EPSRC
Engineering and Physical Sciences Research Council

The University of Nottingham

Molecular Editing of Indoles *via* Formal N-Atom Insertion

and

C–S Cross-Coupling in Micellar Solution

Gemma Valentine

14342648

Supervisor: Dr Liam Ball

Second Supervisor: Prof. Ross Denton

Thesis submitted to the University of Nottingham for the degree of Doctor of Philosophy

March 2023

Table of Contents

Abstract I

Acknowledgements II

List of Abbreviations IV

1. MOLECULAR EDITING OF UNSATURATED HETEROCYCLES VIA FORMAL N-ATOM INSERTION – AN INTRODUCTION 1

1.1 Introduction 2

1.2 Aziridines 9

1.2.1 Aziridine Formation 10

1.2.2 Mechanism of Atkinson's Aziridination 13

1.3 Nitrogen Sources 18

1.3.1 N-Aminoquinazolinones 19

1.3.2 N-Aminophthalimide 20

1.3.3 N-Aminobenzoxazolin-2-one 20

1.3.4 Activated Nitrogen Sources 21

1.4 Strategies for Oxidation 24

1.4.1 Iodine-Based Oxidants 24

1.4.2 Electrochemical Oxidation 25

1.5 Ring Expansion 26

1.6 Aims 30

2. MOLECULAR EDITING OF UNSATURATED HETEROCYCLES VIA FORMAL N-ATOM INSERTION – RESULTS AND DISCUSSION 31

2.1 Aziridination 32

2.1.1 Indole Screening 33

2.1.2 Alternative Nitrogen Sources 36

2.1.3 Synthesis of 6-Fluoroquinazoline 38

2.1.4 Ring Expansion 399

2.2 Beckmann Rearrangement Pathway 41

2.2.1 Mechanism 42

2.2.2 Beckmann Rearrangement of Isatin 44

2.2.3 Beckmann Rearrangement – Results and Discussion 46

2.3 Photocatalytic Pathway 50

3. CONCLUSION AND FUTURE WORK 54

4. EXPERIMENTAL 57

5. REFERENCES 72

6. C–S CROSS-COUPLING IN MICELLAR SOLUTION – AN INTRODUCTION 81

6.1 INTRODUCTION 83

6.2 THIOPHENOL SYNTHESIS 84

6.2.1 Inorganic Sulfur Sources 85

6.2.2 Thiols and Thiolate Salts 87

6.2.3 Thiocarbonyl and Thioester Sources 89

6.3 ISOTHIOURONIUM SALTS AS THIOPHENOL SURROGATES 92

6.3.1 Works of Magné and Ball 93

6.3.2 Scope Limitations 95

6.3.3 Probing the Reaction Mechanism 96

6.3.4 Isothiouronium Reactivity 100

6.4 SURFACTANTS IN ORGANIC SYNTHESIS 102

6.5 AIMS 109

7. C–S CROSS-COUPLING IN MICELLAR SOLUTION – RESULTS AND DISCUSSION 110

7.1 CO-SOLVENT SCREENING 111

7.2 THIOUREA SCREENING 116

7.3 DESIGN OF EXPERIMENTS (DOE) 118

7.4 PRECIPITATION EXPERIMENTS 128

7.5 SCOPE 131

7.6 PHOSPHONIUM INVESTIGATIONS – REACTION MONITORING 133

7.7 DLS 137

8. CONCLUSION AND FUTURE WORK 142

9. EXPERIMENTAL 145

10. REFERENCES 155

Abstract

The research reported in this thesis consists of two distinct projects. The latter of which will be introduced in a subsequent abstract following discussion of the preliminary project.

Molecular editing is a growing research area that involves making late-stage point changes to the core of complex molecular architectures in order to alter their chemical properties. When applied to the pharmaceutical or agricultural industries, late-stage diversification can be used to rapidly expand existing compound libraries to explore new chemical space. Heterocycles have a continuingly large presence in the pharmaceutical industry, and chemistry involving heterocycles continues to be an important area of research. The insertion of a heteroatom such as nitrogen into a ring system would alter a range of physiochemical properties such as polar surface area and would result in changes in solubility and reactivity.

A 2-step route from indole to quinazoline is proposed through aziridination across the 2 and 3 positions of the indole. The first step involves the treatment of various protected indoles with a nitrogen source and phenyliodine(III) diacetate as an oxidant to form an aziridine. The deprotection of this aziridine product at the indolic nitrogen would subsequently allow a ring expansion. In this work, 5-fluoroindole was protected with a variety of protecting groups (tosyl, nosyl, acetyl, Boc, 2,4-dinitrophenyl and benzyl) and their aziridination reactions were investigated. Various nitrogen sources were explored in the aziridination step to give alternative leaving groups for the final ring-expansion step. From the range of aziridines synthesised, the ring expansion of Boc-, nosyl- and acetyl-protected aziridines were focussed on and a variety of conditions were screened.

Alternative methods for conversion of indole-like structures to quinazolines were also explored. The Beckman rearrangement was first investigated, which involved the formation of an oxime of isatin followed by migration initiated under acidic conditions. Additionally, the photo-catalysed C2-C3 ring-opening of Boc-protected indole was studied, which may form quinazoline structures by addition of an ammonia source.

Acknowledgements

Most importantly, I am incredibly fortunate to have had such amazing guidance during my PhD. I'd like to thank Liam Ball for his consistent support and understanding. Through failing projects and a global pandemic you remained encouraging and attentive, providing the perfect balance of wisdom and sarcasm. Your passion for chemistry is evident and contagious. When someone walks into your office for a chat they always leave enthused about their chemistry, even during the difficult parts, which is a tremendous ability to have.

Past members of the Ball group – Lorenzo, Tom, Katie and Aaron – I am thankful for all that you taught me. Aaron, your support in the first two years of my PhD really helped me settle into academic life. You are an excellent mentor and a great person, thank you. I am grateful for starting my PhD in the Ball group alongside other CDT students: Charlie, Desiree and Ben J as an honorary member. Ben J, thank you for your unwavering support and our very important therapy pub sessions. Your efforts to help me acclimatise to outdoor life when pandemic restrictions were lifted were immensely appreciated. Charlie, you are incredibly fun to be around and a very skilled chemist. You're going to do great things. Desiree, thank you for introducing me to yema balls and macaroni salad, one of which I enjoyed.

Alessio and Andy, I thoroughly enjoyed our catchphrase lunchbreaks, though at least now you have the chance to be the first to guess. Martyna, thank you for being there to talk about anything and everything. You're a wonderful person with wonderful earring fashion. Tash, you had some big academic shoes to fill but fill them you have; you're a great chemist. Tash, Sam and Ben L, you're all unhinged and I thank you for that. The Ball group has expanded so much over these four years so it is hard to thoroughly include everyone but Ben S, Sudheesh, Louis and Joseph, thank you for your support. There was never a dull moment in the Ball group, full of interesting discussions both chemistry-related and not. I have thoroughly enjoyed working in this group and I couldn't have asked for better colleagues or friends.

Thank you to my family and friends for being so supportive and patient while I existed in a limited manner during the writing process. In particular, I would like to thank my dad for his contributions to page one of this thesis; it was an excellent Christmas present. Additionally, thank you Maisie (cat) for sometimes sitting on my lap. A special thank you

to Candice Ford who came from Bristol to Nottingham with me for our respective PhDs. I have loved being on this journey alongside you and I am so proud of you for all you have accomplished over the years. Thank you for being a shoulder to cry on during times of stress and an amazing friend to celebrate with during times of joy.

My PhD journey, especially the writing process, would have been made infinitely more difficult without the love and support of my boyfriend, Alex. Thank you for making me tea at all hours and always being there to make me laugh when times were hard. I would also like to thank the various inanimate objects that supported me during the writing process.

I would like to thank the staff in the chemistry and CNL buildings for their assistance. In particular, Shaz and Kev from the analytical team. I will forever fondly remember Shaz regaling us with stories of his youth. I would also like to thank Sue for providing the necessary heaps of coffee required to keep a PhD student afloat, you are a joy. I am appreciative of my fellow CDT students for their friendship and support, and of the CDT admin staff for assisting me over the years.

Finally, I would like to acknowledge Nicole Tsang for her preliminary contributions to the first project reported in this thesis. Additionally, Valentin Magné who developed the foundation of the second project reported in this thesis. Also, thanks to Laura Forfar at Catalysis Consulting for her assistance in DoE design and analysis. I thank the EPSRC for funding and the CDT for giving me this wonderful opportunity.

List of abbreviations

API	Active pharmaceutical ingredients
cryoTEM	Cryogenic transmission electron microscopy
CTAC	Cetrimonium chloride
DLS	Dynamic light scattering
DNB	3,5-Dinitrobenzoate
DoE	Design of experiments
dtbpf	1,1'-Bis(di-*tert*-butylphosphino)ferrocene
EDG	Electron-donating group
EWG	Electron-withdrawing group
FDA	Food and Drug Administration
IBX	2-Iodoxybenzoic acid
LA	Lewis acid
LG	Leaving group
LTA	Lead tetraacetate
m-CPBA	*meta*-Chloroperoxybenzoic acid
mPANI	Mesoporous polyaniline
NBP	*N*-Butyl-2-pyrrolidone
NHC	*N*-heterocyclic carbene
OVAT	One variable a time
PCA	Principle component analysis
PEG	Polyethylene glycol
PG	Propylene glycol
PIDA	Phenyliodine(III) diacetate
PIFA	Phenyliodine(III) bis(trifluoroacetate)
PTS	Polyoxyethanyl-α-tocopheryl sebacate
RE	Reductive elimination
SDS	Sodium dodecyl sulfate
TEMPO	2,2,6,6-Tetramethylpiperidine 1-oxyl
TFE	2,2,2-Trifluoroethanol

Common abbreviations can be accessed at:
https://pubs.acs.org/userimages/ContentEditor/1218717864819/joceah_abbreviations.pdf

1 Molecular Editing of Unsaturated Heterocycles via Formal N-Atom Insertion – An Introduction

1.1 Introduction

The pharmaceutical and agrochemical industries both depend on high throughput of new chemical entities to deliver new, more effective active ingredients to the market. However, only 7% of pharmaceutical drugs that enter preclinical trials actually make it to market (as of 2013).[1] This high rate of failure of newly developed drugs, and the resources required to develop new active ingredients, results in an average cost of taking a new drug to market of roughly $2 billion (as of 2013).[1] Methods that allow late-stage diversification of existing compound libraries expedite the discovery process by alteration of a pre-developed active ingredient, allowing rapid diversification of drug libraries. Molecular editing is one such approach.

"Molecular editing" is a term first coined by Wilson and Danishefsky in 2006[2] to describe the altering of a natural product, increasing or decreasing molecular complexity, through diverted total synthesis. Since then, the term has been further defined as the "insertion, deletion or exchange of atoms in highly functionalised compounds at will and in a highly specific fashion".[3] For ease of classification, Levin and co-workers separated molecular editing into two areas: peripheral editing and skeletal editing (**Figure 1**).[4] Peripheral editing includes transformations that make small-group changes to functionalities external to the molecular core, such as C-H functionalisation. Alternatively, skeletal editing involves the alteration of the core structure itself. This can be further divided into incorporation or exclusion of atoms external to or within a ring system (expansion/contraction) and the addition or removal of units within a ring (insertion/deletion). Skeletal editing also involves the exchange of atoms within a ring, without changing ring size (transmutation). The ability to carry out such transformations would allow facile expansion of current drug and agrochemical libraries, alongside reducing waste and materials consumed if these species were synthesised *via* a *de novo* approach.

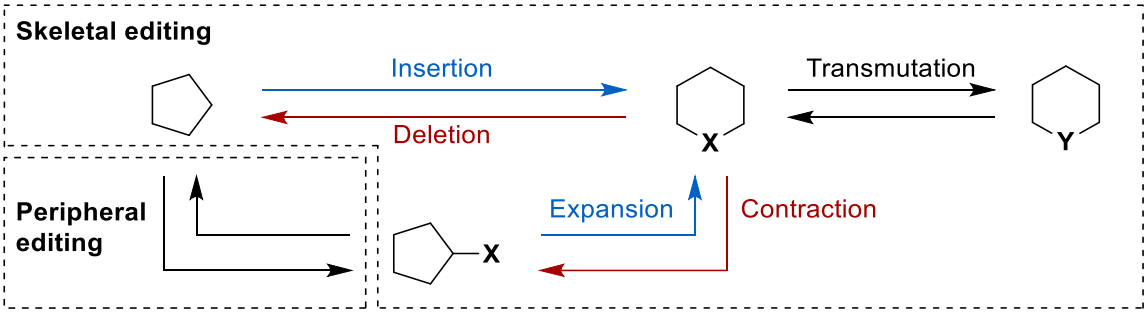


Figure 1 - Molecular editing terms.[5]

Reviews such as that of Joynson and Ball can assist in defining many known transformations within this new classification method.[6] For example, the Favorskii rearrangement allows for the exclusion of a carbonyl from a ring system, formally decreasing the ring size by one unit (**Figure 2a**).[7] Due to fact that the carbonyl remains external to the ring system, this transformation can be categorised as a contraction. Conversely, a transformation reported by Murai and co-workers in 2012 involving a 1,2-carbon migration to a neighbouring nitrogen atom resulted in the formal expansion of these rings by one nitrogen atom (**Figure 2b**).[8]

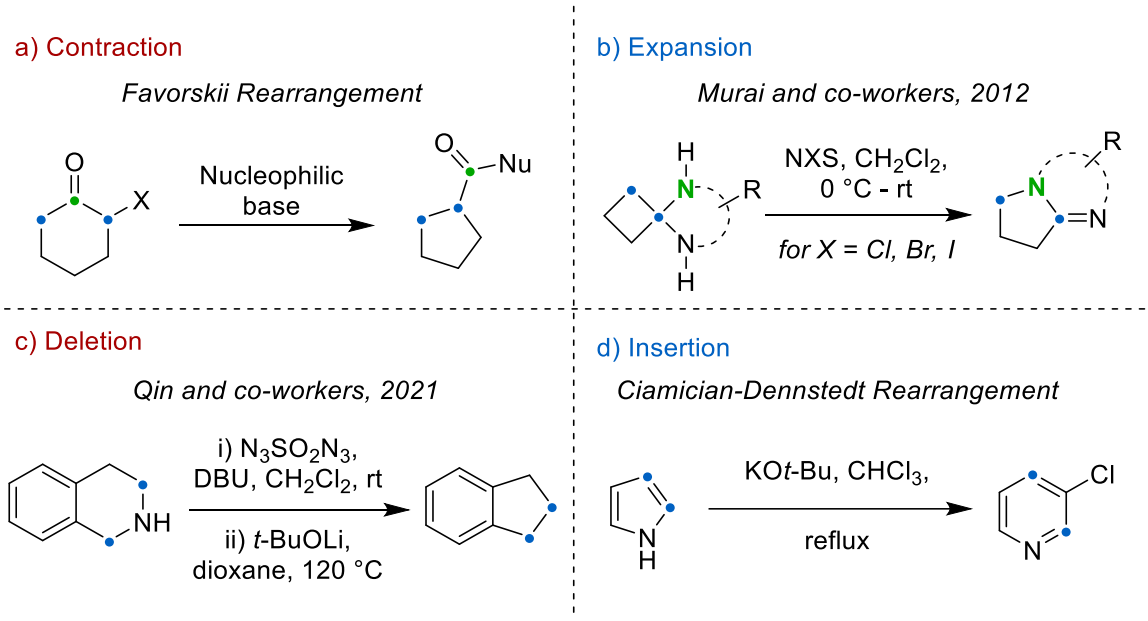


Figure 2 - Examples of transformations that can be categorised as molecular editing: contraction (a),[7] expansion (b),[8] deletion (c)[9] and insertion (d).[10]

Deletion (**Figure 2c**) and insertion (**Figure 2d**) transformations instead involve the complete removal or addition of ring components from the molecule, resulting in a

decrease or increase in ring size respectively. Transformations such as those reported by Qin and co-workers in 2021 can excise a single nitrogen atom from a ring, formally a deletion.[9] An example of an insertion transformation is the Ciamician-Dennstedt rearrangement,[10] formally inserting a carbon atom across the C–C double bond of pyrroles using dichlorocarbene as the reactive species. This insertion not only changes the reactivity of the heterocycle itself but also incorporates a chlorine atom which can be used for further peripheral editing. These examples show how molecular editing transformations can be used to fundamentally change the core structure of a variety of compounds and further expand into unexplored chemical space.

A vast amount of biologically active molecules contain N-heterocycles,[11] some of which are displayed in **Figure 3**. Indeed, between 2015 and 2020, 88% of new FDA approved small-molecule drugs contained *N*-heterocycles.[12] Hence, chemistry which involves the manipulation of these privileged scaffolds is of great interest. As mentioned previously, the facile transformation of existing chemical species to new species is a way to easily explore new chemical space. Considering the Ciamician-Dennstedt rearrangement (**Figure 2d**), transforming one type of heterocycle to another – here pyrrole to pyridine – is a substantial scaffold change with implications of altered chemical properties. However, conceptually, this change in properties could equally be obtained by insertion of a heteroatom instead; using the previous example, this could enable conversion from pyrrole to pyrimidine.

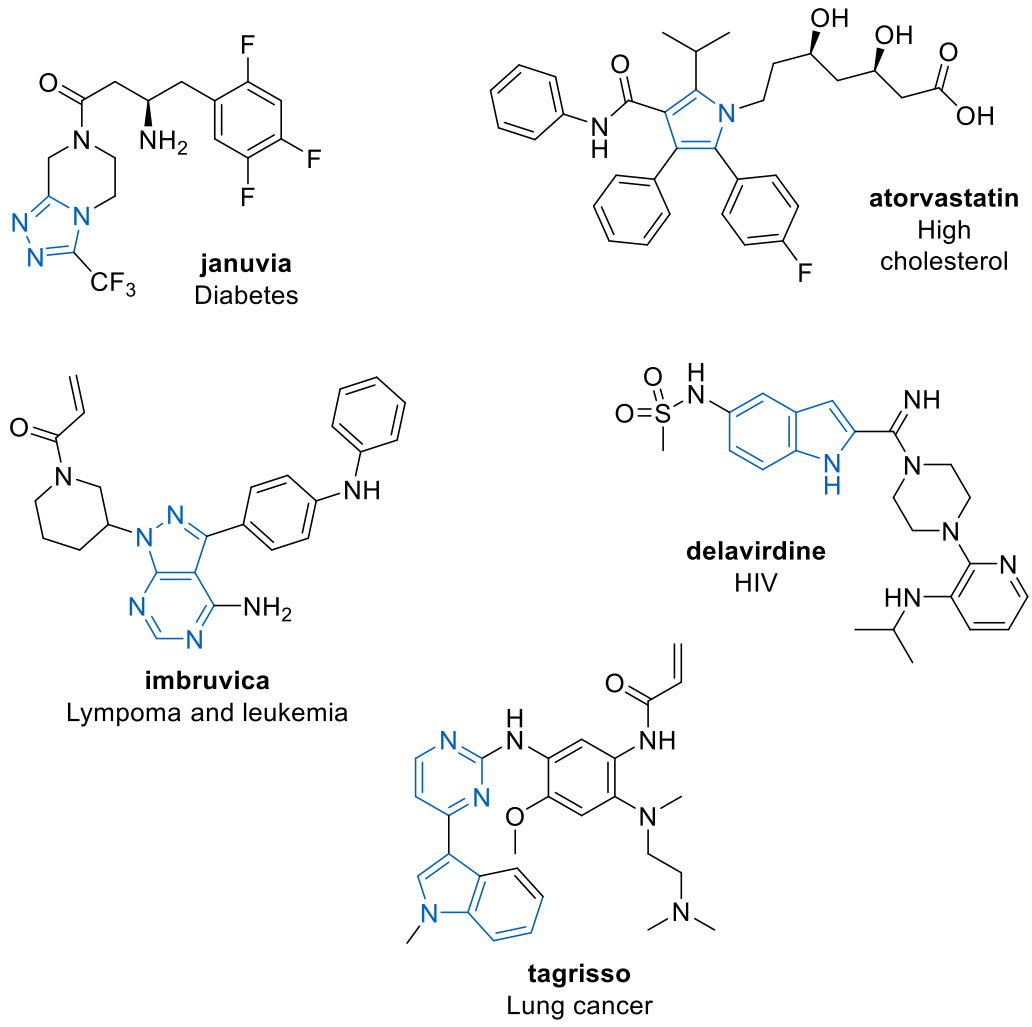
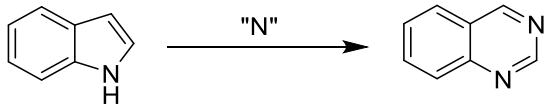


Figure 3 - Examples of pharmaceutical products containing at least one N-heterocycle, and their primary indications.

Despite differing by only a single atom, the insertion of a nitrogen atom into a heterocyclic system would alter a variety of properties that can contribute towards a molecule's pharmacological activity. The introduction of a heteroatom to an organic molecule can alter properties such as hydrophobicity, which can be vital to the binding of a molecule to a protein as well as having an effect on its solubility. **Figure 4** demonstrates the changes that would be made if indole underwent such a ring expansion to give quinazoline. Not only does the molecule become more polar, but its chemistry is also altered; converting from an acidic species to a basic species.

Proposed transformation: 

	Indole	***Quinazoline***
Polar Surface Area	15.8 Å^2	25.8 Å^2
pKaH	−3.6	3.5
cLogP	2.2	1.8

Figure 4 - The effect nitrogen insertion into indole would have on representative properties.[13,14]

A transformation of this type was reported by Narasimhan and Kumar in 1984 for nitrogen insertion into substituted cyclopentadienes (**Figure 5a**) ,[15] and again by Kumar in 1987 for substituted indoles (**Figure 5b**).[16] These routes involved 2 steps: the aziridination of the starting material using a primary amine nitrogen source and oxidant, followed by a fragmentation which resulted in the ring-expanded product. The limited scope presented in these initial papers, where only three cyclopentadienes and three indoles were successfully expanded, mean there is still a lot to be explored in terms of functional group tolerance. In these papers, *N*-aminophthalimide (PhthNH$_2$) is oxidised by lead tetraacetate (LTA) which generates an activated “N” species that adds across a carbon-carbon double bond to form an aziridine. All reagents are used in stoichiometric quantities which results in a low atom economy of 19% for this transformation. This is further worsened by the fact that the stoichiometric lead oxidising species is highly toxic.[17] Aziridination reactions have been widely reported,[18] which gives opportunity to improve the on the conditions reported by Kumar for this transformation – resulting in a transformation that is potentially greener and more feasible on a larger scale.

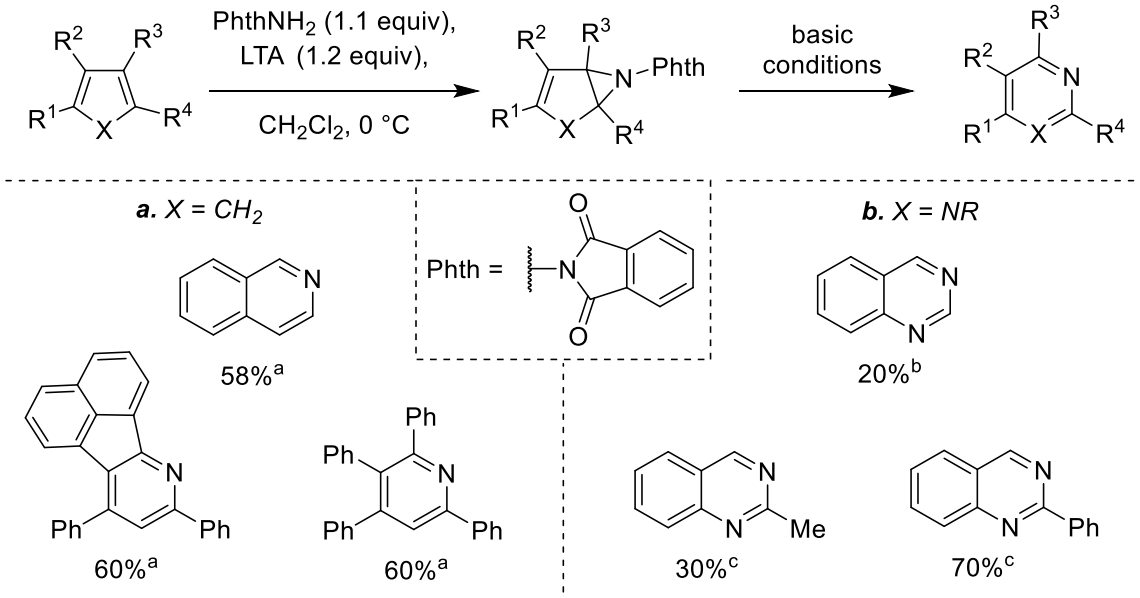


Figure 5 – Two-step ring expansion routes reported for cyclopentadienes (a)[15] and indoles (b).[16] Basic conditions used were: [a]NaH (1.3 equiv), THF, r.t., [b]KOH/MeOH, r.t. for R=SO_2Ph, [c]NaH (3 equiv), DMSO, 0 °C for R=H.

As will be discussed in detail in Chapter 2, attempts to build on Kumar's precedent proved unsuccessful. However, after termination of this project, the N-atom insertion concept was reported by Morandi and co-workers (**Figure 6**).[19] This work will be discussed here for completeness.

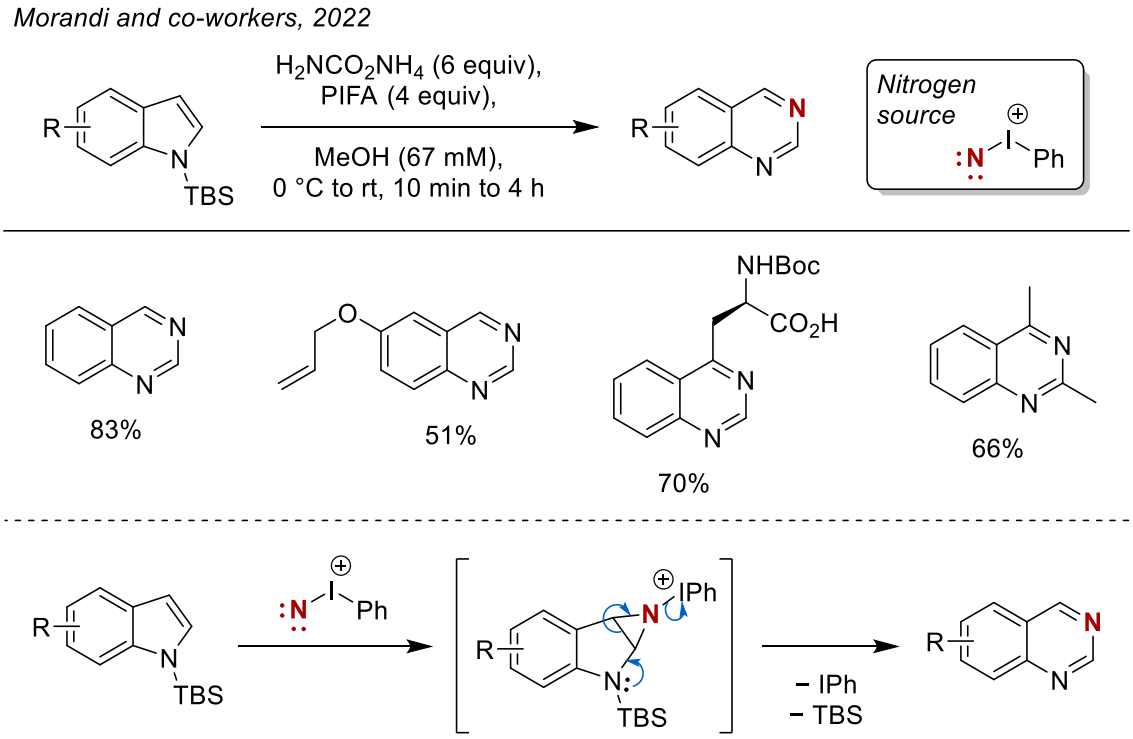


Figure 6 – Transformation reported by Morandi and co-workers, with some highlighted products from the scope and the proposed mechanism.[19]

Morandi utilised an iodonitrene nitrogen source, which allows iodobenzene to act as a leaving group after nitrene addition. The nitrogen source selection proved a crucial factor in the success of this reaction. Of the thirteen different reagents tried, ammonium carbamate gave an initial GC yield of 47% whereas the remaining twelve were unable to surpass 1%. The indoles were protected with a silyl protecting group, which can leave as a cation after ring expansion (**Figure 6**). This is also a key factor as using acetyl, Boc and methyl protecting groups resulted in no more than 4% yield of quinazoline. These conditions were also applied to unprotected indole which gave a GC yield of 1%.

Subsequent sections in the introduction to the work reported in this thesis will touch on each component of the transformation originally proposed by Kumar[16] and discuss the consequences for reactivity. This work focuses on the ring expansion of indoles, however insertion reactions such as this have since been proven possible on pyrrolopyridines.[19]

1.2 Aziridines

Aziridines are highly reactive due to having polarised C–N bonds and a high ring strain of 24.3 kcal mol^{-1}.[20] This reactivity makes this structure synthetically useful and hence their formation has been well-documented.[18] The thermodynamic driving force for ring opening results in their susceptibility to ring-opening on exposure to nucleophiles (**Figure 7a**), a phenomenon which has been widely discussed in literature.[21,22] Ring-opening by anionic nucleophiles can result in polymerisation (**Figure 7b**).[23] This can also be achieved under acidic conditions, where a neutral aziridine can act as the nucleophile towards the, now activated, protonated aziridine.

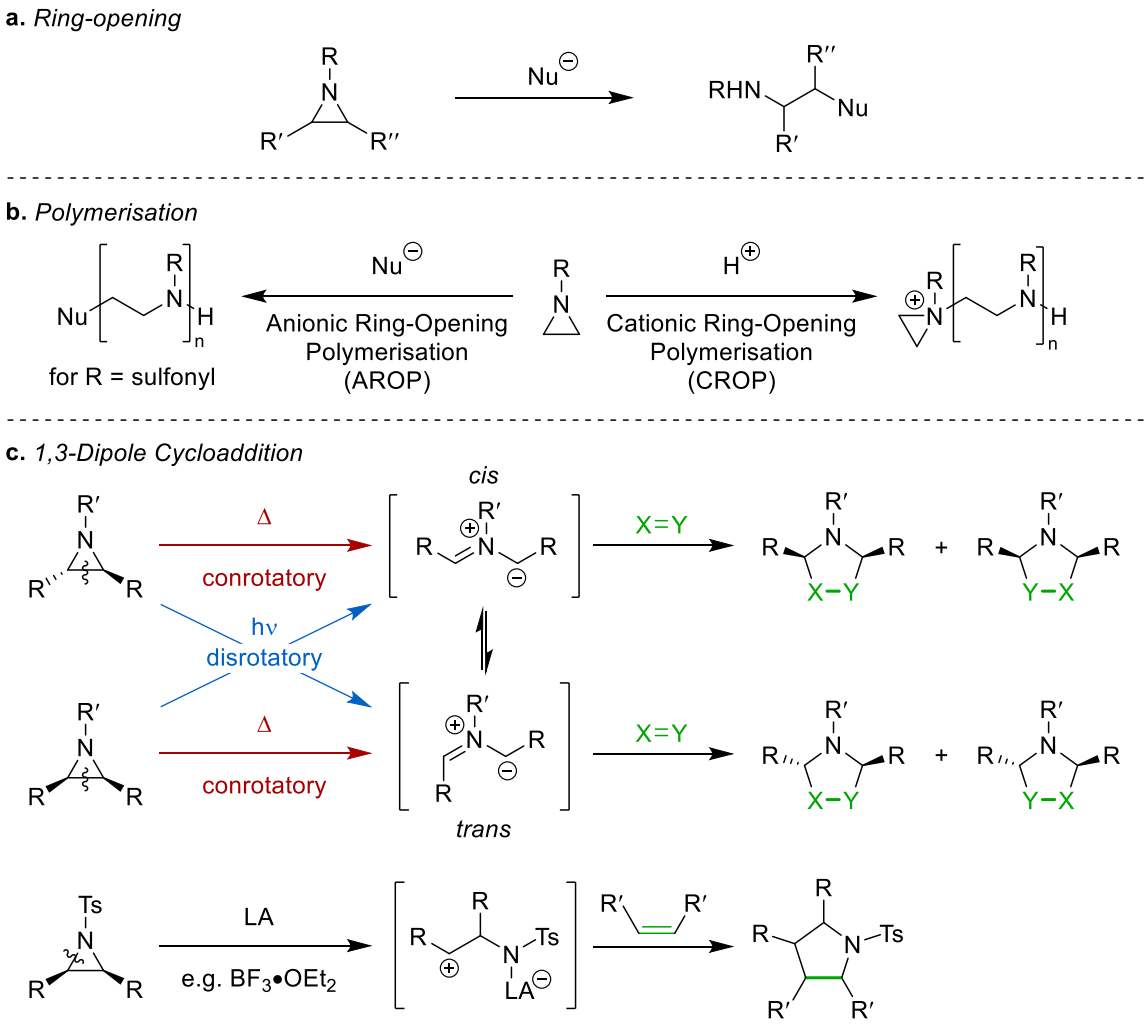


Figure 7 – Reactivity of aziridines.

When exposed to heat or light, aziridines can open by breaking of the C–C bond to give 1,3-dipoles (**Figure 7c**).[24] These can undergo cycloaddition with alkenes, alkynes, and carbonyls[25] following the Woodward-Hoffman rules.[26] The resulting stereochemistry is usually dictated by the generation of either *cis*- or *trans*-orientated substituents of the 1,3-dipolar species, but in some instances, isomerisation can be observed.[25] Alternatively, a 1,3-dipolar species formed through C–N bond breakage can be obtained by addition of a Lewis acid.[27,28] As with the previous example, this can also undergo cycloaddition with alkenes, nitriles and carbonyls.[28]

1.2.1 Aziridine Formation

Examining aziridine synthesis *via* a classic retrosynthetic approach, the disconnections displayed in **Figure 8** can be made. This figure excludes the route that involves C–C bond formation as a final step as this, although possible,[29,30] is synthetically challenging and not a standard route to aziridine functionality.

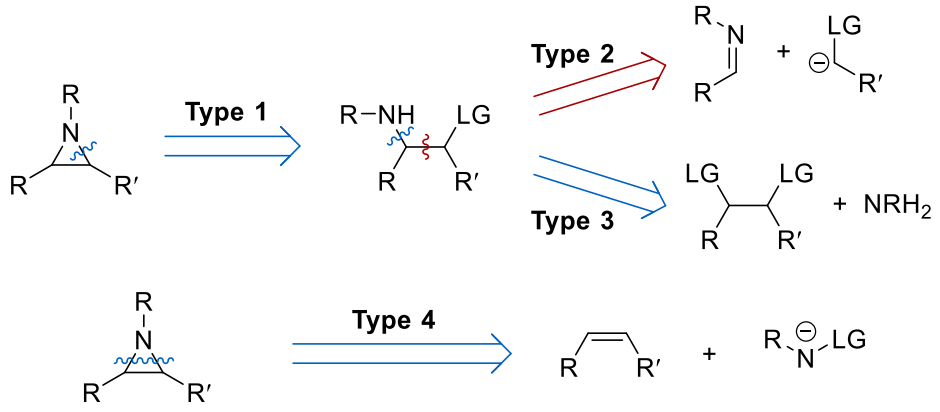


Figure 8 - Aziridine forming reactions via classical disconnection.

C–N bond formation can be achieved through the nucleophilic displacement of a leaving group by an amine (**Figure 8, Type 1**). A reaction of this type was reported in 1888, although initial reports were unsure as to the identity of the product.[31] Wenker reported a similar transformation in 1935 whereby 2-hydroxyethylamine was heated with 96% sulfuric acid, giving an unidentified intermediate that collapsed on addition of base giving aziridine in an overall 19% yield (**Figure 9a**).[32]

Further disconnections can be made at either the C–C bond or the other C–N bond, described herein as Type 2 and Type 3 respectively (**Figure 8**). Another classical method for the synthesis of aziridines is the Aza-Darzens reaction, which falls under Type 2 (**Figure 9b**).[33] This occurs through attack by an anion bearing an α-leaving group, which will be removed *via* attack of the resulting amine. This requires a neighbouring electron-withdrawing group capable of stabilizing the anion, usually carbonyl or nitrile groups but phenyl or alkenyl substituents can suffice.[34] Alternatively, **Figure 9c** demonstrates a Type 3 disconnection through the addition of a nitrogen unit into two neighbouring carbon atoms via two S_N2 reactions.[35] If the epoxide starting material is a single enantiomer, the resulting aziridine is produced in good enantiomeric purity due to the double inversion of stereochemistry.

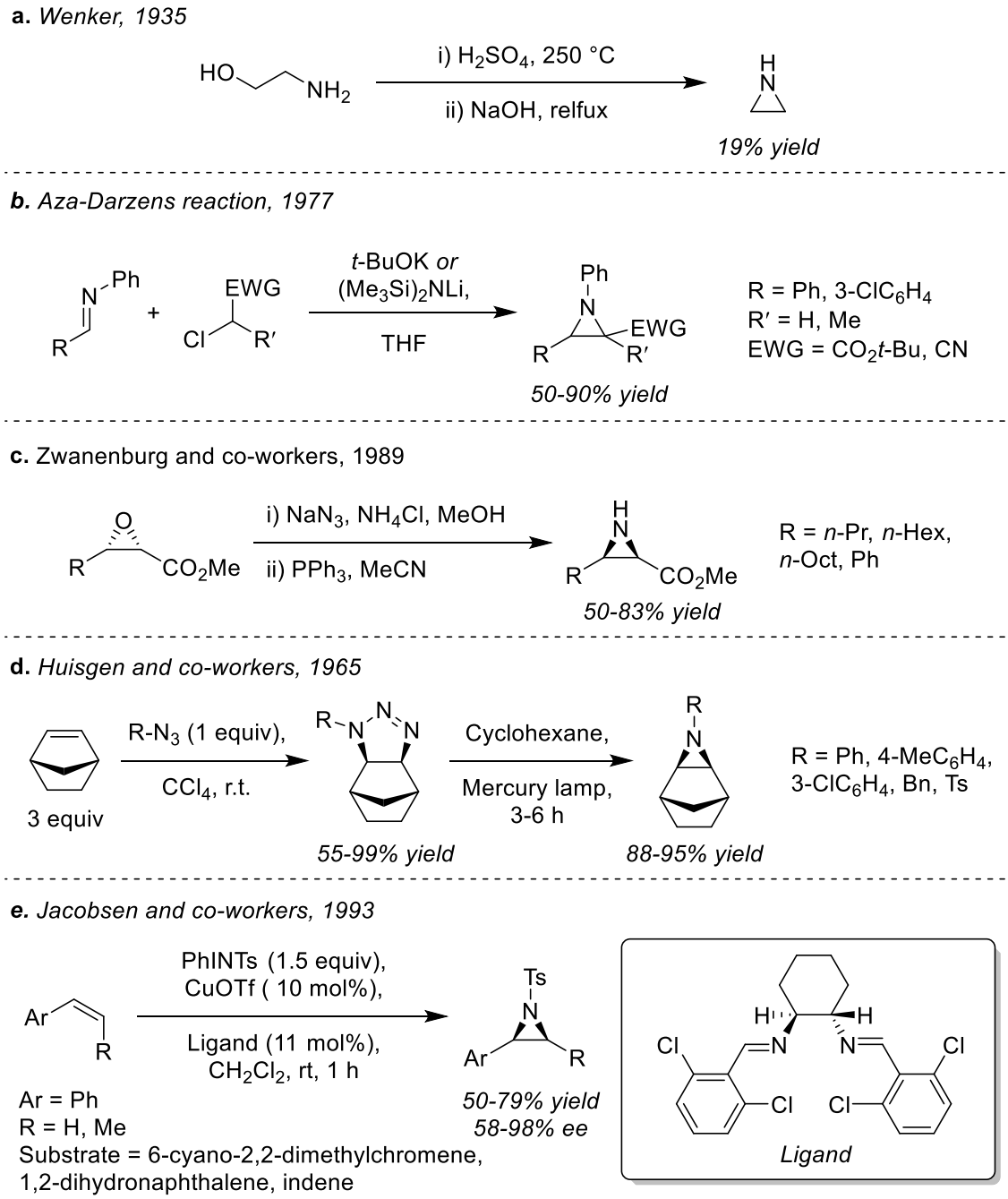


Figure 9 - Examples of aziridine formation conditions.

The final disconnection, Type 4, involves addition of a nitrogen atom across a C–C double bond (**Figure 8**). This can be achieved through initial [3+2] cycloaddition with an azide, forming a 1,2,3-triazole, followed by photodecomposition, as reported by Huisgen and co-workers (**Figure 9d**).[36] Alternative sources of nitrogen such as *N*-tosyliminobenzyliodinane (PhINTs) can react with metals forming stabilised nitrenoids which, when used with a chiral ligand, can give aziridines with high enantiomeric purity (**Figure 9e**).[37,38] This method,

developed by Jacobsen, is designed for the aziridination of *cis*-alkenes, but a complementary method for *trans*-alkenes was first published by Evans in the same year.[39,40]

The aziridine required for the ring expansion of indoles demonstrated by Kumar[16] needs a suitable leaving group at the aziridine nitrogen. One such aziridine synthesis, first reported by Atkinson and Rees, is displayed in **Figure 10**.[41] Aziridines were first synthesised in this manner to explore the electronic states of the nitrogen analogue of a carbene: nitrene.[42] This method requires the reaction of a nitrogen source and oxidising agent with an olefin in stoichiometric amounts. The majority of previous research reported aziridination using *N*-amino heterocycles,[43] primarily *N*-aminoquinazolinone[44,45] and *N*-aminophthalimide.[16] Oxidation of these species is usually carried out by adding stoichiometric amounts of toxic LTA.[43] However, alternative oxidants such as the hypervalent iodine oxidant phenyliodide(III) diacetate (PIDA)[44] have also been investigated.

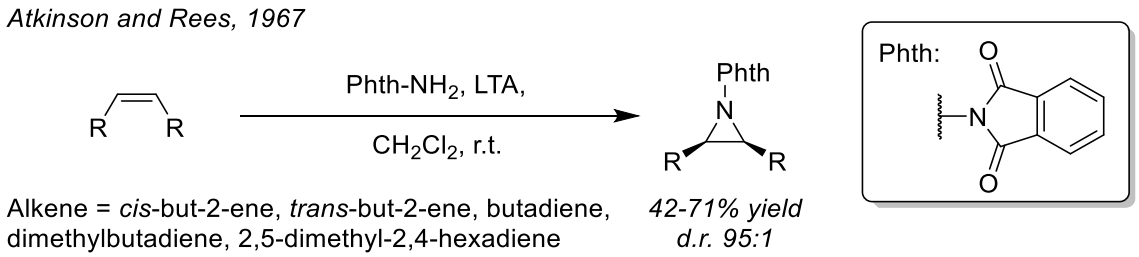


Figure 10 – Reported synthesis of aziridines bearing suitable leaving groups for the proposed transformation.[41]

1.2.2 Mechanism of Atkinson's Aziridination

During the initial investigations into the reactions of LTA and *N*-aminophthalimide with an olefin, it was assumed that a free nitrene intermediate was involved.[45] This nitrene would act in a similar way to that of Skell's carbenes[46] and react in its singlet state to add stereospecifically to the olefin[47] or react in the triplet state to add non-stereospecifically (**Figure 11**).[43]

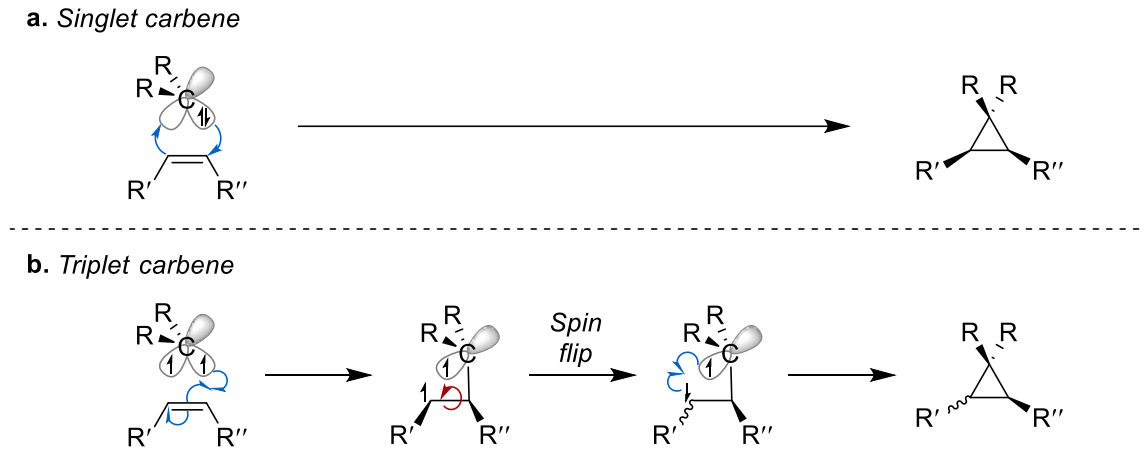
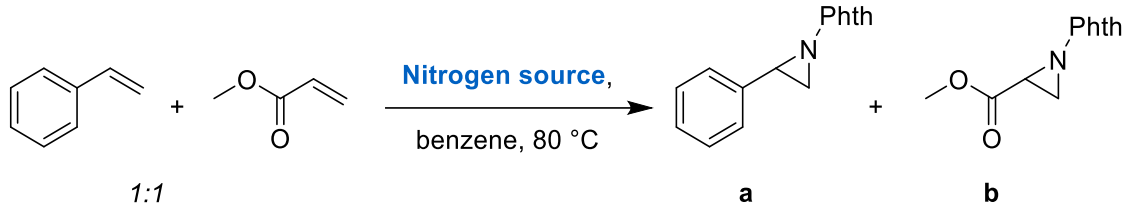


Figure 11 – The mechanisms of reaction of (a) singlet and (b) triplet state carbenes with olefins. The resulting stereoselectivity is displayed, where the red arrow indicates free rotation around the C–C bond.

To investigate the intermediate involved in the reaction with *N*-aminophthalimide and LTA, its selectivity was compared to that of known nitrenes produced by pyrolysis of *N*-phthalimidoaziridines (**Figure 12**).[48] The reagents were combined with a mixture of styrene and methyl acrylate and it was observed that this oxidatively-generated intermediate favoured styrene (1.5:1) whereas the thermally-generated nitrene intermediate favoured methyl acrylate (1:3).[45] This difference in reactivity for olefins with different electronic demands suggested that these aziridinations did not have the same intermediate.



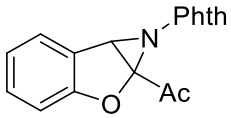
Entry	*Nitrogen source*	*Ratio of formation of a:b*
1	Phth-NH_2, LTA	1.5 : 1
2		1 : 3

Figure 12 – The differing selectivities of nitrenes and the intermediate produced upon oxidation of N-aminophthalimide with LTA when applied to a 1:1 mixture of styrene and methyl acrylate.[45]

Further investigation into this alternative intermediate was carried out by Atkinson and co-workers.[45] NMR spectroscopic studies have shown that oxidised *N*-amino-2-ethylquinazolinone is stable in CH_2Cl_2 at −20 °C. When the temperature is raised, this species reacts with olefins to form aziridines.[49] Upon ^{1}H and ^{13}C NMR spectroscopic analysis at −30 °C, this intermediate was determined to be 3-(acetoxyamino)-2-ethylquinazolinone.[49] Equivalent *N*-acetoxy intermediates are also assumed to exist with nitrogen sources such as *N*-aminophthalimide due to the similarities in stereoselectivity between the two nitrogen sources.[49] The mechanism of formation for these *N*-acetoxy intermediates is displayed in **Figure 13**. Atkinson and co-workers proposed that neither nitrene nor the nitrenium ion could be involved in an equilibrium of active species (**Figure 14**) as no exchange of “N-OAc” acetate or “N-H” protons were observed in a tetra-deuterated acetic acid solution.[45]

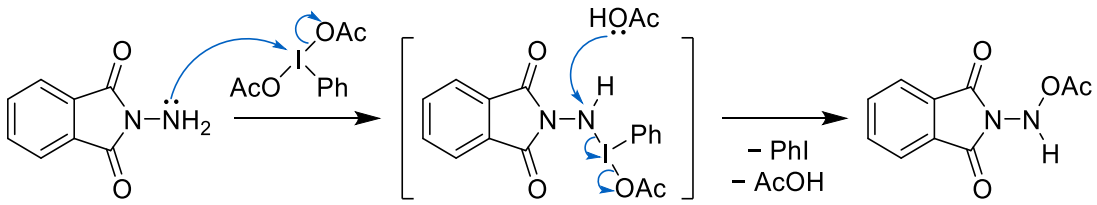


Figure 13 – Oxidation of N-aminophthalimide by PIDA to form the N-acetoxyaminophthalimide species, as described by Krasnova and co-workersl.[44]

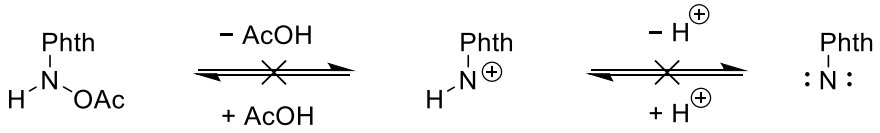


Figure 14 – Equilibrium proposed and disproved by Atkinson and co-workers for the exchange of ions in the active species.[45]

Warming the *N*-acetoxyamino species in the absence of an olefin or other trapping reagent leads to formation of the corresponding tetrazane.[44] If the oxidising agent is still present in solution, this is further oxidised to the tetrazene, which decomposes to give the deaminated species with loss of nitrogen gas (**Figure 15**). This decomposition pathway competes with aziridination and is significant in reactions involving less reactive olefins.[44] This also explains the positive relationship between yield and olefin concentration.[44,45]

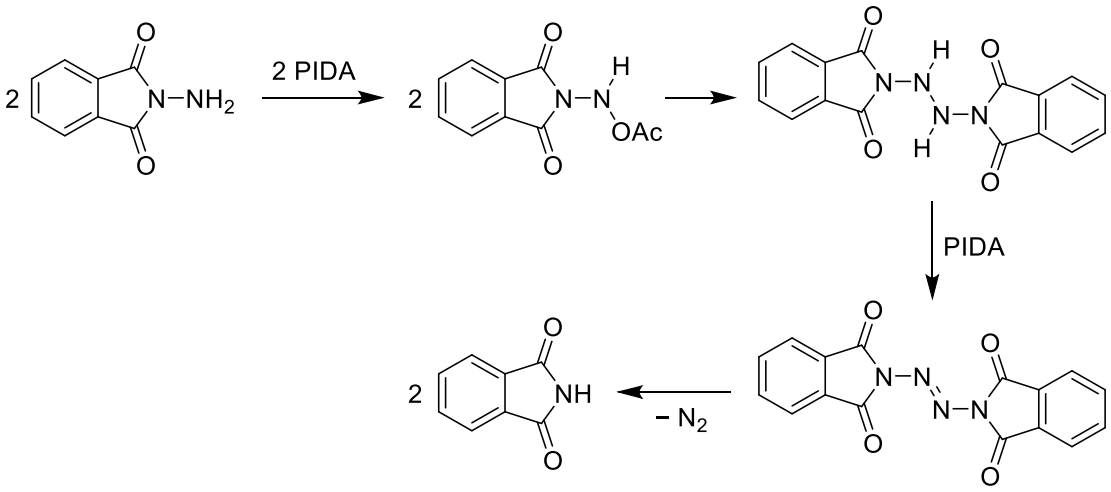
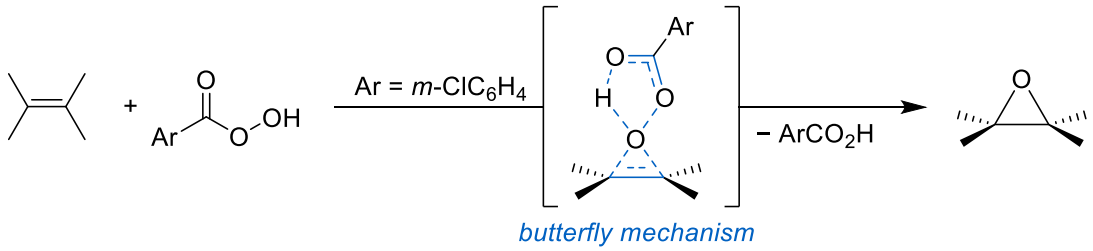


Figure 15 – Decomposition pathway of the activated N-aminophthalimide species by dimerization and loss of nitrogen gas.[44]

McConaghy and Lwowski[42] estimated that these "nitrene" reactions would follow Skell's mechanism for addition of a carbene to an olefin, as mentioned in the previous section (**Figure 11**).[46] Indeed, a similar concerted mechanism akin to these seemed to be taking place. For the *N*-acetoxyamino compounds, this is analogous to the 'butterfly' mechanism proposed by Bartlett for addition of peroxyacids to alkenes to form epoxides (**Figure 16a**).[50] The proposed mechanism for the aziridination of indoles was concerted, as displayed in **Figure 16b**.[45] A publication by Atkinson and Williams stated that this is an asynchronous process, in which the N-C_α bond is formed slightly ahead of the N-C_β bond.[51]

a. *Mechanism proposed by Bartlett for the Prilezhaev reaction*



b. *Mechanism proposed for aziridination of alkenes with N-amino heterocycles*

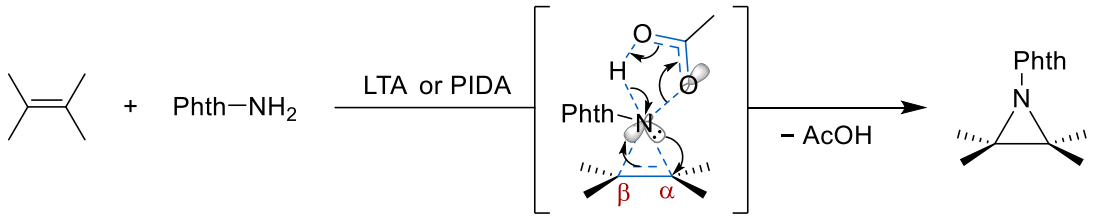
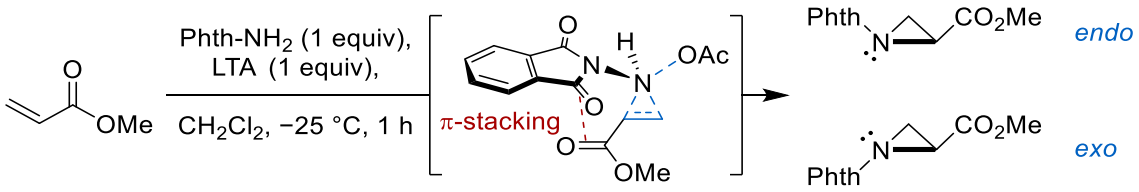


Figure 16 - Proposed concerted mechanisms for the Prilezhaev reaction (a)[50] and the addition of the active N-acetoxyaminophthalimide species across a double bond to form an aziridine with loss of acetic acid (b).[45]

In the aziridination of olefins with *N*-aminophthalimide, the electron withdrawing properties of the phthalimide group results in a high barrier to inversion at the aziridine nitrogen, such that the rate of inversion is essentially zero at −20 °C. This makes it possible to isolate and analyse the individual *exo*- and *endo*-invertomers of such aziridines.[43] Aziridination of methyl acrylate with *N*-aminophthalimide at −30 °C produces the kinetic *endo*-invertomer (**Table 1, entry 1**).[43] This is due to secondary orbital interactions between orbitals of the nitrogen source heterocycles and any substituents on the olefin.[52] Raising the temperature above 0 °C, however, allows conversion into the more thermodynamically stable *exo*-invertomer (**Table 1, entry 2**). When interactions between the phthalimide group and olefin substituents are particularly strong, for example with methyl acrylate due to overlap with the carbonyl group, it can take weeks at room temperature to convert to the more thermodynamically stable invertomer.[43] Studies of *N*-acetoxyaminoquinazolinone showed that the *endo*-invertomer was also the predominant form[53] but, in comparison to *N*-phthalimido aziridines, the rate of inversion at the aziridine nitrogen of *N*-quinazolinone aziridines is much slower.[43]

Table 1 - Investigation into the endo/exo selectivity of the aziridination of methyl acrylate with N-aminophthalimide when solutions remained under −25 °C (entry 1) and when allowed to warm to room temperature (entry 2).[52] The overlap of the methyl acrylate carbonyl with the phthalimide π-system in the endo-invertomer transition state is displayed. Ratios of invertomers were calculated by peak integration from ^{1}H NMR spectroscopic data.



Entry	***Internal temperature of NMR instrument / °C***	***endo : exo***
1	−30	100 : 0
2	25	17 : 83

1.3 Nitrogen Sources

As mentioned previously, the majority of nitrogen sources reported in literature for aziridination across a C–C double bond are *N*-amino heterocycles, the most common of which are displayed in **Figure 17**.[43] Further research has been carried out into other sources such as sulfenylnitrenes[54] and metal-containing compounds.[55] The chemical properties of these nitrogen sources are very important to the aziridination reaction as they can affect the reactivity and selectivity of the compounds.[56] The choice of nitrogen source could also influence the ring expansion step of the route investigated in this thesis, as a more electron withdrawing substituent would increase its leaving group ability. The three *N*-amino heterocyclic structures shown in **Figure 17** – *N*-aminoquinazolinone, *N*-aminophthalimide and *N*-aminobenzoxazolinone – will be discussed in this section, followed by discussion of non-heterocyclic nitrogen sources for completion.

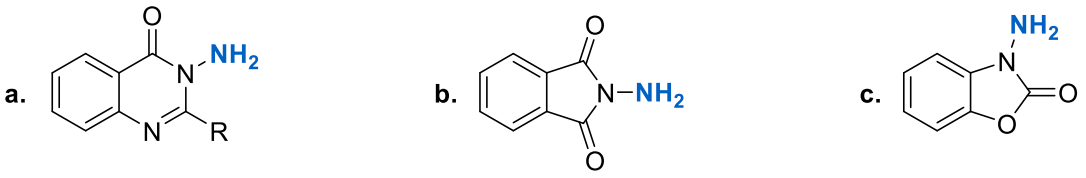


Figure 17 – Different heterocyclic nitrogen sources commonly used in the aziridination of olefins; (a) N-aminoquinazolinones, (b) N-aminophthalimide, (c) N-aminobenzoxazoin-2-one.

1.3.1 N-Aminoquinazolinones

N-Aminoquinazolinone structures were used as nitrogen sources in many of the initial mechanistic investigations into the aziridination of olefins in this manner.[43] As previously stated, the carbonyl group on the quinazoline ring contributes towards the high diastereoselectivity of reactions involving this substrate. Interaction with groups adjacent to the olefin double bond reduces the electrophilicity of the carbonyl, hence increasing the NHOAc lone pair donor ability.[43] Additionally, an advantage of using *N*-aminoquinazolinones over other nitrogen sources is that functionality can be introduced at the 2-position in order to influence reactivity. When an alkyl group is situated on the 2-position of *N*-acetoxyaminoquinazolinone, the species is only stable for a few minutes above 0 °C.[57] Whereas fluorinated groups like CF_3 at the 2-position result in stability at room temperature for hours and can further improve yields.[58] The stability of the *N*-acetoxyamino intermediate is also improved by the removal of acetic acid, which has been found to be a significant yield-limiting factor.[59] One possible explanation for the limited yield is solvolysis in acetic acid.[41] Atkinson suspected that this degradation of active species proceeds through the mechanism displayed in **Figure 18**.[43] Hence, Ulukanli and co-workers found that removal of acetic acid by addition of hexamethyldisilazane almost doubles their yield.[60]

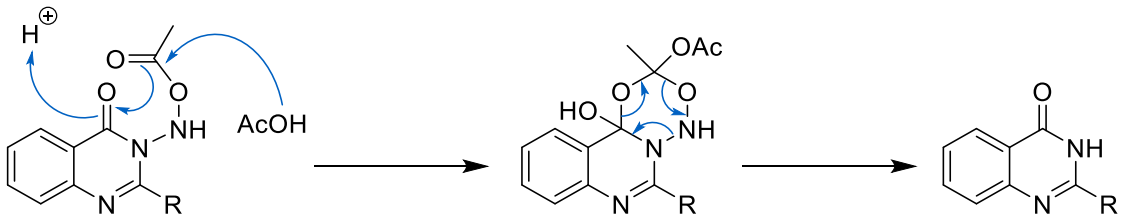


Figure 18 – Suspected mechanism for the solvolysis of the active N-acetoxyquinazolinone species by acetic acid. [43]

1.3.2 N-Aminophthalimide

Parallels can be drawn between aziridination reactions carried out with *N*-aminoquinazolinone and *N*-aminophthalimide, hence they are assumed to have comparable mechanisms.[61] As with *N*-aminoquinazolinones, aziridination with *N*-aminophthalimide is high yielding with good diastereoselectivity.[16] Upon addition to styrene, Atkinson and Kelly[45] found that *N*-aminophthalimide is slightly more selective for the *syn*-invertomer (2.3:1) compared to observations with *N*-aminoquinazolinone (2.1:1). However, *N*-acetoxyaminophthalimide is considerably less stable in solution than *N*-acetoxyaminoquinazolinone.[43] Despite this, the advantage of using *N*-aminophthalimide over *N*-aminoquinazolinone is that it is 13 times cheaper (for 5 g, purchased through Merck).[62]

1.3.3 N-Aminobenzoxazolin-2-one

Atkinson and Rees[41] explored the use of *N*-aminobenzoxazolinone as an aziridinating agent in combination with LTA. Here, benzoxazolone was aminated by hydroxylamine-*O*-sulfonic acid to give the desired substituted hydrazine. Initial comparisons were made with this species and 1-aminobenzotriazole, which reacts with LTA to give the active *N*-acetoxy species, followed by fragmentation to a benzyne with loss of nitrogen gas.[41] However, Aktinson and Rees observed that, despite the fact that oxidation was rapid, no fragmentation occurred.[41] Furthermore, reaction with dienes resulted in 1,2-additions as opposed to the 1,4-additions expected of nitrenes.[63] This was early evidence that suggested the oxidised intermediate was unlikely to be a nitrene. Reactions with *cis*- and *trans*-but-2-ene gave, as expected, the cis- (60%) and trans-aziridines (67%) with very good stereospecificity (95%) (**Figure 19**).[41]

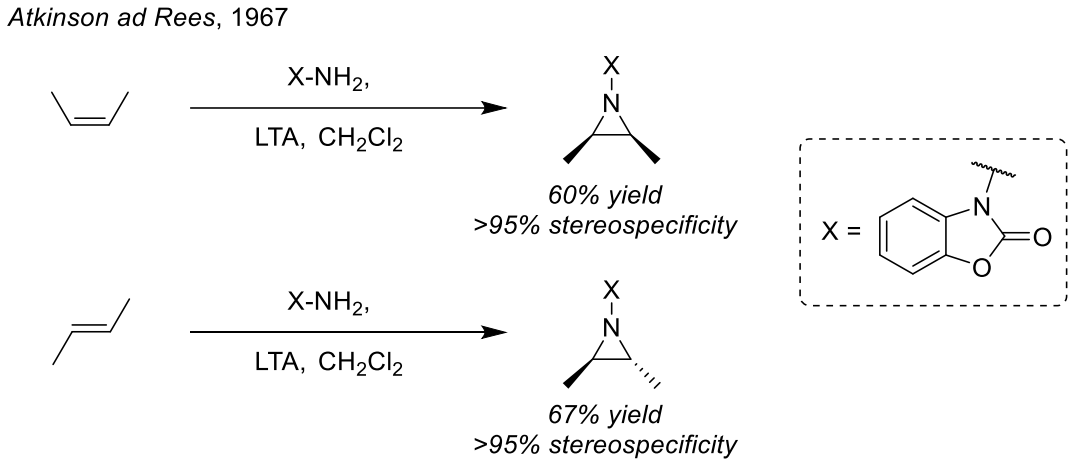


Figure 19 – The stereospecificity displayed in the aziridination of cis- and trans-but-2-enes with N-aminobenzoxazolinone.[41]

1.3.4 Activated Nitrogen Sources

There are nitrogen sources that have been used in aziridination literature that are able to react without the need for an oxidant present in the aziridination process itself. Though stoichiometric amounts of oxidant are not required in the aziridination, these "pre-activated" species must typically be prepared in advance by oxidation, and they do require additional metal catalysts to promote aziridination (**Figure 20**). This is usually achieved by formation of metal nitrenoid species.[38]

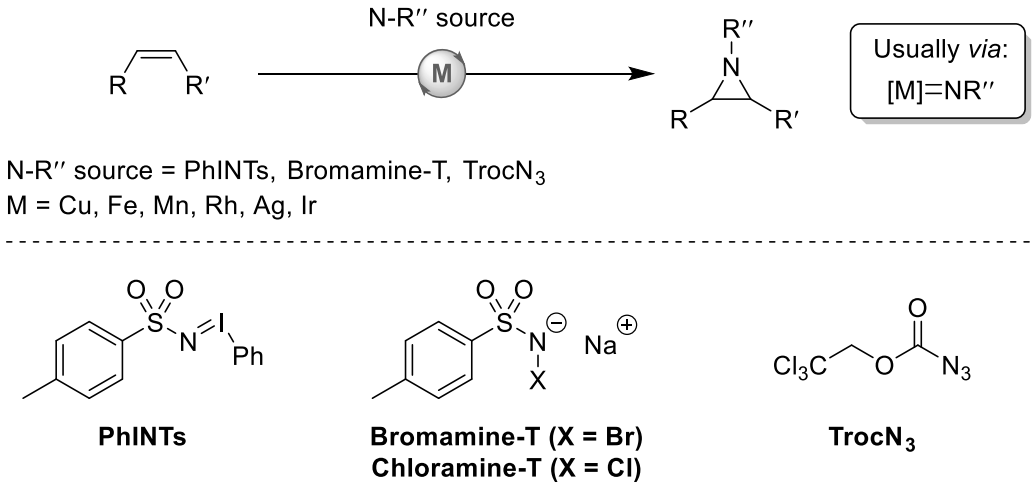
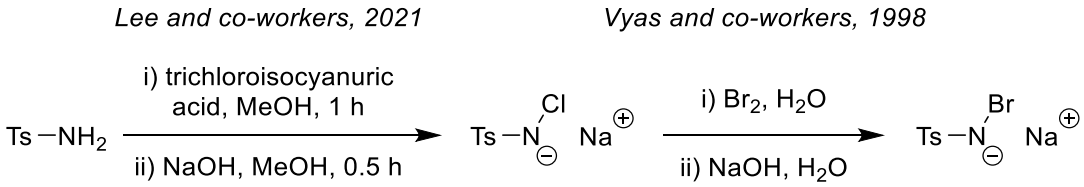


Figure 20 – Metal-catalysed aziridination of olefins and the pre-activated nitrogen sources used.

Azides are well-known for their reactivity and as a result are able to react with olefins without use of an external oxidant. They do, however, require metal catalysis by generation of metal-supported nitrene radicals as the active aziridinating species. These will react like triplet nitrenes through a stepwise addition, as mentioned previously in **Figure 11**. Cobalt(II) porphyrin catalysts are able to stabilise the radicals derived from *N*-Troc, *N*-nosyl and *N*-tosyl azides.[64] Additionally, Schloz and co-workers demonstrated that an iridium-based catalyst can be used in the photocatalysed aziridination of olefins through the controlled photochemical excitation of azides.[65]

Some activated nitrogen sources can be made such *ex situ*. For example, Chloramine-T has been used as an aminating agent for the aziridination of olefins.[66] This reagent can be synthesised by treating tosyl amine with trichloroisocyanuric acid, followed by addition of sodium hydroxide (**Figure 21a**).[67] Alternatively, Chloramine-T is commercially available. The first aziridination publication using Chloramine-T utilised a copper(I) chloride catalyst,[66] however in the same year these authors published an alternative route using molecular iodine as a catalyst.[68] It was proposed that, instead of the catalyst activating the nitrogen source, the iodine reacts with the olefin to generate an iodonium cation which can more readily react with Chloramine-T (**Figure 21b**). In 2004, aziridination of olefins using Chloramine-T was carried out in water using the phase-transfer catalyst and iodide source *n*-Bu_4NI.[69] Aziridination by Chloramine-T has since been catalysed by Fe- and Mn-based catalysts, proposedly through metal-stabilised nitrenes.[70–72]

a. *Synthesis of Chloramine-T and Bromamine-T*



b. *Iodine-catalysed aziridination with Chloramine-T*

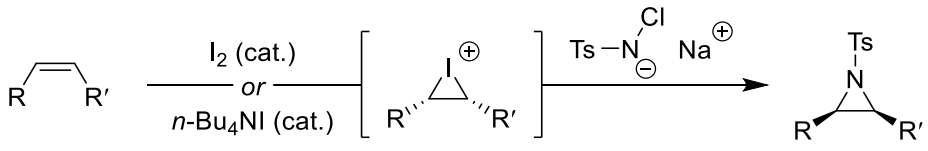


Figure 21 – The synthesis of Chloramine-T from tosyl amine[67] and Bromamine-T from Chloramine-T (a),[73] and the I_2 or n-Bu_4NI catalysed aziridination of olefins with Chloramine-T (b).[68]

Following on from the initial studies in 1998, Vyas and co-workers investigated the comparison of Chloramine-T with its bromine equivalent; Bromamine-T.[73] They synthesised this reagent from Chloramine-T using bromine and sodium hydroxide sequentially (**Figure 21a**). Under the same conditions, they found that Bromamine-T outperformed its chlorine equivalent – giving higher yields of aziridinated olefin for all reported substrates. They suggest that this is due to weaker nitrogen-bromine bonds making the bromide more labile. Bromamine-T has since been used in tandem with other metal catalysts such as Ni(II), Co(II), Fe(III), Mg(II), Mn(II) and Sr(II) chlorides.[74]

One of the more commonly used "pre-activated" nitrogen sources is (*N*-(*p*-tosyl)imino)phenyliodinane (PhINTs). This can be synthesised from tosyl amine through oxidation with PIDA, providing *ex situ* oxidation of the nitrogen source (**Figure 22**).[75] This reagent, though effective, is unstable at room temperature and hence has a short shelf-life.[71,76] Though an additional oxidant is not required for aziridination using PhINTs, a metal catalyst is necessary. This has been used in the asymmetric Cu-catalysed aziridination methods reported by both Jacobsen and Evans.[37,39] Other metals used in the catalysis of aziridinations with PhINTs include Fe,[77,78] Co,[79] Mn,[71,78] and Ag.[80]

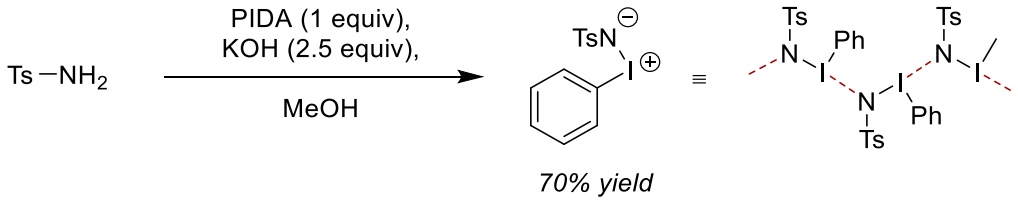


Figure 22 – Synthesis of PhINTs, as reported by Yamada and co-workers,[75] displaying the polymeric intermolecular interactions that more accurately portray the bonding structure of this hypervalent iodine species.[81]

Though these reagents do not require *in situ* oxidation when used for the aziridination of olefins, most require prior oxidation from commercially available compounds. Aziridination of olefins using the nitrogen sources mentioned above have a reliance on stoichiometric oxidant. Options for oxidation methods will be discussed in the following section.

1.4 Strategies for Oxidation

One of the main issues with this aziridination step is the reliance on stoichiometric amounts of oxidant.[43] Reducing the impact that the oxidants have on both resources and the environment would therefore be advantageous. An ideal oxidant would be one that has a low molecular weight, to improve atom economy, and is non-hazardous to humans and to the general environment. Lead tetraacetate was the most widely used oxidant for aziridination of olefins in the early research into this reaction.[43] However, this strong oxidant is highly toxic,[17] difficult to store and difficult to handle.[44] Alternative oxidising species are available and will be discussed in the remainder of this section.

1.4.1 Iodine-Based Oxidants

PIDA is a milder oxidant[44] which is not considered a hazardous substance.[82] Its addition to *N*-aminophthalimide, as described in Section 1.2.2, produces only acetic acid and iodobenzene as by-products.[44] Good yields were obtained when reacted with a range of olefins (**Figure 23a**),[44] and remained relatively unchanged when scaled up to 5 mol.[83] Studies showed that this reagent had relatively high functional group tolerance and was able to react in the presence of nitriles, carbonyls, amides, esters and secondary and tertiary alcohols.[44] As mentioned previously, PIDA can be used *ex situ* to generate PhINTs, which can be used as a nitrogen source in metal-catalysed aziridination reactions.[75] Other variants of this oxidant are available such as phenyliodine(III) bis(trifluoroacetate) (PIFA), as used by Morandi and co-workers in their indole ring expansion conditions.[19] Oxidants of this type can also be made *in situ* by reaction of iodobenzene with *m*-CPBA, generating phenyliodine(III) bis(3-chlorobenzoate).[84] Other iodine-based oxidants that have previously been used in the aziridination of olefins include IBX **(Figure 23b**)[85] and *t*-BuOI (**Figure 23c**),[86] the latter of which is generated *in situ* from t-BuOCl and NaI. Molecular iodine can react with tosyl amine which, when irradiated with visible light, reacts with olefins *via* a radical mechanism to give aziridines (**Figure 23d**).[87] However, this is only possible when one R group is capable of stabilising a radical on the adjacent carbon.

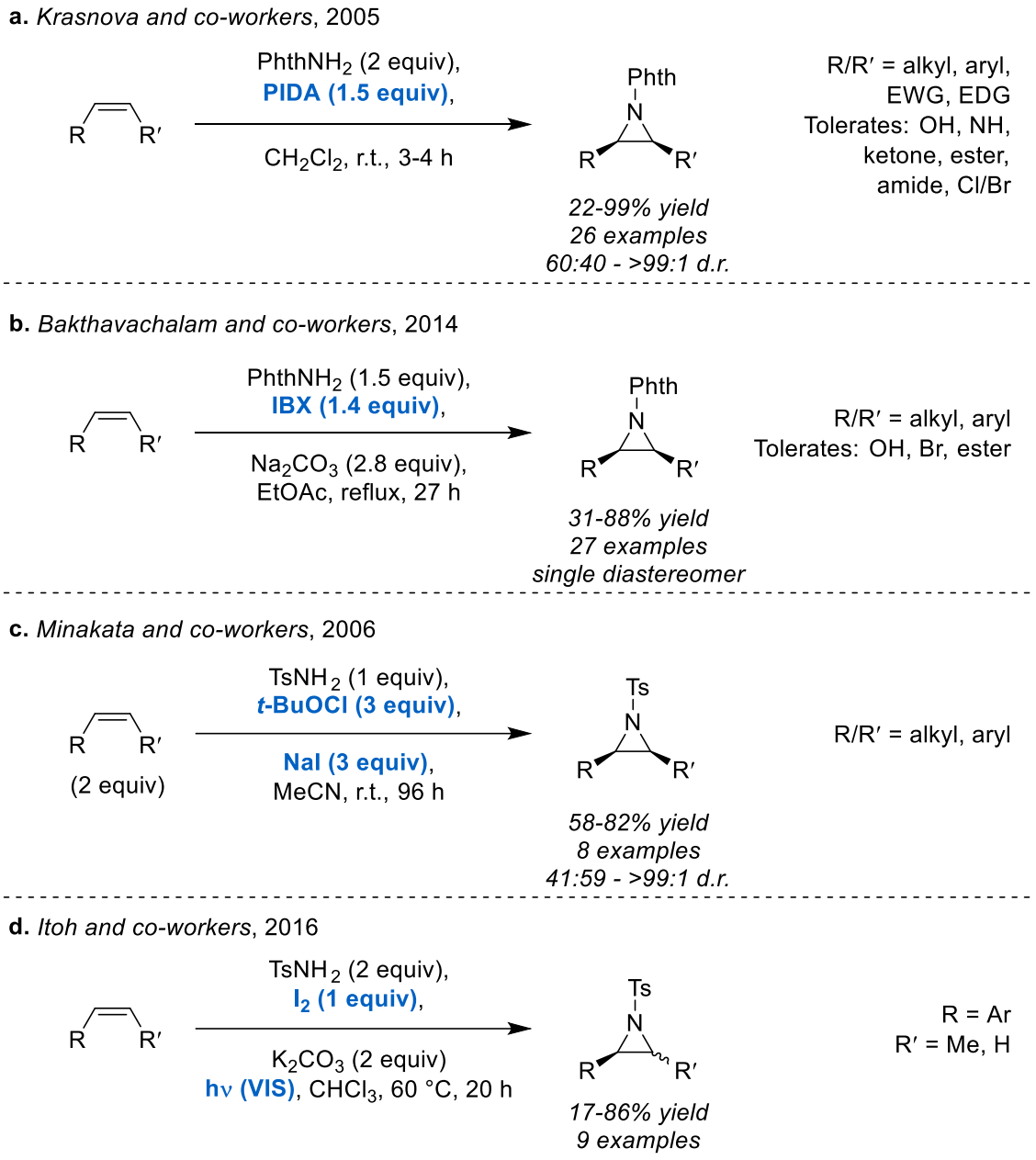


Figure 23 – Use of iodine-based oxidants PIDA (a),[44] IBX (b),[85] t-BuOI (c)[86] and I_2 (d)[87] in the aziridination of olefins.

1.4.2 Electrochemical Oxidation

One of the main issues with this aziridination method is that all reagents are used in stoichiometric quantities. This problem could potentially be solved with electrochemistry.

Due to the similar oxidation potentials for both the olefin and amine,[83] it is very difficult to selectively oxidise the amine. However, the phenomenon of 'overpotential' introduces a way to electronically discriminate between species. Overpotential is the additional potential difference, above the thermodynamically expected potential, required experimentally for a particular reaction to take place. The olefin and amine can hence be distinguished by varying conditions such that one reaction is more kinetically favoured at one electrode than the other.[88] Siu and co-workers calculated that +1.80 V was required to initiate the oxidation of *N*-aminophthalimide in MeCN in the absence of oxidant (**Figure 24**).[88] This reaction was carried out at room temperature using two platinum electrodes with triethylamine and acetic acid as the electrolyte. The addition of the triethylammonium acetate salt as the electrolyte was found to be a vital part of the reaction. This suggests that a similar *N*-acetoxyamino intermediate is present, further supported by similar stereochemical distributions.[88]

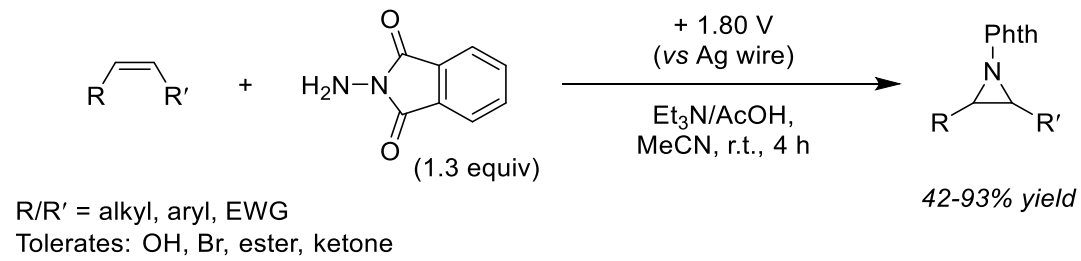


Figure 24 – Electrochemical aziridination of alkenes, as reported by Siu and co-workers.[89]

A variety of olefins were aziridinated using this method in very high yields. The selectivity of this method means that this can be achieved with minimal side reactions.[83] This method has already been tested on a multigram scale.[88] Unfortunately, indoles would be easier to oxidise than the alkenes investigated in these studies and hence the selective oxidation of indole over the amine would be more difficult.

1.5 Ring Expansion

In 1987, Kumar published a paper describing how indoles could be converted to quinazolines through the aziridination of indole, followed by addition of base to facilitate ring expansion.[16] Two different conditions were used in this publication for the ring

expansion step for both protected and unprotected indoles. For *N*-(phenylsulfonyl)indole, methanolic potassium hydroxide can be added to induce the ring expansion to form quinazoline (20%) and the deprotected indole (80%) (**Figure 25, conditions 1**). For unprotected indoles, sodium hydride in DMSO was used (**Figure 25, conditions 2**). The latter conditions were applied to four substituted indoles: 2-methylindole, 2-phenylindole, 1,2,3,4-tetrahydrocarbazole and 1-oxo-1,2,3,4-tetrahydrocarbazole. Ring expansion was successful for 2-methylindole and 2-phenylindole, giving both the desired quinazolines (30% and 70%, respectively) along with *N*-phthalimido-3-aminoindoles as side-products (30% and 10%, respectively). Treatment of 1,2,3,4-tetrahydrocarbazole and 1-oxo-1,2,3,4-tetrahydrocarbazole with DMSO/NaH, however, instead resulted in the formation of carbazole (85%) and 1-hydroxycarbazole (70%) respectively.

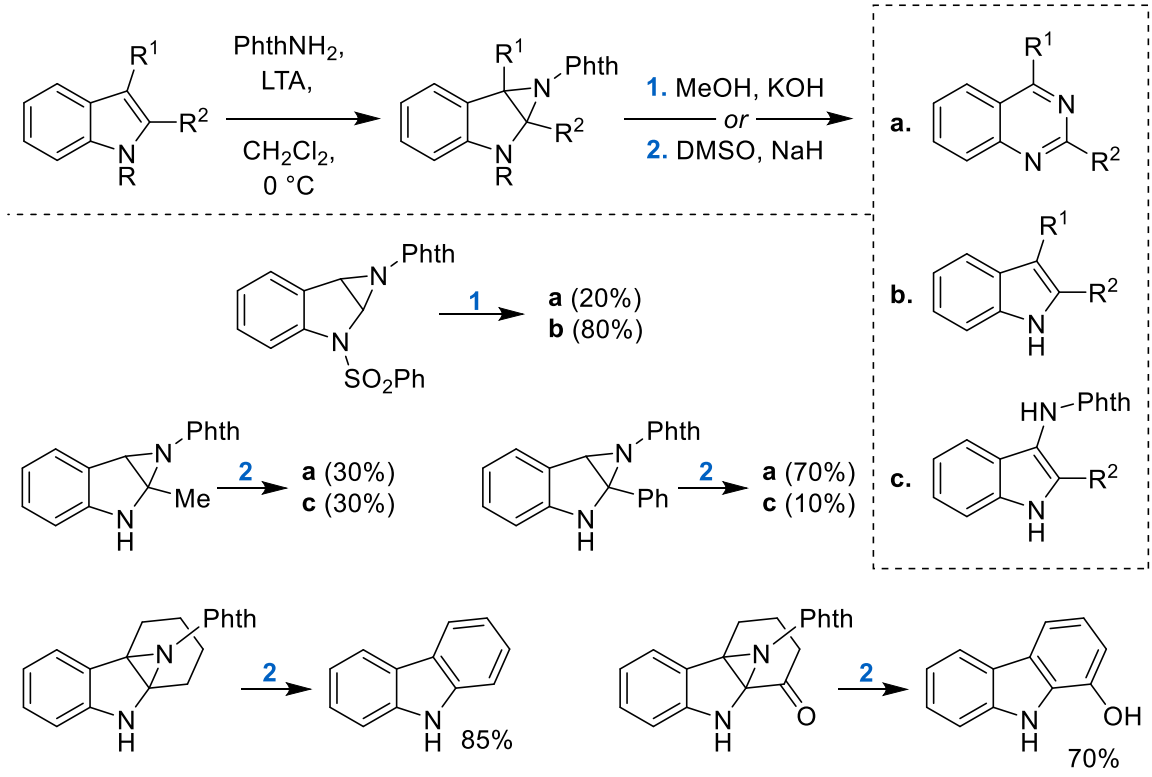


Figure 25 – Transformations reported by Kumar for the ring expansion of protected and unprotected indoles.[16]

The exact mechanism for the ring-opening step was not explored within this paper.[16] However, parallels can be drawn between this reaction and the previously mentioned Ciamician-Dennstedt reaction (**Figure 26**).[10] This instead inserts carbon atoms into rings

through cyclopropanes *via* generation of dihalocarbenes or, in some instances, monohalocarbenes.[90]

Ciamician-Dennstedt rearrangement

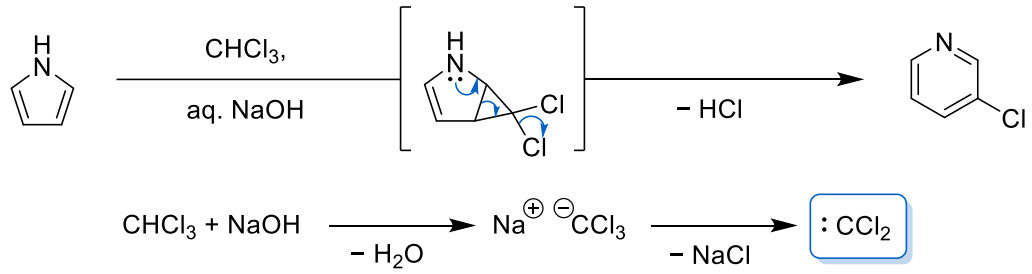


Figure 26 – The mechanism for the Ciamician-Dennstedt ring expansion of pyrrole.[10,91,92]

The ring expansion of indoles to quinazolines reported by Morandi and co-workers, though utilising a different nitrogen source to Kumar's reported procedure, also occurs *via* aziridine formation.[19] Based on computational studies reported in this publication, this proceeds *via* the nucleophilic attack of an iodonitrene from the 3-position of a protected indole, which can then cyclise as shown in **Figure 27**. Morandi and co-workers propose that the ring expansion is initiated from the lone pair of the indoline nitrogen, breaking the C2-C3 bond and resulting in the expulsion of iodobenzene. The labile silyl group can then leave as a silylium cation.

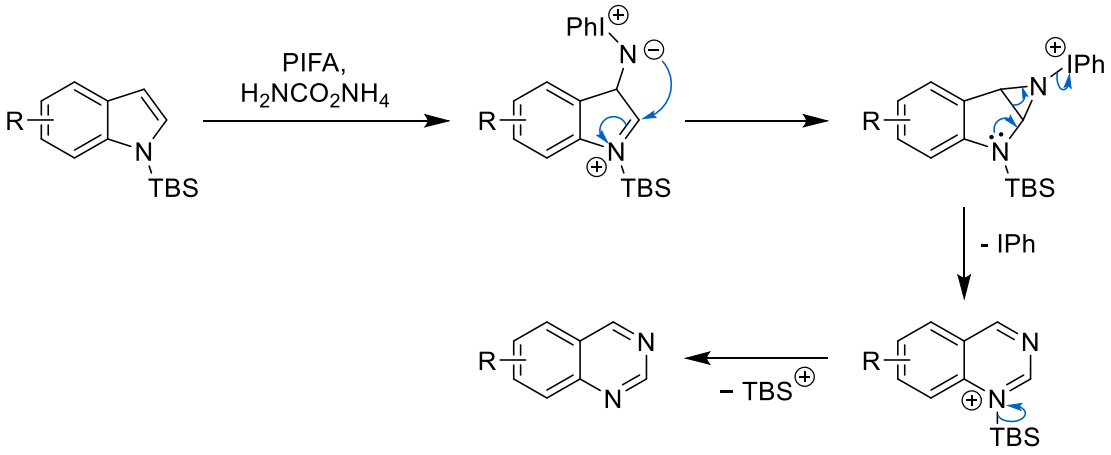


Figure 27 – The mechanism for the ring expansion of indole as reported by Morandi and co-workers.[19]

These mechanisms all involve the departure of a leaving group situated at the aziridine nitrogen, or equivalent. An indole ring expansion method reported by Xu and co-workers

in 2018 instead utilised a leaving group at the C3 position of indole (**Figure 28**).[93] They proposed a fragmentation that results in the expulsion of N_2 from an azide group at the C3 position of the indoline, giving the corresponding 4-aminoquinazolines. The authors suggested that the origin of this electron movement is at the aziridine nitrogen, however it can equally be assumed to originate from the indoline nitrogen. Though a promising synthetic route, this is only applicable in the synthesis of 4-aminoquinazolines also containing aryl groups at the C2 position. An indole with 2-(*n*-butyl) substitution was tried but gave only trace amounts of ring-expanded product under these conditions.

Xu and co-workers, 2018

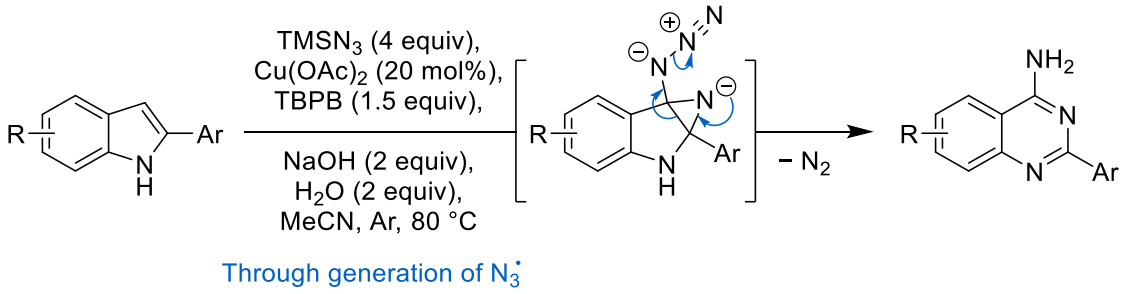


Figure 28 – The proposed mechanism for the copper-catalysed ring-expansion of 2-arylindoles using azide radicals to form 4-amino-2-arylquinazolines.[93]

1.6 Aims

The aim of this work was to develop a general, mild and convenient method for the N-atom ring expansion of indoles. We envisaged that this would be achieved in two steps by aziridination followed by ring-expansion to give a quinazoline. In the initial stages of this work, aziridination conditions were screened. These were based on the conditions reported by Kumar,[16] but using a safer, more sustainable hypervalent iodine oxidant in place of LTA. Each aspect of the proposed transformation was to be investigated:

1. Screen a range of protecting groups on 5-fluoroindole for the aziridination step to not only test scope, but to also allow for options for the removal of the protecting group.
2. Explore alternative nitrogen sources, mainly focussing on nitrogen sources with large literature precedent such as *N*-aminoquinazolinones.
3. With the library of aziridines obtained from these previous steps, test different methods for removal of the protecting groups to allow for ring expansion.

Furthermore, alternative methods of nitrogen insertion into indoles to give quinazoline-based systems were to be explored. Namely, the Beckmann rearrangement of isatin and a photocatalyzed oxidative ring-opening of Boc-protected indole[94] followed by ring closure with introduction of a nitrogen source.

2 Molecular Editing of Unsaturated Heterocycles via Formal N-Atom Insertion – Results and Discussion

2.1 Aziridination

Each component of the initial aziridination step was to be systematically investigated. The first stage of this investigation was to start from previously reported conditions and build upon them. Preliminary experiments performed by Nicole Tsang identified the working conditions illustrated in **Figure 29**. While an important proof of concept for this first step, full optimisation had not been performed and reaction scope was not established.

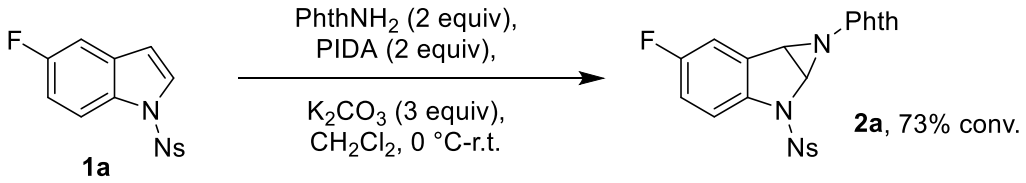
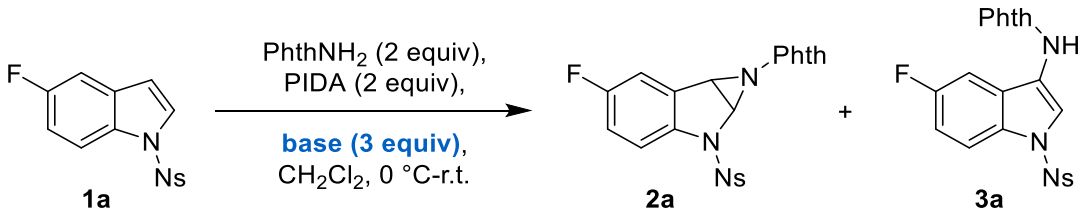


*Figure 29 – Standard reaction conditions used for the aziridination of protected indoles as optimised by Nicole Tsang, using tosyl protected indole **1a** as an example. Yield given as percentage conversion, calculated from relative ^{19}F NMR spectroscopy peak intensities. Percentage conversion defined as consumption of indole starting material.*

After this initial experimentation, the next steps were to investigate each aspect of the reaction, as stated in the aims. The first of these to be investigated was the base used. The presence of acetic acid in the reaction mixture has been shown to negatively impact the yield of the olefin aziridination reaction.[59] This was further confirmed by Nicole Tsang's work, as reaction in the absence of base resulted in no conversion of the indole starting material (**Table 2, entry 1**). Different bases were screened to investigate any impacts this may have on the reaction's outcome (**Table 2**). The organic bases pyridine and triethylamine were initially tested due to their solubility in CH_2Cl_2 (**Table 2, entries 2 and 3**). Unfortunately, use of these bases gave no conversion from indole. This may be due to reaction of the bases with PIDA which consumes oxidant and also reduces the amount of the base available to quench the acetic acid produced. Investigations into inorganic bases found that potassium carbonate, sodium carbonate and potassium phosphate gave the best yields. From these results, potassium carbonate was selected for use in subsequent reactions.

*Table 2 – Base tests using standard aziridination conditions. Aqueous pKaH values are stated. Conditions: N-nosyl-5-fluoro-indole (0.05 mmol), N-aminophthalimide (0.1 mmol), PIDA (0.10 mmol), base (0.15 mmol) and CH_2Cl_2 (0.75 mL). [a]Reaction times reported as the time at which maximal relative ^{19}F NMR spectroscopy yields were observed. [b]Values reported calculated from relative intensities of assigned indole (**1a**), aziridine (**2a**) and side-product (**3a**) peaks by ^{19}F NMR spectroscopy. [c]Result obtained by Nicole Tsang.*



Entry	*Base*	*pK_{aH}*	*Time / h[a]*	*% 2a[b]*	*% 3a[b]*
1[c]	None	-	18	0	19
2	Pyridine	5.2	15	0	0
3	NEt_3	10.8	24	0	0
4	$NaHCO_3$	6.4	14	0	59
5	Na_2HPO_4	7.1	15	15	54
6	Li_2CO_3	10.3	2	53	8
7	**Na_2CO_3**	**10.3**	**6**	**76**	**0**
8	**K_2CO_3**	**10.3**	**6**	**75**	**0**
9	Cs_2CO_3	10.3	65	46	2
10	Na_3PO_4	12.4	2	64	3
11	**K_3PO_4**	**12.4**	**7**	**77**	**0**

2.1.1 Indole Screening

Different protected indoles were investigated in this route from indoles to quinazolines. Having a wide library of aziridinated indoles provides options for different methods of removing the protecting group in the subsequent ring expansion step. 5-Fluoroindole was thus protected with eight different protecting groups: nosyl (**1a**), tosyl (**1b**), acetyl (**1c**), Boc (**1d**), 2,4-dinitrophenyl (**1e**), benzyl (**1f**), trifluoroacetyl (**1g**) and trichloroacetyl (**1h**). All eight protected indoles were subjected to standard aziridination conditions (**Figure 30**).

The protection of 5-fluoroindole with 2,4-dinitrophenylsulfonyl and triflyl groups was also attempted, but no protected indoles were obtained from these reactions. The standard aziridination conditions were also applied to unprotected 5-fluoroindole.

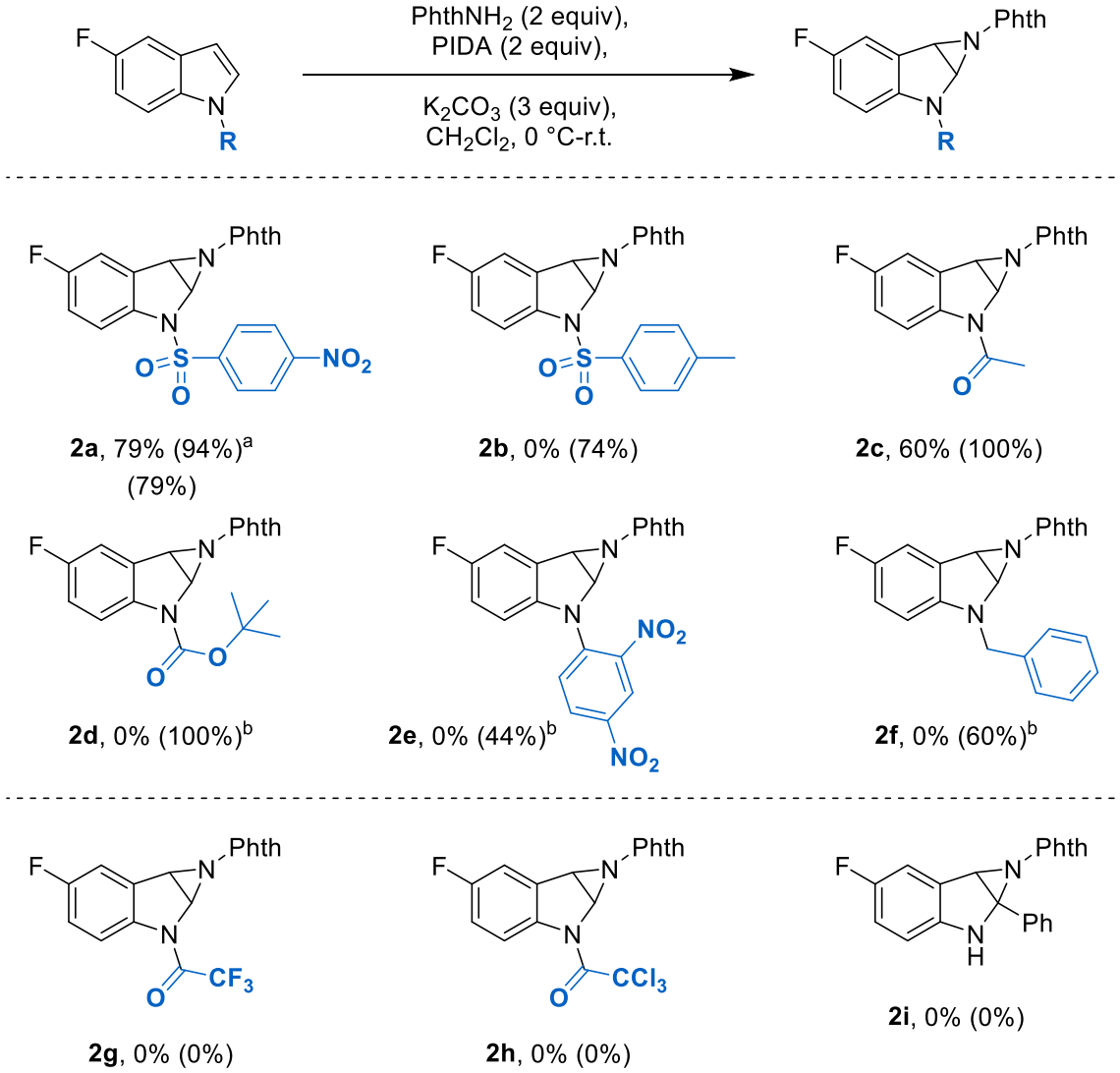


Figure 30 – Aziridination of protected and unprotected indoles under standard aziridination conditions. Yields reported as isolated yield, with percentage conversion in parentheses as determined by relative peak intensity by ^{19}F NMR spectroscopy. Percentage conversion defined as consumption of indole starting material. [a]4 equiv of K_2CO_3 was used. [b]Compound identity inferred from spectroscopic analysis of crude mixture.

Aziridination of *N*-nosyl-5-fluoroindole (**1a**) under these conditions was achieved with 79% conversion, based on relative peak intensities of the aziridine and indole peaks by ^{19}F NMR spectroscopy. When four equivalents of base were used, a higher conversion of 94%

was observed, giving **2a** in a 79% isolated yield. Applying the stated reaction conditions to **1b** gave aziridine **2b** with a slightly lower conversion (74%). Attempts were made to isolate this aziridine, however the compound degraded during the work-up process. Further analysis of this degradation product identified it as the aziridine-opened indole **3b** (**Figure 31**). In the initial paper published by Kumar,[16] treatment of unprotected aziridines with DMSO/NaH afforded both the desired quinazolines and 3-substituted indoles that had undergone a similar ring-opening transformation. Though 3-aminoindoles themselves are sought after for their biological activity,[95–99] this research remained focussed on the indole ring-expansion methodology. In this work, samples were taken at each stage of the work-up of **2b** and analysed by ^{1}H and ^{19}F NMR spectroscopy to determine the stage at which decomposition occurred. It was found that the use of $MgSO_4$ as a drying agent aided in the degradation of this aziridine. A possible explanation for this activity is that the aziridine is sensitive to Lewis acids. Following this investigation, Na_2SO_4 was used as an alternative, less Lewis-acidic drying agent for the work-up of all aziridines.

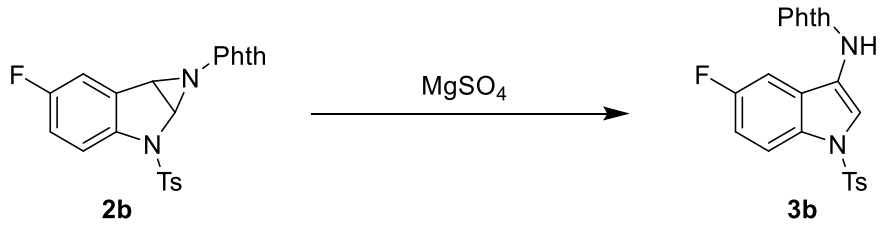


*Figure 31 – Ring-opening degradation of aziridine **2b** upon exposure to $MgSO_4$.*

Indole **1c** successfully reacted to form aziridine **2c** with 100% conversion (by ^{19}F NMR spectroscopy) within four hours and was isolated as a white powder. Indole **1d** seemingly formed aziridine **2d** with 100% conversion, based on the characteristic aziridine doublets commonly observed around δ_H 5.9 and 4.5 ppm. However, isolation of this aziridine resulted in a change in chemical shifts suggesting that decomposition had occurred, but it was unclear in what way. Mass spectrometry of this isolated compound displayed the expected aziridine masses for the $[M+H]^+$ and $[M+Na]^+$ ions but these masses are identical to those of the ring-opened side-product, so the formation of either compound cannot be confirmed. Similarly, characteristic aziridine peaks were observed following the attempted aziridination of indoles **1e** and **1f**. Over time, however, ^{19}F NMR spectroscopy indicated degradation of aziridines to unidentified side-products.

A C2-substituted indole was investigated to probe the effect of sterics on the reaction. When the standard aziridination conditions were applied to 2-phenylindole (**2i**), a new type of degradation product, **4i**, was observed (**Figure 32**). Analysis by mass spectrometry revealed a peak corresponding to the $[M+H]^+$ ion (calcd. for $C_{22}H_{14}N_3O_2^+$: 352.1081; found 352.1079). H^1 NMR spectroscopy data also indicated an absence of protons on both the C2 and C3 positions. This is assumed to be accessible through the ring opening of aziridine, much like in the ring-opening degradation of **2b** to **3b**. The driving force for this extra oxidation may be the conjugated system formed.

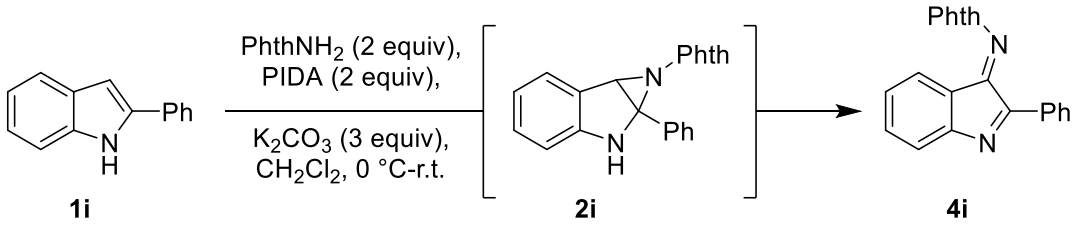


*Figure 32 – The ring-opening degradation of assumed aziridine **2i** when exposed to the standard aziridination conditions.*

Aziridination is possible for a variety of protecting groups, which provides several options for the subsequent ring-expanding step. Isolated yields vary from poor to good, but this may be circumvented by undertaking the subsequent ring expansion without prior isolation of the aziridine, as will be explored in a subsequent section. Next, nitrogen sources were investigated to assess the scope of the aziridination and the stability of the resulting aziridines. Additionally, this would further add to the library of aziridinated indoles being built up for subsequent ring expansion studies. The nosyl-protected indole was used for these studies due to the much higher stability of the resulting aziridine compared to other protected indoles.

2.1.2 Alternative Nitrogen Sources

Following the successful aziridination using *N*-aminophthalimide reported in the previous sub-section, other possible nitrogen sources for this aziridination were screened for addition to indole **1a**. These *N*-, *O*- and *S*-amino compounds were used in the same manner as previous aziridination reactions (**Figure 33**). These compounds were chosen due to the precedent in literature for aziridination using identical or similar reagents. *N*,*N*-

Disubstituted hydrazines are most commonly seen in literature,[43] but there is also mention of hydroxylamines[100] and sulfenamides[101] in the aziridination of some olefins. Unfortunately, other than the indole starting material, no new indole-derived peaks were observed by ^{1}H or ^{19}F NMR spectroscopy for any of the nine nitrogen sources. Instead, consumption of PIDA as indicated by ^{1}H NMR spectroscopy was observed.

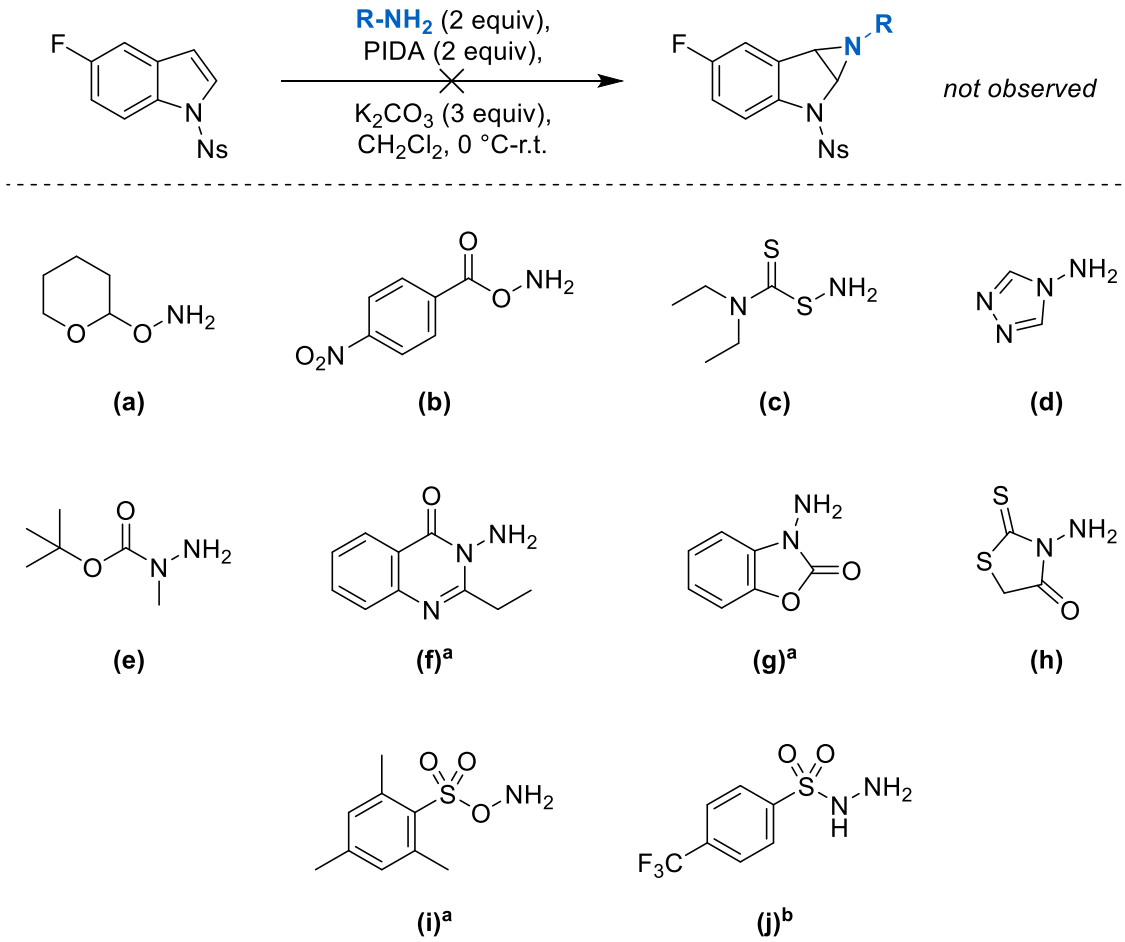


*Figure 33 – Alternative nitrogen sources used for aziridination of N-nosyl-5-fluoroindole **1a**, using the standard conditions: nosyl indole (0.05 mmol), nitrogen source "X-NH_2" (0.10 mmol), PIDA (0.10 mmol) and K_2CO_3 (0.15 mmol) in CH_2Cl_2 (0.75 mL). [a]Provided by Charlie Swan. [b]Provided by Aaron Senior.*

Particular nitrogen sources of note include 3-amino-2-ethylquinazolin-4(3*H*)-one (**Figure 33, f**) and 3-aminobenzoxazolin-2-one (**Figure 33, g**) as they feature in olefin aziridination literature.[43,47] When 3-amino-2-ethylquinazolin-4(3*H*)-one, **f**, was used, the results were unclear as the ^{1}H NMR spectra were complex. Use of 3-aminobenzoxazolin-2-one **g** under

these conditions resulted in no conversion from indole, while observing the conversion of PIDA to iodobenzene by ^{1}H NMR spectroscopy.

Unfortunately, no aziridines were synthesised by using the nitrogen sources stated in **Figure 33,** other than *N*-aminophthalimide. Hence, no further additions to the aziridine library for ring expansion were made. Nevertheless, the ring expansion of the accessible aziridines is the logical next step.

2.1.3 Synthesis of 6-Fluoroquinazoline

The only analytical data previously reported for the desired product of indole ring-expansion, 6-fluoroquinazoline, was a melting point.[102] In order to facilitate optimisation of the ring expansion step it was considered prudent to have access to an authentic sample of the quinazoline as an analytical standard. Hence, an alternative synthesis was explored (**Figure 34**). The 3-step method involved first heating 5-fluoroanthranilic acid (**5**) at reflux in formamide to give quinazolinone **6**.[103] Next, **6** was heated at reflux with thionyl chloride[104] which gave chloroquinoline **7**. The third and final step was achieved by using a combination of $PdCl_2$(dppf), $NaBH_4$ and TMEDA in THF.[105] Isolation proved challenging, and much material was lost in the purification process but a sufficient amount of pure 6-fluoroquinazoline (**8**) was obtained for analysis.

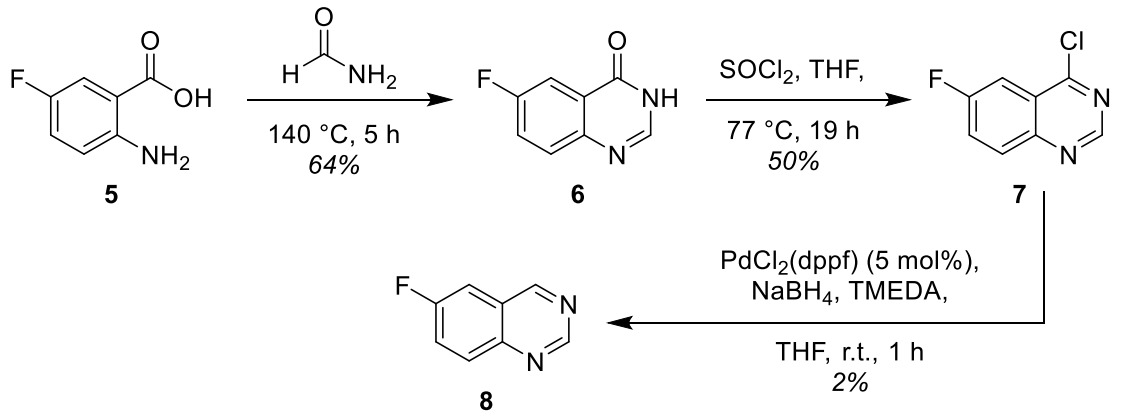


*Figure 34 – Conditions used in the alternative synthesis of 6-fluoroquinazoline (**8**). Yields are given as isolated yield.*

2.1.4 Ring Expansion

In the preliminary work on this project, carried out by Nicole Tsang, some ring expansion conditions were attempted on nosyl- and tosyl-protected indole aziridines (**Figure 35**). She aimed to remove the tosyl group using the two conditions reported in the original paper by Kumar;[16] KOH/MeOH and NaH/DMSO. To remove the nosyl group, she subjected **2a** to thiophenol and base. Use of these conditions unfortunately resulted in degradation as deduced from complex ^{1}H and ^{19}F NMR spectra.

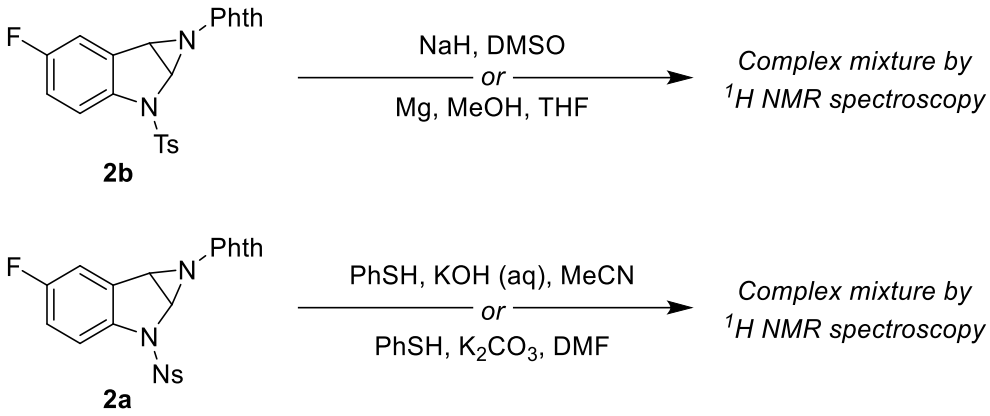
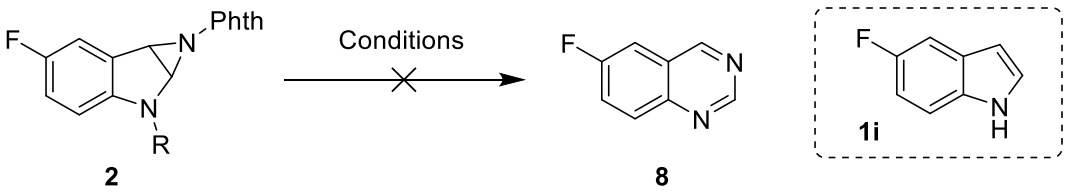


Figure 35 – Ring expansion methods tried by Nicole Tsang.

These conditions, along with some others, were applied to **2a** as shown in **Table 3** (**entries 1-5**). In these repetitions, 4-fluorothiophenol was used due to safety. Thiophenol is fatal by inhalation, in contact with skin and if inhaled whereas 4-fluorothiophenol is reportedly an irritant.[82] Use of a fluorinated reagent also gives the ability to track progress *via* ^{19}F NMR spectroscopy. When **2a** was subjected to 4-fluorothiophenol, both with and without base, multiple new species were observed by ^{19}F NMR spectroscopy. The major peak observed was that of 4-fluorothiophenol but, unfortunately, none of these new species aligned with confirmed data for **8** (**Table 3, entries 1-2**). Magnesium and activated zinc metal were then used as reducing agents to remove the nosyl group (**Table 3, entries 3-4 respectively**), however both resulted in degradation. Interestingly, magnesium specifically removed the aziridine giving the original protected indole **1a**. Finally, Kumar had shown that methanolic potassium hydroxide could be used as a method of removing a phenylsulfonyl protecting group from an aziridinated indole.[16] When these conditions were applied to **2a** (**Table 3, entry 5**), a mix of products was observed by ^{19}F NMR

spectroscopy. One significant peak observed was that of unprotected 5-fluoroindole (**1i**), as also observed by Kumar;[16] but unfortunately no ring-expansion was observed.

*Table 3 - Conditions used for the deprotection of indole aziridines. Percentage conversion and yield of **8** were determined by ^{1}H and ^{19}F NMR spectroscopy. Percentage conversion defined as consumption of aziridine starting material, measured by relative peak intensities. [a]Conditions applied to crude aziridine solution.*



2 **8**

Entry	*R*	*Conditions*	*%conv.*	*%yield*
1	Ns (**2a**)	4-FC_6H_4SH, K_2CO_3, THF, r.t., inert	99	0
2	Ns (**2a**)	4-FC_6H_4SH, THF, 0 °C - r.t., inert	96	0
3	Ns (**2a**)	Mg, MeOH, r.t., inert	100	0
4	Ns (**2a**)	Zn (activated), THF/sat. aq NH_4Cl (1:1), r.t.	100	0
5	Ns (**2a**)	10% KOH/MeOH, 0 °C - r.t.	100	0
6	Ac (**2c**)	*t*-BuOK, EtOAc, r.t., inert	0	0
7	Ac (**2c**)	KOH, THF/H_2O (1:1), 50 °C	97	0
8	Ac (**2c**)	BF_3•Et_2O, PhOH, Et_2O, r.t., inert	100	0
9	Ac (**2c**)	BF_3•Et_2O, 4-FC_6H_4SH, Et_2O, r.t., inert	100	0
10	Ac (**2c**)	$Bi(OTf)_3$, PhOH, THF, r.t., inert	100	0
11	Ac (**2c**)	MeMgBr (3 M in Et_2O), THF, r.t., inert	96	0
12	Ac (**2c**)	*i*-PrMgBr (3 M in 2-MeTHF), THF, r.t., inert	100	0
13	Ac (**2c**)	4-FC_6H_4MgBr (2M in Et_2O), THF, r.t., inert	98	0
14[a]	Boc (**2d**)	180 °C	100	0
15[a]	Boc (**2d**)	TFA, CH_2Cl_2, 0 °C – r.t.	97	0
16[a]	Boc (**2d**)	TBAF, CH_2Cl_2, reflux	100	0
17[a]	Boc (**2d**)	Montmorillonite K10, 45 °C, CH_2Cl_2, inert	100	0
18[a]	Boc (**2d**)	$Sn(OTf)_2$, CH_2Cl_2, 45 °C, inert	100	0

One aziridine of interest in this work was **2c** due to its relatively stable nature compared to other aziridines. For this deprotection, a variety of nucleophiles were used both with and without catalysis from Lewis acids (**Table 3, entries 6-13**). It was observed that use of

Lewis acids often catalysed the incorrect ring-opening route (c.f. formation of **3b**, **Figure 31**), presumably by coordinating to the aziridine nitrogen. Some Grignard reagents were tried due to the preferable reaction with carbonyls (**Table 3, entries 11-13**).[106] These reactions gave complex ^{1}H and ^{19}F NMR spectra, indicating degradation.

Focus was then shifted onto Boc-protected indoles. As mentioned previously, however, the isolation of this aziridine resulted in degradation such that the ring expansion had to be telescoped without prior isolation. A wide variety of Boc-deprotection conditions have been previously reported and hence there were many options available. The conditions applied are shown in **Table 3** (**entries 14-18**). Firstly, heating of the reaction mixture to 180 °C resulted in complex ^{1}H and ^{19}F NMR spectra (**Table 3, entry 14**). This could be due to the fact that the aziridine ring is unstable at this temperature and can open in a variety of undesired ways. This may also be the reason why treatment with trifluoroacetic acid (TFA) resulted in complex ^{1}H and ^{19}F NMR spectra (**Table 3, entry 15**). Highly acidic conditions are known to increase reactivity of aziridines as protonation of the aziridine nitrogen improves is electrophilicity and increases its susceptibility to attack.[107] TBAF, montmorillonite K10 and $Sn(OTf)_2$ were also added to the crude aziridine mixture (**Table 3, entries 16-18**). In all of these experiments an intractable mix of unidentified products was formed, with no observable amount of **8**.

Following these experiments, it became clear that this route may not be suitable for its intended purpose. In order to be used for late-stage modification, the proposed ring-expansion needs to be facile and with broad functional group compatibility. If conditions for this transformation were found, they are likely to be incredibly specific with a narrow substrate scope. Hence, alternative routes from indoles to quinazolines *via* nitrogen insertion were investigated.

2.2 Beckmann Rearrangement Pathway

Continuing our investigation, we aimed to explore other methods to transform indole structures into quinazolines. Overall, this involves the insertion of a nitrogen atom into the core indole structure. One alternative method of nitrogen insertion into a chain is through the more well-known Beckmann rearrangement. Following its discovery in 1886,[108] much research has been carried out into the understanding and application of this

transformation. The rearrangement itself consists of forming an oxime from a ketone, then activation, migration and attack of water to give an amide (**Figure 36**). This type of migration is incredibly synthetically useful and has hence been used in industry for processes such as the synthesis of ε-caprolactam from cyclohexanone.[109]

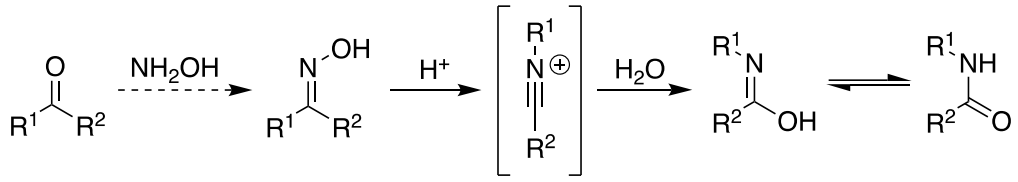


Figure 36 - A typical acid-catalysed Beckmann rearrangement, often starting from the respective ketones which can be converted to oximes by exposure to hydroxylamine.

2.2.1 Mechanism

Oximes are usually formed through the condensation reactions of hydroxylamines with ketones (**Figure 37**).[110] In the Beckmann rearrangement, the oxime will then be activated, for example by protonation at the oxime oxygen. Next is the irreversible migration of the R group *anti* to the protonated OH group, eliminating water.[111] The cationic intermediate can then be attacked by a nucleophile. If attacked by water, this gives an amide.

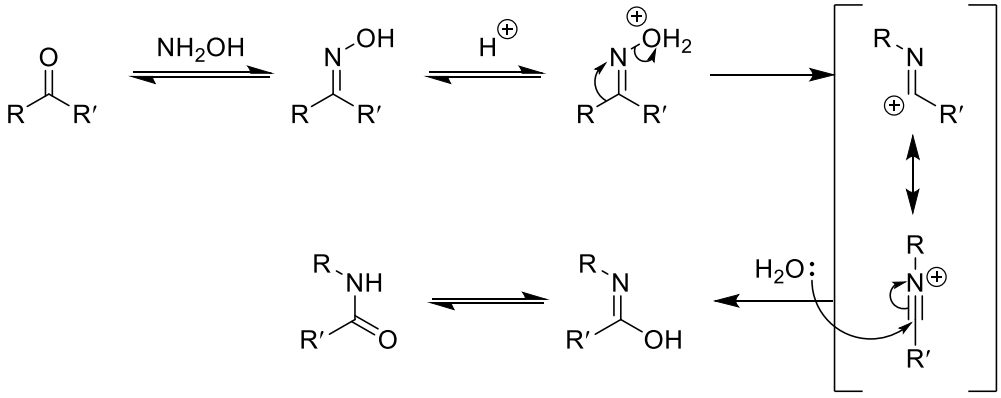


Figure 37 - Generally accepted mechanism for the Beckmann rearrangement, with attack of water to quench the carbocation giving an amide.

As indicated in **Figure 37**, the migrating group must be *trans* to the leaving group for the migration to occur. Therefore, the outcome of the migration is dictated by which *E/Z*

isomers of the oxime are present. However, in acidic media, *E/Z* isomerization of oximes may be possible, which allows for interconversion of the two isomers (**Figure 38**).[112] Protonation at nitrogen weakens the N-C π-bond, decreasing the energy required for isomerization.[113] Computational studies[114] on this type of interconversion state that this can occur through three pathways: pure inversion, pure rotation, or a mixture of the two. On a neutral oxime, the average activation energy calculated in this paper is 41 kcalmol^{-1} but, as mentioned previously, this is reduced by protonation.[114]

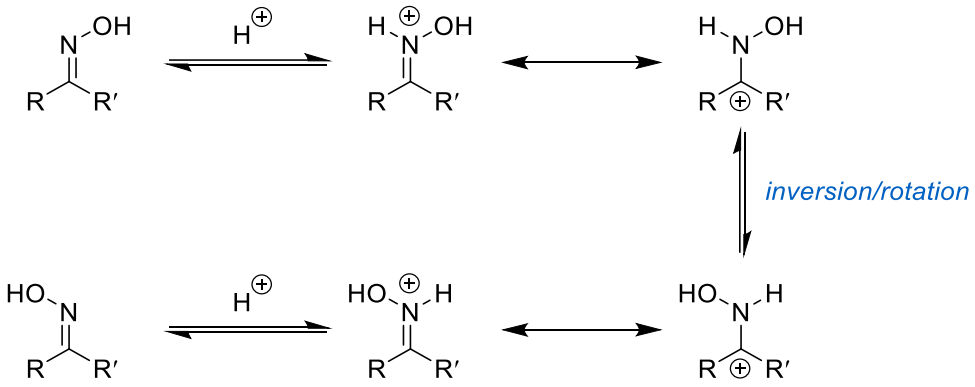


Figure 38 - Acid-catalysed E/Z isomerization of oximes.

This isomerization can result in R group migration being instead determined in part by relative rates and hence the migratory aptitude of each group.[115] This follows the standard migratory aptitudes for other rearrangements, such as the pinacol rearrangement.[116] For example, a mixture of pure *Z*-isomer of the oxime-*O*-tosylate of pentan-2-one in the presence of tosic acid gives only the product derived from the *E*-isomer due to preferrable migration of the propyl group over the methyl group (**Figure 39**).[111]

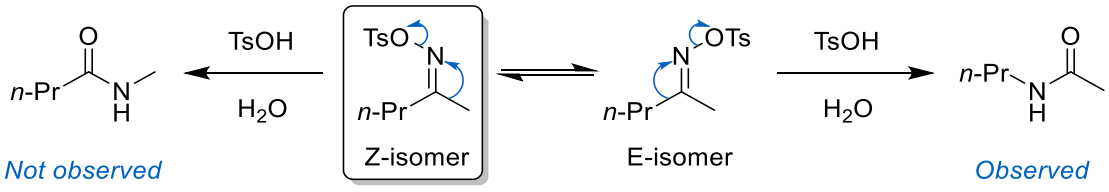


Figure 39 – Preferential group migration of an n-propyl group over a methyl group.

Reactions involving the oximes derived from acetone, acetophenone and cyclohexanone were analysed by use of B3LYP calculations to investigate whether these reactions proceeded through a purely concerted mechanism.[117] Of these compounds, it was found that only cyclohexanone proceeded in a pure concerted mechanism in the solvents

modelled ($H_3O^+(H_2O)_6$ and $H^+(AcOH)_3$). Interestingly, the phenyl group of acetophenone was found to migrate through a bridged phenonium-like π complex (**Figure 40a**). The authors found that both acetone and acetophenone gave the nitrilium ion as an intermediate (**Figure 40b**).[117] This nitrilium ion can be trapped by a variety of nucleophiles to give alternative outcomes for the Beckmann rearrangement.[118–120]

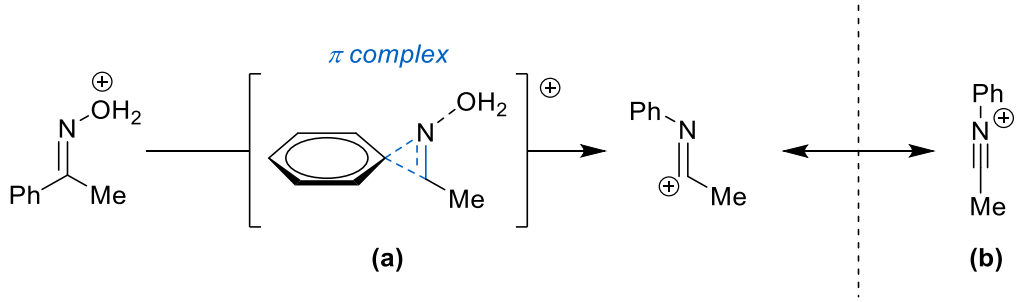


Figure 40 – Phenonium intermediate formed during phenyl group migration (a) and nitrilium intermediate formed after phenyl group migration (b).[117]

Over the last century, many different reagents have been used to catalyse the Beckmann rearrangement.[121] In general, metal-containing Lewis acids are the most used catalysts. These work by coordinating to the oxime oxygen, improving its leaving group ability. Aluminium-based Lewis acids are efficient at catalysing the reaction.[122] However, some such as $AlCl_3$ are affected by the water produced in the rearrangements.[123] Other metal catalysts investigated were $InBr_3$/AgOTf,[124] $HgCl_2$,[125], $Ga(OTf)_3$,[115] and Sc(OTf).[123] The Beckmann rearrangement of arylketones has also been achieved by electrochemistry via an alternative radical mechanism.[126]

2.2.2 Beckmann Rearrangement of Isatin

Isatin is the 2,3-diketo derivative of indole, hence containing both a ketone and amide moiety. Reaction of isatin with hydroxylamine under standard conditions yields the isatin-3-oxime, as expected due to the higher reactivity of ketones compared to that of amides (**Figure 41a**). Formation of isatin-2-oxime is more difficult but has been reported as accessible[127] through methods displayed in **Figure 41b**. It is also possible to form oximes at both carbonyls by reaction of isatin-2-imine with hydroxylamine (**Figure 41c**).[128]

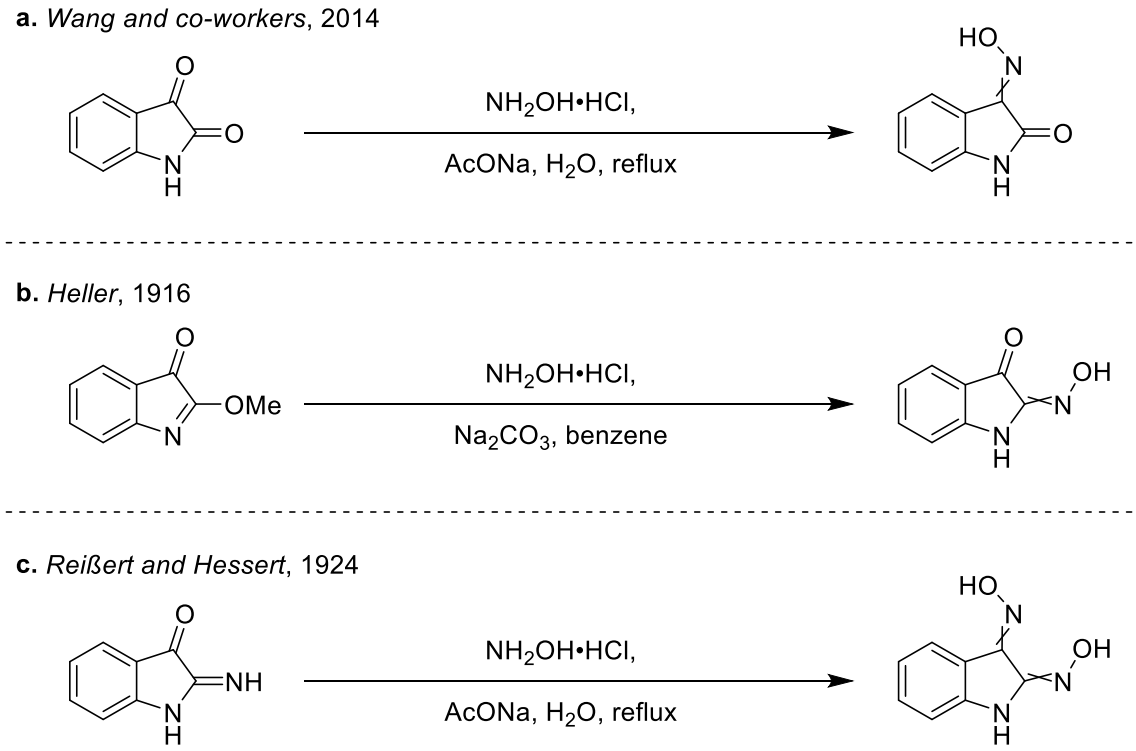


Figure 41 - Synthesis of (a) isatin-3-oxime,[129] (b) isatin-2-oxime[127] and (c) isatin-2,3-dioxime.[128]

Once the oximes of isatin have been synthesised, the next step is the Beckmann rearrangement. In 2020, the one-pot Beckmann rearrangement of isatin was reported through the isatin-3-oxime.[130] The authors used thiamine (vitamin B_1) to catalyse the Beckmann rearrangement of a range of substrates and obtained moderate yields. As expected, this proceeded through migration of the adjacent aryl group to give quinoxaline-2,3-diol (**Figure 42a**). This migration goes through the *Z*-oxime which is preferrable due to hydrogen bonding between the oxime OH and the neighbouring carbonyl oxygen.

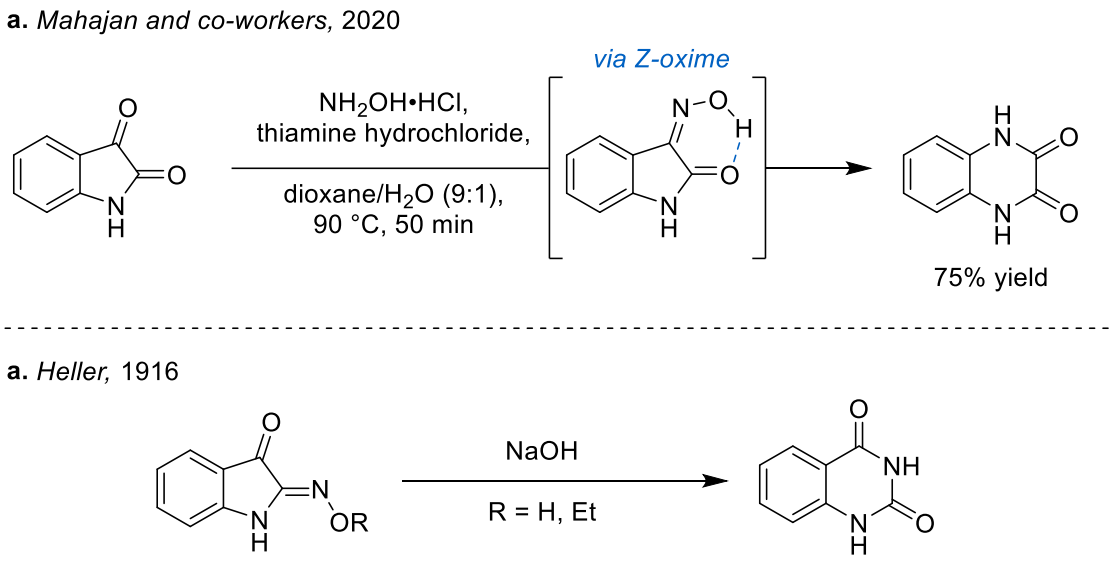


Figure 42 - Beckmann rearrangements on (a) isatin-3-oxime[130] and (b) isatin-2-oxime.[127]

In the interest of forming quinazoline-based ring systems from indole-based ring systems, the opposite migration to the route reported by Mahajan and co-workers must occur. This can be achieved through synthesis of isatin-2-oximes and treatment with aqueous base (**Figure 42b**).[127] This gives 2,4-quinazolinedione which could then be converted to the quinazoline. Both transformations displayed in **Figure 42** would achieve the desired introduction of heteroatoms into the ring, however quinazoline formation remains the focus of the following investigation.

2.2.3 Beckmann Rearrangement – Results and Discussion

Akin to the aziridination pathway, a nitrogen atom can be formally inserted into a nitrogen-containing heterocycle via a different ring-expansion – the Beckmann rearrangement.[108] The initial oxime formation step was carried out on isatin (**9**) using standard conditions, namely hydroxylamine hydrochloride then base (**Figure 43**). This process occurred with 100% conversion of isatin, and afforded oxime **10** with an isolated yield of 35% after recrystallisation. Often, better leaving groups than H_2O are required to encourage the Beckmann rearrangement. As such, the *O*-tosylate **11** was synthesised by reaction of the oxime with tosyl chloride in the presence of NaOH.[131] This gave the isatin-3-oxime *O*-tosylate (**11**) with 100% conversion and a 12% isolated yield.

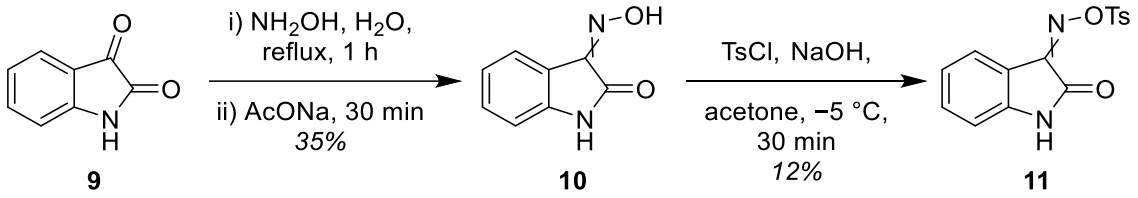


*Figure 43 - Conditions for oxime (**10**) and oxime tosylate (**11**) formation from isatin (**9**).*

Once oxime **10** was obtained, the next step is the Lewis acid-catalysed ring expansion. The outcome of this reaction would depend upon the oxime diastereomer formed in the previous step, as this directs which group will migrate (**Figure 44**). The *Z*-isomer undergoes ring expansion by migration of the C-aryl bond and, with quenching of the carbocation by water, gives quinoxaline-2,3-diol (**12**, **Figure 44a**). The *E*-isomer however expands by migration of the C-carbonyl bond, giving quinazoline-2,4-diol (**13, Figure 44b**). As previously mentioned, a reported Beckmann rearrangement of isatin-3-oxime gave solely **12**.[130] The ^{1}H NMR spectrum of **10** suggested the presence of only one diastereomer. However, upon transformation into **11**, there is a clear presence of two isomers in a 1:1 ratio. This may be the result of a conformational preference of the *Z*-isomer of **10** due to hydrogen bonding with the adjacent carbonyl oxygen, displayed by the red dashed line in **Figure 44a**. For *O*-tosylate **11**, however, hydrogen bonding is no longer possible and no clear preference of isomer is displayed.

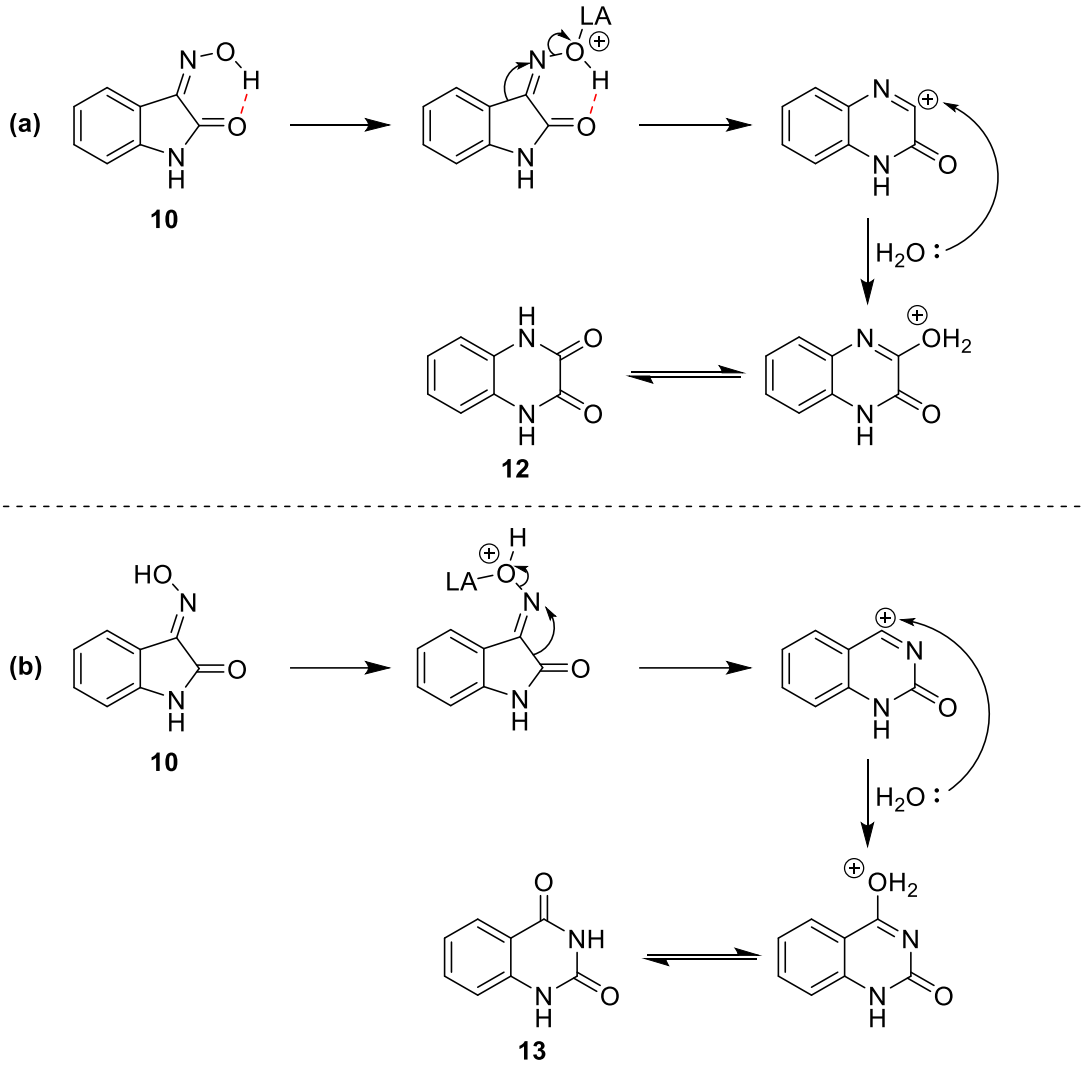
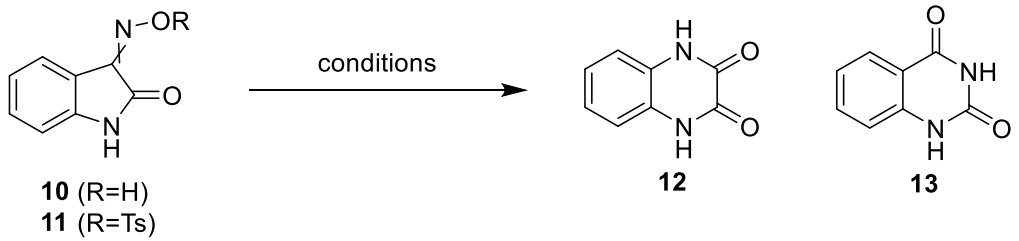


*Figure 44 - The Beckmann rearrangement mechanism for each isomer of oxime, resulting in either quinoxaline-2,3-diol (**12**) or quinazoline-2,4,-diol (**13**).*

There is literature precedent for unsubstituted (OH) oximes undergoing Beckmann rearrangements under acidic conditions,[111] so this was the first set of conditions tried (**Table 4, entry 1**). Oxime **10** was stirred in a solution of sulfuric acid for 24 h with no change to the starting material. These reaction conditions were repeated on tosylate **11** to the same end (**Table 4, entry 2**). Two further conditions were tried where TFA and $Bi(OTf)_3$ were used as activators in CH_2Cl_2 with 1 drop of water for carbocation capture (**Table 4, entries 3 and 4**). These also gave zero conversion from **11** after heating to 60 °C for 46 hours.

*Table 4 - Beckmann rearrangement conditions tried on isatin-3-oximes. Percentage conversion of **10/11** and percentage yield of **12/13** characterised by ^{1}H NMR spectroscopy. Percentage conversion defined as consumption of oxime starting material (**10/11**), measured by relative peak intensities. All reactions unless otherwise stated were carried out on a 0.025 mmol scale in 0.75 mL of respective solvents. [a]Performed on a 0.15 mmol scale in 2.5 mL H_2O.*



10 (R=H)
11 (R=Ts)

12 **13**

Entry	***R***	***Conditions***	***%conv.***	***%yield of 12/13***
1[a]	H (**10**)	H_2SO_4, water, 90 °C, 72 h	0	0
2	Ts (**11**)	H_2SO_4, water, 90 °C, 92 h	0	0
3	Ts (**11**)	TFA, CH_2Cl_2, 1 drop water, 60 °C, 46 h	0	0
4	Ts (**11**)	$Bi(OTf)_3$, CH_2Cl_2, 1 drop water, 60 °C, 46 h	0	0

If a better leaving group is required, this involves a 2-step process to make the species needed for the Beckmann rearrangement (c.f. **Figure 43**). Instead, it may be possible to make such a species in one step by using a substituted hydroxylamine. Initial investigation into this used *O*-mesityl sulfonyl hydroxylamine, which was provided by Charlie Swan. This hydroxylamine was added to isatin **9** in acetonitrile at room temperature and the reaction was monitored by ^{1}H NMR spectroscopy (**Figure 45**). Two new species were observed, one of which could be attributed to the oxime **14** and one that was identified as 2-aminobenzonitrile (**15**). This type of reaction is known as a Beckmann fragmentation and is a common side-reaction which can be assisted by neighbouring heteroatoms.[132,133] The mechanism for this fragmentation is displayed in **Figure 45**.[111] The oxime is formed which can then undergo a fragmentation, leaving a reactive isocyanate group which can be attacked by any nucleophiles present, such as water. This side-reaction could theoretically be avoided by protecting the isatin nitrogen, reducing the availability of the nitrogen lone pair.

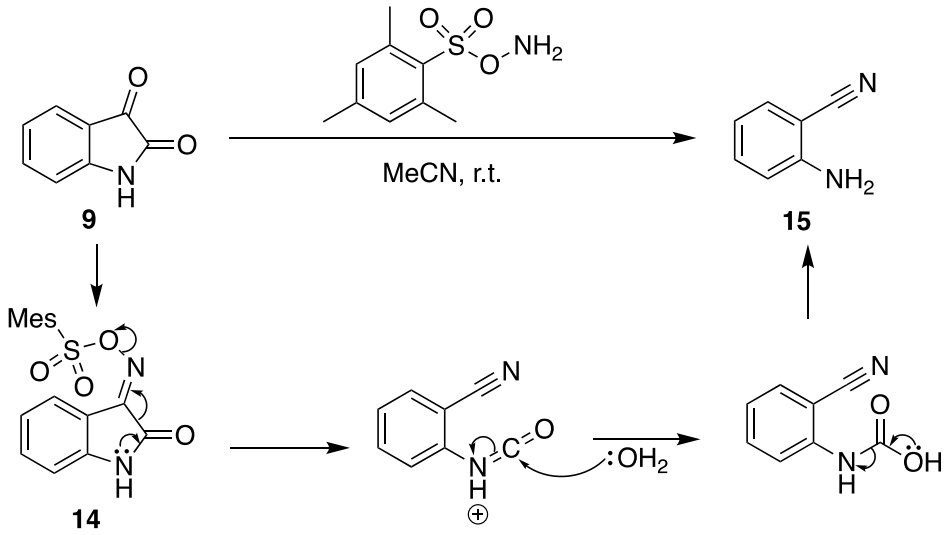


*Figure 45 - The Beckmann fragmentation observed when reacting isatin (**9**) with mesityl sulfonyl hydroxylamine in acetonitrile at room temperature, accompanied by a plausible mechanism.[111]*

Initial investigation into the use of the Beckmann rearrangement in the ring expansion of indole-like structures gave no observable yield of ring-expanded product. In parallel to this research, another alternative pathway from indoles to quinazolines was explored. This will be discussed in the following section.

2.3 Photocatalytic Pathway

Instead of a ring expansion reaction, quinazolines may be synthesised from indoles by ring cleavage then ring re-forming. A biomimetic[134] oxidative cleavage of the indole C2-C3 bond was first reported by Witkop using Pt/O_2.[135] This transformation, since termed the Witkop oxidation, has traditionally been achieved under a number of conditions (**Figure 46a**).[136] This was then further developed by Winterfeldt who introduced a one-pot Witkop oxidation and Camps cyclisation to give quinolones.[137] The combination of these two steps is known as the Witkop-Winterfeldt oxidation (**Figure 46b**).

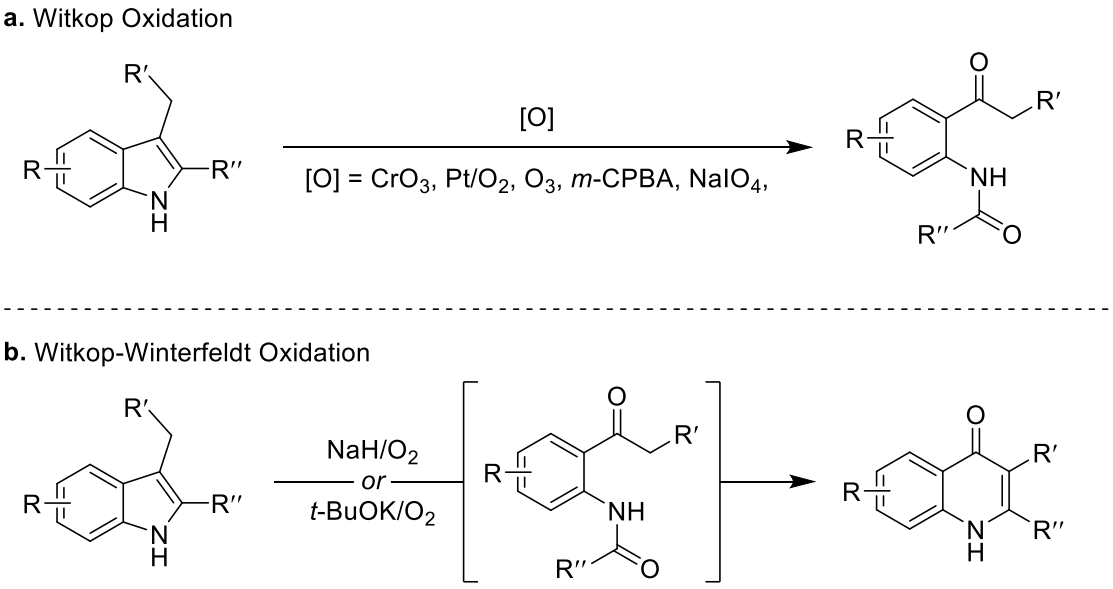


Figure 46 – Common conditions for the Witkop oxidation of indoles to 2-ketoacetanilide derivatives (a)[136] and the Witkop-Winterfeldt oxidation towards the formation of quinolones (b).[137]

With the purpose of moving away from strong oxidants, photochemical pathways have also been developed. One such method involves exposure of *N*-Boc-indole and catalytic amounts of methylene blue in air to blue LED light (**Figure 47**).[94] The products of these reactions could be cyclised with addition of nitrogen through introduction of ammonia. The green aspects of this photocatalyzed route, including the benign photosensitizer, make this an appealing alternative route to quinazolines.

Wu and co-workers, 2018

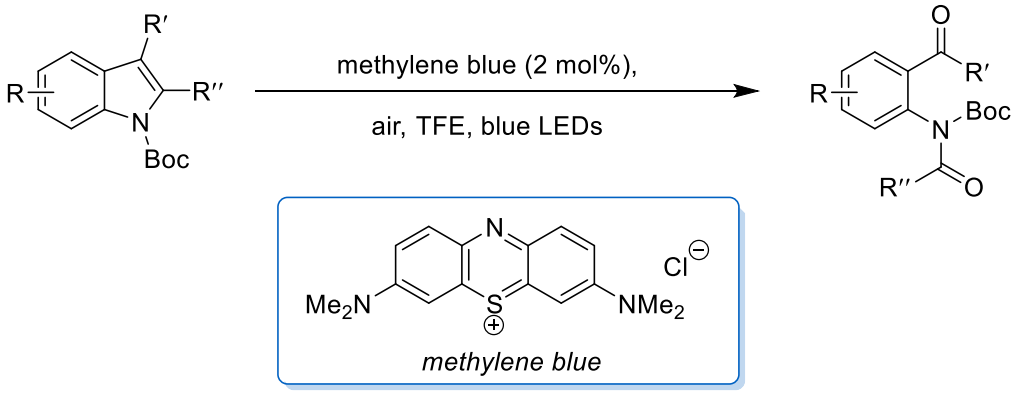
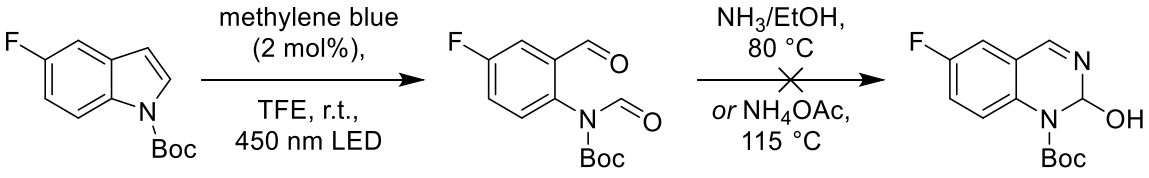


Figure 47 – The photocatalysed Witkop oxidation of Boc-protected indoles reported by Wu and co-workers.[94]

We have successfully replicated the photocatalysed Witkop oxidation on a 0.1 and 0.3 mmol scale with a maximum of 71% conversion (**Figure 48**). Unfortunately, due the instability of this dicarbonyl product (**16**) on silica gel, and the fact that this product presents as an oil, separation of **1d** and **16** proved difficult. Due to this separation issue, the crude mixture was telescoped through to the next stage of this route. This involved introduction of nitrogen by imine formation then subsequent ring-closure. Two potential reagents for this transformation were ammonia in methanol and ammonium acetate. These reagents were both used neat and were stirred at 80 °C and 115 °C respectively. Unfortunately, both reactions yielded complex ^{19}F and ^{1}H NMR spectra.



1d **16** **17**

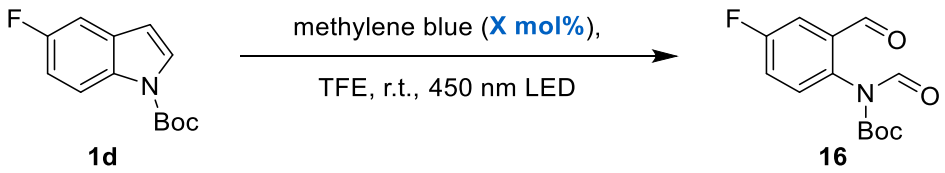
1d:16 = 1:2.5

71% conversion

*Figure 48 - Photocatalytic Witkop oxidation of N-Boc-5-fluoroindole giving a 1:2.5 mixture of indole **1d** and ring-opened product **16** as observed by ^{19}F NMR spectroscopy. Ring closing was attempted using ammonia in methanol and ammonium acetate but expected product **17** was not observed by ^{1}H or ^{19}F NMR spectroscopy.*

In an attempt to increase conversion of **1d** from 71%, the reaction conditions were varied as shown in **Table 5**. The previous method stated in **Figure 48** allowed air exchange through needles in the septum of a sealed microwave tube (**Table 5, entry 1**). Interestingly, increasing the air exchange by removing the septum resulted in a lower conversion (**Table 5, entry 2**). **Table 5, entry 3** displays another interesting observation, whereby increasing the catalyst concentration decreases the conversion. A potential reason for this is that methylene blue is very strongly blue in colour and hence reflects blue light. It could be that, in the more concentrated sample, light cannot penetrate far into the solution and hence reaction can only occur at the very surface of the vessel.[138]

*Table 5 - The effect of changing air flow and catalyst concentration on percentage conversion. Percentage conversion defined as consumption of indole starting material **1d**, measured by relative peak intensities. [a]Percentage conversion calculated from relative ^{19}F NMR spectroscopy integrals of **1d** and **16**.*



Entry	*Air flow*	*methylene blue / mol%*	*%conv[a]*
1	Needles in septum	2	71
2	Open	2	50
3	Needles in septum	20	23

Following these initial investigations, a deeper look into the literature surrounding this route revealed a publication from 1974 describing the exact route intended for this research.[139] Maeda and co-workers irradiated a mixture of indole, methylene blue and ammonium formate with visible light and achieved a one-pot synthesis of quinazoline in good yields (**Figure 49**). In light of this, further investigation into this route was not made.

Maeda and co-workers, 1974

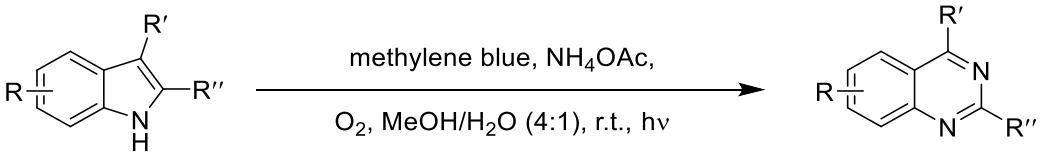


Figure 49 - The route from substituted indoles to quinazolines through the Witkop oxidation as reported by Maeda and co-workers.[139]

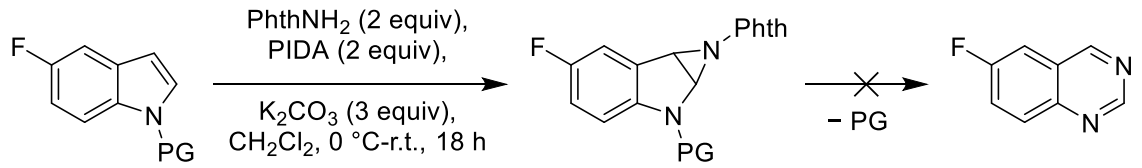
3 Conclusions and Future Work

Molecular editing as a branch of organic synthesis has been more thoroughly defined in recent years.[6,140] The molecular editing, or more precisely skeletal editing, of heterocyclic core structures by the insertion of a heteroatom can result in large changes in chemical properties. Given the prevalence of heterocycles in biologically active substances, editing their core skeletal structure can allow for expansion of existing drug and agrochemical libraries. In the first two chapters of this thesis, the ring expansion of indole-based structures by one nitrogen atom to give quinazoline-based structures was investigated. To this end, three 2-step routes were proposed (**Figure 50**).

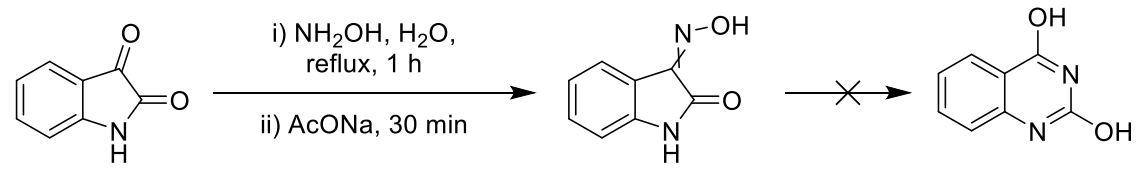
Firstly, a route from indole to quinazoline through aziridination across the 2 and 3 positions of indole was explored (**Figure 50a**), inspired by a route previously reported by Kumar.[16] In this thesis, a variety of aziridination conditions were screened using $PhI(OAc)_2$ as an oxidant which is safer and more sustainable than the $Pb(OAc)_4$ used in previous olefin aziridination literature. Six protected 5-fluoroindole substrates were synthesised (tosyl, nosyl, acetyl, Boc, 2,4-dinitrophenyl and benzyl) and used in aziridination reactions under the conditions stated in **Figure 50a**. However, isolation was a consistent problem due to degradation by ring opening. Nitrogen sources were screened but only *N*-aminophthalimide successfully gave the corresponding aziridine.

A variety of conditions for protecting group removal, and hence ring-expansion, were attempted on nosyl-, acetyl- and Boc-protected indoles. Unfortunately, these attempts resulted in complex mixtures and, after obtaining the relevant analytical data through an alternative synthesis, the presence of the desired 6-fluoroquinazoline was not observed. Following this research, a similar method was published by Morandi which reported the successful ring-expansion of indoles to quinazoline.[19] One key aspect of this route was the use of a silyl protecting group, as other protecting groups result in vastly decreased yields.

a. *Aziridination pathway*



b. *Beckmann rearrangement pathway*



c. *Photocatalytic pathway*

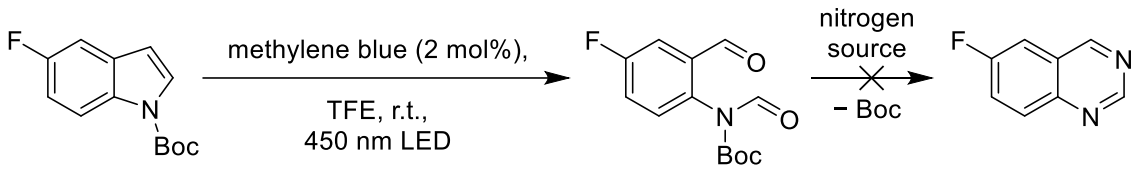


Figure 50 – The three 2-step routes from indole-like structures to quinazoline-like structures explored in the first half of this thesis.

As a result of the issues associated with the aziridination route, alternative routes from indole structures to quinazoline structures were investigated. The second of the 2-step routes discussed was the Beckmann rearrangement (**Figure 50b**). Isatin derivatives may be converted to oximes on treatment with hydroxylamine, then a Lewis-acid-promoted migration can occur to give quinazoline-2,4-diol. The oxime and oxime-*O*-tosylate of isatin were isolated and some preliminary experiments were carried out to promote ring-expansion. The conditions tried did not give the desired outcome.

Finally, a photo-catalysed ring-opening of *N*-Boc-5-fluoroindole was explored as a route to quinazoline (**Figure 50c**). Though the indole ring was successfully opened, separation of the ring-opened structure and the indole starting material proved challenging. Telescoping the crude mixture through to the ring-closing step by addition of ammonia sources resulted in degradation of the ring-opened product. Additionally, further investigation into this route revealed the existence of a closely related methodology.[139]

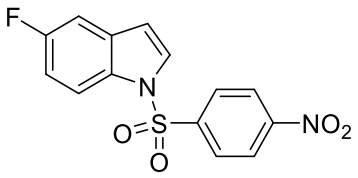
Following investigation into these three routes, it was determined that this transformation was no longer sufficiently novel to warrant further studies. Hence, the focus of the remainder of this thesis will shift to the C–S cross-coupling of aryl iodides with thiourea in micelle solutions.

4 Experimental

General

Reagents were purchased from commercial suppliers and used as supplied. Anhydrous solvents were obtained from in-house solvent purification systems (Inert® Prosolv; dried by passage through activated alumina columns under pressure of Ar). Reactions requiring inert conditions were conducted in flame-dried glassware under an atmosphere of nitrogen using standard Schlenk techniques. NMR spectra were recorded at 298 K on Bruker Advance-III spectrometers operating at nominal ^{1}H frequencies of 400 MHz. Chemical shifts (δ) are given in ppm and referenced to residual solvent peaks for ^{1}H ($CDCl_3$: δ_H= 7.26) and $^{13}C\{^{1}H\}$ ($CDCl_3$: δ_C = 77. 16). Signals are reported at singlet (s), doublet (d), triplet (t), quartet (q), apparent (app), multiplet (m), broad (br) or combinations of the above. High resolution mass spectroscopy (HRMS was performed using a Bruker MicroTOF spectrometer, with an electrospray ionisation (ESI) ion source. Infrared (IR) spectra were recorded on a Bruker Alpha platinum-ATR with diamond window. Melting points were measured on a Gallenkamp apparatus. Photochemistry was achieved using a HepatoChem EvoluChem(TM) PhotoRedOx Box and HCK1012-01-002 (450-455nm) LED lamp operating at 18 W with samples kept between 5-7 cm from the light source.

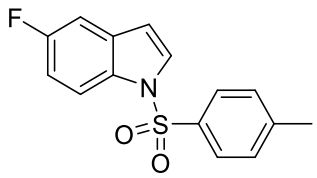
5-Fluoro-1-((4-nitrophenyl)sulfonyl)-1*H*-indole (1a)



Prepared following a literature procedure.[141] A solution of 5-fluoroindole (1.00 g, 7.40 mmol) in THF (15.0 mL) was added under an atmosphere of dinitrogen to a stirring

suspension of NaH (444 mg, 11.1 mmol) in THF (14.8 mL) and stirred for 30 minutes at room temperature. A solution of nosyl chloride (1.80 g, 8.14 mmol) in THF (28.6 mL) was added dropwise at 0 °C and stirred for 18 h at room temperature. The resulting solution was diluted with saturated aqueous $NaHCO_3$ solution (20 mL) and extracted with EtOAc (3 × 20 mL). The combined organic phases were washed with water (30 mL) then dried over Na_2SO_4. After removal of the solvent under reduced pressure, the crude product was washed with diethyl ether to give a pale orange powder of 5-fluoro-1-((4-nitrophenyl)sulfonyl)-1*H*-indole **1a** (1.07 g, 3.34 mmol, 45%). **m.p.** 126-128 °C; **^{1}H NMR (400 MHz, $CDCl_3$)** δ = 8.31 (appdt, *J* = 9.2, 2.2 Hz, 2H), 8.05 (appdt, *J* = 9.2, 2.2 Hz, 2H), 7.96 (dd, *J* = 9.0, 4.4 Hz, 1H), 7.60 (d, *J* = 3.7 Hz, 1H), 7.22 (dd, *J* = 8.5, 2.5 Hz, 1H), 7.11 (apptd, *J* = 9.0, 2.5 Hz, 1H), 6.71 (dd, *J* = 0.6, 3.7 Hz, 1H); **^{13}C{^{1}H} NMR (101 MHz, $CDCl_3$)** δ = 160.0 (d, *J* = 241.6 Hz), 150.7, 143.1, 132.0 (d, *J* = 10.2 Hz), 131.1, 128.0, 127.7, 124.6, 114.5 (d, *J* = 9.6 Hz), 113.4 (d, *J* = 25.8 Hz), 110.6 (d, *J* = 4.0 Hz), 107.5 (d, *J* = 24.1 Hz); **^{19}F NMR (376 MHz, $CDCl_3$)** δ = −118.5 (app td, *J* = 8.8, 4.3 Hz); **ν_{max}(neat)/cm^{-1}:** 3148, 3109, 3074, 1592, 1377, 1349, 1211, 1173, 1129, 1115, 1106, 856, 763, 737, 721, 680, 646, 606, 574, 464; **HRMS** calcd. for $C_{14}H_8FN_2O_4$: 319.0194 $[M-H]^-$; found (ESI^-) 319.0197.

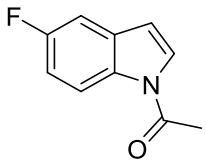
5-Fluoro-1-((4-methylphenyl)sulfonyl)-1*H*-indole (1b)



Prepared following a literature procedure.[141] A suspension of 5-fluoroindole (500 mg, 3.70 mmol) in THF (8.30 mL) was added under an atmosphere of dinitrogen to a stirring suspension of NaH (222 mg, 5.55 mmol) in THF (8.30 mL) and stirred for 30 minutes at room temperature. A solution of tosyl chloride (776 mg, 4.07 mmol) in THF (4.20 mL) was added dropwise and stirred for 18 h at room temperature. The resulting solution quenched by dilution with water (5 mL) and extracted with EtOAc (3 × 5 mL). The combined organic phases were washed with saturated $NaHCO_3$ solution (5 mL) and brine (5 mL), then dried over anhydrous Na_2SO_4. After removal of the solvent under reduced pressure, the crude product was purified by passage through a plug of silica gel, using pentane as an eluent,

to give a pale yellow powder of 5-fluoro-1-((4-methylphenyl)sulfonyl)-1*H*-indole **1b** (939 mg, 3.25 mmol, 88%). **m.p.** 103-106 °C (lit. 107-109 °C);[142] **^{1}H NMR (400 MHz, $CDCl_3$)** δ = 7.95 (dd, *J* = 9.0, 4.4 Hz, 1H), 7.76 (apptd, *J* = 8.3, 1.8 Hz, 2H), 7.61 (d, *J* = 3.7 Hz, 1H), 7.25 (d, *J* = 8.3 Hz, 2H), 7.19 (dd, *J* = 9.0, 2.5 Hz, 1H), 7.05 (apptd, *J* = 9.0, 2.5 Hz, 1H), 6.63 (dd, *J* = 3.7, 0.6 Hz, 1H), 2.37 (s, 3H); **^{13}C{^{1}H} NMR (101 MHz, $CDCl_3$)** δ = 159.6 (d, *J* = 240.2 Hz), 145.1, 135.1, 131.7 (d, *J* = 10.2 Hz), 131.2, 130.0, 128.1, 126.8, 114.6 (d, *J* = 9.4 Hz), 112.6 (d, *J* = 25.7 Hz), 108.9 (d, *J* = 4.1 Hz), 106.9 (d, *J* = 24.0 Hz), 21.5; **^{19}F NMR (376 MHz, $CDCl_3$)** δ = −120.0 (apptd, *J* = 9.0, 4.5 Hz; **ν_{max}(neat)/cm^{-1}:** 3139, 3120, 2955, 2927, 2854, 1591, 1458, 1442, 1367, 1346, 1214, 1184, 1165, 1132, 1111, 1088, 991, 948, 809, 797, 760, 724, 671, 591, 574, 538, 524, 493, 472, 428; **HRMS** calcd. for $C_{15}H_{13}FNO_2S^+$: 290.0646 $[M+H]^+$; found (ESI^+) 290.0648. Data are in agreement with literature.[142]

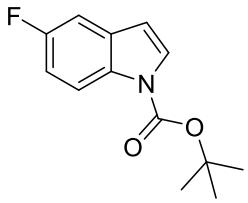
1-(5-Fluoro-1*H*-indol-1-yl)ethan-1-one (1c)



Prepared following a literature procedure.[143] Powdered NaOH (100 mg, 2.50 mmol) was added to a stirred solution of 5-fluoroindole (135 mg, 1.00 mmol) and tetrabutylammonium hydrogensulfate (3.00 mg, 0.01 mmol) in CH_2Cl_2 (2.60 mL) under an atmosphere of dinitrogen. A solution of acetyl chloride (118 mg, 1.50 mmol) in CH_2Cl_2 (0.92 mL) was then added dropwise and the resulting solution was stirred at room temperature for 24 h (until no further conversion was observed by NMR spectroscopy). Purification of the crude product was achieved by flash chromatography through silica gel using toluene as the eluent, giving 1-(5-fluoro-1*H*-indol-1-yl)ethan-1-one as a red powder **1c** (92 mg, 0.52 mmol, 52%). **m.p.** 58-65 °C; **^{1}H NMR (400 MHz, $CDCl_3$)** δ = 8.43 (dd, *J* = 8.8, 4.7 Hz, 1H), 7.48 (d, *J* = 3.7 Hz, 1H), 7.24 (dd, *J* = 8.8, 2.6 Hz, 1H), 7.10 (apptd, *J* = 9.1, 2.6 Hz, 1H), 6.63 (d, *J* = 3.7 Hz, 1H), 2.66 (s, 3H); **^{13}C{^{1}H} NMR (101 MHz, $CDCl_3$)** δ = 168.4, 159.7 (d, *J* = 240.2 Hz), 132.0, 131.4 (d, *J* = 10.1 Hz), 126.7 117.6 (d, *J* = 9.1 Hz), 112.8 (d, *J* = 24.8 Hz), 108.9 (d, *J* = 4.0 Hz), 106.4 (d, *J* = 23.8 Hz), 23.7; **^{19}F NMR (376 MHz, $CDCl_3$)** δ = −119.4 (apptd, *J* = 9.2, 4.6 Hz); **ν_{max}(neat)/cm^{-1}:** 3152, 3104, 2924, 2852, 1702, 1593,

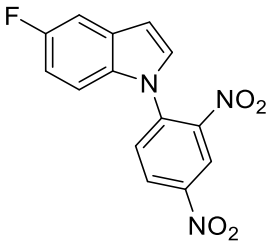
1460, 1442, 1367, 1326, 1255, 1188, 1171, 1133, 1107, 949, 811, 796, 759, 723, 630, 592, 522, 480, 430; **HRMS** calcd. for $C_{10}H_9FNO^+$: 178.0663 $[M+H]^+$; found (ESI^+) 178.0664. Data are in agreement with literature.[143]

Tert-butyl 5-fluoro-1*H*-indole-1-carboxylate (1d)



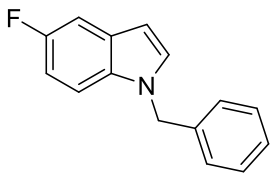
Prepared following a literature procedure.[144] A solution of 5-fluoroindole (405 mg, 3.00 mmol), di-*tert*-butyl dicarbonate (0.80 mL, 3.60 mmol) and 4-dimethylaminopyridine (37.0 mg, 0.30 mmol) in THF (12.0 mL) was stirred at room temperature for 18 h. The crude product was purified by filtering through a silica plug using 5% EtOH in cyclohexane as an eluent to give *tert*-butyl 5-fluoro-1*H*-indole-1-carboxylate as a yellow oil **1d** (664 mg, 2.82 mmol, 94%). **^{1}H NMR (400 MHz, $CDCl_3$)** δ = 8.11 (br s, 1H), 7.65 (d, *J* = 3.6 Hz, 1H), 7.23 (dd, *J* = 9.0, 2.5 Hz, 1H), 7.05 (apptd, *J* = 9.0, 2.5 Hz, 1H), 6.55 (d, *J* = 3.6 Hz, 1H), 1.69 (s, 9H); **^{13}C{^{1}H} NMR (101 MHz, $CDCl_3$)** δ = 159.2 (d, *J* = 238.7 Hz), 149.5, 131.6, 131.4 (d, *J* = 10.2 Hz), 127.4, 116.0 (d, *J* = 9.1 Hz), 112.0 (d, *J* = 25.0 Hz), 107.0 (d, *J* = 3.9 Hz), 106.3 (d, *J* = 23.8 Hz), 83.9, 28.2; **^{19}F NMR (376 MHz, $CDCl_3$)** δ = −121.2 (br q, *J* = 8.0 Hz); **ν_{max}(neat)/cm^{-1}:** 3105, 2981, 2929, 1703, 1593, 1461, 1443, 1370, 1256, 1166, 1133, 1108, 1086, 949, 810, 797, 759, 723, 632, 615, 523, 430; **HRMS** mass not found as not sufficiently ionisable. Data are in agreement with literature.[145]

1-(2,4-Dinitrobenzene)-5-fluoro-1*H*-indole (1e)



Prepared following a literature procedure.[146] A solution of 5-fluoroindole (68 mg, 0.50 mmol), 1-chloro-2,4-dinitrobenzene (124 mg, 0.61 mmol), copper(I) iodide (19.5 mg, 0.10 mmol), and K_2CO_3 (138 mg, 1.00 mmol) in DMF (5.00 mL) was stirred at 120 °C for 20 h (until full conversion was observed by TLC (1:1 EtOAc/cyclohexane). Once cooled, the reaction mixture was poured into water (7 mL) and the product was extracted with EtOAc (3 × 5 mL). The combined organic phases were dried with Na_2SO_4 and solvent was removed under reduced pressure to give red crystals of 1-(2,4-dinitrobenzene)-5-fluoro-1*H*-indole **1e** (42.4 mg, 0.14 mmol, 28%). **m.p.** 142-145 °C (lit. 151-153 °C);[146] **^{1}H NMR (400 MHz, $CDCl_3$)** δ = 8.94 (d, *J* = 2.6 Hz, 1H), 8.63 (dd, *J* = 8.8, 2.6 Hz, 1H), 7.87 (d, *J* = 8.8 Hz, 1H), 7.37 (dd, *J* = 8.9, 2.5 Hz, 1H), 7.20 (d, *J* = 3.4 Hz, 1H), 7.14 (dd, *J* = 9.0, 4.1 Hz, 1H), 7.03 (apptd, *J* = 9.0, 2.5 Hz, 1H), 6.80 (dd, *J* = 3.4, 0.6 Hz, 1H); **^{13}C{^{1}H} NMR (101 MHz, $CDCl_3$)** δ = 159.2 (d, *J* = 238.7 Hz), 146.4, 145.7, 137.8, 132.4, 130.3 (d, *J* = 10.0 Hz), 129.8, 128.8, 128.2, 121.9, 112.2 (d, *J* = 26.5 Hz), 110.2 (d, *J* = 9.6 Hz), 107.3 (d, *J* = 4.4 Hz), 107.1 (d, *J* = 23.9 Hz); **^{19}F NMR (376 MHz, $CDCl_3$)** δ = −121.5 (apptd, *J* = 8.9, 4.1 Hz); **ν_{max}(neat)/cm^{-1}:** 3100, 2923, 2855, 1731, 1599, 1520, 1466, 1447, 1337, 1280, 1246, 1207, 1134, 908, 844, 798, 769, 729, 427; **HRMS** calcd. for $C_{14}H_9FN_3O_4^+$: 302.0572 $[M+H]^+$; found (ESI^+) 302.0577. Data are in agreement with literature.[146]

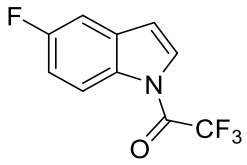
1-Benzyl-5-fluoro-1*H*-indole (1f)



Prepared following a literature procedure.[147] A solution of 5-fluoroindole (135 mg, 1.00 mmol) in DMF (1.00 mL) was added dropwise to a suspension of NaH (48.0 mg, 1.20 mmol) in DMF (1.00 mL) at 0 °C and stirred for 30 minutes. Benzyl bromide (0.20 mL, 1.68 mmol) was then added dropwise at 0 °C and stirred for 21 h (until full conversion was observed by TLC, 1:3 EtOAc/cyclohexane). The reaction was quenched with water (5 mL) and the product was extracted with EtOAc (3 × 5 mL). The combined organic phases were washed with 5% aq. LiCl solution (4 × 15 mL) and water (2 × 15 mL). The organic phase was dried with $MgSO_4$ and the solvent was removed under reduced pressure to give pink crystals of 1-benzyl-5-fluoro-1*H*-indole **1f** (92.3 mg, 0.41 mmol, 41%). **m.p.** 53-55 °C; **^{1}H**

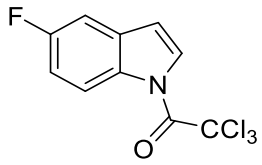
NMR (400 MHz, $CDCl_3$) δ = 7.36-7.29 (m, 4H), 7.21-7.16 (m, 2H), 7.12 (d, *J* = 6.6 Hz, 2H), 6.93 (apptd, *J* = 9.1, 2.4 Hz, 1H), 6.53 (d, *J* = 3.0 Hz, 1H), 5.33 (s, 2H); **$^{13}C\{^1H\}$ NMR (101 MHz, $CDCl_3$)** δ = 157.9 (d, *J* = 234.0 Hz), 137.2, 132.9, 129.9, 128.8, 128.4, 127.8, 126.7, 110.3 (d, *J* = 9.8 Hz), 110.1 (d, *J* = 26.3 Hz), 105.7 (d, *J* = 23.3 Hz), 101.6 (d, *J* = 4.7 Hz), 50.4; **^{19}F NMR (376 MHz, $CDCl_3$)** δ = −125.4 (apptd, *J* = 9.5, 4.4 Hz); **ν_{max}(neat)/cm^{-1}:** 3068, 3029, 2917, 2863, 1622, 1578, 1486, 1439, 1222, 1184, 1116, 866, 800, 752, 724, 706, 689, 622, 469, 432; **HRMS** calcd. for $C_{15}H_{13}FN^+$: 226.1027 $[M+H]^+$; found (ESI^+) 226.1036. Data are in agreement with literature.[147]

2,2,2-Trifluoro-1-(5-fluoro-1*H*-indol-1-yl)ethan-1-one (2g)



Prepared following a literature procedure.[148] A solution of 5-fluoroindole (203 mg, 1.50 mmol) and sodium hydride (120 mg, 3.00 mmol) in THF (5.00 mL) was stirred at 0 °C for 30 minutes. After which, trifluoroacetic anhydride (0.30 mL, 2.16 mmol) was added and the reaction was allowed to warm to room temperature and stirred for 24 hours. The reaction was diluted with ethyl acetate, washed with water then with brine, and the organic phase was dried over Na_2SO_4. After removal of solvent under reduced pressure, the compound was purified by recrystallization using ethyl acetate and cyclohexane as the counter-solvent. This gave 2,2,2-trifluoro-1-(5-fluoro-1*H*-indol-1-yl)ethan-1-one as an off-white powder **2g** (184 mg, 0.80 mmol, 53%). **m.p.** 230 °C (dec); **^1H NMR (400 MHz, $CDCl_3$)** δ = 8.87 (br s, 1H), 8.13-8.09 (m, 2H), 7.44 (dd, *J* = 8.9, 4.2 Hz, 1H), 7.15 (apptd, *J* = 8.9, 2.6 Hz, 1H); **$^{13}C\{^1H\}$ NMR (101 MHz, $CDCl_3$)** δ = 160.5, 160.3 (d, *J* = 240.7 Hz), 135.2, 126.9 (d, *J* = 11.1 Hz), 115.7, 113.0 (d, *J* = 26.5 Hz), 112.6 (d, *J* = 9.6 Hz), 108.1 (d, *J* = 25.5 Hz), 103.6, CF_3 signal not observed; **^{19}F NMR (376 MHz, $CDCl_3$)** δ = −72.6 (d, *J* = 1.0 Hz, 3F), −118.5 (apptd, *J* = 9.1, 4.2 Hz, 1F); **ν_{max}(neat)/cm^{-1}:** 3234, 3129, 1639, 1473, 1429, 1140, 898, 810, 728; **HRMS** calcd. for $C_{10}H_5F_4NO$: 232.0380 $[M+H]^+$; found (ESI^+) 232.0381.

2,2,2-Trichloro-1-(5-fluoro-1*H*-indol-1-yl)ethan-1-one (2h)

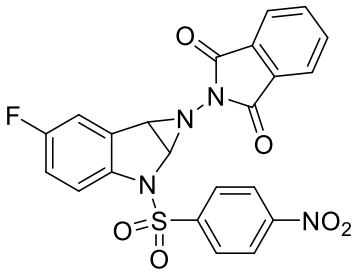


Prepared following a literature procedure.[148] A solution of 5-fluoroindole (203 mg, 1.50 mmol) and sodium hydride (120 mg, 3.00 mmol) in THF (5.00 mL) was stirred at 0 °C for 30 minutes. After which, trichloroacetyl chloride (0.20 mL, 1.09 mmol) was added and the reaction was allowed to warm to room temperature and stirred for 23 hours. The reaction was diluted with ethyl acetate, washed with water then with brine, and the organic phase was dried over Na_2SO_4. After removal of solvent under reduced pressure, the compound was purified by recrystallization using diethyl ether and cyclohexane as the counter-solvent. This gave 2,2,2-trichloro-1-(5-fluoro-1*H*-indol-1-yl)ethan-1-one as a brown powder **2h** (52 mg, 0.19 mmol, 12%). **m.p.** 174-176 °C; **^{1}H NMR (400 MHz, $CDCl_3$)** δ = 7.97 (dd, *J* = 9.0, 4.5 Hz, 1H), 7.51 (d, *J* = 3.7 Hz, 1H), 7.33 (dd, *J* = 8.7, 2.6 Hz, 1H), 7.14 (apptd, *J* = 9.0, 2.6 Hz, 1H), 6.73 (dd, *J* = 3.7, 0.8 Hz, 1H); **^{13}C{^{1}H} NMR (101 MHz, $CDCl_3$)** δ = 159.7 (d, *J* = 240.6 Hz), 148.3, 132,5, 131.2 (d *J* = 10.2 Hz), 128.1, 115.9 (d, *J* = 9.3 Hz), 112.9 (d, *J* = 25.4 Hz), 108.8 (d, *J* = 4.0), 106.9 (d, *J* = 24.1 Hz), CCl_3 signal not observed; **^{19}F NMR (376 MHz, $CDCl_3$)** δ = −119.13 (apptd, *J* = 8.9, 4.5 Hz); **ν_{max}(neat)/cm^{-1}:** 3163, 3110, 3078, 1711, 1619, 1594, 1461, 1254, 1137, 948, 851; **HRMS** mass not found as not sufficiently ionisable.

General procedure for the aziridination of protected indoles.

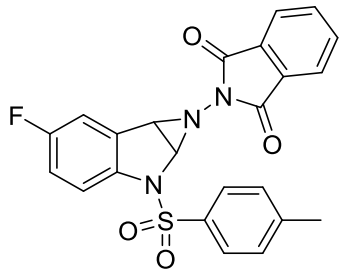
A solution of phenyliodine(III) diacetate (32.2 mg, 0.10 mmol) in CH_2Cl_2 (0.25 mL) was added dropwise to a stirred suspension of protected 5-fluoroindole (0.05 mmol), *N*-aminophthalimide (12.2 mg, 0.10 mmol) and K_2CO_3 (20.7 mg, 0.15 mmol) in CH_2Cl_2 (0.50 mL) at 0 °C. This solution was then allowed to warm to room temperature and stirred for 18 h. When the reaction was complete, as indicated by NMR spectroscopy, the reaction was diluted with Et_2O (5 mL). The resulting precipitate was filtered and washed with Et_2O (3 × 5 mL) and water (3 × 5 mL). The solid was then dissolved in EtOAc (10 mL), the organic phase was dried with Na_2SO_4 and the solvent was removed under reduced pressure to give the aziridine product.

2-(5-Fluoro-2-((4-nitrophenyl)sulfonyl)-2,6b-dihydroazirino[2,3-*b*]indol-1(1a*H*)-yl)isoindoline-1,3-dione (2a)



Synthesized according to the general procedure but on a 0.45 mmol scale and with 4 equivalents of K_2CO_3 (249 mg, 1.80 mmol) The resulting compound was isolated as a yellow powder **2a** (155 mg, 0.36 mmol, 79%). **m.p.** 183-186 °C; **^{1}H NMR (400 MHz, $CDCl_3$)** δ = 8.53-8.49 (m, 2H), 8.34-8.30 (m, 2H), 7.89-7.84 (m, 2H), 7.82-7.76 (m, 2H), 7.54 (dd, *J* = 8.6, 4.3 Hz, 1H), 7.39 (dd, *J* = 8.6, 2.5 Hz, 1H), 7.09 (apptd, *J* = 8.9, 2.5 Hz, 1H), 5.87 (d, *J* = 5.4 Hz, 1H), 4.50 (d, *J* = 5.4 Hz, 1H); **^{13}C{^{1}H} NMR (101 MHz, $CDCl_3$)** δ = 166.5, 159.9 (d, *J* = 243.4 Hz), 150.7, 143.1, 138.0, 135.0, 134.7, 131.3 (d, *J* = 3.8 Hz), 129.9, 128.8, 126.3 (d, *J* = 9.5 Hz), 122.1, 115.5 (d, *J* = 9.5 Hz), 114.4 (d, *J* = 25.9 Hz), 114.1, 105.0 (d, *J* = 25.0 Hz); **^{19}F NMR (376 MHz, $CDCl_3$)** δ = −117.5 (apptd, *J* = 7.7, 4.2 Hz); **ν_{max}(neat)/cm^{-1}:** 3109, 3088, 2927, 2852, 1732, 1607, 1530, 1374, 1353, 1180, 1143, 742, 579; **HRMS** calcd. for $C_{22}H_{13}FN_4O_6SNa^+$: 503.0432 $[M+Na]^+$; found (ESI^+) 503.0433.

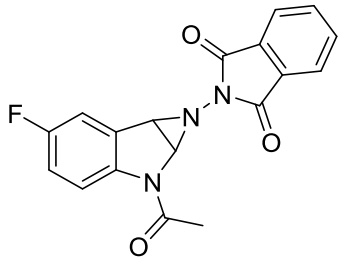
2-(5-Fluoro-2-((4-methylphenyl)sulfonyl)-2,6b-dihydroazirino[2,3-*b*]indol-1(1a*H*)-yl)isoindoline-1,3-dione (2b)



Synthesized according to the general procedure but not isolated. **^{1}H NMR (400 MHz, $CDCl_3$)** δ = 8.10-8.05 (m, 2H), 7.91-7.84 (m, 4H), 7.77-7.72 (m, 2H), 7.48 (dd, *J* = 8.9, 4.2

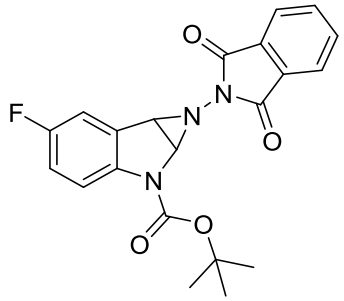
Hz, 1H), 7.35 (dd, *J* = 7.6, 2.7 Hz, 1H), 7.03 (apptd, *J* = 8.9, 2.7 Hz, 1H), 5.92 (d, *J* = 5.4 Hz, 1H), 4.48 (d, *J* = 5.4 Hz, 1H), 2.37 (s, 3H); **$^{13}C\{^{1}H\}$ NMR (101 MHz, $CDCl_3$)** δ = Clear spectrum could not be obtained due to instability of compound; **^{19}F NMR (376 MHz, $CDCl_3$)** δ = −119.0 (apptd, *J* = 8.6, 4.4 Hz); **HRMS** calcd. for $C_{23}H_{16}FN_3O_4S$: 450.0918 $[M+H]^+$; found (ESI^+) 450.0907.

2-(2-Acetyl-5-fluoro-2,6b-dihydroazirino[2,3-*b*]indol-1(1a*H*)-yl)isoindoline-1,3-dione (2c)



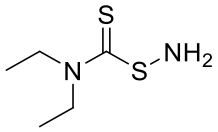
Synthesized according to the general procedure. Isolated as a white powder **2c** (201 mg, 0.60 mmol, 60%). **m.p.** 170 °C (dec); **^{1}H NMR (400 MHz, DMSO-d_6)** mixture of rotamers observed, peaks identified as from either isomer A or B in the 3:1 mixture of A:B. δ = 8.04 (dd, *J* = 8.8, 4.8 Hz, 1H, A), 7.89-7.82 (m, 4H, A), 7.80 (dd, *J* = 9.0, 4.5 Hz, 1H, B), 7.72-7.65 (m, 4H, B), 7.56 (dd, *J* = 7.9, 2.7 Hz, 1H, A), 7.42 (dd, *J* = 8.3, 2.5 Hz, 1H, B), 7.23 (apptd, *J* = 8.8, 2.7 Hz, 1H, A), 7.03 (apptd, *J* = 9.0, 2.5 Hz, 1H, B), 6.06 (d, *J* = 4.4 Hz, 1H, B), 6.03 (d, *J* = 5.4 Hz, 1H, A), 4.96 (d, *J* = 4.4 Hz, 1H, B), 4.83 (d, *J* = 5.4 Hz, 1H, A), 2.69 (s, 3H, A), 2.59 (s, 3H, B); **$^{13}C\{^{1}H\}$ NMR (101 MHz, DMSO-d_6)** δ = 169.2, 166.6, 158.8 (d, *J* = 238.1 Hz), 135.2, 131.3, 130.6 (d, *J* = 3.8 Hz), 130.5, 124.7 (d, *J* = 10.0 Hz), 123.9, 118.0 (d, *J* = 8.8 Hz), 113.3 (d, *J* = 24.9 Hz), 109.3, 104.7 (d, *J* = 24.9 Hz), 24.0; **^{19}F NMR (376 MHz, DMSO-d_6)** mixture of isomers observed, peaks identified as from either isomer A or B in the 3:1 mixture of A:B δ = −118.7 (apptd, *J* = 8.6, 4.6 Hz, A), −119.1 (apptd, *J* = 8.7, 4.7 Hz, B); **ν_{max}(neat)/cm^{-1}:** 3093, 2980, 1764, 1704, 1688, 1606, 1475, 1383, 1363, 1312, 1247, 1137, 1024, 888, 833, 712, 524; **HRMS** calcd. for $C_{18}H_{13}FN_3O_3^+$: 338.0936 $[M+H]^+$; found (ESI^+) 338.0935 .

***tert*-Butyl 1-(1,3-dioxoisoindolin-2-yl)-5-fluoro-1a,6b-dihydroazirino[2,3-*b*]indole-2(1*H*)-carboxylate (2d)**



Synthesized according to the general procedure. Isolation attempted but degradation suspected, resulting compounds obtained as a yellow oil **2d**. **^{1}H NMR (400 MHz, $CDCl_3$)** δ = Clear spectrum could not be obtained due to instability of compound; **^{13}C{^{1}H} NMR (101 MHz, $CDCl_3$)** δ = Clear spectrum could not be obtained due to instability of compound; **^{19}F NMR (376 MHz, $CDCl_3$)** δ = −120.1 (br s); **ν_{max}(neat)/cm^{-1}:** 3192 (br), 3061, 2981, 2718, 1721, 1603, 1468, 1370, 1305, 1256, 1140, 1117, 1070, 1050, 709, 667, 645, 548, 532; **HRMS** calcd. for $C_{21}H_{19}FN_3O_4^+$: 396.1354 $[M+H]^+$; found (ESI^+) 396.1360.

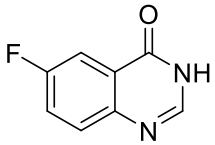
***N*-((Aminothio)carbonothioyl)-*N*-ethylethanamine**



Prepared following a literature procedure.[149] A solution of hydroxylamine-*O*-sulfonic acid (254 mg, 2.24 mmol) and sodium hydroxide (90.0 mg, 2.25 mmol) in water (2.30 mL) was added dropwise to a solution of sodium diethyldithiocarbamate trihydrate (340 mg, 1.51 mmol) in water (2.30 mL) at 0 °C and stirred for 6 h. The suspension was filtered to give a pale-yellow solid which was further washed with water. The solid was washed with CH_2Cl_2 then the filtered solution was collected. The solvent was removed under reduced pressure to give *N*-((aminothio)carbonothioyl)-*N*-ethylethanamine as a yellow oil (170 mg, 103 mmol, 69%). **^{1}H NMR (400 MHz, $CDCl_3$)** δ = 4.05 (q, *J* = 7.2 Hz, 2H), 3.62 (q, *J* = 7.2 Hz, 2H), 3.11 (s, 2H), 1.31 (t, *J* = 7.2 Hz, 6H); **^{13}C{^{1}H} NMR (101 MHz, $CDCl_3$)** δ = 204.5, 50.2,

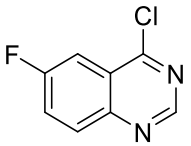
12.6; **HRMS** calcd. for $C_5H_{13}N_2S_2^+$: 165.0515 $[M+H]^+$; found (ESI^+) 165.0517. Data are in agreement with literature.[149]

6-Fluoroquinazolin-4(3*H*)-one (6)



Prepared following a literature procedure.[103] A solution of 2-amino-5-fluorobenzoic acid (465 mg, 3.00 mmol) in formamide (1.00 mL) was heated at 140 °C and stirred for 5 h. The reaction was allowed to cool to room temperature then was quenched with ice-cold water (8.00 mL) resulting in the formation of a precipitate. The precipitate was collected by filtration and washed with ice-cold water. The remaining solid was washed through with ethyl acetate and the resulting solution was collected. The solvent was removed under reduced pressure to give 6-fluoroquinazolin-4(3*H*)-one as a white powder **6** (316 mg, 1.93 mmol, 64%). **m.p.** 255-256 °C (lit. 260-261 °C);[103] **^{1}H NMR (400 MHz, DMSO-d$_6$)** δ = 12.37 (br s, 1H), 8.10 (s, 1H), 7.82-7.68 (m, 3H); **^{13}C{^{1}H} NMR (101 MHz, DMSO-d$_6$)** δ = 160.7 (d, *J* = 3.2 Hz), 160.5 (d, *J* = 245.5 Hz), 146.1, 145.4 (d, *J* = 2.0 Hz), 130.6 (d, *J* = 8.5 Hz), 124.4 (d, *J* = 8.5 Hz), 123.3 (d, *J* = 24.0 Hz), 110.9 (d, *J* = 23.2 Hz); **^{19}F NMR (376 MHz, DMSO-d$_6$)** δ = −112.0 (apptd, *J* = 8.3, 4.8 Hz); **ν_{max}(neat)/cm^{-1}:** 3153, 3017, 2927, 2852, 1658, 1618, 1333, 1152, 910, 831; **HRMS** calcd. for $C_8H_5FN_2NaO^+$: 187.0279 $[M+Na]^+$; found (ESI^+) 187.0277. Data are in agreement with literature.[103]

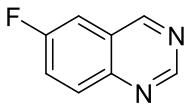
4-Chloro-6-fluoroquinazoline (7)



Prepared following a literature procedure.[104] A solution of 6-fluoroquinazolin-4(3*H*)-one (82 mg, 0.50 mmol) and DMF (3 drops) in thionyl chloride (1.00 mL) was heated at 77 °C under an atmosphere of dinitrogen and stirred for 19 h. The solvent was removed in vacuo and

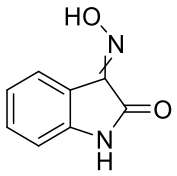
the remaining residue was dissolved in CH_2Cl_2. The resulting solution was washed with saturated aq. $NaHCO_3$ solution then brine. The organic phase was dried over Na_2SO_4 and the solvent was removed under reduced pressure to give 4-chloro-6-fluoroquinazoline as a white powder **7** (46 mg, 0.25 mmol, 50%). **m.p.** 218 °C (dec); **^{1}H NMR (400 MHz, DMSO-d_6)** δ = 9.14 (s, 1H), 8.24 (dd, *J* = 9.1, 5.2 Hz, 1H), 8.13-8.05 (m, 2H); **^{13}C{^{1}H} NMR (101 MHz, DMSO-d_6)** δ = 160.6 (d, *J* =245.3 Hz), 160.5 (d, *J* = 3.3 Hz), 145.7, 145.2, 130.0 (d, *J* = 8.4 Hz), 124.3 (d, *J* = 8.2 Hz), 123.4 (d, *J* = 23.8 Hz), 111.1 (d, *J* = 23.2 Hz); **^{19}F NMR (376 MHz, DMSO-d_6)** δ = −106.8 (ddd, *J* = 8.3, 8.2, 5.0 Hz); **ν_{max}(neat)/cm^{-1}:** 3066, 2996, 2922, 2852, 2686, 2623, 2576, 1780, 1649, 1489, 1265, 1163, 861; **HRMS** calcd. for $C_8H_5Cl^{35}FN_2^+$: 183.0120 [M+H]$^+$; found (ESI$^+$) 183.0120.

6-Fluoroquinazoline (8)



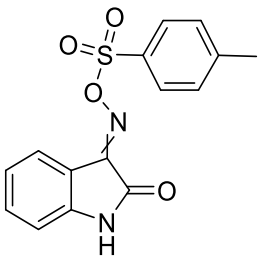
Prepared following a literature procedure.[105] To a solution of 4-chloro-6-fluoroquinazoline (65.0 mg, 0.36 mmol) in THF (7.00 mL) was added $PdCl_2$(dppf) (13 mg, 0.02 mmol), TMEDA (0.18 mL, 1.20 mmol) and $NaBH_4$ (46 mg, 1.22 mmol) consecutively under an atmosphere of dinitrogen. The solution was stirred at room temperature for 1.5 hours. The reaction was quenched with brine then the organics were extracted with diethyl ether. The combined organic fractions were combined and dried over Na_2SO_4 then the solvent was removed under reduced pressure. The resulting yellow oil was purified by preparative TLC (5:1 EtOAc/cyclohexane) to give 6-fluoroquinazoline as a white powder **8** (1.1 mg, 0.01 mmol, 2%). **m.p.** 133-135 °C (lit. 140 °C);[102] **^{1}H NMR (400 MHz, $CDCl_3$)** δ = 9.43 (s, 1H), 9.36 (s, 1H), 8.13 (dd, *J* = 9.2, 5.0 Hz, 1H), 7.75 (ddd, *J* = 9.2, 8.3, 2.8 Hz, 1H), 7.60 (dd, *J* = 7.8, 2.8 Hz, 1H); **^{13}C{^{1}H} NMR (101 MHz, $CDCl_3$)** δ = 160.8 (d, *J* = 252.4 Hz), 159.6 (d, *J* = 5.5 Hz), 154.7 (d, *J* = 2.9 Hz), 147.2, 131.3 (d, *J* = 8.7 Hz), 125.6 (d, *J* = 9.2 Hz), 124.9 (d, *J* = 26.0 Hz), 110.2 (d, *J* = 21.8 Hz); **^{19}F NMR (376 MHz, $CDCl_3$)** δ = −109.1 (apptd, *J* = 8.1, 5.0 Hz); **ν_{max}(neat)/cm^{-1}:** 3137, 2920, 2851, 2744, 1724, 1574, 1499, 1247, 1143, 1032, 836, 819; **HRMS** calcd. for $C_8H_5FN_2$: 149.0510 [M+H]$^+$; found (ESI$^+$) 149.0517.

3-(Hydroxyimino)indolin-2-one (10)



Prepared following a literature procedure.[129] A solution of isatin (735 mg, 5.00 mmol) and hydroxylamine hydrochloride (378 mg, 5.44 mmol) in water (10.0 mL) was stirred at 100 °C for 1 h. Sodium acetate (410 mg, 5.00 mmol) was added and the reaction was stirred for a further 1 h at 100 °C. The precipitate was then filtered and the solid was dissolved in acetone and dried over $MgSO_4$. The solvent was removed under reduced pressure and the product was recrystalised from methanol, giving 3-(hydroxyimino)indolin-2-one as orange crystals **10** (283 mg, 1.75 mmol, 35%). **m.p.** 232 °C (dec); **^{1}H NMR (400 MHz, DMSO-d$_6$)** δ = 13.28 (s, 1H), 10.68 (s, 1H), 7.94 (dd, J = 7.5, 1.3 Hz, 1H), 7.35 (apptd, *J* = 7.7, 1.3 Hz, 1H), 7.02, (apptd, *J* = 7.5, 1.0 Hz, 1H), 6.88 (d, *J* = 7.7 Hz, 1H); **^{13}C{^{1}H} NMR (101 MHz, DMSO-d$_6$)** δ = 164.9, 144.7, 143.0, 132.6, 127.5, 122.5, 116.4, 110.7; **ν_{max}(neat)/cm^{-1}:** 3169, 3072, 2884, 1703, 1615, 1456, 1340, 1187, 1021, 1007, 744, 642; **HRMS** calcd. for $C_8H_6N_2O_2$: 161.0357 $[M-H]^-$; found (ESI^-) 161.0353. Data are in agreement with literature.[150]

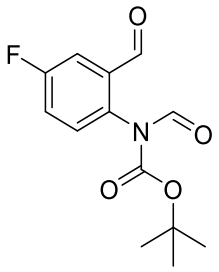
3-((Tosyloxy)imino)indolin-2-one (11)



Prepared following a literature procedure.[131] An aqueous sodium hydroxide solution (2M, 0.50 mL) was added dropwise to a stirred solution of 3-(hydroxyimino)indolin-2-one **10** (162 mg, 1.00 mmol) and *p*-toluenesulfonyl chloride (210 mg, 1.10 mmol) in acetone (3.00 mL), which was cooled to −5 °C in a salt ice bath. The reaction was stirred for 0.5 h then quenched by dilution with H_2O. The resulting precipitate was filtered and dried, giving 3-

((tosyloxy)imino)indolin-2-one **11** as yellow microfibres (38.0 mg, 0.12 mmol, 12%). **m.p.** 255 °C (dec); **^{1}H NMR (400 MHz, DMSO-d$_6$)** mixture of isomers observed, peaks identified as from either isomer A or B by COSY. Tosyl hydrogens appear as one set of peaks; δ = 10.74 (s, 1H), 8.20 – 8.18 (m, 1H, B), 8.18 – 8.16 (m, 1H, A), 8.09 (dd, *J* = 7.9, 1.3 Hz, 1H, B), 8.01 – 7.98 (m, 2H), 7.90 (dd, *J* = 8.0, 1.6 Hz, 1H, A), 7.78 (apptd, *J* = 8.0, 1.6 Hz, 1H, A), 7.72 (apptd, *J* = 7.9, 1.3 Hz, 1H, B), 7.59 – 7.56 (m, 2H), 7.42 (apptd, *J* = 7.7, 1.0 Hz, 1H, B), 7.38 (td, *J* = 7.6, 1.1 Hz, 1H, A), 2.45 (s, 3H); **^{13}C{^{1}H} NMR (101 MHz, DMSO-d$_6$)** peaks identified as from either isomer A or B by HSQC and HMBC. Tosyl carbons appear as one set of peaks δ = 163.3 (B), 152.0 (A), 149.4 (B), 148.7 (A), 147.1, 142.9 (B), 139.9 (A), 136.1 (B), 135.0 (A), 134.5, 133.8 (A), 131.0, 129.4, 129.1 (B), 126.2 (B), 126.0 (A), 122.6 (A), 116.6 (B), 115.7 (B), 104.2 (A), 21.7; **ν_{max}(neat)/cm^{-1}:** 3123, 3074, 3034, 2970, 2927, 2224, 1757, 1711, 1588, 1556, 1460, 1387, 1344, 1176, 942, 886, 696; **HRMS** calcd. for $C_{15}H_{12}N_2NaO_4S$: 339.0410 [M+Na]$^+$; found (ESI$^+$) 339.0421.

***tert*-Butyl (4-fluoro-2-formylphenyl)(formyl)carbamate (16)**



Prepared following a literature procedure.[94] A microwave tube charged with *tert*-butyl 5-fluoro-1*H*-indole-1-carboxylate **1d** (71.9 mg, 0.3 mmol), methylene blue (2 mg, 2 mol%) and TFE (3 mL) was irradiated under LED light (450 nm). The reaction was stirred at room temperature for 22.5 h then quenched with water. The organics were extracted with ethyl acetate and were washed with copious amounts of brine. The organic layer was then dried over $MgSO_4$ then the solvent was removed under reduced pressure. This gave a crude yellow oil of *tert*-butyl 5-fluoro-1*H*-indole-1-carboxylate (**1d**) and *tert*-butyl (4-fluoro-2-formylphenyl)(formyl)carbamate (**9**) (77 mg, 1:2.5 **1d**:**16**). **^{1}H NMR (400 MHz, CDCl$_3$)** δ = 9.93 (d, *J* = 1.4 Hz, 1H), 9.44 (s, 1H), 7.64 (dd, *J* = 8.0, 3.0 Hz, 1H), 7.91 (ddd, *J* = 8.7, 7.5, 3.0 Hz, 1H), 7.25 (dd, *J* = 8.7, 4.7 Hz, 1H), 1.50 (s, 9H); **^{13}C{^{1}H} NMR (101 MHz, CDCl$_3$)** δ = 193.7 (d, *J* = 2.2 Hz), 188.0 (d, *J* = 1.6 Hz), 163.0, 160.7 (d, *J* = 231.2 Hz)

133.8 (d, *J* = 6.4 Hz), 132.3 (d, *J* = 7.8 Hz), 121.6 (d, *J* = 22.8 Hz), 120.4 (d, *J* = 6.5 Hz), 118.6 (d, *J* = 23.4 Hz), 85.5, 27.9; **^{19}F NMR (376 MHz, $CDCl_3$)** δ = −110.2 (tdd, *J* = 7.7, 4.6, 1.4 Hz); **ν_{max}(neat)/cm^{-1}:** 3291, 2978, 2929, 2856, 1699, 1672, 1526, 1494, 1254, 1143, 781; **HRMS** calcd. for $C_{13}H_{14}FNNaO_4$: 290.0799 [M+Na]$^+$; found (ESI$^+$) 290.0794.

5 References

1 J. A. DiMasi, H. G. Grabowski and R. W. Hansen, *J. Health Econ.*, 2016, **47**, 20-33.

2 R. M. Wilson and S. J. Danishefsky, *J. Org. Chem.*, 2006, **71**, 8329–8351.

3 K. R. Campos, P. J. Coleman, J. C. Alvarez, S. D. Dreher, R. M. Garbaccio, N. K. Terrett, R. D. Tillyer, M. D. Truppo and E. R. Parmee, *Science*, 2019, **363**.

4 J. Jurczyk, J. Woo, S. F. Kim, B. D. Dherange, R. Sarpong and M. D. Levin, *Nature Synthesis*, 2022, **1**, 352–364.

5 B. D. Dherange, P. Q. Kelly, J. P. Liles, M. S. Sigman and M. D. Levin, *J. Am. Chem. Soc.*, 2021, **143**, 11337–11344.

6 B. W. Joynson and L. T. Ball, *Helv. Chim. Acta*, 2023, **106**, e2022001.

7 A. E. Favorskii, *Zhur. Russ. Khim. Obshch.*, 1892, **24**, 254.

8 K. Murai, H. Komatsu, R. Nagao and H. Fujioka, *Org. Lett.*, 2012, **14**, 772–775.

9 H. Qin, W. Cai, S. Wang, T. Guo, G. Li and H. Lu, *Angew. Chem. Int. Ed.*, 2021, **60**, 20678–20683.

10 G. L. Ciamician and M. Dennstedt, *Ber. Dtsch. Chem. Ges.*, 1881, **14**, 1153–1163.

11 D. C. Blakemore, L. Castro, I. Churcher, D. C. Rees, A. W. Thomas, D. M. Wilson and A. Wood, *Nat. Chem.*, 2018, **10**, 383–394.

12 P. Bhutani, G. Joshi, N. Raja, N. Bachhav, P. K. Rajanna, H. Bhutani, A. T. Paul and R. Kumar, *J. Med. Chem.*, 2021, **64**, 2339–2381.

13 K. Kamaraju, J. Smith, J. Wang, V. Roy, H. O. Sintim, W. E. Bentley and S. Sukharev, *Biochemistry*, 2011, **50**, 6983–6993.

14 J. G. Kettle and R. A. Ward, *J. Chem. Inf. Model*, 2010, **50**, 525–533.

15 K. Narasimhan and P. R. Kumar, *Heterocycles*, 1984, **22**, 1369–1375.

16 P. R. Kumar, *Heterocycles*, 1987, **26**, 1257–1262.

17 D. R. Jurberg, *Lead and Human Health: An Update*, American Council on Science and Health, New York, 2000.

18 G. S. Singh and T. H. Tabane, in *Green Synthetic Approaches for Biologically Relevant Heterocycles*, 2014, pp. 163–184.

19 J. C. Reisenbauer, O. Green, A. Franchino, P. Finkelstein and B. Morandi, *Science*, 2022, **377**, 1104–1109.

20 K. M. Morgan, J. A. Ellis, J. Lee, A. Fulton, S. L. Wilson, P. S. Dupart and R. Dastoori, *J. Org. Chem.*, 2013, **78**, 4303–4311.

21 X. E. Hu, *Tetrahedron*, 2004, **60**, 2701–2743.

22 S. Sabir, G. Kumar, V. P. Verma and J. L. Jat, *ChemistrySelect*, 2018, **3**, 3702–3711.

23 T. Gleede, L. Reisman, E. Rieger, P. C. Mbarushimana, P. A. Rupar and F. R. Wurm, *Polym. Chem.*, 2019, **10**, 3257–3283.

24 Rolf. Huisgen, Wolfgang. Scheer and Helmut. Huber, *J. Am. Chem. Soc.*, 1967, **89**, 1753–1755.

25 A. Meyer and J. Ryan, *Molecules*, 2016, **21**, 935.

26 R. B. Woodward and R. Hoffmann, *J. Am. Chem. Soc.*, 1965, **87**, 395–397.

27 I. Ungureanu, P. Klotz and A. Mann, *Angew. Chem.*, 2000, **112**, 4790–4792.

28 S. Gandhi, A. Bisai, B. A. B. Prasad and V. K. Singh, *J. Org. Chem.*, 2007, **72**, 2133–2142.

29 A. L. Schwan and J. Warkentin, *J. Chem. Soc. Chem. Commun.*, 1986, 1721.

30 M. Joucla, J. Mortier and R. Bureau, *Tetrahedron Lett.*, 1987, **28**, 2975–2976.

31 S. Gabriel, *Ber. Dtsch. Chem. Ges.*, 1888, **21**, 1049–1057.

32 H. Wenker, *J. Am. Chem. Soc.*, 1935, **57**, 2328–2328.

33 J. C. Antilla and W. D. Wulff, *J. Am. Chem. Soc.*, 1999, **121**, 5099–5100.

34 S. Harada, N. Kowase, N. Tabuchi, T. Taguchi, Y. Dobashi, A. Dobashi and Y. Hanzawa, *Tetrahedron*, 1998, **54**, 753–766.

35 J. Legters, L. Thijs and B. Zwanenburg, *Tetrahedron Lett.*, 1989, **30**, 4881–4884.

36 R. Huisgen, L. Möbius, G. Müller, H. Stangl, G. Szeimies and J. M. Vernon, *Chem. Ber.*, 1965, **98**, 3992–4013.

37 Z. Li, K. R. Conser and E. N. Jacobsen, *J. Am. Chem. Soc.*, 1993, **115**, 5326–5327.

38 Z. Li, R. W. Quan and E. N. Jacobsen, *J. Am. Chem. Soc.*, 1995, **117**, 5889–5890.

39 D. A. Evans, M. M. Faul, M. T. Bilodeau, B. A. Anderson and D. M. Barnes, *J. Am. Chem. Soc.*, 1993, **115**, 5328–5329.

40 D. A. Evans, M. T. Bilodeau and M. M. Faul, *J. Am. Chem. Soc.*, 1994, **116**, 2742–2753.

41 R. S. Atkinson and C. W. Rees, *Chem. Commun.*, 1967, 1230–1231.

42 J. S. McConaghy and W. Lwowski, *J. Am. Chem. Soc.*, 1967, **89**, 2357–2364.

43 R. S. Atkinson, *Tetrahedron*, 1999, **55**, 1519–1559.

44 L. B. Krasnova, R. M. Hili, O. v Chernoloz and A. K. Yudin, *Arkivoc*, 2004, **2005**, 26–38.

45 R. S. Atkinson and B. J. Kelly, *J. Chem. Soc. Chem. Commun.*, 1987, **2**, 1362–1363.

46 P. S. Skell and R. C. Woodworth, *J. Am. Chem. Soc.*, 1957, **79**, 6577.

47 R. S. Atkinson and C. W. Rees, *J. Chem. Soc. C*, 1969, 772–778.

48 D. W. Jones, *J. Chem. Soc. Chem. Commun.*, 1972, 884.

49 R. S. Atkinson, M. Grimshire, B. J. Kelly and D. O. Chemistry, *Tetrahedron*, 1989, **45**, 2875–2886.

50 Paul. D. Bartlett, *Rec. Chem. Prog.*, 1950, **11**, 45–51.

51 R. S. Atkinson and P. J. Williams, *J. Chem. Soc., Perkin Trans. 2*, 1996, 205.

52 R. S. Atkinson and J. R. Malpass, *J. Chem. Soc. Perkin 1*, 1977, 2242–2249.

53 R. S. Atkinson, J. Fawcett, D. R. Russell and P. J. Williams, *Tetrahedron Lett.*, 1995, **36**, 3241–3244.

54 R. S. Atkinson and Brian. D. Judkins, *J. Chem. Soc. Perkin 1*, 1981, **1**, 2615–2619.

55 K. M. Gillespie, E. J. Crust, R. J. Deeth and P. Scott, *Chem. Commun.*, 2001, 785–786.

56 A. Subbarai, O. S. Rao and W. Lwowski, *J. Org. Chem.*, 1989, **54**, 3945–3952.

57 R. S. Atkinson, M. P. Coogan and I. S. T. Lochrie, *J. Chem. Soc. Perkin 1*, 1997, 897–900.

58 R. S. Atkinson, M. P. Coogan and C. L. Cornell, *J. Chem. Soc. Perkin 1*, 1996, 157.

59 R. S. Atkinson, E. Barker and S. Ulukanli, *J. Chem. Soc. Perkin 1*, 1998, **3**, 583–590.

60 S. Ulukanli, S. Karabuga, A. Celik and C. Kazaz, *Tetrahedron Lett.*, 2005, **46**, 197–199.

61 R. S. Atkinson and R. Martin, *J. Chem. Soc. Chem. Commun.*, 1974, **10**, 386–388.

62 Merck Structure Search. Available at: https://www.sigmaaldrich.com/GB/en/structure-search (Accessed 20 March 2023)

63 R. Appel and O. Buchner, *Angew. Chem.*, 1962, **74**, 430–431.

64 M. Goswami, V. Lyaskovskyy, S. R. Domingos, W. J. Buma, S. Woutersen, O. Troeppner, I. Ivanović-Burmazović, H. Lu, X. Cui, X. P. Zhang, E. J. Reijerse, S. DeBeer, M. M. van Schooneveld, F. F. Pfaff, K. Ray and B. de Bruin, *J. Am. Chem. Soc.*, 2015, **137**, 5468–5479.

65 S. O. Scholz, E. P. Farney, S. Kim, D. M. Bates and T. P. Yoon, *Angew. Chem. Int. Ed.*, 2016, **55**, 2239–2242.

66 T. Ando, S. Minakata, I. Ryu and M. Komatsu, *Tetrahedron Lett.*, 1998, **39**, 309–312.

67 W. Lee, H. J. Jeon, H. Jung, D. Kim, S. Seo and S. Chang, *Chem.*, 2021, **7**, 495–508.

68 T. Ando, D. Kano, S. Minakata, I. Ryu and M. Komatsu, *Tetrahedron*, 1998, **54**, 13485–13494.

69 H. Wu, L. Xu, C. Xia, J. Ge and L. Yang, *Synth. Commun.*, 2005, **35**, 1413–1417.

70 L. Simkhovich and Z. Gross, *Tetrahedron Lett.*, 2001, **42**, 8089–8092.

71 D. K. Wolgemuth, S. D. Elmore, J. D. Cope, P. E. Sheridan, S. L. Stokes and J. P. Emerson, *Catal. Commun.*, 2021, **150**, 106275.

72 M. J. Zdilla and M. M. Abu-Omar, *J. Am. Chem. Soc.*, 2006, **128**, 16971–16979.

73 R. Vyas, Bhanu. M. Chanda and A. v. Bedekar, *Tetrahedron Lett.*, 1998, **39**, 4715–4716.

74 B. M. Chanda, R. Vyas and A. v. Bedekar, *J. Org. Chem.*, 2001, **66**, 30–34.

75 Y. Yamada, T. Yamamoto and M. Okawara, *Chem. Lett.*, 1975, **4**, 361–362.

76 S. L. Jain, V. B. Sharma and B. Sain, *Tetrahedron Lett.*, 2004, **45**, 8731–8732.

77 B. D. Heuss, M. F. Mayer, S. Dennis and M. M. Hossain, *Inorganica Chim. Acta*, 2003, **342**, 301–304.

78 D. Mansuy, J.-P. Mahy, A. Dureault, G. Bedi and P. Battioni, *J. Chem. Soc. Chem. Commun.*, 1984, 1161.

79 X. Riart-Ferrer, P. Sang, J. Tao, H. Xu, L.-M. Jin, H. Lu, X. Cui, L. Wojtas and X. P. Zhang, *Chem.*, 2021, **7**, 1120–1134.

80 Y. Cui and C. He, *J. Am. Chem. Soc.*, 2003, **125**, 16202–16203.

81 A. K. Mishra, M. M. Olmstead, J. J. Ellison and P. P. Power, *Inorg. Chem.*, 1995, **34**, 3210–3214.

82 Merck, https://www.sigmaaldrich.com/united-kingdom.html, (Accessed 30 August 2019).

83 I. D. G. Watson, L. Yu and A. K. Yudin, *Acc. Chem. Res.*, 2006, **39**, 194–206.

84 J. Li, P. W. H. Chan and C.-M. Che, *Org. Lett.*, 2005, **7**, 5801–5804.

85 A. Bakthavachalam, H.-C. Chuang and T.-H. Yan, *Tetrahedron*, 2014, **70**, 5884–5894.

86 S. Minakata, Y. Morino, Y. Oderaotoshi and M. Komatsu, *Chem. Commun.*, 2006, 3337.

87 K. Matsuzawa, Y. Nagasawa, E. Yamaguchi, N. Tada and A. Itoh, *Synthesis*, 2016, **48**, 2845–2850.

88 T. Siu, C. J. Picard and A. K. Yudin, *J. Org. Chem.*, 2005, **70**, 932–937.

89 T. Siu and A. K. Yudin, *J. Am. Chem. Soc.*, 2002, **124**, 530–531.

90 J. Hine, *J. Am. Chem. Soc.*, 1950, **72**, 2438–2445.

91 H. Wynberg, *Chem. Rev.*, 1960, **60**, 169–184.

92 H. Wynberg and Egbert. W. Meijer, *Org. React.*, 2004, **28**, 1–36.

93 M.-M. Xu, W.-B. Cao, X.-P. Xu and S.-J. Ji, *Chem. Commun.*, 2018, **54**, 12602–12605.

94 K. Wu, C. Fang, S. Kaur, P. Liu and T. Wang, *Synthesis*, 2018, **50**, 2897–2907.

95 R. H. Bahekar, M. R. Jain, A. Goel, D. N. Patel, V. M. Prajapati, A. A. Gupta, P. A. Jadav and P. R. Patel, *Bioorg. Med. Chem.*, 2007, **15**, 3248–3265.

96 A. Pews-Davtyan, A. Tillack, A.-C. Schmöle, S. Ortinau, M. J. Frech, A. Rolfs and M. Beller, *Org. Biomol. Chem.*, 2010, **8**, 1149.

97 R. Romagnoli, P. G. Baraldi, T. Sarkar, M. D. Carrion, C. L. Cara, O. Cruz-Lopez, D. Preti, M. A. Tabrizi, M. Tolomeo, S. Grimaudo, A. Di Cristina, N. Zonta, J. Balzarini, A. Brancale, H.-P. Hsieh and E. Hamel, *J. Med. Chem.*, 2008, **51**, 1464–1468.

98 J. Lavrado, K. Gani, P. A. Nobre, S. A. Santos, P. Figueiredo, D. Lopes, V. do Rosário, J. Gut, P. J. Rosenthal, R. Moreira and A. Paulo, *Bioorg. Med. Chem. Lett.*, 2010, **20**, 5634–5637.

99 E. Arzel, P. Rocca, P. Grellier, M. Labaeïd, F. Frappier, F. Guéritte, C. Gaspard, F. Marsais, A. Godard and G. Quéguiner, *J. Med. Chem.*, 2001, **44**, 949–960.

100 E. Vedejs and H. Sano, *Tetrahedron Lett.*, 1992, **33**, 3261-3264.

101 R. S. Atkinson and B. D. Judkins, *J. Chem. Soc. Chem. Commun.*, 1979, **19**, 832-833.

102 W. L. F. Armarego and J. I. C. Smith, *J. Chem. Soc. B*, 1967, 449-454.

103 S. S. Kulkarni, S. Singh, Janki. R. Shah, W.-K. Low and T. T. Talele, *Eur J. Med. Chem.*, 2012, **50**, 264–273.

104 Q. Zhang, Y. Li, B. Zhang, B. Lu and J. Li, *Bioorg. Med. Chem. Lett.*, 2017, **27**, 4885–4888.

105 G. Chelucci and S. Figus, *J. Mol. Catal. A Chem.*, 2014, **393**, 191–209.

106 R. M. Peltzer, J. Gauss, O. Eisenstein and M. Cascella, *J. Am. Chem. Soc.*, 2020, **142**, 2984–2994.

107 J. Ranjith and H.-J. Ha, *Molecules*, 2021, **26**, 1774.

108 E. Beckmann, *Ber. Dtsch. Chem. Ges.*, 1886, **19**, 988–993.

109 J. S. Zhang, K. Wang, Y. C. Lu and G. S. Luo, *Reactors, Kinetics and Catalysis*, 2011, **58**, 925–931.

110 T. Sahyoun, A. Arrault and R. Schneider, *Molecules*, 2019, **24**, 2470.

111 R. E. Gawley, *Org. React.*, 1988, **35**, 1–60.

112 S. Nsikabaka, W. Harb and M. F. Ruiz-López, *Journal of Molecular Structure (Theochem)*, 2006, **764**, 161–166.

113 W. Z. Heldt, *J. Org. Chem.*, 1961, **26**, 1695–1702.

114 J. Gálves and A. Guirado, *J. Comput. Chem.*, 2010, **31**, 520–531.

115 P. Yan, P. Batamack, G. K. Surya Prakash and G. A. Olah, *Catal. Letters*, 2005, **103**, 165–168.

116 C. J. Collins, *Q. Rev. Chem. Soc.*, 1960, **14**, 357–377.

117 S. Yamabe, N. Suchida and S. Yamazaki, *J. Org. Chem.*, 2005, **70**, 10638–10644.

118 K. Hattori, Y. Matsumura, T. Miyazaki, K. Maruoka and H. Yamamoto, *J. Am. Chem. Soc.*, 1981, **103**, 7368–7370.

119 T. Yokomatsu, Y. Yoshida, N. Nakabayashi and S. Shibuya, *J. Org. Chem.*, 1994, **59**, 7562–7564.

120 S. Sakane, Y. Matsumura, Y. Yamamura, Y. Ishida, K. Maruoka and H. Yamamoto, *J. Am. Chem. Soc.*, 1983, **105**, 672–674.

121 K. Kaur and S. Srivastava, *New J. Chem.*, 2020, **44**, 18530–18572.

122 K. Maruoka, T. Miyazaki, M. Ando, Y. Matsumura, S. Sakane, K. Hattori and H. Yamamoto, *J. Am. Chem. Soc.*, 1983, **105**, 2831–2843.

123 J. Yeon Shin, D. Jung Jung and S. Lee, *ACS Catal.*, 2013, **3**, 525–528.

124 V. K. Tandon, A. K. Awasthi, H. K. Maurya and P. Mishra, *J. Heterocycl. Chem.*, 2012, **49**, 424–427.

125 C. Ramalingan and Y.-T. Park, *J. Org. Chem.*, 2007, **72**, 4536–4538.

126 L. Tang, Z.-L. Wang, Y.-H. He and Z. Guan, *ChemSusChem*, 2020, **13**, 4929–4936.

127 G. Heller, *Ber. Dtsch. Chem. Ges.*, 1916, **49**, 2757–2774.

128 A. Reißert and K. Hessert, *Ber. Dtsch. Chem. Ges.*, 1924, **57**, 964–972.

129 Z. Wang, C. Wang, Y. Sun, N. Zhang, Z. Liu and J. Liu, *Tetrahedron*, 2014, **70**, 906–913.

130 S. Mahajan, N. Slathia and K. K. Kapoor, *Tetrahedron Lett*, 2020, **61**, 151859.

131 A. P. Stankevicius, P. B. Terentiev, L. N. Yanushiene and P. V. Vainauskas, *Chem. Heterocycl. Compd.*, 2003, **39**, 1645–1646.

132 E. W. . Colvin, S. Malchenko, R. A. Raphael and J. S. Roberts, *J. Chem. Soc. Perkin 1*, 1973, **18**, 1989–1997.

133 M. S. Laxmisha and G. S. R. Subba Rao, *Tetrahedron Lett.*, 2000, **41**, 3759–3761.

134 J. Basran, I. Efimov, N. Chauhan, S. J. Thackray, J. L. Krupa, G. Eaton, G. A. Griffith, C. G. Mowat, S. Handa and E. Lloyd Raven, *J. Am. Chem. Soc.*, 2011, **133**, 16251–16257.

135 B. Witkop and G. Graser, *Liebigs Ann. Chem.*, 1944, **556**, 103–114.

136 J. Xu, L. Liang, H. Zheng, Y. R. Chi and R. Tong, *Nat Commun*, 2019, **10**, 4754.

137 E. Winterfeldt, *Liebigs Ann. Chem.*, 1971, **745**, 23–30.

138 K. C. Harper, E. G. Moschetta, S. v. Bordawekar and S. J. Wittenberger, *ACS Cent. Sci.*, 2019, **5**, 109–115.

139 K. Maeda, T. Mishima and T. Hayashi, *Bull. Chem. Soc. Jpn.*, 1974, **47**, 334–338.

140 J. Jurczyk, J. Woo, S. F. Kim, B. D. Dherange, R. Sarpong and M. D. Levin, *Nat. Synth.*, 2022, **1**, 352–364.

141 C. W. Williams, R. Shenje and S. France, *J. Org. Chem.*, 2016, **81**, 8253–8267.

142 M. Tredwell, S. M. Preshlock, N. J. Taylor, S. Gruber, M. Huiban, J. Passchier, J. Mercier, C. Génicot and V. Gouverneur, *Angew. Chem. Int. Ed.*, 2014, **53**, 7751–7755.

143 J. Zhou, P. Hu, M. Zhang, S. Huang, M. Wang and W. Su, *Chem. Eur. J.*, 2010, **16**, 5876-5881.

144 J. E. Jakobsson, G. Grønnevik and P. J. Riss, *Chem. Commun.*, 2017, **53**, 12906-12909.

145 Y. Yi, Z. Fan and C. Xi, *Green Chemistry*, 2022, **24**, 7894–7899.

146 V. Soni, U. N. Patel and B. Punji, *RSC Adv.*, 2015, **5**, 57472-57481.

147 K. Nemoto, S. Tanaka, M. Konno, S. Onozawa, M. Chiba, Y. Tanaka, Y. Sasaki, R. Okubo and T. Hattori, *Tetrahedron*, 2016, **72**, 734-745.

148 L. Li, K. Yuan, Q. Jia and Y. Jia, *Angew. Chem. Int. Ed.*, 2019, **58**, 6074–6078.

149 S. Isao and Y. Katsumi, *Bull. Chem. Soc. Jpn.*, 1986, **59**, 2017–2018.

150 W.-T. Wei, W.-M. Zhu, W.-W. Ying, Y. Wu, Y.-L. Huang and H. Liang, *Org. Biomol. Chem.*, 2017, **15**, 5254–5257.

6 C–S Cross-Coupling in Micellar Solution – An Introduction

Abstract

The prominence of thiophenols and their derivatives in biologically active substances is tarnished by their often toxic, malodourous and air-sensitive nature. Previous research in the Ball group highlighted the use of isothiouronium salts as crystalline, odourless and bench-stable thiophenol surrogates. This work involved the Ni-catalysed cross-coupling of aryl iodides with thiourea in *N*-methyl-2-pyrrolidone (NMP). However, NMP is now a restricted substance by REACH regulations due to its substantial reproductive toxicity. We endeavoured to find a green alternative.

Micelle solutions have previously been used to facilitate metal-catalysed cross-coupling reactions, allowing for use of water as the bulk solvent. The work reported in this thesis demonstrates that this benign solvent system can be applied to the C–S cross-coupling reaction previously investigated in the Ball group. The solvent system was investigated, and co-solvents were utilised to improve yields. The selection and proportion of co-solvent has a substantial impact on the outcome of the reaction. The effects of co-solvent on micelle structure was investigated using dynamic light scattering (DLS) to determine average micelle diameter.

Due to the large number of variables involved in this method, the process of reaction optimisation was expedited by use of Design of Experiments (DoE), facilitated by Catalysis Consulting. An isolation procedure was developed then used in a substrate scope, which highlighted the wide range of functional groups tolerated by this method. Finally, the observed generation of aryl phosphonium salts as a side-product of this reaction prompted some initial mechanistic studies.

6.1 Introduction

Thiophenol derivatives are important motifs in the pharmaceutical,[1,2] agrochemical[3] and organic electronics industries.[4] Some compounds of note are indicated in **Figure 51**.

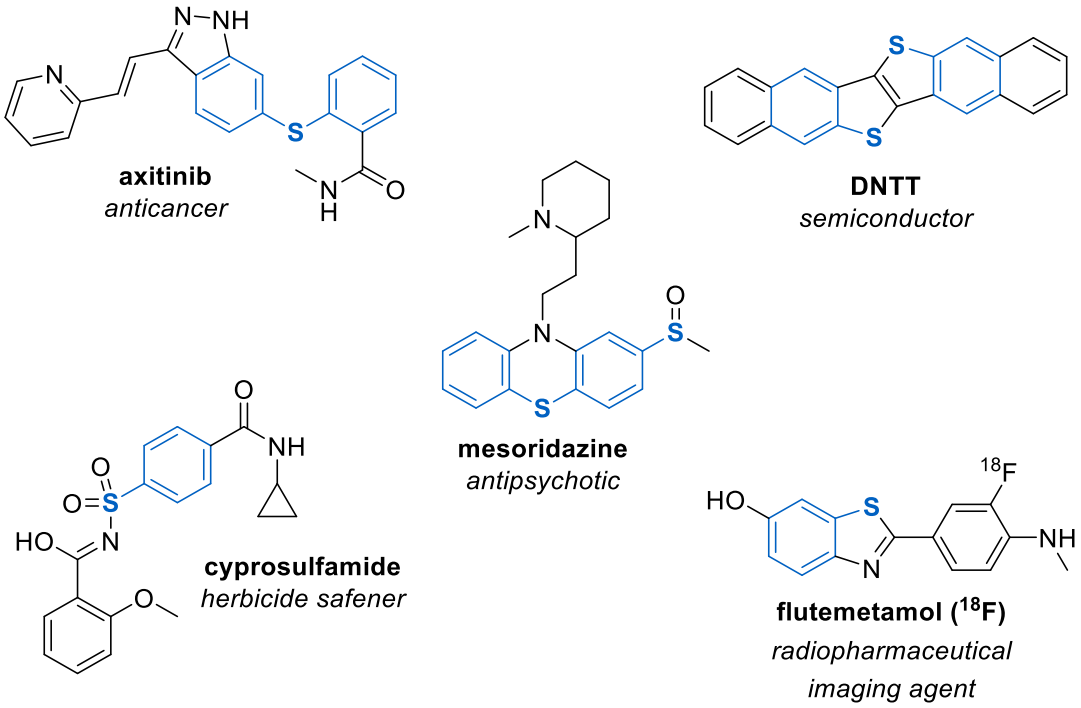


Figure 51 – Thiophenol substructures in compounds of importance.

The range of oxidation states available to sulfur results in a large library of sulfur-based functional groups. When designing a route to a desired sulfur-containing product, a possible starting material can be a thiophenol. As shown in **Figure 52**, thiophenols can be derivatised to sulfonamides, sulfonyl chlorides, sulfones and sulfoxides.[5,6] Thiols can take part in S_NAr reactions, for example with 2-halopyridines.[7] Aryl alkyl thioethers can be obtained from the respective alkyl bromides *via* a nucleophilic substitution reaction.[8] Diaryl thioethers can be obtained through a variety of metal-catalysed cross-coupling tactics, such as Migita[9] or Ullmann-type[10] cross-couplings.

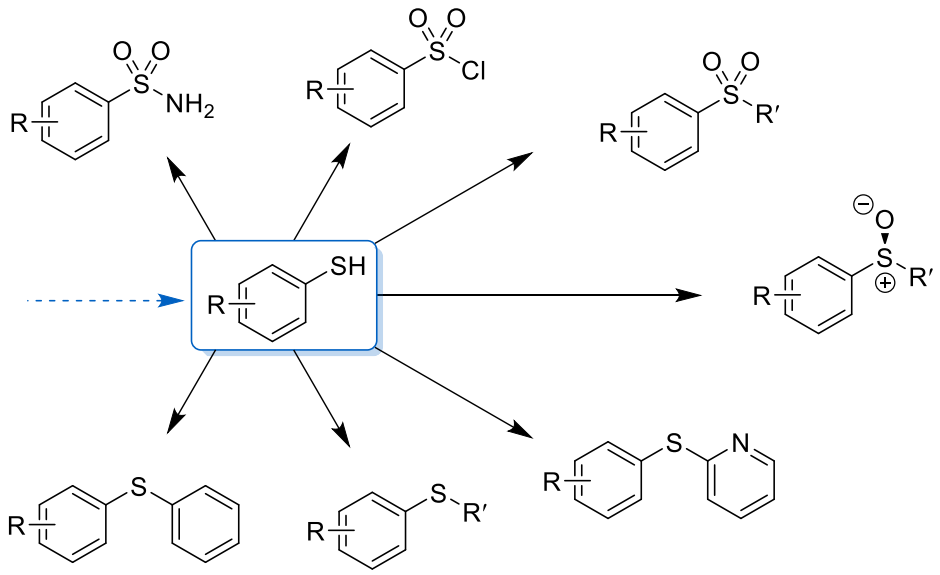


Figure 52 – The various sulfur functional groups accessible from thiophenol as a universal precursor.

However, there are a variety of issues associated with the use of thiophenol as a starting material. Thiophenols are often toxic, have a pungent odour, and are easily oxidised in air to the corresponding disulfide.[11] Additionally, thiols are known to poison metal-catalysts.[12] Despite their synthetic utility, thiophenols have relatively limited commercial availability. For example, using Merck's structure search function, a search for thiophenol substructures gave 74 results as opposed to the 664 obtained for the isoelectronic phenol substructure. As a result, access to thiophenols often requires *de novo* synthesis which can be both costly and onerous. Furthermore, the factors mentioned above have resulted in reduced synthetic options in comparison with phenols.[13] In the following section, a variety of available thiophenol syntheses will be discussed.

6.2 Thiophenol Synthesis

This section will focus on methods for the synthesis of thiophenols that involve C–S bond formation. Though it should be noted that thiophenols can be accessed by reduction of higher oxidation states such as sulfonyl chlorides,[14] this ultimately requires the preparation of the sulfonyl chloride functional group. This, in turn, requires C–S bond formation. In these C–S bond forming reactions, the choice of sulfur source is a challenge to

researchers. As mentioned in the section above, use of thiols as a sulfur source has a variety of disadvantages.[11] In the remainder of this section, aryl-S forming reactions have been organised on the basis of the sulfur source used: inorganic, thiol-based and thiocarbonyl-based sources.

6.2.1 Inorganic Sulfur Sources

Elemental sulfur, S_8, is the simplest of sulfur sources and is readily available commercially.[15] This has been used as a sulfur source in the copper-catalysed C–S bond-forming reaction reported by Jiang and co-workers in 2009 (**Figure 53a**).[16] The polysulfide product of this reaction can then be converted into the thiophenol on treatment with either $NaBH_4$ or an acidic PPh_3 solution. Though this route uses a convenient sulfur source, the conditions used in the release of the thiophenol functionality would not be applicable to a wide range of functional groups. Furthermore, the generation of Ph_3PS as a by-product will negatively impact atom economy and leads to the requirement of additional purification steps. To avoid this, the polysulfide can be used directly in further functionalisation reactions.[17]

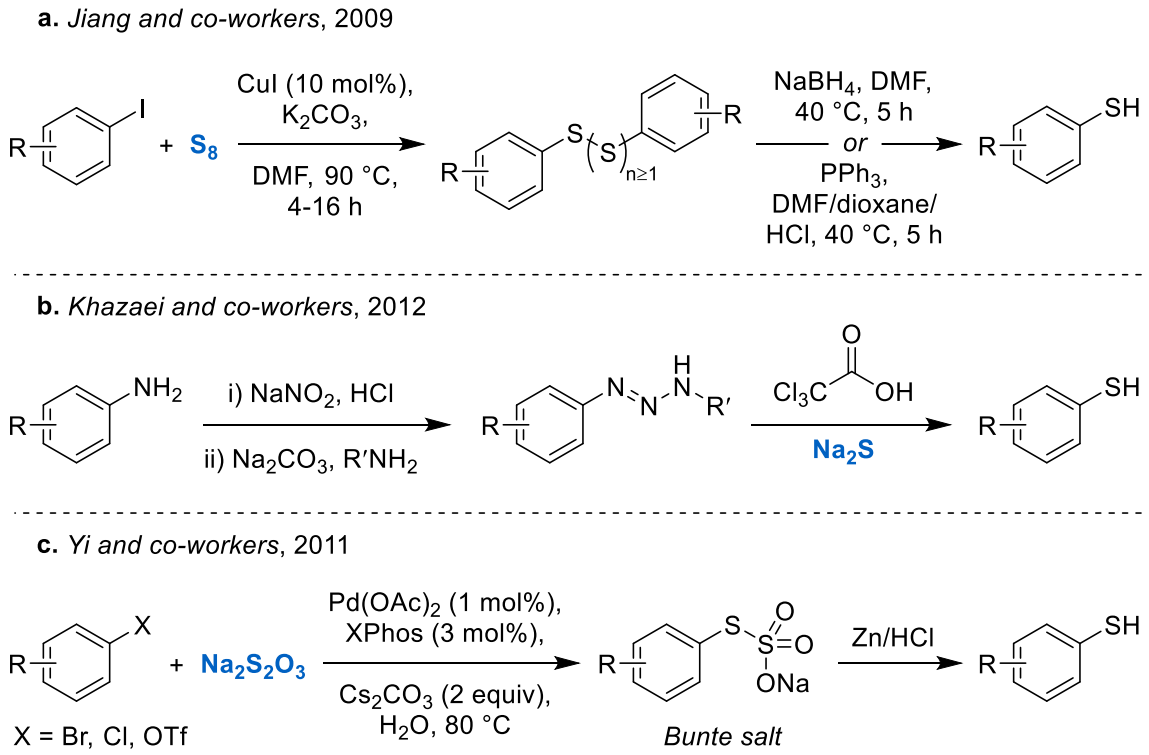


Figure 53 – Use of inorganic sulfur sources in the synthesis of thiophenols.

Sulfide salts are also relatively simple sulfur sources, with salts such as Na_2S being used in paper processing. Khazaei and co-workers reported a route from anilines to thiophenols using Na_2S as their sulfur source (**Figure 53b**).[18] They initially formed diazonium salts, which were then treated with primary amines and isolated as the more stable substituted triazenes. This is followed by the one-pot acid-catalysed regeneration of the diazonium salt then reaction with hydrogen sulfide, generated from reaction of Na_2S with acid. However, this route comes with substantial hazards. Firstly, diazonium salts are known explosion hazards.[19] Furthermore, the H_2S gas generated from Na_2S is toxic and malodourous. Other sulfur salts such as $Na_2S_2O_3$ can be used as milder alternatives, as shown in the work by Yi and co-workers in 2011 (**Figure 53c**).[20] This is a 2-step process that involved the formation of a Bunte salt[21] from an aryl halide then the reduction to the thiol species. Akin to the route shown in **Figure 53a**, the final step involves a relatively strong reductant that results in poor functional group tolerance. As with this previous example, these Bunte salts can be used directly in diversification reactions such as the addition of Grignard reagents to form thioethers.[22]

6.2.2 Thiols and Thiolate Salts

Although thiols themselves are difficult to work with, some modifications can be made to improve the handling of these reagents. Shaw utilised sodium 1-propanethiolate, a less toxic and less volatile analogue of 1-propanethiol, in their transition metal-free route to thiophenols (**Figure 54a**).[23] This is also possible with sodium methylthiolate.[24] These routes do, however, still rely on thiols in the formation of the thiolate salt, and generate sulfides as malodourous co-products. The route reported by Shaw is also sensitive to water and required thorough drying of all reagents to obtain good yields.

The unpleasant odour emitted by thiols can be reduced by use of higher molecular weight thiols with lower volatility, as used by Itoh and Mase (**Figure 54b**).[25] Here, they used 2-ethylhexyl 3-mercaptopropionate, which is not malodourous,[26] in a Pd-catalysed Migita-type coupling.[27] The isolatable thioethers can then go through a base-catalysed retro-Michael elimination to release the thiophenol moiety. One can think of these thioethers as a base-sensitive protecting group for other transformations around the ring.[28] Alternatively, the thiophenol can be released *in situ*, hence avoiding exposure to the toxic and malodourous compound. They can thus be used as thiophenol surrogates when accessing other sulfur functional groups, for example in the one-pot synthesis of diaryl thioethers.[29,30] Unfortunately, the synthesis proposed by Itoh and Mase for this thiophenol surrogate utilises high temperatures and, though the larger thiol gives the advantages noted above, it negatively impacts the atom economy. Furthermore, each step requires column chromatography which is both wasteful and unpleasant for thiols and their alkyl ethers.

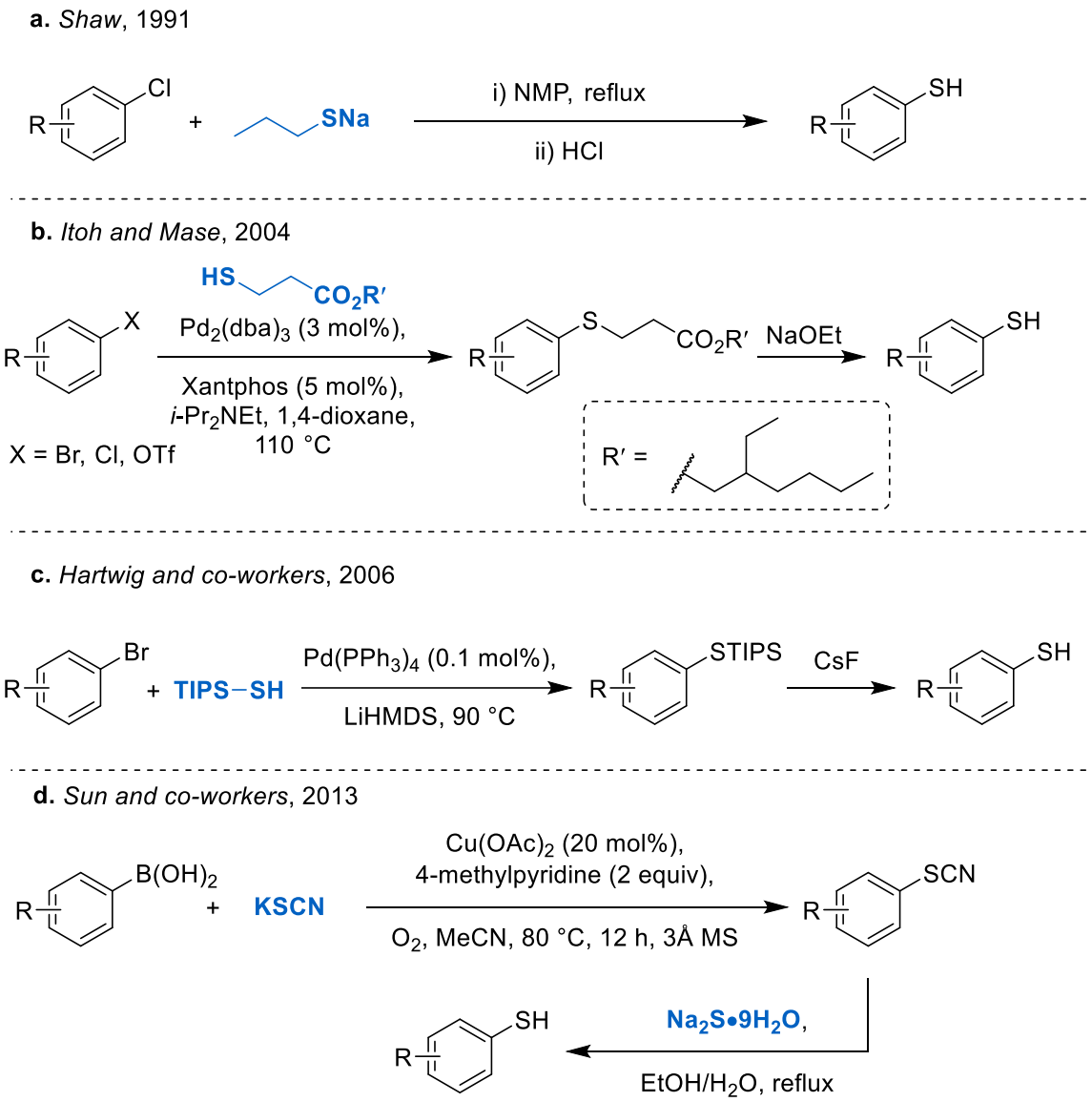


Figure 54 – Use of thiols and thiolate salts in the synthesis of thiophenols.

The concept of thiophenol surrogates was explored further by Hartwig and co-workers in 2006 (**Figure 54c**),[31] inspired by the synthesis of a TIPS-protected thiophenol reported by Kreis and Bräse.[32] These air-stable surrogates are synthesised through a palladium-catalysed cross-coupling of aryl bromides with triisopropylsilanethiol (TIPS-SH). A similar transformation can also be carried out on aryl triflates.[33] The TIPS-protected thiophenols can then be deprotected using fluoride sources such as caesium fluoride. Akin to the surrogate reported by Itoh and Mase, this too can be used directly in the formation of diaryl thioethers, releasing the thiophenol *in situ*.[31] Again, this route does required high temperatures to achieve the desired yields. Additionally, a strong base is required, and the

sulfur source is expensive when purchased on scale and is reported to give off a foul odour.[34]

A more economical sulfur source was used by Sun and co-workers in their Cu-catalysed synthesis of aryl thiocyanates from the corresponding boronic acids (**Figure 54d**). The use of copper as a catalyst is a greener option than the previously mentioned palladium catalysts. Unfortunately, the deprotection of this surrogate is not as convenient. Sun and co-workers used the sodium sulfide sulfur source discussed previously which generates hydrogen sulfide in protic environments. An alternative deprotection method is treatment with $LiAlH_4$ which comes with its own disadvantages, especially in terms of functional group tolerance.[35] However, aryl thiocyanates have been widely used as thiophenol surrogates in a variety of diversification reactions.[36–39]

6.2.3 Thiocarbonyl and Thioester Sources

Utilising thiocarbonyl sulfur sources in the C–S bond forming step of thiophenol syntheses often gives stabilised, isolatable species. The innate reactivity of carbonyl structures also enables milder deprotection methods through simple hydrolysis. Such routes will be discussed in this section. One of the first recorded thiophenol C–S bond forming reactions involved the use of a thiocarbonyl, namely a xanthate, as its sulfur source (**Figure 55a**). In the original paper by Leuckart, the later-named Leuckart thiophenol synthesis gently heats aryl diazonium salts with potassium ethyl xanthate.[40] As referenced in Section 6.2.1, diazonium salts are known to be explosive. Further papers have been published on this route that instead use aryl boronic acids[41] and aryl halides[42] as more suitable starting materials. Both updated methods do however utilise copper catalysts and high temperatures.

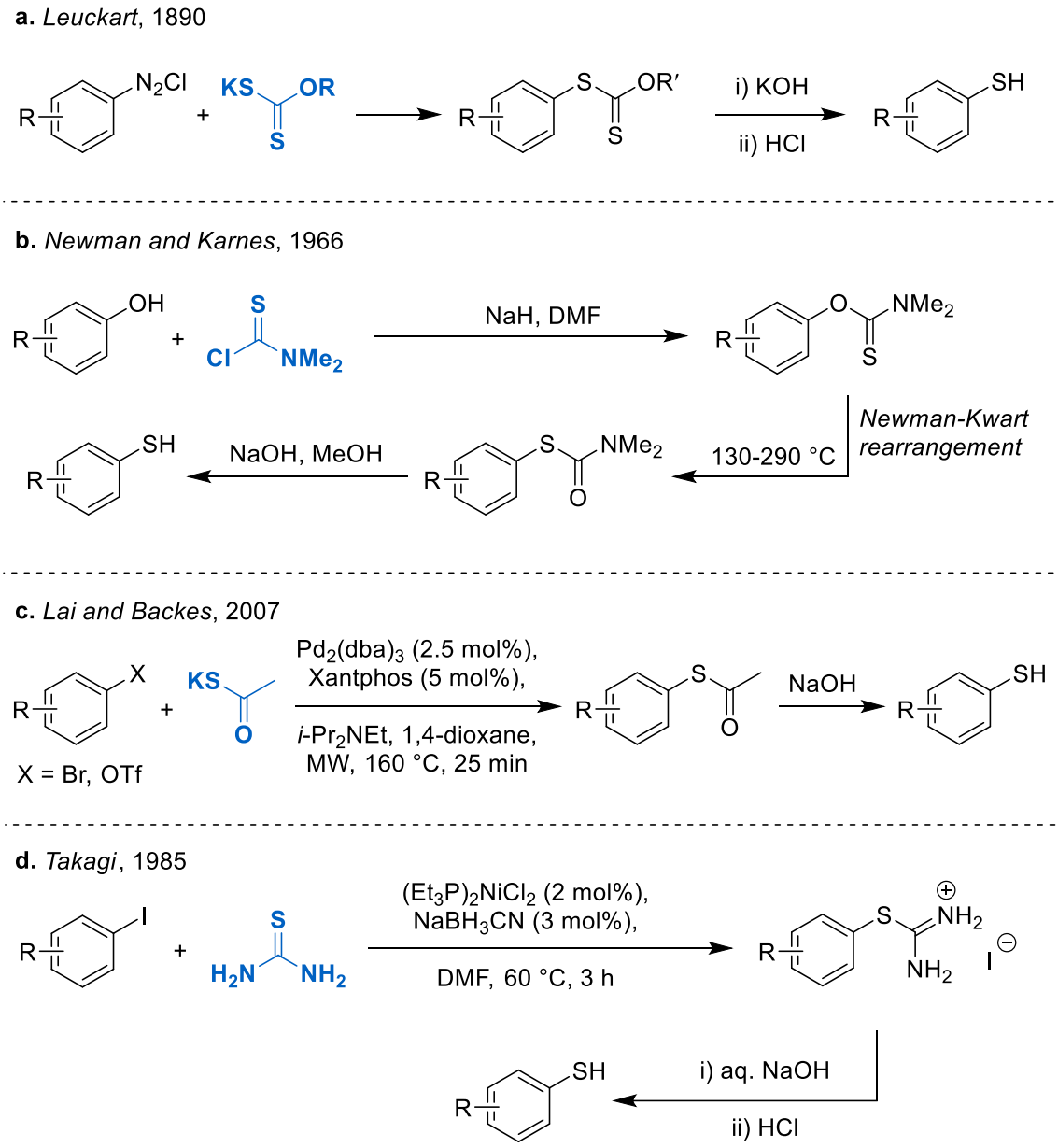


Figure 55 – Use of thiocarbonyls in the synthesis of thiophenols.

Another named reaction in the library of standard aryl C–S forming reactions is the Newman-Kwart rearrangement (**Figure 55b**).[43] Dimethylthiocarbamoyl chloride is the mild but relatively expensive sulfur source used in the initial synthesis of *O*-aryl thiocarbamates from phenols. Next follows a thermally induced rearrangement to the more thermodynamically stable *S*-aryl thiocarbamate. The often extremely high temperature required for this transformation – particularly for electron-rich phenol derivatives – is a disadvantage of this route. This has been overcome in recent years using Pd-catalysis,[44]

photocatalysis[45] and electrocatalysis.[46] The thiophenol functionality can then be released by hydrolysis.

Following the discussion of a TIPS-protected thiophenol in the prior sub-section, thioacetates can also be utilised to pre-install protecting groups during thiophenol synthesis (**Figure 55c**).[47] These do indeed act as thiophenol surrogates and undergo direct functionalisation of the sulfur group.[48–50] Once again, this route is disadvantaged by high temperature requirements, though with microwave-assisted short reaction times. The method reported by Lai and Backes tolerated some electron-withdrawing and electron-donating groups.[47] Two identified incompatibilities were -NHCBz and -NO_2 substituents due to either decomposition or unwanted side-reactivity. An additional weakness of this route is the malodourous thioacetate starting material, which is also a skin sensitiser.

The final route mentioned in this sub-section was first published by Takagi in 1985.[51] They reported the Ni-catalysed cross-coupling of aryl iodides with thiourea at milder temperatures compared to the previously stated routes (**Figure 55d**). This method is also base-free and does not use, or produce, explosive diazonium salts. This route involves the formation of isothiouronium salts as air-stable, odourless, crystalline thiophenol surrogates. The isothiouronium salts synthesised in the first step have an advantage over the earlier mentioned thiophenol surrogates in that they are salts. Hence, they can be purified by precipitation from solution without the need for column chromatography. This same group went on to apply these conditions in the synthesis of 2-benzothiazolamines[52] and in a one-pot cross-coupling to give diaryl thioethers.[53] The reaction works well with aryl iodides but not with aryl chlorides; arylbromides are borderline cases, with electron-poor examples being suitable for the coupling. Various N-substitutions on thiourea are also effective,[54] but, from an atom-economy point of view, the parent (unsubstituted) thiourea is preferable. Though smaller in molecular weight and inexpensive, thiourea is a reprotoxic and carcinogenic substance. The toxic reductant used in this route could also cause issues with certain functional groups, as the authors did not report a successful transformation for easily reduced substances. Furthermore, sodium cyanoborohydride can be a source of hydrogen and sodium cyanide.[55,56]

The synthesis of isothiouronium salts in the manner reported by Takagi was further investigated by the Ball group, culminating in a publication in 2019 (**Figure 56**).[57] The

method designed by Magné and Ball had reduced catalyst loadings, a broad scope and a more benign reductant in comparison with Takagi's reported method.[51]

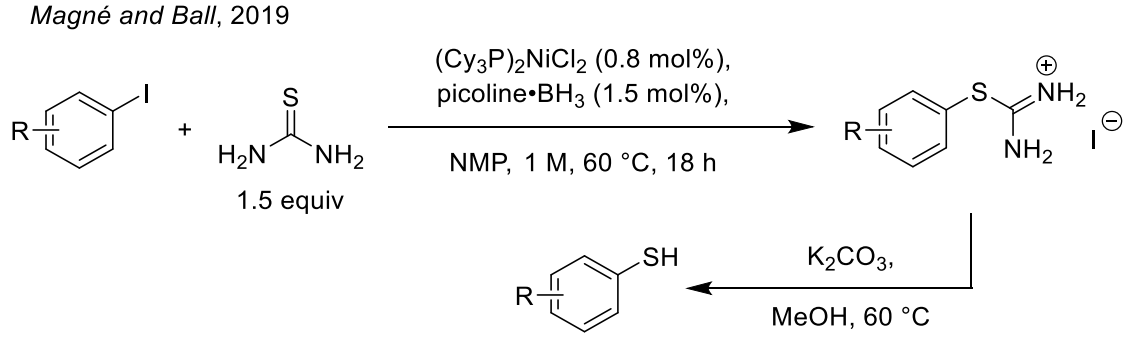


Figure 56 – Method for isothiouronium salt synthesis and subsequent deprotection reported by Magné and Ball.[57]

The work of Magné and Ball demonstrates a milder synthetic route to thiophenol surrogates which are odourless and easily isolated. The details of this method and the chemistry of isothiouronium salts in general will be discussed in the following section.

6.3 Isothiouronium Salts as Thiophenol Surrogates

This section will begin with a brief discussion on *S*-alkyl isothiouronium salts as these were first used to display how this functional group can be used as a thiol surrogate. One of the first reported uses of isothiouronium salts as a route to thiols came from Frank and Smith in 1946 (**Figure 57**).[58] They synthesised these salts in a harsh manner: heating alkyl alcohols at reflux with thiourea in concentrated hydrobromic acid. To this mixture, a solution of sodium hydroxide was added and refluxed further to give the thiol. Since then, milder methods were used as a route to thiols or as thiophenol surrogates from alcohols[59] and alkyl halides.[60,61] These often do not require metal catalysis as this is a simple S_N2, or occasionally S_N1, process.[62,63] A different approach is needed for the synthesis of aromatic thiols, such as the previously mentioned routes by Takagi and Magné and Ball.[57] Although these reports utilised catalysts based on earth-abundant nickel in their cross-coupling, the same transformation can also be achieved with Fe nanocomposites[64] and Cu(I) catalysts.[65] In addition to their potential as thiophenol surrogates, some *S*-aryl isothiouronium salts have shown activity as antimicrobial agents.[66]

Frank and Smith, 1946

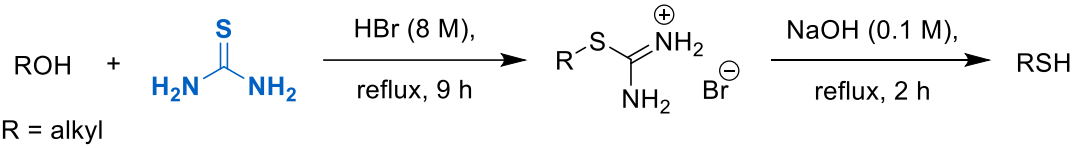


Figure 57 – Synthesis of S-alkyl isothiouronium salts.[58]

In this thesis, focus is given to the formation of aryl C–S bonds as a vital step in routes towards valuable compounds containing thiophenol derivatives. For the purpose of introducing the work reported in this thesis, the remainder of this section will focus on the work carried out by Magné and Ball as the current best-in-class for the synthesis of *S*-aryl isothiouronium salts.[57]

6.3.1 Works of Magné and Ball

In this initial report in 2019, the Ni-catalysed C–S cross-coupling of aryl iodides with thiourea was optimised as displayed in **Figure 58**.[57] $(Cy_3P)_2NiCl_2$ was used as the catalyst with a low catalyst loading of 0.8 mol%. The authors found that monodentate phosphine ligands gave better results than bidentate or non-phosphine ligands. Picoline borane complex was used to activate the catalyst and was also used in low amounts. During the process of optimisation, they carried out control reactions to test the robustness of their conditions. They found that carrying out the reaction in the absence of picoline borane or in the absence of catalyst resulted in no product formation. An anaerobic atmosphere is also vital to reactivity, as is common in Ni—catalysed systems.[57] Of the 25 solvents screened for this method, polar solvents worked best, with the best yields observed using NMP. The robustness of this transformation towards water was proven by using a 10% solution by volume of water in NMP. This did decrease yield but by less than 20%. Increasing the concentration of aryl iodide in the solution increased yields. The optimised conditions used 1 M solutions to reflect this, but without impacting reagent solubility.

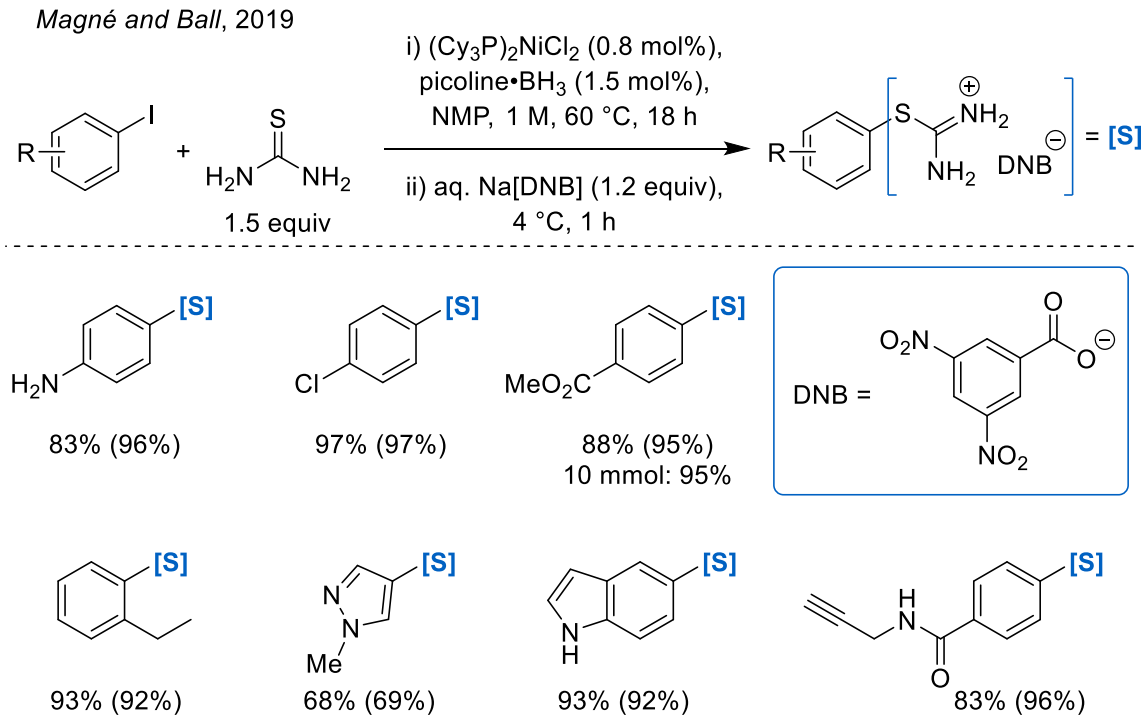


Figure 58 – Select scope from the publication by Magné and Ball in 2019.[57] Yields are reported as isolated yields, with yields in parenthesis calculated using NMR spectroscopy. Reactions were performed on a 1 mmol scale unless stated otherwise.

Isothiouronium iodide salts generated in the first step were unfortunately soluble in the chosen solvent – NMP. Precipitation of the desired compound was thus achieved through a subsequent anion metathesis step. Thermally stable and inexpensive sodium 3,5-dinitrobenzoate was added to the crude solution and the resulting isothiouronium salt precipitated out of solution in just 1 hour. This gave air, light and moisture-stable salts as odourless, free-flowing powders which are bench-stable for at least 4 years. The authors suggested that these salts could therefore be suitable for use in high-throughput experimentation.

These optimised reaction and isolation conditions were then used to synthesise 59 isothiouronium salts, some of which are highlighted in **Figure 58**.[57] Where the isolated yield was significantly lower than the yield calculated by NMR spectroscopic analysis of the crude reaction mixture, the authors suggested this is due to a generic isolation procedure being used as opposed to optimised conditions for that particular substrate. Magné and Ball have demonstrated that this reaction is scalable, with minimal change in yield between 1, 10 and 100 mmol scale. This reaction tolerates complex substrates with

multiple functional groups, including challenging heterocycles.[67] Though the scope is extensive, this method does not come without its limitations.

6.3.2 *Scope Limitations*

Aryl iodides, though commercially available, are the least commercially available of the aryl halides.[68] Aryl chlorides are unreactive under Magné and Ball's conditions,[57] as also reported by Takagi.[51] Fortunately, boronic esters and triflates are also tolerated in this reaction which allows for subsequent alternative cross-couplings. This route cannot claim chemoselectivity, however, as bromides can also cross-couple with thiourea under these conditions. Competition experiments carried out on 4-bromoiodobenzene revealed that the rate of C-I bond activation was roughly 10 times greater than C-Br activation (**Figure 59**). As a result of this, the authors were able to selectively cross-couple with the C-I bond by limiting thiourea concentrations.

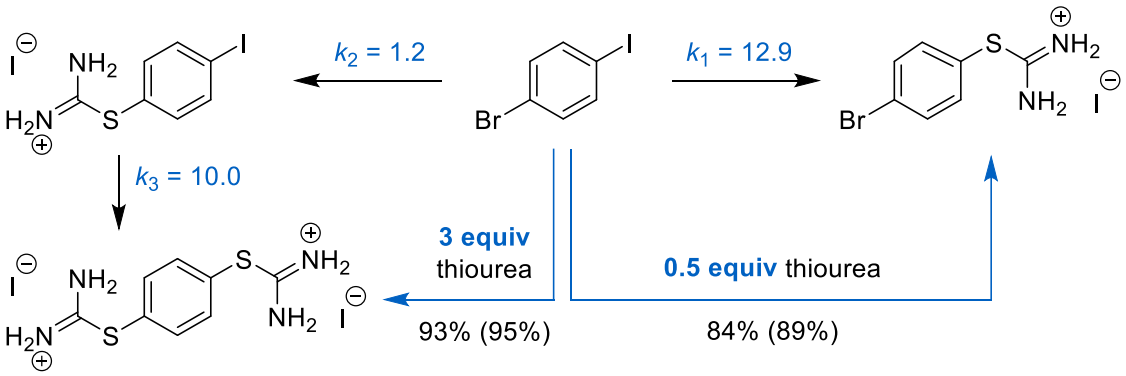


Figure 59 – Relative rates calculated for the cross-coupling of thiourea with each halide of 4-bromoiodobenzene under the standard reaction conditions: $(Cy_3P)_2NiCl_2$ (0.8 mol%), picoline borane (1.5 mol%), thiourea (1.5 equiv), NMP. Alterations to these conditions are displayed over the blue arrows, giving the indicated salts. Yields are reported as isolated yields, with yields in parenthesis calculated by NMR spectroscopy.[57]

Ortho-substitution provides a steric challenge for cross-coupling reactions.[69] These conditions give good to excellent yields for *o*-Me, *o*-OMe and *o*-Et substitution, but no conversion was observed with 2-iodomesitylene. Hence, steric hinderance is tolerated up to a point. Aliphatic amines are also incompatible with this method, likely due to being basic enough to convert the isothiouronium group prematurely to the thiophenol which can

then poison the metal catalyst.[12] This issue was solved by prior protonation of the amine, forming a salt which eliminated unwanted side-reactivity. Other substrate incompatibilities can give an insight into the currently unknown mechanism of the reaction.

6.3.3 Probing the Reaction Mechanism

Pd-catalysed cross-coupling reactions typically proceed through a Pd(0)/Pd(II) catalytic cycle (**Figure 60a**).[70] Nickel catalysts, however, do not always follow the same cycle due to their ability to easily access other oxidation states, such as Ni(I) and Ni(III).[71] The Ni-C bond has lower homolytic bond strength than Pd-C bonds[72] and therefore the likelihood of a radical pathway occurring is higher for Ni-catalysed cross-couplings.[73] Mechanistic research carried out by Zhang and co-workers into the Suzuki-Miyaura cross-coupling using $Ni(NHC)_n$ catalysts suggested the presence of an alternative catalytic cycle.[74] Their proposed mechanism, displayed in **Figure 60b**, involved a 2-electron Ni(I)/Ni(III) cycle. Initial activation of the catalyst was required through a radical-generating single-electron oxidation of Ni(0) to Ni(I). It is noted, however, that this cycle was proposed based on data from catalysts with more sterically demanding NHCs. When less sterically demanding NHCs were used, they proposed that a conventional Ni(0)/Ni(II) cycle was dominant. It has been observed that the mechanism of Ni-catalysed cross-couplings can be influenced by ligand selection,[75] steric demand[76] and substrate choice.[77] Its mechanistic malleability results in great difficulty when attempting to decipher the species involved in the catalytic cycle of any given Ni-catalysed system.

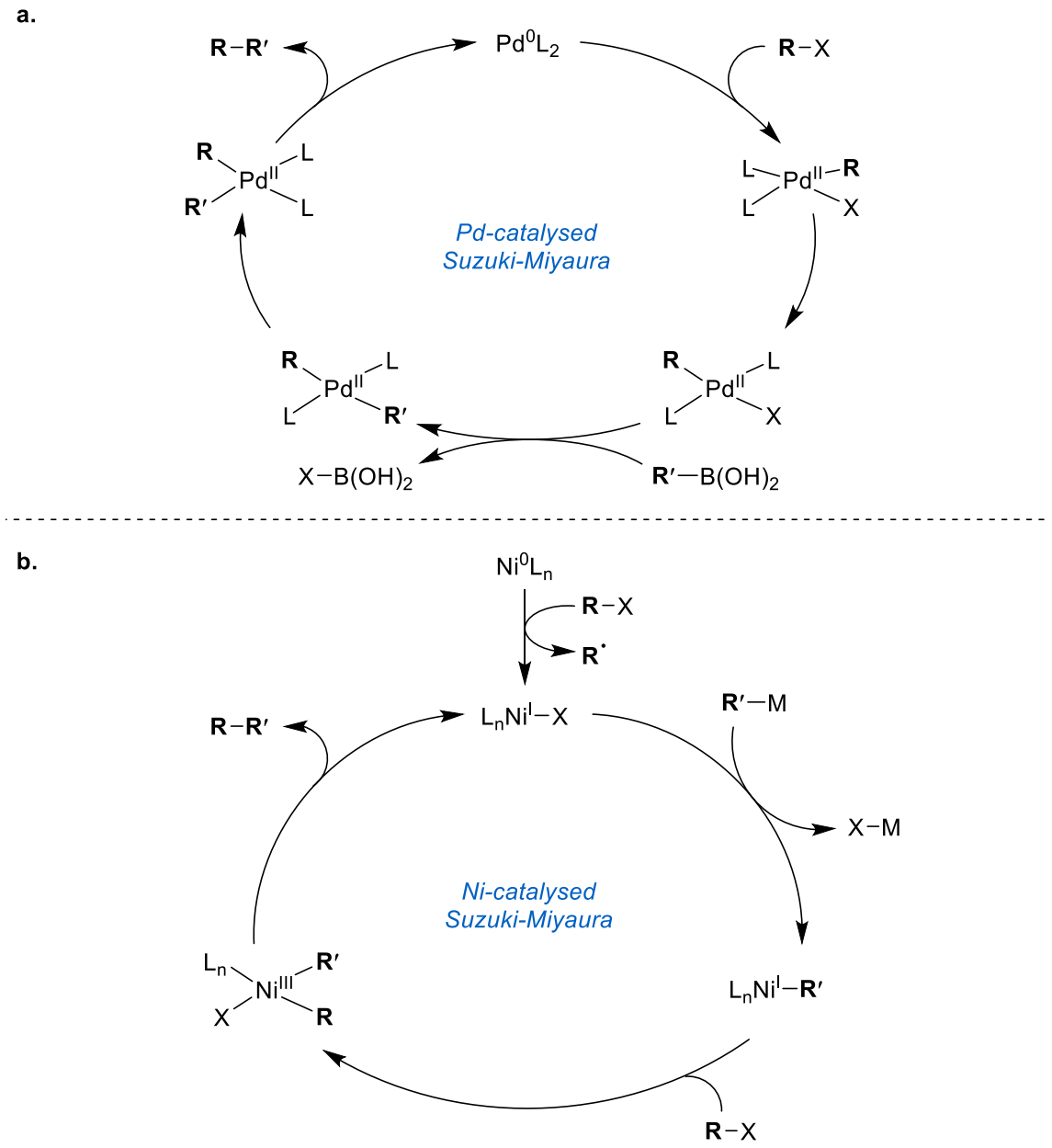


Figure 60 – The general mechanism for the Pd-catalysed Suzuki-Miyaura cross-coupling (a)[70] and the proposed mechanism for the Ni-catalysed Suzuki-Miyaura cross-coupling (b).[74]

The research reported by Ball and Magné presented some preliminary mechanistic investigations into the species present in the Ni-catalysed cross-coupling of aryl iodides with thiourea. Though the mechanism has not yet been deduced, these findings will now be discussed. From the substrate scope investigated, the substrates displayed in **Figure 61** proved incompatible with the reaction conditions. Both nitro[78] and azo[79] groups are known to act as radical sinks, suggesting the involvement of radical species. Alternatively,

nitro groups can undergo oxygen atom transfer with Ni(0) species and azo groups can also act as π-acidic ligands for Ni(0) species.[80] These could be reasons for decreased activity as opposed to any radical-based interference. In addition, 4-iodoimidazole displayed decreased reactivity, which is also observed in Ni-catalysed $S_{RN}1$ reactions,[81] as a result of fragmentation of radicals to form imidazole anions.[82] This also could suggest the involvement of a radical-based catalytic cycle.

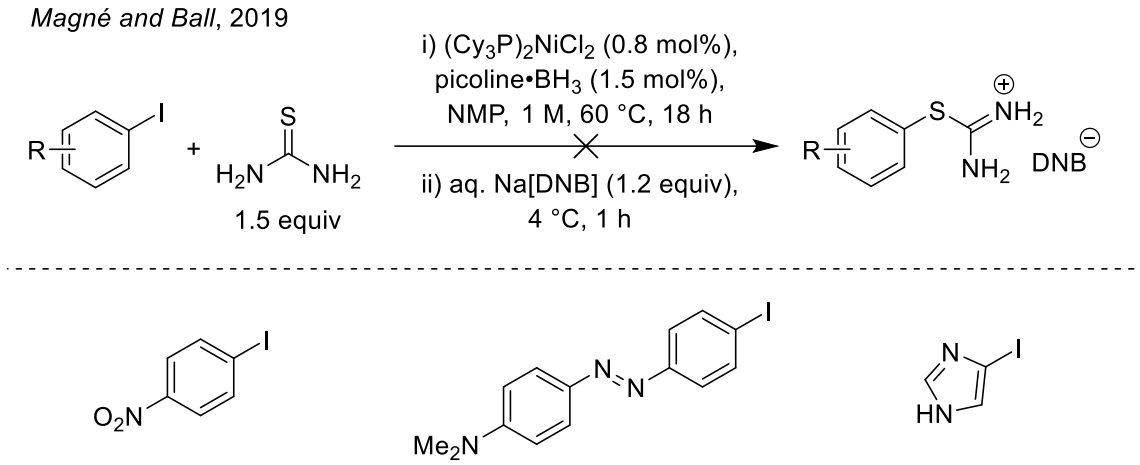
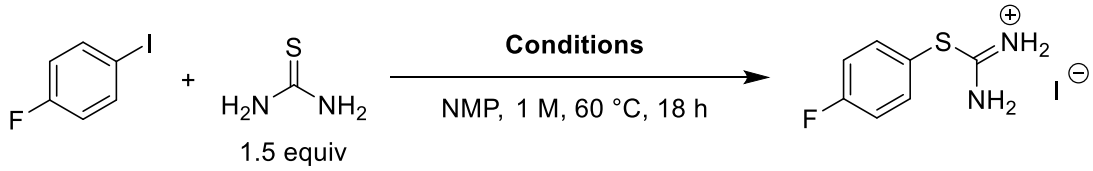


Figure 61 – Potentially mechanistically impactful unreactive substrates.[57]

To further probe the mechanism involved in this method, Magné and Ball added 1,4-dinitrobenzene (**Table 6, entry 2**) and TEMPO (**Table 6, entry 3**) to a reaction that would otherwise yield excellent results (**Table 6, entry 1**). TEMPO acts as a radical trap,[83] as do compounds containing nitro groups, as mentioned previously. The impact that 1,4-dinitrobenze has as an additive suggests that the unsuitability of 4-iodonitrobenzene as a substrate is not for lack of reactivity at the C-I bond, but due to incompatibility of the nitro group. These data could suggest a radical-based catalytic cycle but, as before, both results can have alternative explanations. This incompatibility with nitro groups has also been noted for Ni(0)-catalysed systems,[84] and TEMPO is known to react with other organometallic species.[85]

Table 6 – Mechanism-probing experiments carried out by Magné and Ball.[57] Yields reported as calculated yields using ^{19}F NMR spectroscopy.



Entry	***Conditions***	***Yield of isothio-uronium salt / %***
1	$(Cy_3P)_2NiCl_2$ (0.8 mol%), picoline•BH_3 (1.5 mol%)	>99
2	As entry 1, 1,4-dinitrobenzene (0.2 equiv)	0
3	As entry 1, TEMPO (1 equiv)	0
4	$(Cy_3P)_2NiCl$(*o*-tol) (0.8 mol%)	0
5	$(Cy_3P)_2NiCl$(*o*-tol) (0.8 mol%), picoline•BH_3 (1.5 mol%)	>99
6	$Ni(cod)_2$ (0.8 mol%), PCy_3 (1.6 mol%)	35

The function of picoline borane in this system is unknown.[57] To probe its function, Magné and Ball synthesised a plausible catalytic intermediate: $(Cy_3P)_2NiCl$(*o*-tol). Analogues of this could be generated during catalysis from aryl iodide and a Ni(0) species through a variety of mechanistic routes.[86] Using this potentially "pre-activated" catalyst without the presence of picoline borane resulted in no observable yield (**Table 6, entry 4**). Reactivity was restored, however, by addition of picoline borane with this complex (**Table 6, entry 5**). If indeed this coupling does proceed through a Ni(0)/Ni(II) catalytic cycle, then using a Ni(0) catalyst should theoretically negate the requirement for catalyst pre-activation, a potential function of picoline borane. Some isothiouronium salt was produced using $Ni(cod)_2$ as a Ni(0) source, as displayed in **Table 6, entry 6**. This is a promising result, however it is known that other Ni oxidation states are accessible from Ni(0) and aryl iodide mixtures.[87]

The species present in this cross-coupling reaction are not yet clear, and much work is to be done to determine the precise catalytic cycle involved in this system.

6.3.4 *Isothiouronium Reactivity*

As stated in prior sections, isothiouronium salts can be used directly in further diversification reactions to access other sulfur functionalities. The 2019 report by Magné and Ball displayed the versatility of these salts, as shown in **Figure 62**.[57] The thiophenol functionality can be released quantitatively by treatment with K_2CO_3 in methanol at 60 °C.[88] Oxychlorination can be achieved by treatment with NCS and the resulting sulfonyl chloride can be converted to the corresponding sulfonamide with ammonium hydroxide. Alternatively, the isothiouronium salt can be converted directly to the sulfonamide through a modification of Bull's oxyamination procedure.[89] The isothiouronium functionality itself can be utilised to generate 2-thiopyrimidines by condensation with a diketone. The authors demonstrated that, when treated with a base to release thiophenol *in situ*, S_N2 and conjugate addition reactions are viable to form *S*-alkyl bonds. *S*-Aryl bonds can be formed through either S_NAr or other cross-coupling methods. Swan and co-workers reported a photocatalysed route to non-symmetrical diaryl thioethers from these isothiouronium salts.[90]

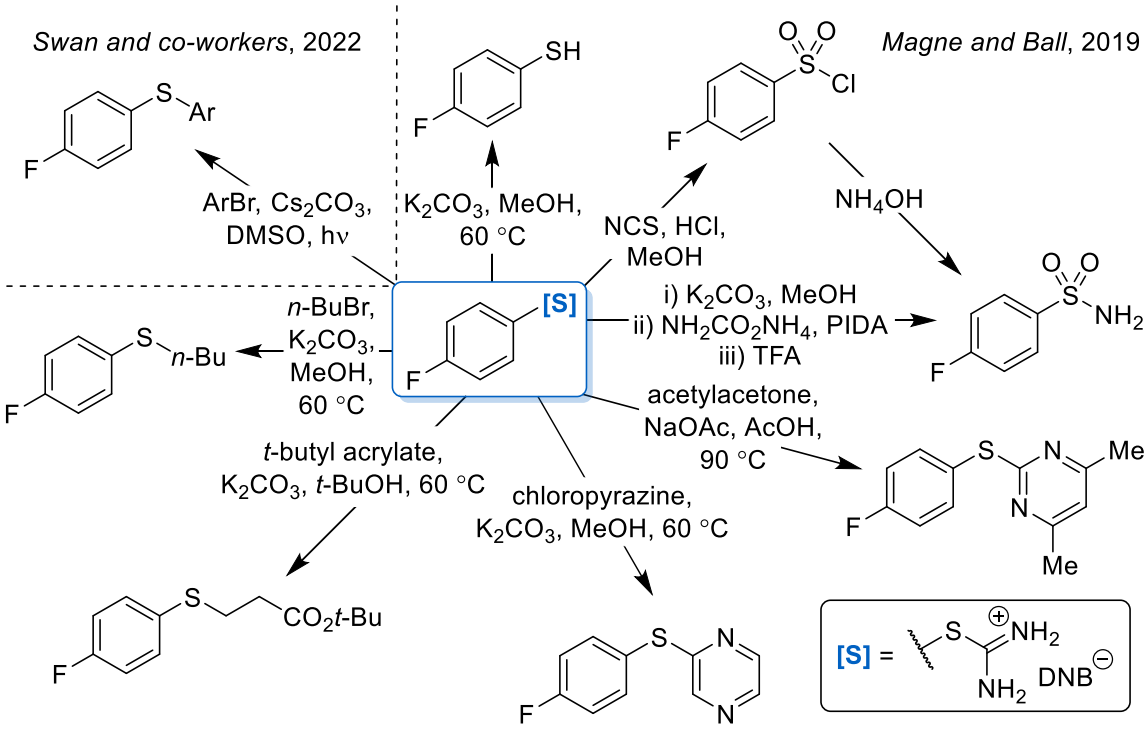
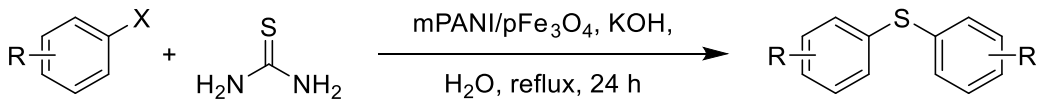


Figure 62 – Functionalisation of sulfur groups from isothiouronium salts.[57,90]

A selection of these routes were utilised in the synthesis of biologically active molecules chlorbenside, celecoxib and vortioxetine.[57] These would usually involve the undesirable handling of thiophenol, but this can be bypassed by *in situ* release from the corresponding isothiouronium salt using this method. Previous reports of one-pot methods from aryl halides to thioethers have been published for symmetrical diaryl (**Figure 63a**)[64] and aryl-alkyl thioethers (**Figure 63b**).[65]

a. *Damodara and co-workers*, 2013



b. *Firouzabadi and co-workers*, 2010

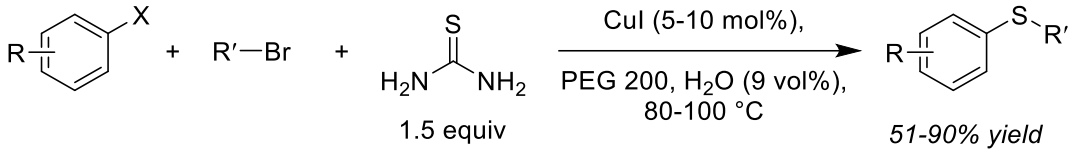


Figure 63 – Examples of one-pot isothiouronium syntheses followed by aryl halide cross-couplings.[64,65]

One major drawback of the route published by Magné and Ball is the choice of solvent. The authors note that polar solvents were preferred in this system and the solvent that gave the best results was NMP.[57] This solvent's toxicity has resulted in its restriction under current REACH guidelines.[91] In contrast, both of the routes outlined in **Figure 63** utilise water as their primary solvent. From a green chemistry point of view, this is the ideal solvent.[92–95] Robustness tests on the method published by Magné and Ball indicated that the reaction tolerated at least 10 vol% water with a minor decrease in yield.[57] Despite this, it is likely that reproducing these conditions in solely water as a solvent will cause solubility issues. A potential solution to this problem would be to use an aqueous micelle solution as solvent for this method.

6.4 Surfactants in Organic Synthesis

The 5th of the 12 green chemistry principles reported by Anastas and Warner stated that organic solvents "should be made unnecessary wherever possible and, innocuous when used".[96] This is emphasized by the fact that 80-90% of waste produced by pharmaceutical plants by mass can be attributed to solvents.[97,98] It is clear that both the volume and choice of solvents used will have a large impact on green metrics.[99] A range of guides have been made available in previous years in an attempt to assist researchers in responsible solvent selection.[100,101] The solvent selected by nature, in which a broad range of chemical transformations are possible,[102] is water. This readily available, non-flammable, non-toxic solvent has desirable properties such as its easily tuneable pH and a high heat capacity which allows exothermic reactions to be more easily controlled.[102]

However, there are disadvantages associated with using water as a solvent that constrain its use is organic synthesis. Primarily, lipophilic reagents and catalysts will not be soluble, resulting in biphasic mixtures.[103] This exclusion of lipophilic compounds from the bulk hydrogen bonding matrix is called the "hydrophobic effect".[104] Though seemingly a disadvantage, Breslow described how the Diels-Alder reaction of lipophilic dienes and dienophiles can be accelerated when water is used as a solvent as a result of the hydrophobic effect.[105] This finding initiated further investigations into reactions in, or on, water.[103]

One such approach to solubilisation of lipophilic compounds in a hydrophilic environment employs amphiphilic compounds to mediate between the two phases.[102] Surfactants aggregate in water to form areas of lipophilicity within the aqueous solvent. Non-polar reagents will be soluble within these lipophilic areas, giving microheterogeneous areas of high concentration for the reaction to take place in.[106,107] This property has led to many describing the structures formed, such as micelles, as "nanoreactors".[108,109] Well-known surfactants such as SDS (**Figure 64**), which can be found in detergents,[110] have found roles in facilitating organic reactions.[111–113] Surfactants can be categorised based on the charge on the polar group, as indicated in **Figure 64**. They can be anionic, such as SDS and the phospholipids present in cells,[114] cationic such as cetrimonium chloride (CTAC),[115] or non-ionic.

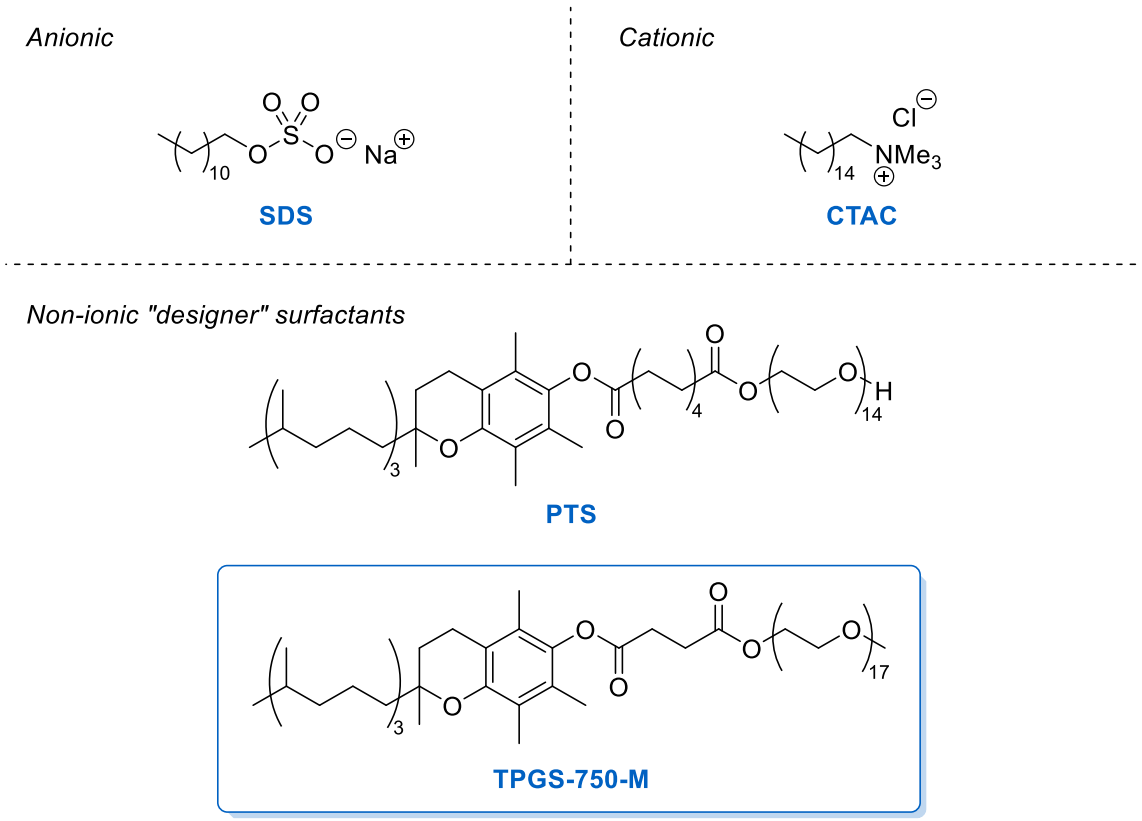


Figure 64 – Examples of anionic, cationic and non-ionic surfactants.

PTS (**Figure 64**) was originally synthesised by researchers at the National Research Council for the purpose of solubilising lipophilic coenzyme CoQ_{10}, a dietary supplement.[116,117] It was observed that PTS can successfully form translucent solutions of CoQ_{10} and other lipophilic compounds in water.[118] This property led researchers to investigate its use for the purpose of organic synthesis.[111,119] The Lipshutz group in particular have pioneered this field, firstly applying PTS to a wide range of cross-coupling reactions using water as the bulk solvent.[118,120] To demonstrate its practicality in organic synthesis, Lipshutz and co-workers successfully carried out Heck,[107] Suzuki-Miyaura[121] and Sonogashira[122] cross-couplings and olefin metathesis (**Figure 65**).[123,124]

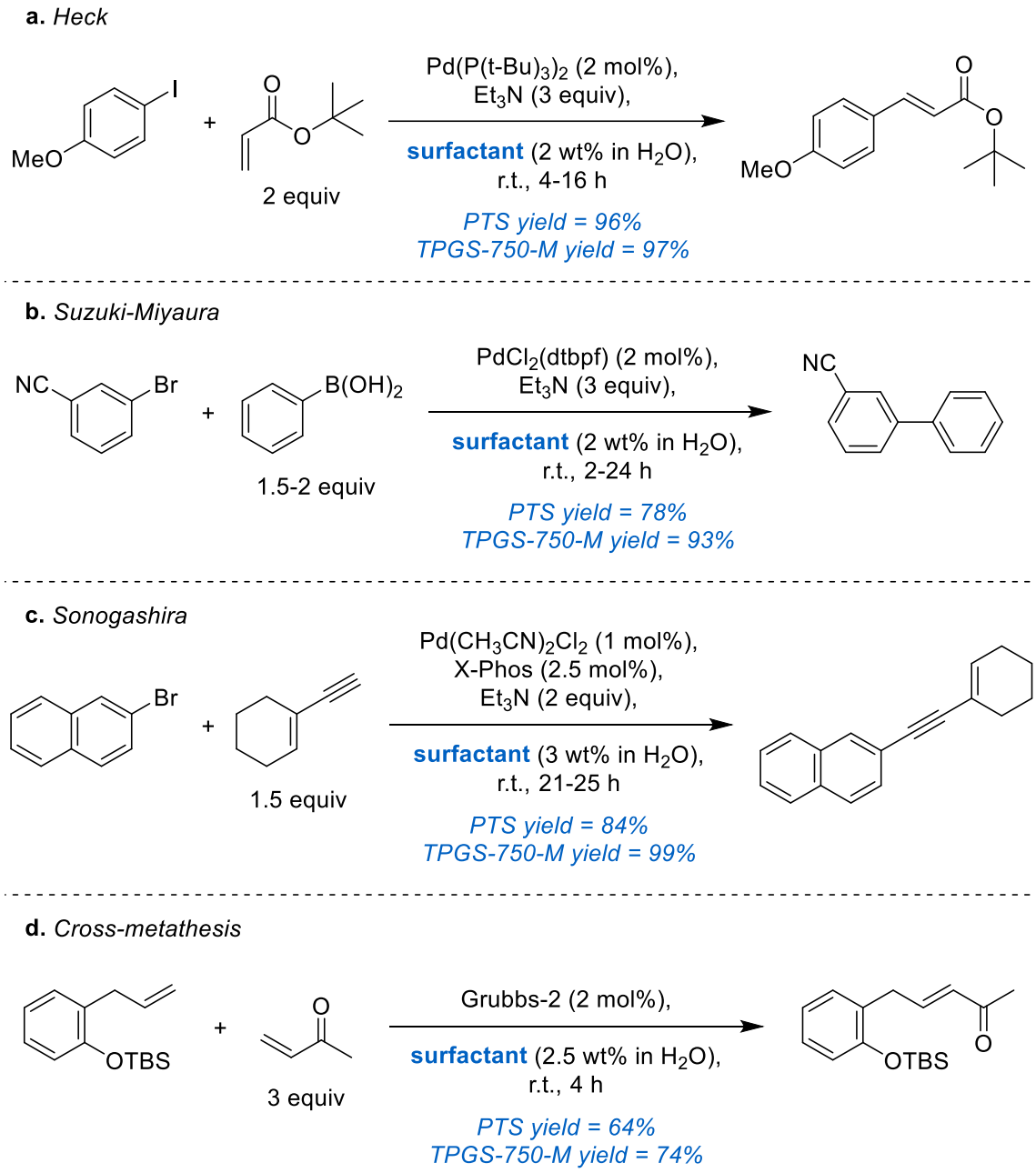


Figure 65 – Cross-coupling reactions in surfactant solutions, as reported by Lipshutz and co-workers in 2011.[125]

Lipshutz went on to develop "designer surfactants", surfactants designed specifically for facilitating cross-coupling reactions. One surfactant developed in this group of note was TPGS-750-M (**Figure 66a**).[125] The authors incorporated the concept of "benign by design" in their efforts to develop the next generation of surfactants for organic synthesis.[103,126] TPGS-750-M consists of non-toxic vitamin E, a readily available cross-linker and a

polyethylene glycol (PEG) chain. From DFT analysis incorporating a solvent model, Andersson and co-workers proposed that micellar structures such as that displayed in **Figure 66b** form in 2 wt% solutions of TPGS-750-M in water.[127] This was further supported by cryoTEM imaging. Lipshutz and co-workers found this surfactant outperformed PTS when used in the previously described cross-coupling examples (**Figure 65**).[125]

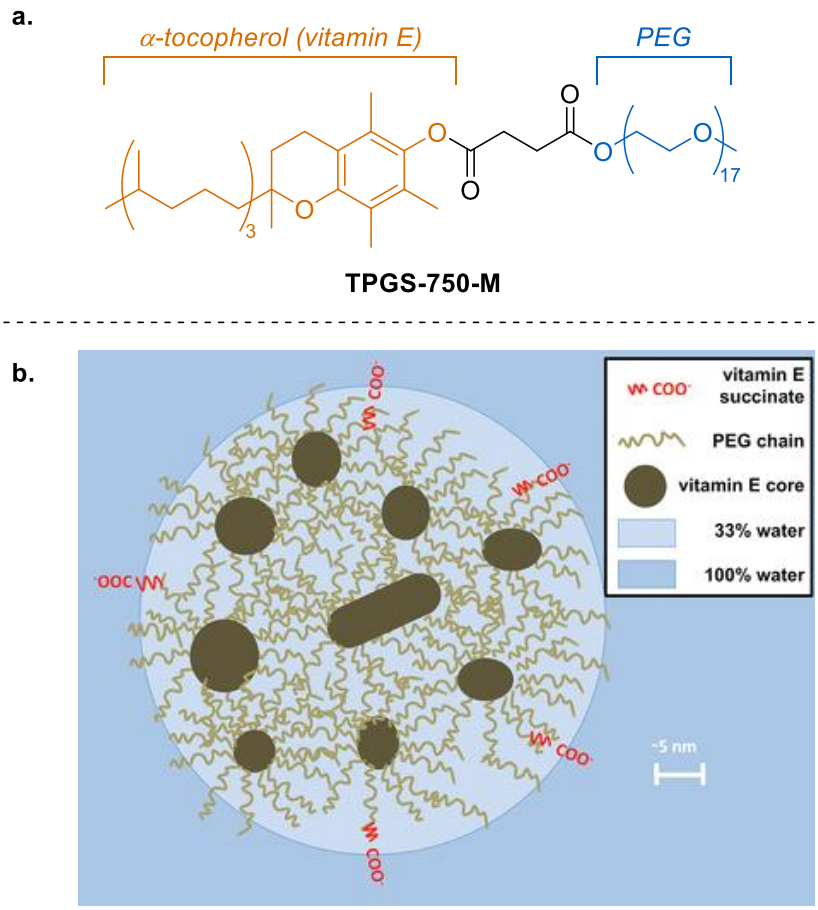
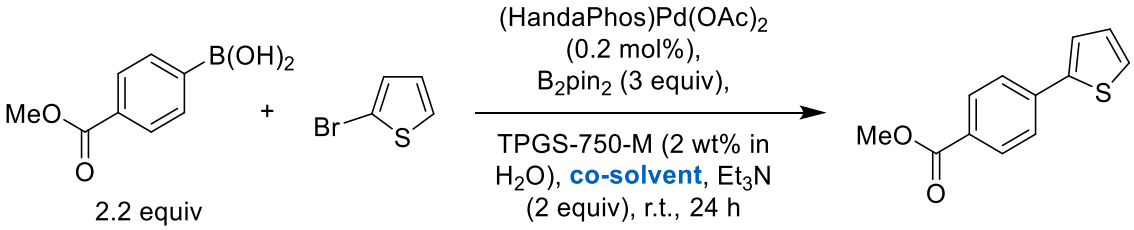


Figure 66 – The structure of TPGS-750-M (a) and the micelle structures formed in water (b), as proposed by Lipshutz and co-workers.[127]

The size of the micelles formed can give an indication of the suitability of a surfactant to organic synthesis. Lipshutz published a set of "rules" for micellar catalysis, one of which stated that micelles should be larger than 10 nm and smaller than 100 nm in diameter with the ideal range between 45-60 nm.[128] However, the size of micelle formed in solution is not solely dictated by the choice of surfactant. A well-known phenomenon in micelle chemistry, swelling, can be used to increase micelle diameter. Co-solvents can be incorporated into the micelle structure, resulting in enlarged micelles.[129] The effect of co-

solvent usage on cross-couplings in micelle solutions was highlighted by Gabriel and co-workers, one example of which is displayed in **Table 7**.[130]

Table 7 – The effect of co-solvent on the outcome of a Suzuki-Miyaura cross-coupling in TPGS-750-M solutions. Yields were reported as isolated yields and average particle size was determined by DLS measurements.[130]



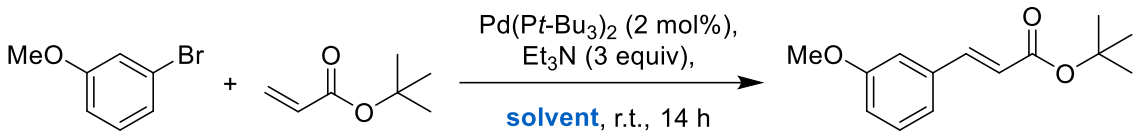
Entry	*Co-solvent*	*Yield / %*	*Average micelle diameter / nm*
1	None	46	57
2	10 vol% THF	81	129

The authors used dynamic light scattering (DLS) to measure the average particle size in 2 wt% solutions of TPGS-750-M in water. They observed that micelles more than doubled in size when solutions also contained 10 vol% of THF. This is echoed by an increase in yield obtained from the displayed Suzuki-Miyaura cross-coupling in solutions containing 10 vol% THF. Though it is worth noting that the DLS measurements were taken without the additional reagents, so the exact value may differ under reaction conditions. Correlation does not equal causation, hence the authors noted that other factors may influence the yield, such as the influence of co-solvent on initial reagent solubility.

Changing factors such as the concentration of salts in the water medium can also influence the outcome of reactions in micelles. Lipshutz and co-workers reported that carrying out Heck cross-couplings using 3 M aq. NaCl solutions instead of water resulted in boosted yields (**Table 8**).[131] This is proposed to occur due to the "salting out" effect. Increasing the amount of NaCl in solution impacts the hydrogen bonding network,[132] resulting in H_2O being drawn away from the micelles and hence an increase the size of the micelles.[133] This was reflected in the DLS measurements taken and the impact of salt concentration varied between inorganic salts.[131] Further to this, the authors analysed the micelles by cryoTEM and found that 5 wt% PTS solutions in water produced primarily spherical micelles. When 3 M aq. NaCl solutions were used, however, an interconnected network of

worm-like structures were observed. This change in micelle structure could be an alternative reason for enhanced reactivity.

Table 8 – The salt effect on Heck reactions in micelle solutions.[131]



Entry	*Solvent*	*Yield / %*	*Average micelle diameter / nm*
1	5 wt% PTS in H_2O	46	25
2	5 wt% PTS in 3 M aq. NaCl	81	110

Surfactant design has also allowed for other external factors to influence micelle properties.[134] Surfactants that have pH-sensitive functionalities can provide tuneable solutions, whereby altering the pH results in switching between micelle and worm-like structures.[135] Some surfactants can also be thermally influenced to induce structural changes.[136]

In the previous sub-sections, the importance of aromatic C–S bond formation was highlighted. C–S cross-coupling in micelle solution was reported by Yu and co-workers in 2021; a product of the Lipshutz group (**Figure 67**).[137] This Ni-catalysed Migita-type cross coupling used a 2 wt% solution of TPGS-750-M in water as a solvent. Both diaryl and alkyl-aryl thioethers were synthesised under these conditions in poor to excellent yields. This method provides precedent for C–S cross-coupling in micelle solutions, however it comes with the plethora of issues mentioned previously for reactions using thiols.

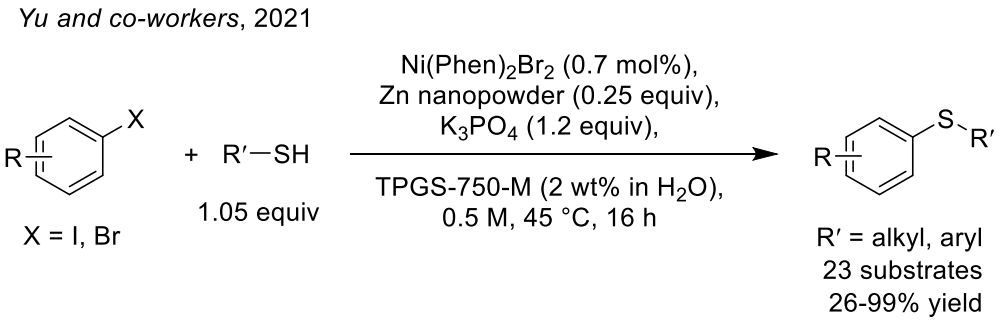


Figure 67 – Migita-type cross-coupling of thiols and aryl halides reported by Yu and co-workers.[137]

Though an excellent option in the design of more sustainable methods, micelle solutions will not be suitable solvent systems for some reactions. There will be routes with inherent

water-sensitivity that continue to be optimal under anhydrous conditions.[92] Fortunately, the cross-coupling method reported by Magné and Ball has a demonstrated tolerance towards 10 vol% water in NMP.[57] Additionally, this method favours polar solvents and gives better yields at higher concentrations. These characteristics suggest that the route proposed by Magné and Ball could be well-suited to application to use in micelle solvent systems. Due to the toxicity and restricted status of NMP, replacement of this solvent with micelle solutions would be a step towards a more sustainable route.

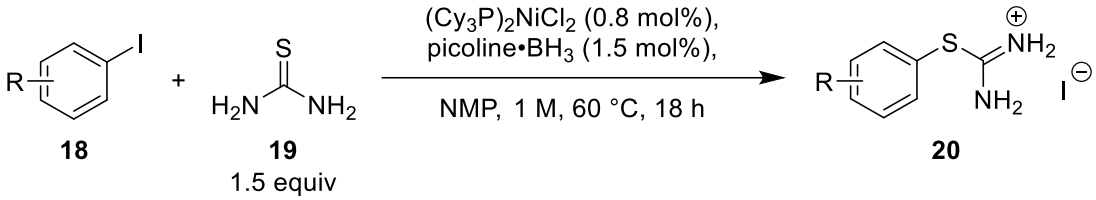
6.5 Aims

The focus of this project was to develop a method for synthesising isothiouronium salts in micelle solutions. Based on the method reported by Magné and Ball,[57] the nickel-catalysed cross-coupling of aryl iodides with thiourea in TPGS-750-M solutions was to be investigated. Due to the change in solvent from NMP, the effects of solvent and co-solvent on reaction outcome required exploration. To determine the effects that co-solvents had on micelle swelling, the solutions were to be analysed using DLS. A precipitation method was developed in a variety of solvent systems and with varying levels of *N*-substitution on thiourea to probe the effect of changing solvent on ease of precipitation.

To expedite the optimisation process, DoE designs were performed in collaboration with Catalysis Consulting. Following this, the optimised conditions were to be used in a substrate scope to explore functional group tolerance. Initial mechanism-probing experiments were reported by Magné and Ball, but the species involved in this cross-coupling are still unknown. The new factors introduced into this route may provide further insight and allow for additional mechanistic studies.

7 C–S Cross-Coupling in Micellar Solution – Results and Discussion

When investigating the synthesis of isothiouronium salts in micelle solutions, we first looked to the optimised conditions reported by Magné and Ball in 2019 (**Figure 68**).[57] These conditions are a logical starting point, but have been optimised for use of NMP as a solvent. The same conditions may not be applicable to micelle solutions.



18 **19** 1.5 equiv **20**

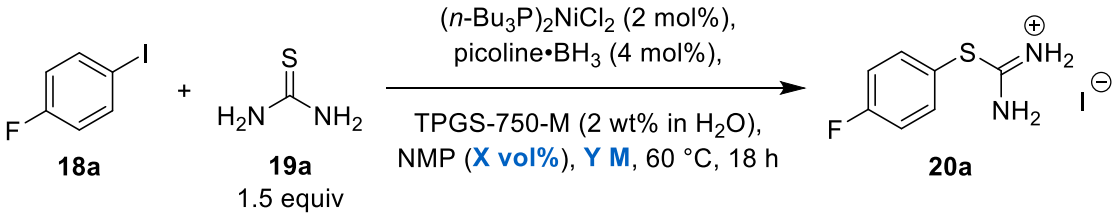
*Figure 68 – Optimised conditions for the nickel-catalysed cross-coupling of aryl iodides (**18**) and thiourea (**19**) in NMP reported by Magné and Ball.[57]*

The previous section highlighted TPGS-750-M as a surfactant that is widely applicable to a range of cross-coupling methods.[125] Therefore, we selected this surfactant for our investigations. We expected that there could be solubility issues with some reagents, hence the previously mentioned co-solvent effect may be required in this design.

7.1 Co-solvent Screening

The drive of this project was to utilise aqueous micellar media in place of toxic organic solvents. As such, preliminary experimentation involved the use of 2 wt% solutions of TPGS-750-M as the sole solvent. In this study, we utilised $(n\text{-}Bu_3P)_2NiCl_2$ as a precatalyst, as opposed to $(Cy_3P)_2NiCl_2$ used by Magné and Ball.[57] This is due to the fact that the former complex was previously observed to be more readily soluble in various solvents,[57] as we expected this would be an issue in water-based systems. Applying the reaction conditions displayed in **Table 9** at both 0.2 M and 0.4 M initial concentrations of aryl iodide **18a** with solely 2 wt% TPGS-750-M in degassed water gave no observable conversion by ^{19}F NMR spectroscopy (**Table 9, entry 1**). This stands in contrast to the fact that, under the same conditions, using degassed NMP as the solvent gave excellent yields (**Table 9, entry 5**).

Table 9 – The effect of changing the volume fraction of NMP in the solvent system on conversion. *[a]Percentage conversion was determined by relative peak intensity by ^{19}F NMR spectroscopy. [b]Degassed water used in the place of surfactant solution.*



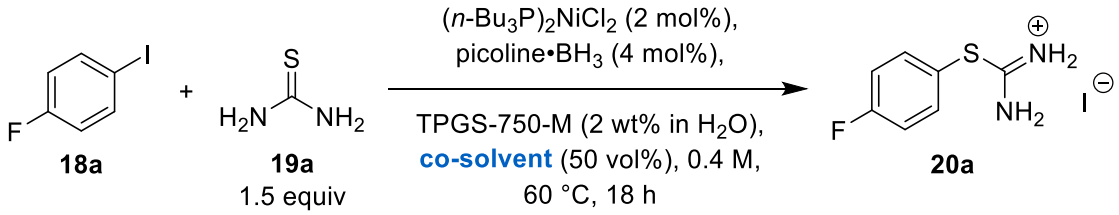
Entry	*Proportion of NMP in solvent system / vol%*	*Conversion / %[a] (0.2 M)*	*Conversion / %[a] (0.4 M)*
1	0	0	4
2	20	0	53
3	50	32 (3[b])	77
4	80	40 (15[b])	81
5	100	94	95

As mentioned in the introductory section for this work, co-solvents can be used to improve yields. Co-solvents can aid reagent solubility and promote micelle swelling, providing a greater volume for the reaction to take place in. For these initial co-solvent tests, we used NMP as the co-solvent as neat NMP had been previously identified as an excellent medium for this reaction.[57] At both 0.2 M and 0.4 M initial aryl iodide concentrations, conversions are seen to increase with increasing proportions of co-solvent (**Table 9, entries 2-4**). It can also be observed that increasing the initial aryl iodide concentration results in improved conversion throughout, aligning with observations by Magné and Ball.[57] To confirm the beneficial role of TPGS-750-M, reactions with 50 and 80 vol% NMP were repeated using degassed water in place of the 2 wt% TPGS-750-M solution (**Table 9, entries 3 and 4**). Greatly diminished conversions were observed under these conditions, highlighting the importance of surfactant in this system.

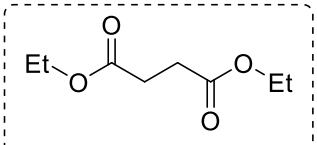
Given that the purpose of this project was to synthesise isothiouronium salts in a system that no longer uses NMP as a solvent, focus was next given to screening alternative co-solvents for this reaction. A variety of co-solvents were screened using the 50 vol% reaction conditions mentioned previously, the results of which are displayed in **Table 10**. For the solvents giving higher yields (**Table 10, entries 7-10**), these were also carried out with 20 vol% co-solvent. Taking into consideration the observations of Magné,[57] only polar

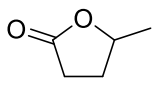
co-solvents were screened. We observed that the solvent choice had a great influence on the outcome of the reaction. This is likely due to a combination of polarity, miscibility in water and compound solubility.

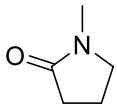
*Table 10 – Co-solvent screen for the synthesis of **20a** in micelle solutions. NMR yields were calculated from ^{19}F NMR spectroscopic data using bis(4-trifluoromethyl)benzene as an internal standard. Yields in parenthesis were obtained using 20 vol% co-solvent.*



Entry	*Co-solvent*	*NMR yield / %*
1	diethyl succinate	1
2	*t*-amyl alcohol	6
3	THF	10
4	acetone	16
5	tetraethylurea	24
6	γ-valerolactone	47
7	IPA	64 (21)
8	MeCN	70 (15)
9	DMSO	71 (18)
10	NMP	77 (53)


diethyl succinate


γ-valerolactone

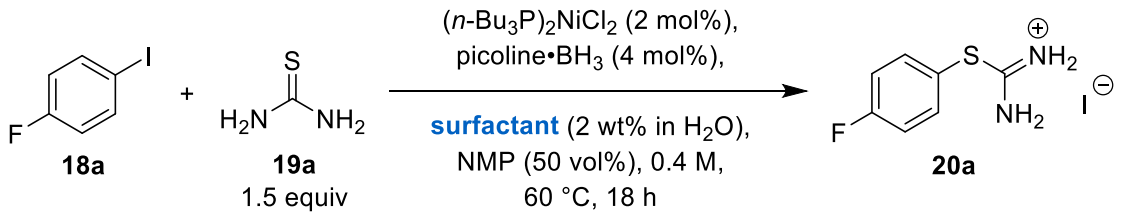

NMP

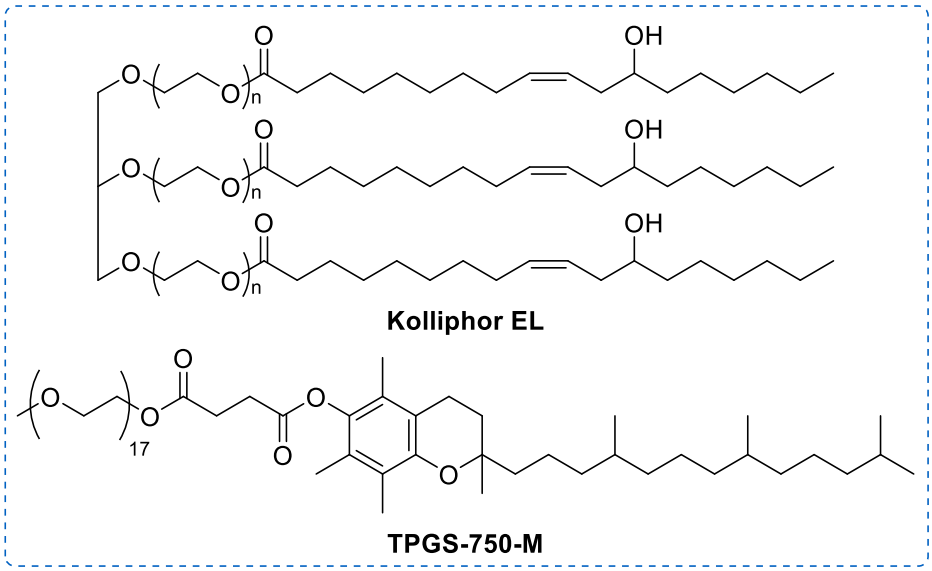
Magné and Ball noted that use of aerobic atmosphere in their method resulted in significantly reduced yields (<10%).[57] To ensure removal of oxygen from the system, all co-solvents were degassed by bubbling dinitrogen for a minimum of 30 minutes. Deionised water was instead degassed through three rounds of freeze-pump-thaw under an atmosphere of dinitrogen. Though these precautions were taken in this work, this oxygen-sensitivity was only reported using neat NMP as a solvent.[57] Previous literature reported the use of Kolliphor EL as a surfactant for oxygen-sensitive chemistry.[138] The authors displayed the ability of this surfactant to exclude oxygen from the micelles, allowing oxygen-sensitive chemistry such as Suzuki-Miyaura cross-couplings to occur without the

need to degas the surrounding system. Given this precedent for oxygen-sensitive reactions in Kolliphor EL micelles, it was hypothesised that this could be applied to our method. If successful, the need to degas the system would be avoided, with practical benefits especially on scale.

Therefore, we tried our transformation using both 2 wt% TPGS-750-M and Kolliphor EL solutions under different inertion regimes (**Table 11**). **Table 11 entries 1-3** used aqueous surfactant solutions that were degassed by freeze-pump-thaw but vary by the extent to which degassing was applied to the co-solvent, if present. Finally, **Table 11 entry 4** displays the results of using surfactant solutions that were not degassed, and which were performed under an aerobic atmosphere. An overall negligible improvement in yield for Kolliphor EL in comparison with TPGS-750-M was found. Comparing results from using degassed or technical grade NMP under an inert atmosphere (**Table 11, entry 2 vs 3**), there was a surprisingly marginal decrease yield when using NMP that had not been degassed. The detrimental effect that oxygen has on the method reported by Magné and Ball suggests that oxygen can be present in NMP.[57] Perhaps the segregation of reagents provided by both surfactants decreases the interaction between the reaction site, presumably within the micelle, and wherever oxygen is distributed within that system.

*Table 11 – Comparative study of the effects of oxygen on the synthesis of **20a** in micellar solutions. Yields are given as calculated NMR yields calculated from ^{19}F NMR spectroscopic data using bis(4-trifluoromethyl)benzene as an internal standard. Surfactant solutions are 2 wt% solution of surfactant in degassed H_2O. [a]Surfactant solution was prepared using H_2O that was not degassed.*





Entry	Co-solvent	Atmosphere	TPGS-750-M yield / %	*Kolliphor EL yield / %*
1	None	N_2	4	7
2	Degassed NMP	N_2	77	79
3	Technical grade NMP	N_2	70	71
4	Technical grade NMP	air	0[a]	0[a]

When this reaction was performed without degassing the surfactant solution or NMP, and in an aerobic atmosphere, this resulted in no observable yield (**Table 11, entry 4**). Unfortunately, the use of Kolliphor EL in these aerobic conditions did not produce the desired effect reported by Mattiello and co-workers for other cross-couplings.[138] One possible reason for this difference in observation could be due to the fact that these authors did not use co-solvents in their solvent systems. Co-solvents may disrupt the

“barrier” that exists between the micelle interior and exterior, allowing for dispersion of oxygen throughout. Since co-solvents have proven vital in this synthetic design, TPGS-750-M remained the chosen surfactant. Following these initial results for co-solvent screening, 50 vol% co-solvent solutions were used when other aspects of this method were investigated.

7.2 Thiourea Screening

Given that this solvent system is composed of water and micelles with lipophilic cores, and supposing the reactions do take place inside the micelles,[139] having a water-soluble reagent may decrease yields. If we were to alter the thiourea by increasing its lipophilicity, this may increase availability in the area where the reaction is presumably taking place. To this effect, we carried out our reaction with a variety of *N*-substituted thioureas (**Figure 69**). This used both 2 wt% solutions of TPGS-750-M in water with 50 vol% NMP and solely NMP, the latter represented in parenthesis.

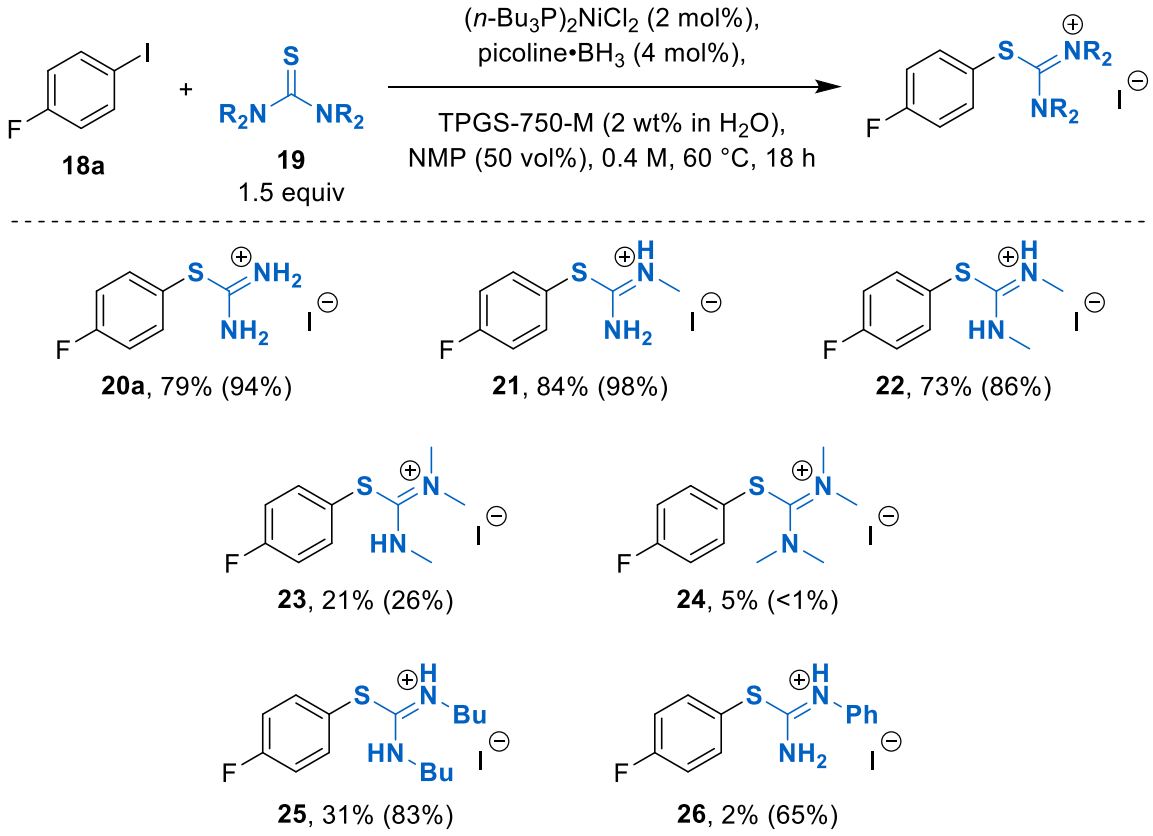


Figure 69 – Cross-coupling of 4-fluoroiodobenzene with a variety of thioureas. Yields are given as calculated NMR yields calculated from ^{19}F NMR spectroscopic data using bis(4-trifluoromethyl)benzene as an internal standard.

The best yields observed for both solvent systems were obtained when using *N*-methylthiourea as a sulfur source (**21**). Increasing the number of *N*-methyl groups on thiourea after this results in a decrease in yield for both solvent systems. The purpose of investigating the effect of thiourea substitution in solely NMP is to provide a benchmark for the efficacy of thioureas in the cross-coupling, but disregarding any effects caused by being in an aqueous micelle solution. For example, changing the *N*-substitution can alter its nucleophilicity and steric properties. One could hence assume that any difference in yields between the two solvent systems could provide information about its activity within the aqueous micelle media irrespective of its general activity in this cross-coupling. When *N,N'*-dibutyl (**25**) and *N*-phenyl (**26**) thioureas were used, the observed yields were disproportionately low in the surfactant solution compared to the difference between yields for the various methylated thioureas. Lippincott and co-workers suggested that their Suzuki-Miyaura cross-coupling in TPGS-750-M solutions occurred within the long PEG

chains (c.f. **Figure 66b**, Section 6.4), based on the partition coefficients of their reagents.[139] The fact that the two most lipophilic thioureas in **Figure 69** are disproportionately less reactive is consistent with this suggestion. These thioureas may be too soluble in the lipophilic cores of the micelle and not as available in the area in which the reaction is proposed to occur. However, an alternative explanation for decreased availability is due to their insolubility in water, though unlikely as the solutions were visibly homogenous at the end of the reaction.

As a result of this investigation, unsubstituted thiourea was selected for further optimisation. Though slightly higher yields are observed with *N*-methylthiourea, the difference is minimal and is outweighed by the lower cost and lower molecular weight of thiourea, hence minimising unnecessary mass. Despite the preliminary optimisation by Magné and Ball of their Ni-catalysed synthesis of isothiouronium salts in NMP, the change in solvent system mandates separate optimisation. Given the large number of variables that could have a bearing on the reaction outcome – catalyst loading, reductant equivalents, co-solvent selection, vol% co-solvent, initial aryl iodide concentration, temperature, etc - DoE was used to expedite optimisation.

7.3 Design of Experiments (DoE)

The standard practice often employed in reaction optimisation involves changing one variable at a time, also known as OVAT optimisation. Other remaining variables are kept constant to identify relationships between the changing variable and the outcome of the reaction. For example, one would investigate a range in one variable, such as temperature, to find the optimum for a set of conditions. This optimum temperature is then used in the optimisation of other variables, such as concentration, maintaining the “optimum” temperature. This approach limits the amount of condition space explored and can often lead to the inaccurate identification of optimum conditions. This is displayed in **Figure 70**, where identifying the optimum in Variable 1, then in Variable 2, misses the true area of highest yield.

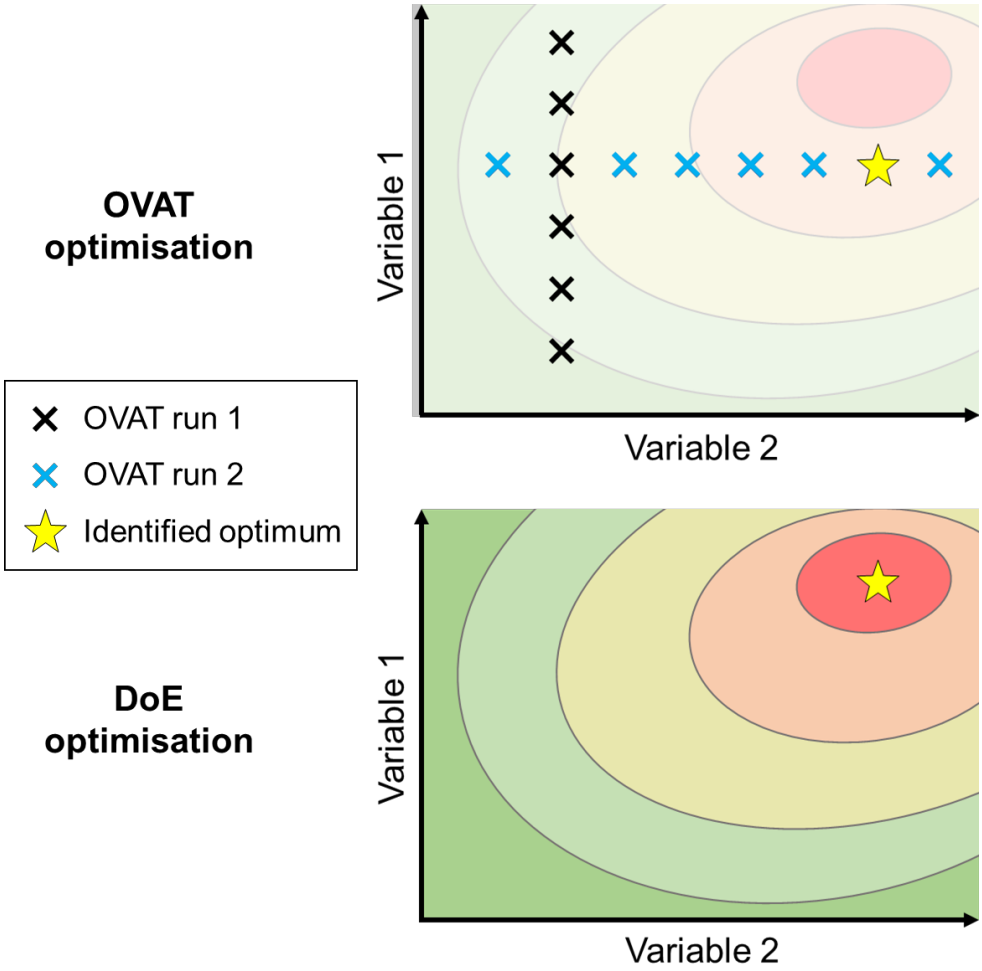


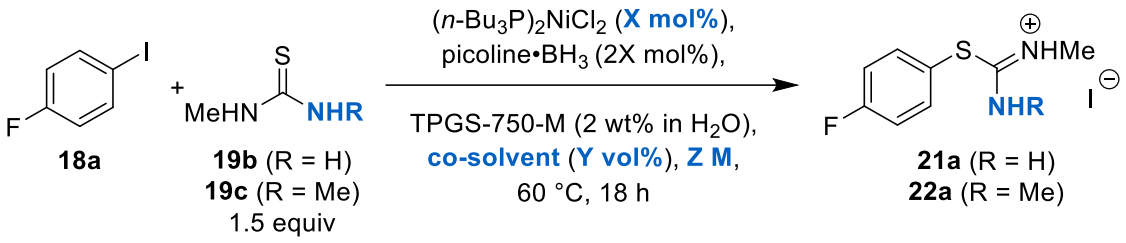
Figure 70 – Comparison between optimums identified using one variable at a time (OVAT) and design of experiments (DoE) methods during optimisation.

In order to obtain a full picture of the ways in which each variable impacts the reaction outcome, the reaction can be investigated using design of experiments (DoE).[140–142] Through this method, a set number of conditions are explored, changing multiple variables at the same time. The outcomes of which are inputted into mathematical models to generate a contour plot of conversion akin to that displayed in **Figure 70**. DoE has an advantage over the OVAT approach as it allows the user to carry out far fewer reactions to get a full picture of the impact multiple variables have on the reaction. This can also reveal variable interactions that may not be obvious from OVAT data. In the area of API process development, where the development of new products often has short timescales, DoE is a useful tool to increase efficiency. The decrease in the number of reactions

necessary to optimise a process that a well-formulated design provides will also reduce the amount of waste produced in the development of such processes.

In the transformation reported in this thesis, there are many variables such as catalyst loading, reductant equivalents, thiourea choice, initial aryl iodide concentration, co-solvent selection, volume fraction of co-solvent and surfactant concentration. As such, an OVAT approach would be unsuitable for this optimisation process. Instead, we worked alongside Dr Laura Forfar at Catalysis Consulting to apply DoE to our optimisation. Of the variables that we could have chosen to include in our design, some were excluded for simplicity of design. In the first design, we chose to investigate the mol% of nickel catalyst, substituents on thiourea (*N*-methyl or *N*,*N'*-dimethyl), initial aryl iodide concentration, vol% and type of co-solvent (**Table 12**). Co-solvents were selected from a map of 136 solvents, generated from principle component analysis (PCA) of those solvents, collating many solvent properties into a more manageable 2- or 3-dimensional space. This allowed us to choose three solvents of differing polarity, polarizability and hydrogen bonding ability which more efficiently explored this solvent space. In this design, we chose propylene glycol (PG), γ-valerolactone and *N*-butyl-2-pyrrolidone (NBP). The ranges of variables explored, and the results of each run, are displayed in **Table 12**. This design incorporated three centre points, highlighted in the table (runs 1,4 and 19), as a tool to probe reproducibility and hence model validity.

Table 12 – DoE design investigating the following variables: co-solvent, vol% of co-solvent, substitution of thiourea (either N-methyl or N,N'-dimethylthiourea), mol% of Ni-catalyst and initial aryl iodide concentration. Yields are given as calculated from ^{19}F NMR spectroscopic data using bis(4-trifluoromethyl)benzene as an internal standard.



Run	Co-solvent	Co-solvent / vol%	Thiourea	Ni-cat. / mol%	$[18a]_0$ / M	Yield / %
1	**GV**	**30**	**19b**	**3**	**0.6**	**64**
2	PG	10	**19c**	1	0.4	2
3	NBP	50	**19c**	5	0.8	84
4	**GV**	**30**	**19b**	**3**	**0.6**	**72**
5	NBP	10	**19c**	1	0.8	51
6	NBP	50	**19b**	5	0.4	72
7	PG	50	**19c**	5	0.4	66
8	PG	50	**19c**	1	0.8	72
9	NBP	50	**19b**	1	0.8	77
10	PG	50	**19b**	5	0.8	87
11	GV	30	**19c**	3	0.6	69
12	PG	10	**19b**	5	0.4	18
13	PG	50	**19b**	1	0.4	5
14	NBP	10	**19c**	5	0.4	45
15	PG	10	**19b**	1	0.8	16
16	NBP	10	**19b**	5	0.8	59
17	NBP	50	**19c**	1	0.4	27
18	NBP	10	**19b**	1	0.4	0
19	**GV**	**30**	**19b**	**3**	**0.6**	**64**
20	PG	10	**19c**	5	0.8	44

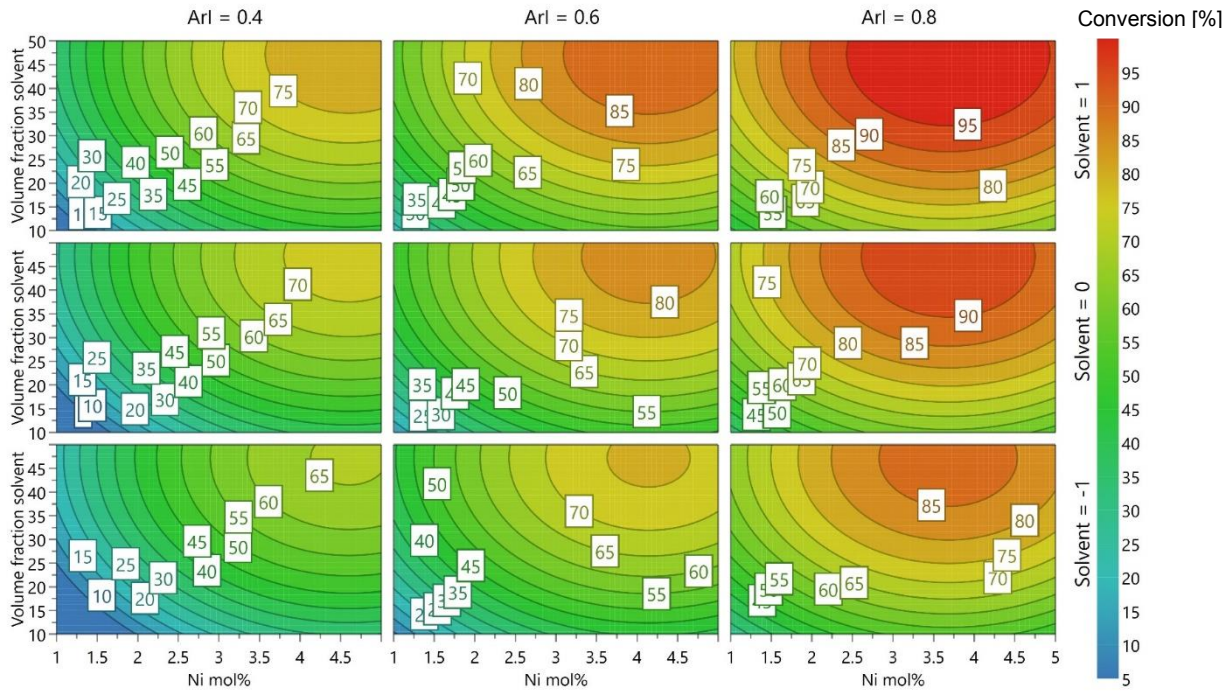


*Figure 71 – Contour plot produced from DoE analysis of data stated in **Table 12** and 12 additional experiments added to improve model validity. Selected solvents: −1 = PG, 0 = γ-valerolactone, 1 = NBP. The values associated with the contour lines represent predicted percentage conversion.*

The results from **Table 12** were used to generate a model of the effect each variable has on the reaction outcome. This can be summarised in the contour plots displayed in **Figure 71**. The solvent choice did appear to have an effect on the predicted reaction outcome, but to a lesser extent than expected. PG gave the lowest predicted yields; likely due to forming biphasic solutions with water. In general, the predicted conversion is higher under high aryl iodide concentrations. This is consistent with the observations of Magné and Ball for their method using NMP as the solvent. As demonstrated in Section 7.1, increasing the volume fraction of co-solvent results in increased yields. However, the contour plot suggests that for each co-solvent this effect reaches a maximum at 45-50 vol% of co-solvent. The effect of increasing the volume fraction of co-solvent past 50% however remains unknown as this was outside the scope of this DoE design.

This model predicts that up to 3.5-4.5 mol% catalyst loading, there is a positive relationship between percentage conversion and catalyst loading. After which, increasing the catalyst loading seemingly lowers the predicted conversion. The relationships between variables can be summarised in these contour plots but can be seen more clearly when in the form

of interaction plots. The interaction plot between catalyst loading and aryl iodide concentration displays this relationship between catalyst loading and predicted conversion for both high (0.8 M) and low (0.4 M) initial aryl iodide concentration (**Figure 72**).

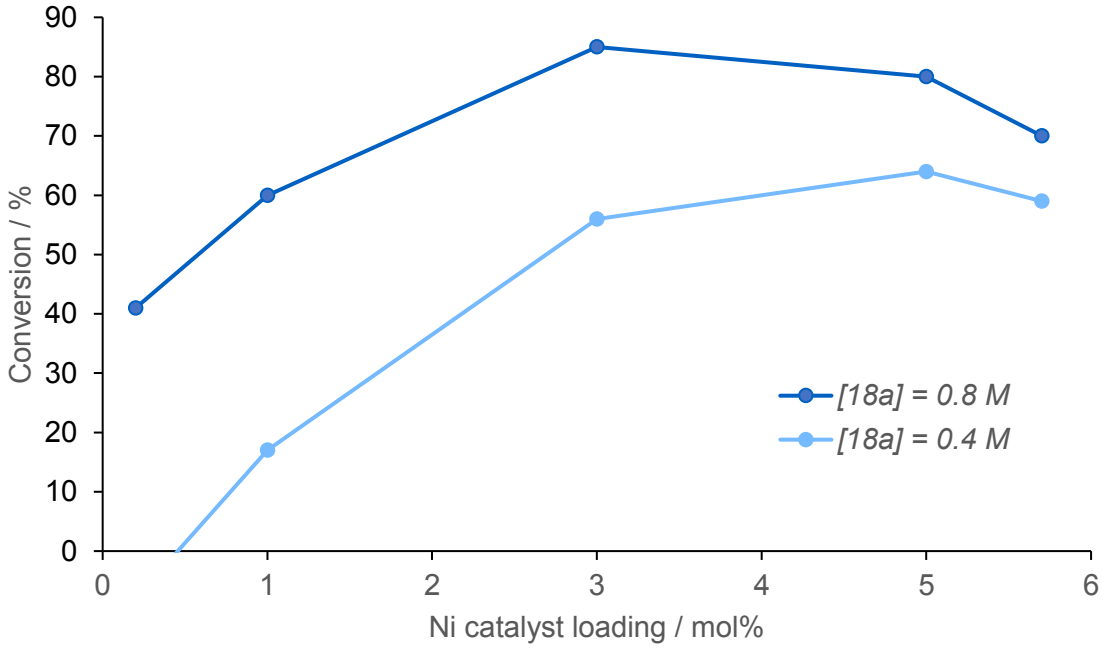


Figure 72 – Interaction plot between nickel catalyst loading and initial aryl iodide concentration.

This trend was repeated experimentally for higher aryl iodide concentrations and a similar plateau was observed at 3 mol% nickel catalyst (**Figure 73**). The experimental yields observed likely differed from predicted as the reactions were run at 1 M initial aryl iodide concentration as opposed to the 0.8 M solutions used in this DoE design. Additionally, the conversions were predicted from a range of solvents as opposed to the experimental yields, where IPA was used as a co-solvent.

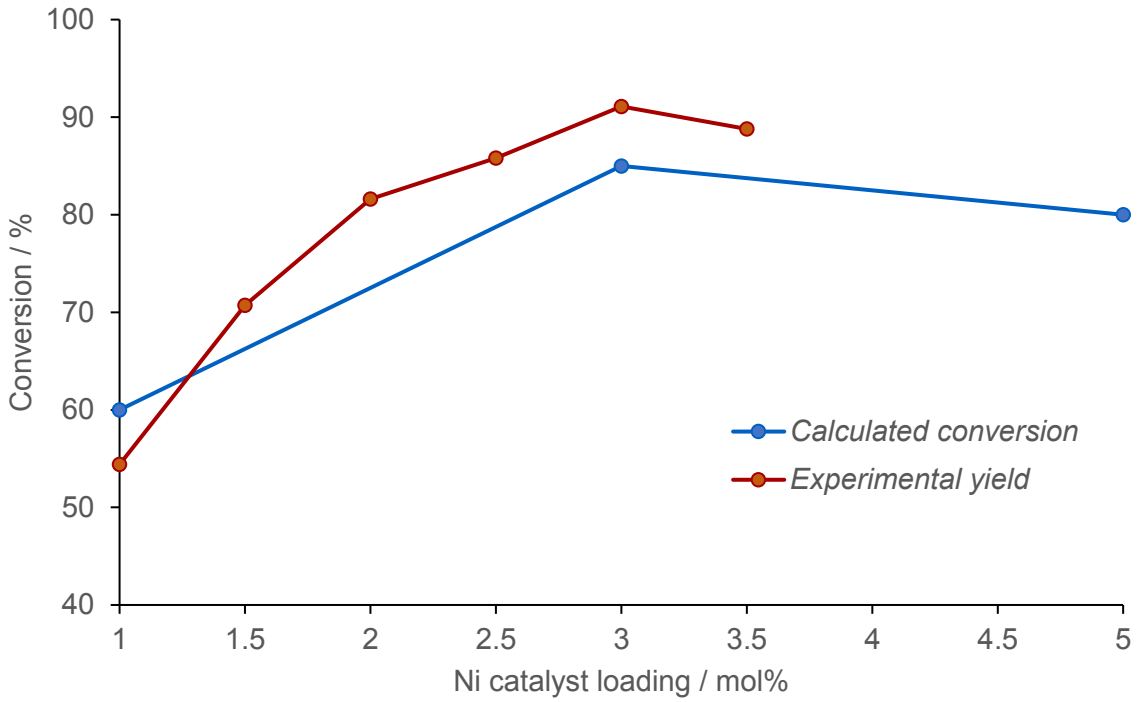
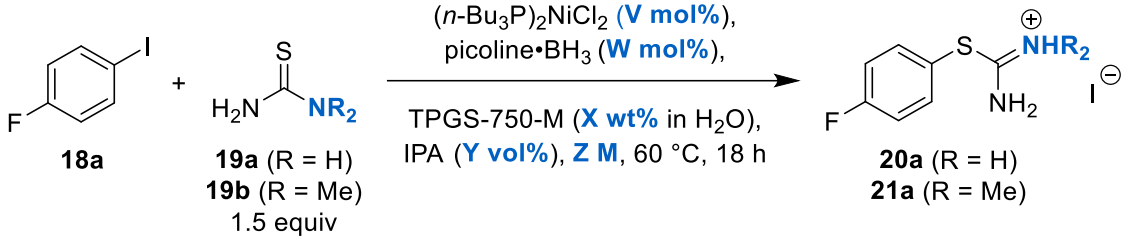


*Figure 73 – Repetition of relationship between catalyst loading and conversion predicted by DoE. Calculated conversions were taken from **Figure 72** for high aryl iodide concentrations ([**18a**]$_0$ = 0.8 M). Experimental yields were obtained using the following conditions: 4-fluoroiodobenzene **18a** (0.5 mmol), thiourea (1.5 equiv), picoline borane (2 equivalents in relation to Ni mol%), TPGS-750-M (2 wt% in H_2O), 50 vol% IPA, [**18a**]$_0$ = 1 M at 60 °C for 18 h. Experimental yields determined by NMR spectroscopy using 4,4'-bis(trifluoromethyl)biphenyl as an internal standard.*

An additional DoE design was performed incorporating other variables of this cross-coupling (**Table 13**). For this design, IPA was used as the co-solvent due to its performance in the initial screening reactions and its environmentally benign nature. We, again, opted to investigate *N*-substitution at thiourea, but instead with unsubstituted thiourea and *N*-methylthiourea. Additionally, the equivalents of reductant with respect to Ni-catalyst and the amount of TPGS-750-M in the aqueous solution were incorporated into our design. Catalyst loading and initial aryl iodide concentration remained variables in this design. The variable ranges explored and the results of each run are displayed in **Table 13**, again highlighting the centre points included to test reproducibility.

Table 13 - DoE design investigating the following variables: vol% of co-solvent, substitution of thiourea (either unsubstituted or N-methyl), mol% of Ni-catalyst, equivalents of picoline borane in relation to Ni mol%, initial aryl iodide concentration and wt% of TPGS-750-M in water. Yields are given as calculated from ^{19}F NMR spectroscopic data using bis(4-trifluoromethyl)benzene as an internal standard.



Run	*Co-solvent / vol%*	*Thiourea*	*Ni-cat. / mol%*	*picoline•BH_3 equiv*	*$[18a]_0$ / M*	*Surfactant / wt%*	*Yield / %*
1	10	19a	5	2	0.6	2	9
2	50	19a	1	2	0.6	5	58
3	**30**	**19a**	**3**	**1.5**	**0.4**	**3.5**	**35**
4	10	19b	1	2	0.6	2	9
5	50	19a	5	2	0.2	2	55
6	10	19b	5	1	0.2	2	0
7	50	19a	1	1	0.6	2	40
8	50	19b	5	1	0.6	2	78
9	10	19a	1	1	0.2	2	0
10	50	19a	5	1	0.2	5	52
11	10	19a	5	1	0.6	5	0
12	50	19b	1	1	0.2	5	12
13	10	19b	1	1	0.6	5	0
14	**30**	**19a**	**3**	**1.5**	**0.4**	**3.5**	**40**
15	50	19b	1	2	0.2	2	24
16	10	19b	5	2	0.2	5	34
17	50	19b	5	2	0.6	5	81
18	10	19a	1	2	0.2	5	11
19	**30**	**19a**	**3**	**1.5**	**0.4**	**3.5**	**39**
20	30	19b	3	1.5	0.4	3.5	54

After the results of the design had been analysed, we observed different contour plots for thiourea and *N*-methylthiourea. These are displayed in **Figure 74** and **Figure 75** respectively. As expected, some observations were similar to the previous design. Increasing initial aryl iodide concentration increases the predicted conversion. Volume fraction of IPA increases up to a maximum around 45 vol%, as reported in the previous design. Seemingly this change is more impactful for reactions with thiourea in comparison with *N*-methylthiourea. Again, the catalyst loading had a positive relationship with the predicted conversion, but this was not as clear as with the previous design. There was also a positive relationship between the equivalents with respect to nickel catalyst and picoline borane complex, the reductant, and predicted conversion. This may be due to either the necessity of reductant in the activation of the nickel catalyst or the instability of picoline borane in water. The amount of surfactant in the aqueous solution was excluded from these contour plots as we found this variable had little to no effect on the reaction outcome. This may be a result of a lack of variability in surfactant structure between 2-5 wt% TPGS-750-M, the two extremes of surfactant concentration explored. From this point forward we elected to use 2 wt% solutions in water in order to reduce unnecessary waste and for easier solution preparation.

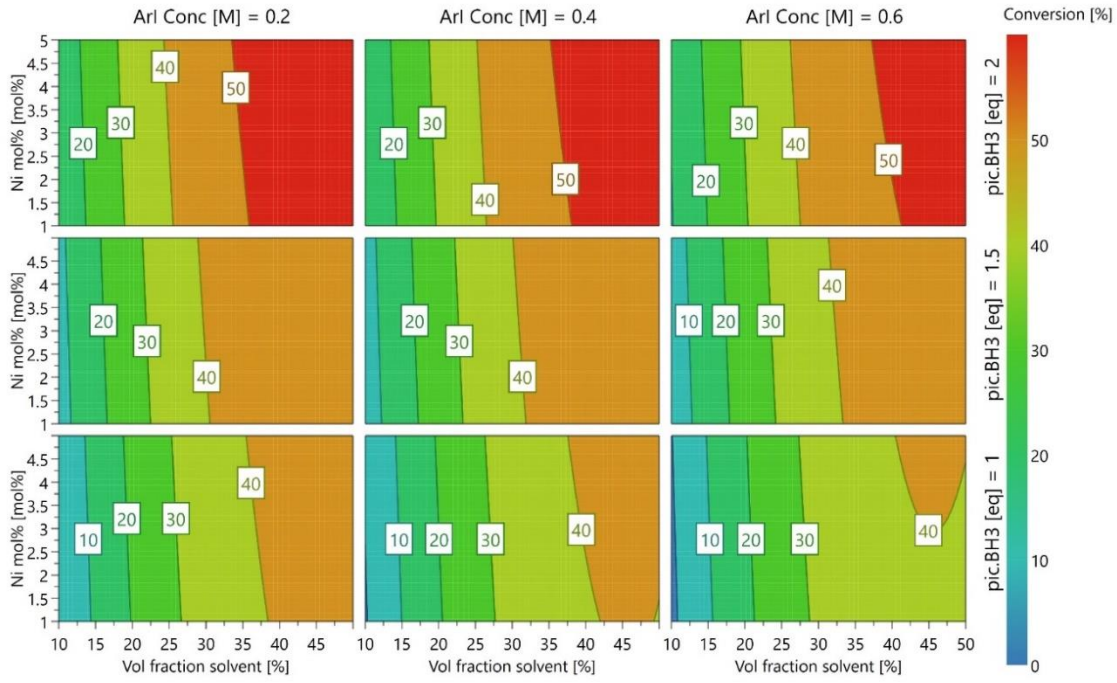


Figure 74 – Contour plot for unsubstituted thiourea produced from DoE analysis of data stated in ***Table 13*** *and 4 additional experiments added to improve model validity. The values associated with the contour lines represent predicted percentage conversion.*

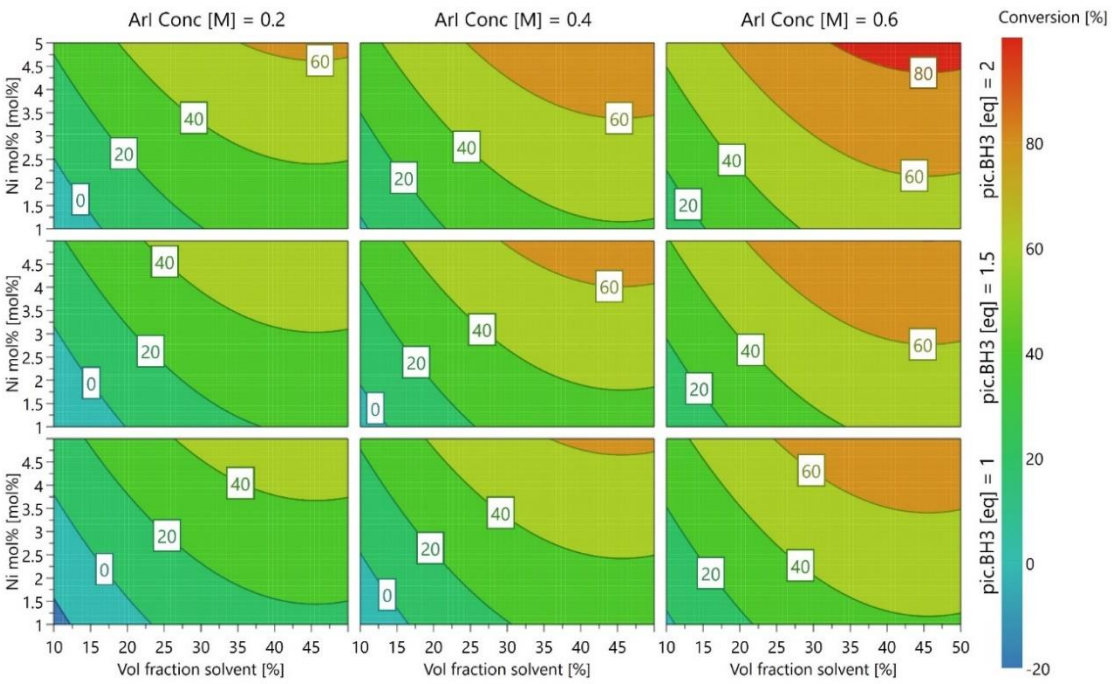


*Figure 75 – Contour plot for N-methylthiourea produced from DoE analysis of data stated in **Table 13** and 4 additional experiments added to improve model validity. The values associated with the contour lines represent predicted percentage conversion.*

Comparing the two contour plots in in **Figure 74** and **Figure 75**, one can notice a difference in the relationship with catalyst loading. As previously mentioned, this can be displayed more clearly with an interaction plot. **Figure 76** indicates that reactions utilising *N*-methylthiourea display the expected positive relationship between catalyst loading and predicted conversion. However, using higher catalyst loading with unsubstituted thiourea results in a negligible increase in predicted conversion in comparison with low catalyst loading. This observed difference in sensitivities to catalyst loading between the thioureas may be used in future experimentation to better understand the mechanistic nuances of this route.

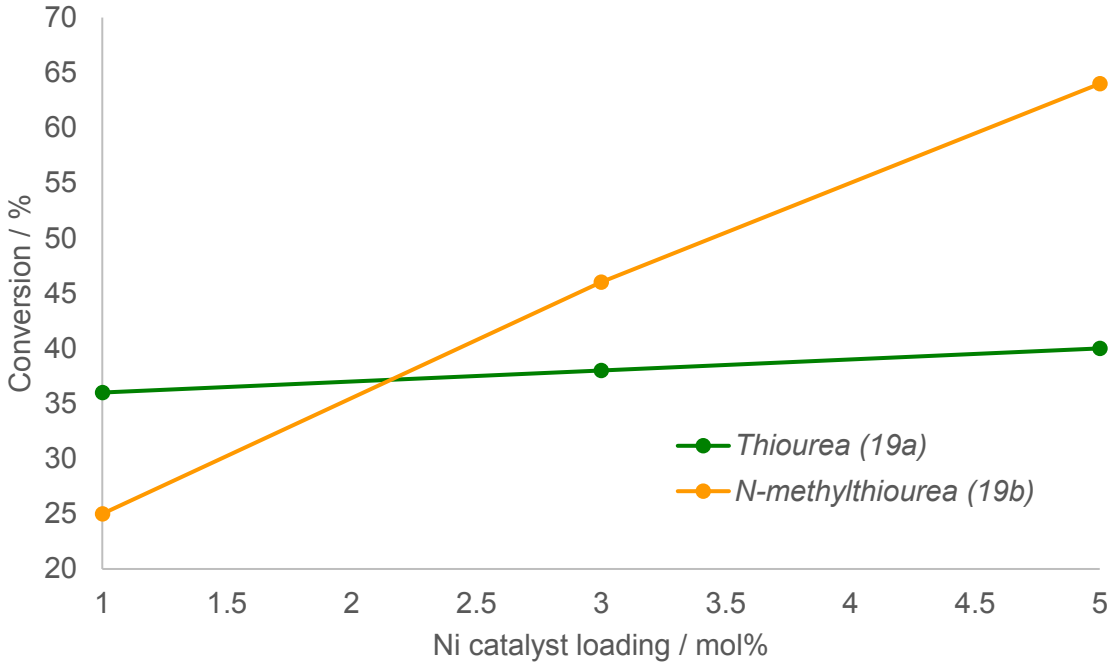


Figure 76 – Interaction plot between mol% of nickel catalyst and thiourea substitution.

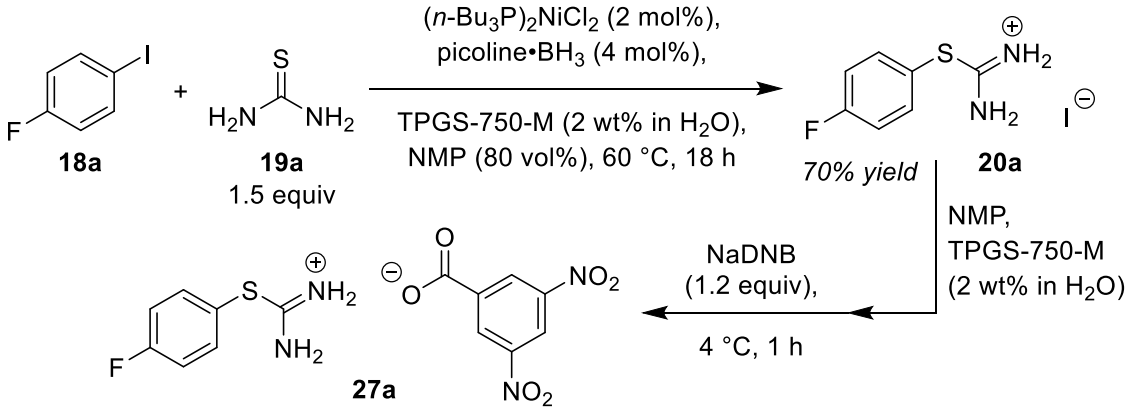
This observation can be used to maximise conversion at either lower or higher catalyst loading by selection of either thiourea. **Figure 76** indicated that yields can be maximised by using *N*-methylthiourea (**19b**) at higher catalyst loading. Though higher yields were obtained using *N*-methylthiourea, thiourea is both lower in molecular weight and less expensive than its *N*-methyl counterpart, as discussed in the previous section. In the method reported by Magné and Ball,[57] substituted thioureas were not explored. While *N*-methylthiourea has proven to give slightly higher yields than its unsubstituted counterpart, we must ensure that the isolation of their salts are as facile.

7.4 Precipitation Experiments

The chromatography-free isolation of the isothiouronium salts produced by Magné and Ball is one of the major advantages of this route.[57] In their methodology, precipitation was facilitated by anion metathesis with sodium 3,5-dinitrobenzoate, resulting in the precipitation of the isothiouronium 3,5-dinitrobenzoate salts from aqueous NMP. In this thesis, however, we carry out the reaction in micelle solutions. This could pose a problem for isolation if the salts do not precipitate from the surfactant solutions. To test this, an

aqueous solution of 3,5-dinitrobenzoate was added to solutions of *S*-(4-fluorophenyl)isothiouronium iodide (**20a**) with varying volume fractions of co-solvent (**Table 14**). This was achieved by synthesising **20a** in surfactant solutions with 80 vol% NMP, giving a 70% yield as calculated from ^{19}F NMR spectroscopic data against an internal standard. This solution was then made up to 20, 50 and 80 vol% NMP solutions by adding the required amount of NMP and surfactant solution. To these solutions, a 0.2 M aqueous solution of sodium 3,5-dinitrobenzoate was added and the resulting solution was placed in a fridge for one hour. Following this, the solid precipitate was removed and the supernatant analysed by ^{19}F NMR spectroscopy against an internal standard. The remaining isothiouronium salt in solution was then compared to the initial calculated 70% yield to determine the percentage precipitation.

Table 14 – Precipitation test in TPGS-750-M solutions with 80, 50 and 20 vol% NMP. Percentage precipitation determined from the ^{19}F NMR spectroscopic analysis of the supernatant solution compared to the 70% NMR yield obtained in the preliminary step. NMR yields were determined using 2,2,2-trifluoroethanol as an internal standard.



Entry	*NMP / vol%*	Precipitation / %
1	80	98
2	50	98
3	20	97

The data in **Table 14** indicate that the isothiouronium 3,5-dinitrobenzoate salt **27a** precipitates excellently from all three solutions. Next, we endeavoured to investigate the effect of thiourea substitution on precipitation (**Figure 77**). Substituted isothiouronium iodide salts were prepared using TPGS-750-M solutions with 50 vol% NMP. A 0.2 M

aqueous solution of sodium 3,5-dinitrobenzoate was then added to each and the solutions were placed in a fridge for up to 18 hours. As previously noted, precipitation of *N*-unsubstituted isothiouronium salts requires only one hour for excellent precipitation. The *N*-substituted thiourea samples however performed poorly overall.

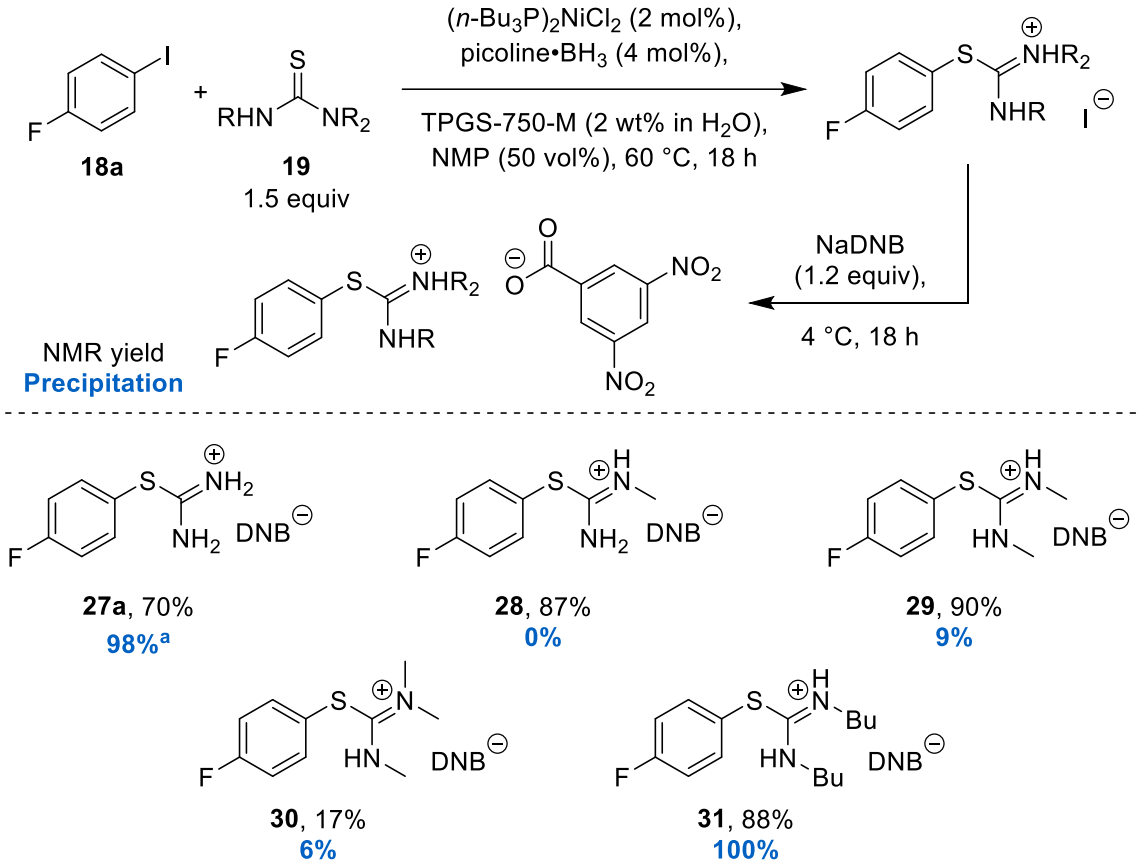


Figure 77 – Precipitation of isothiouronium salts synthesised using a variety of substituted thioureas. TPGS-750-M solutions with 80, 50 and 20 vol% NMP. Percentage precipitation (blue) was determined from the ^{19}F NMR spectroscopic analysis of the supernatant solution compared to the calculated yield (black). NMR yields were determined using 2,2,2-trifluoroethanol as an internal standard.

Despite the increased spectroscopic yields observed using *N*-methylthiourea in this cross-coupling reaction, their salts do not precipitate out of solution under these conditions. Isothiouronium salts from *N,N'*-dimethyl (**29**) and *N,N,N'*-trimethyl (**30**) substituted thioureas also did not precipitate well. Contrary to this trend, *N,N'*-dibutyl salt **31** precipitated fully out of solution. This may be due to the increased lipophilicity and hence decreased solubility of these salts in the aqueous solution. From these data, thiourea

remains the preferential sulfur source due its lower cost and its decreased contribution to the overall atom economy of this route in comparison with *N,N'*-dibutylthiourea. With this confirmation of ease of separation, and the optimisation reported in the previous section, we next set out to investigate the scope of this system.

7.5 Scope

Our research into this cross-coupling route led us to the optimised conditions stated in **Figure 78**. We applied these conditions to a range of aryl iodides and isolated the corresponding isothiouronium 3,5-dinitrobenzoate salts *via* the method mentioned in the previous section. Generally, these optimised conditions produced the respective isothiouronium salts in good to excellent yields. From these results, one can see that this reaction tolerates electron-withdrawing groups, electron-donating groups, free alcohols, free amines free acids, aldehydes and some nitrogen-containing heterocycles. Of particular note, the reactive hydrazine group of **27l** remained untouched in this reaction. These were performed on a 0.5 mmol scale with respect to aryl iodide but the synthesis of **27g** was also performed on a 10 mmol scale, giving excellent yields for both.

For comparison, the isolated yields reported by Magné and Ball using their method are stated in **Figure 78** in blue.[57] Use of the conditions reported in this thesis gives mostly comparable yields, with the exception of isothiouronium salts **27d** and **27o**. Though Magné and Ball's synthesis using NMP is preferable for these two examples, the use of a micelle solution in this manner is a valid substitution for the majority of these substrates. Isolation issues arose with lipophilic aryl iodides such as **27j**, **27p** and, to the point of isolation incapability, **27r**. During isolation, these compounds formed incredibly fine particulates that passed through even glass filter paper. *ortho*-Substitution was not well-tolerated under these conditions (**27d**), to a larger extent than was reported for the method proposed by Magné and Ball. In some instances, unreacted aryl iodide persisted in the resulting precipitate which would hence require further purification. Compounds **27k** and **27o** were isolated as 2:9 and 10:9 ratios of aryl iodide and isothiouronium salt respectively. Applying these conditions to aryl iodide **27q** did not give the desired isothiouronium salt, but instead resulted in a complex mixture by ^{1}H NMR spectroscopy.

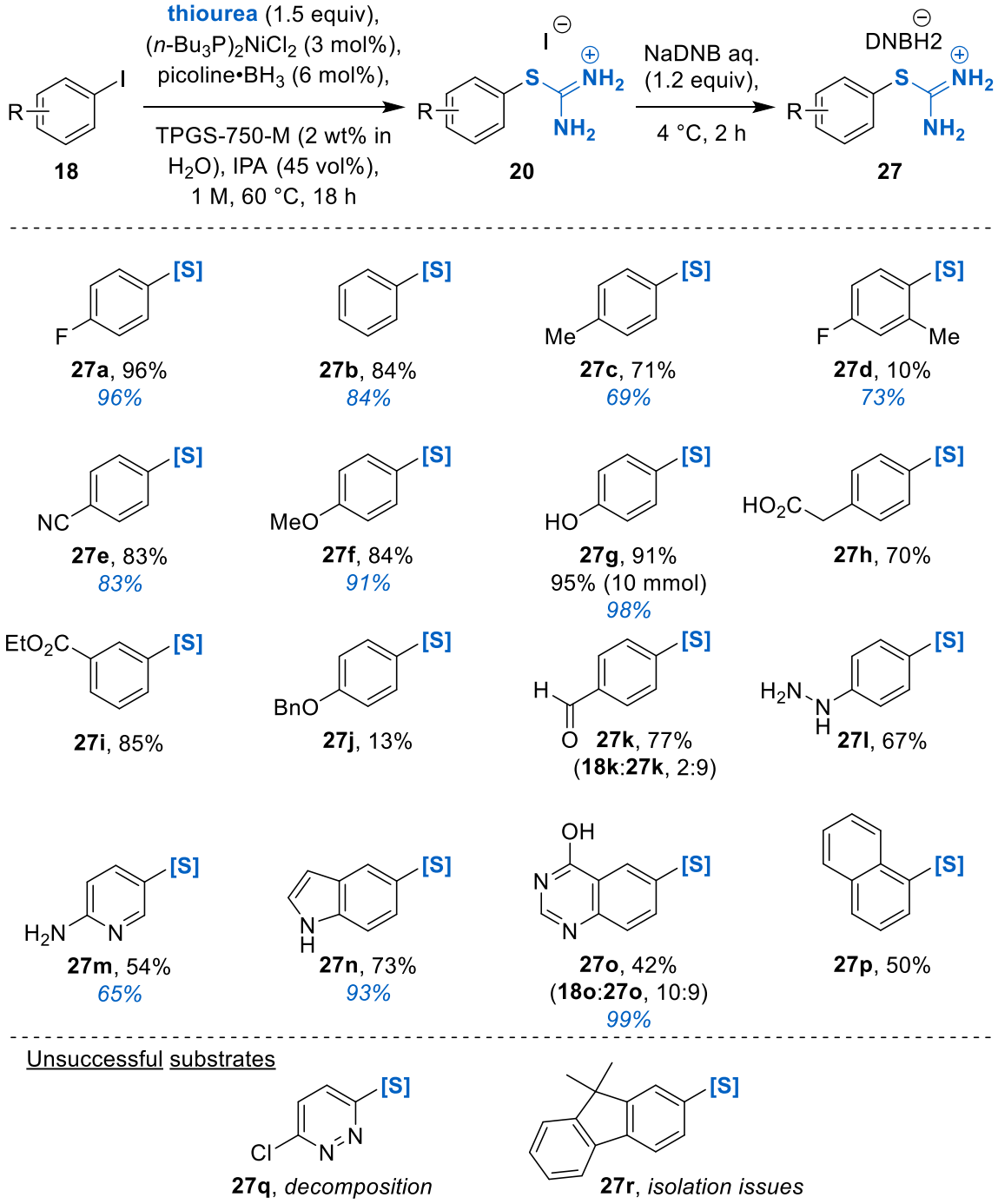


Figure 78 – Scope of the nickel-catalysed cross-coupling of aryl iodides with thiourea in TPGS-750-M solutions (2 wt% in H_2O) with 45 vol% IPA. Yields are reported as isolated yields. ***27k*** *and* ***27o*** *were obtained as mixtures of aryl iodide and isothiouronium salts – ratios are reported in brackets. Yields in blue represent isolated yields reported by Magné and Ball.*[57]

Quantitative yields could not be obtained in this route due to the generation of side-products. One of the two major side products was protodeiodinated arene (ArH) in amounts commensurate to picoline borane. The other, Ar(*n*-Bu)$_3$P$^+$, is of particular interest to the nature of the reaction, a discussion of which will be given in the following section.

7.6 Phosphonium Investigations – Reaction Monitoring

While studying this transformation, one consistent side-product observed was a peak at δ_F = −104 ppm in the ^{19}F NMR spectrum. We found this to be consistent with a phosphonium salt such as **33** (**Figure 79**).[143] Though the exact mechanism of this cross-coupling reaction is not yet known, a C–P reductive elimination from a Ni complex akin to **32** to form arylated phosphonium salts is known.[144–146]

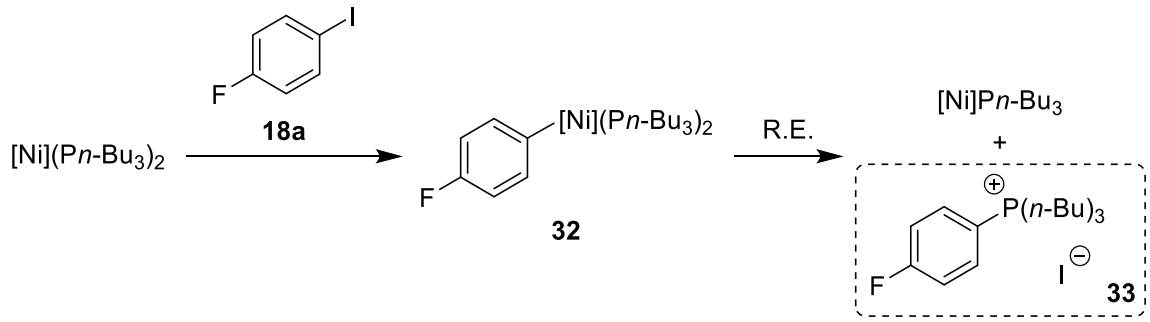


*Figure 79 – Suspected formation of the phosphonium salt **33** by reductive elimination.*

Magné and Ball found that nickel ligand choice greatly affected their reaction outcome.[57] Due to the fact that the generation of this phosphonium species involves the removal of a ligand from the nickel catalyst, this process may be hindering the reaction. To probe this, we monitored the reaction for 3.5 h by ^{19}F NMR spectroscopy to track this side-reaction. The conditions used for this investigation are stated in **Figure 80**. We chose to use *N*-methylthiourea in this instance due to its solubility in NMP in comparison to thiourea. The catalyst loading was also raised in this reaction in an endeavour to decrease reaction times and facilitate monitoring by both ^{31}P and ^{19}F NMR spectroscopy.

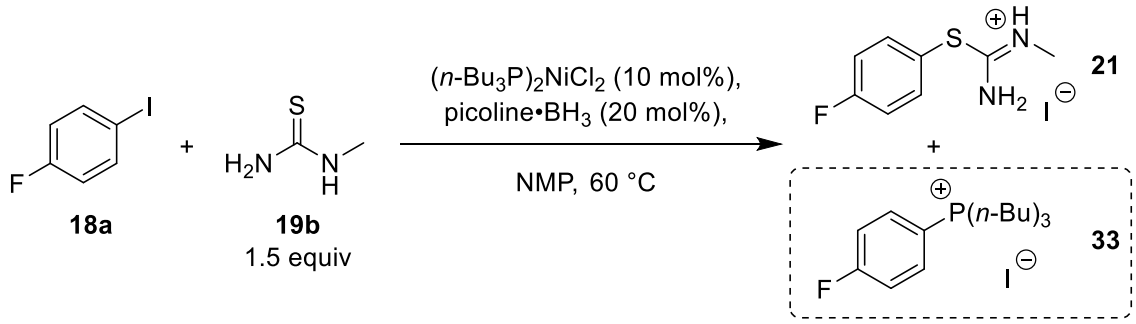


*Figure 80 – The conditions for the reaction monitoring experiment used to track formation of phosphonium salt **33**.*

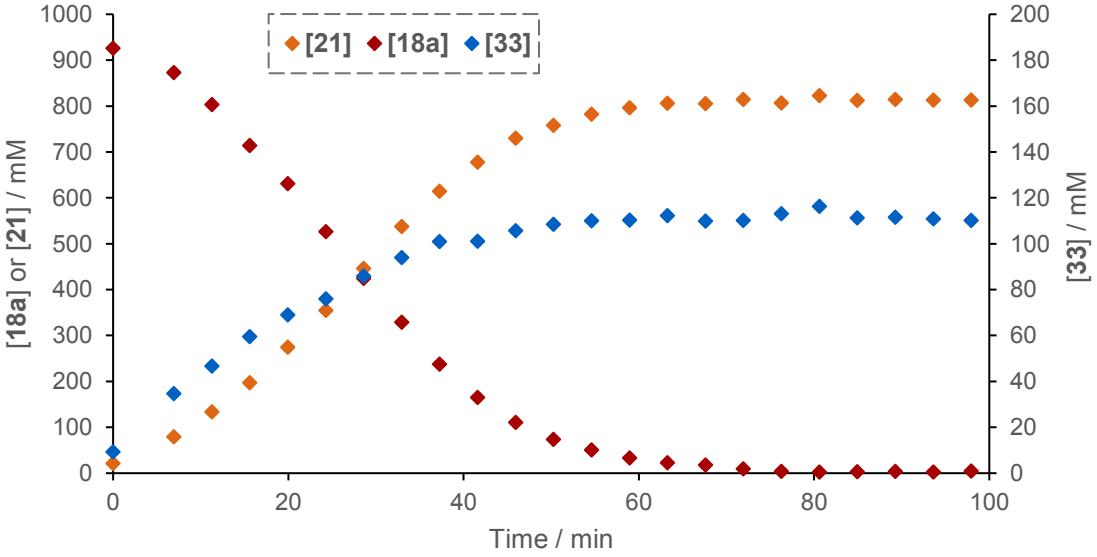


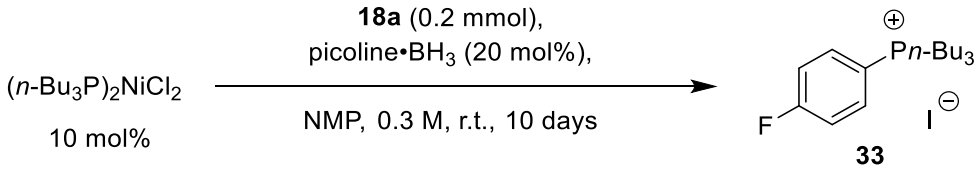
*Figure 81 – A plot of time against concentration of **18a**, **21** and **33** as calculated by ^{19}F NMR spectroscopy using 2,2,2-trifluoroethanol as an internal standard. The y-axis on the left denotes [**18a**] and [**21**], whereas the right axis relates to [**33**].*

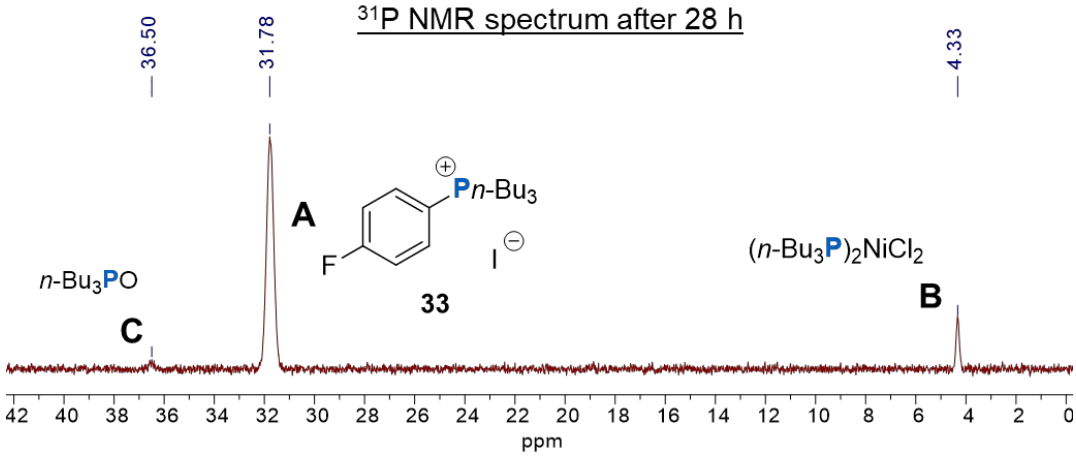
The results of this investigation are summarised in **Figure 81**. It can be seen that formation of this phosphonium species begins from the start of the reaction and continues throughout, reaching its plateau after 60 minutes. This graph also provides further information about the isothiouronium synthesis itself, in particular when observing consumption of **18a** over time. There is a slight sigmoidal profile in the first 10 minutes, which could indicate a catalyst activation process. Subsequently, in the main phase of the reaction there is seemingly a linear correlation between concentration and time for the consumption of aryl iodide. This suggests that the reaction is pseudo zeroth order with respect to aryl iodide concentration. In a Ni(0)/(Ni(II) cycle this would be consistent with a

slow reductive elimination. This contradicts the relationship between aryl iodide concentration and conversion predicted in both DoE models. This disparity could hint at greater mechanistic complexity.

We observed that the formation of phosphonium salt **33** and isothiouronium salt **21** occurs simultaneously. Importantly, the rate of C–S bond formation does not seem to depend on how much phosphonium is formed. Given that the yield of both species plateau at a similar time, the reaction may be prematurely terminating as a result of phosphonium formation. To test this, we first tracked the formation of phosphonium by ^{31}P NMR spectroscopy. This was performed on a solution of 4-fluoroiodobenzene (**18a**), (*n*-$Bu_3P)_2NiCl_2$ and picoline borane complex in NMP in a Young's NMR tube (**Table 15**). The solution of NMP was not deuterated, however a sealed capillary of DMSO-d_6 was added to lock the sample. Over ten days, we observed a decrease in a peak at δ_P 4.3 ppm. This aligns with previous literature for the nickel catalyst at δ_P 5.4 ppm, taking the change in solvent into account.[147] We observed an increase in a peak at δ_P 31.8 ppm which we assigned as the phosphonium peak (**33**). This is based on literature data for phenyltributylphosphonium chloride which resonated at δ_P 30.1 ppm in $CDCl_3$.[148] Another species seen to increase over time is a small peak at δ_P 36.5 ppm. This is likely the phosphine oxide produced from residual oxygen in the reaction solvent. The literature shift for tributylphosphine oxide has been reported as δ_P 44.7 ppm in $CDCl_3$.[143]

*Table 15 – Phosphine species **33** developing over 10 days, as followed by ^{31}P NMR spectroscopy. Proportions calculated from the relative peak intensities by ^{31}P NMR spectroscopy.*





Entry	***Time / h***	***Proportion A***	***Proportion B***	***Proportion C***
1	6	0.85	0.15	0
2	28	0.88	0.09	0.03
3	232	0.98	0	0.02

When we observed no remaining phosphine associated with the nickel catalyst, the resulting solution existed as a clear bright blue solution as opposed to the initial deep red colour resulting from the nickel catalyst. The phosphine species observed in this solution were predominately the phosphonium species **33** but with a small amount of the suspected phosphine oxide. To this solution, aryl iodide, thiourea and NMP were added to make the solution up to the standard reaction conditions (**Figure 82**). When this solution was stirred at 60 °C for 18 h, an 87% conversion was observed by ^{19}F NMR spectroscopy.

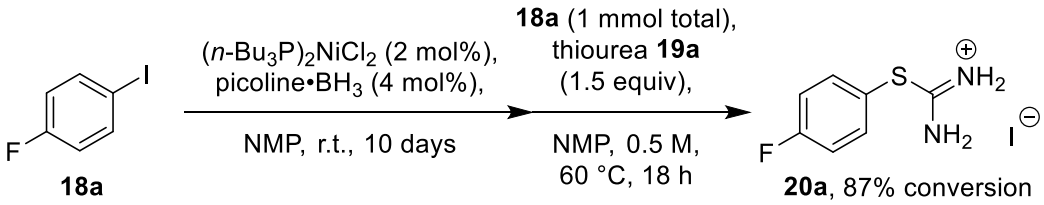


*Figure 82 – Investigation into the effect of phosphonium formation on the synthesis of **20a**. Percentage conversion as calculated from ^{19}F NMR spectroscopic data.*

As previously mentioned, the mechanism for this transformation is not yet known. The fact that the reaction tolerates the lack of tributylphosphine as a ligand for nickel could provide an insight into the mechanism of the reaction. This is particularly interesting given that Magné and Ball observed that the ligand on the nickel catalyst had a large influence on yield.[57] Furthermore, the ligand used in that study, tri(cyclohexyl)phosphine, was applied to the reaction conditions reported in this thesis (**Figure 83**). In this instance, we observed no generation of phosphonium side-product. This could be due to the more sterically hindered cyclohexyl group preventing the proposed reductive elimination step.

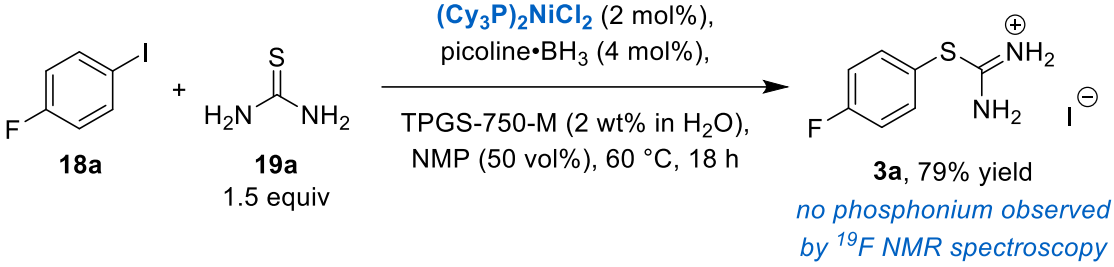


Figure 83 – Standard reaction conditions for the synthesis of isothiouronium salts applied to the catalyst used in the report by Magné and Ball.[57] Yields are given as calculated from ^{19}F NMR spectroscopic data using bis(4-trifluoromethyl)benzene as an internal standard.

7.7 DLS

During the optimisation of this route, it became clear that a co-solvent was required in order to improve yields. This, as mentioned previously, may be due to a combination of increased solubility of reagents and the swelling of micelles. We used dynamic light scattering (DLS) to analyse the effect that co-solvent has on the average size of the micelles in 2 wt% solutions of TPGS-750-M in water. DLS involves the passage of a laser through solutions and the analysis of the fluctuation of intensity observed on the other

side.[149] The light is scattered by any micelles that move into the path of the laser. The average diameter of these micelles can be calculated from the timeframe over which the particle is scattering the laser. Three different co-solvents were used to investigate their effect on average micelle diameter: IPA, acetonitrile and DMSO. For each co-solvent, TPGS-750-M solutions containing 0, 15, 30 and 45 vol% co-solvent were analysed. The results of which are displayed in **Table 16**.

Table 16 – The average diameter recorded in 2 wt% TPGS-750-M solutions in water with varying proportions of co-solvent using DLS.

Entry	***Co-solvent***	***Average micelle diameter in X vol% co-solvent / nm***			
		0 vol%	***15 vol%***	***30 vol%***	***45 vol%***
1	MeCN	8	9	9	8
2	DMSO	8	26	33	58
3	IPA	9	33	108	463

As samples with no co-solvent were measured three times, the reproducibility of these results is displayed. Interestingly, addition of increasing proportions of acetonitrile has a negligible effect on the micelle size. For DMSO and IPA, however, we do see a trend of increasing micelle size with increasing proportions of co-solvent. We observed that each increment of IPA had a much larger effect on the size of micelles than DMSO. Making a solution using our optimised conditions of 45 vol% IPA gave micelles averaging 463 nm in diameter. This theoretically provides a larger volume available for the reaction to take place in. Though the previously mentioned report by Lipshutz in 2018 stated that micelles for organic synthesis should be in the range of 10-100 nm, with an ideal size of 50-60 nm.[128] The authors suggested that larger micelles suffer from decreased exchange between the aqueous and lipophilic phases. However, Shen and co-workers later discussed how the suitability of micelle size varied by the size of reagents.[150]

Further information can be obtained from the particle size distribution charts generated from the DLS measurements of each series of co-solvent data. **Figure 84a** displays the previously discussed negligible change in micelle size when increasing volume fractions of acetonitrile are added. The size distribution chart of DMSO solutions (**Figure 84b**) does indeed show the trend of increasing average particle size as the volume fraction of DMSO is increased, as stated in **Table 16**. However, this chart also demonstrates that TPGS-750-M solutions with DMSO contain multiple structure populations. This phenomenon can

be seen more clearly in the distribution chart where IPA was used as a co-solvent (**Figure 84c**). This bimodal distribution suggests the presence of a different surfactant structure within this micelle. Here, both populations increase in size with increasing amounts of IPA, with only the larger population existing in 45 vol% solutions of IPA. Without cryoTEM imaging, the structures associated with these populations remain unknown. Though, DLS assumes spherical particles when calculating size and hence can produce more complicated charts when non-spherical structures are present.[151] This could be the reasoning behind the more complex distributions observed when using DMSO as a co-solvent.

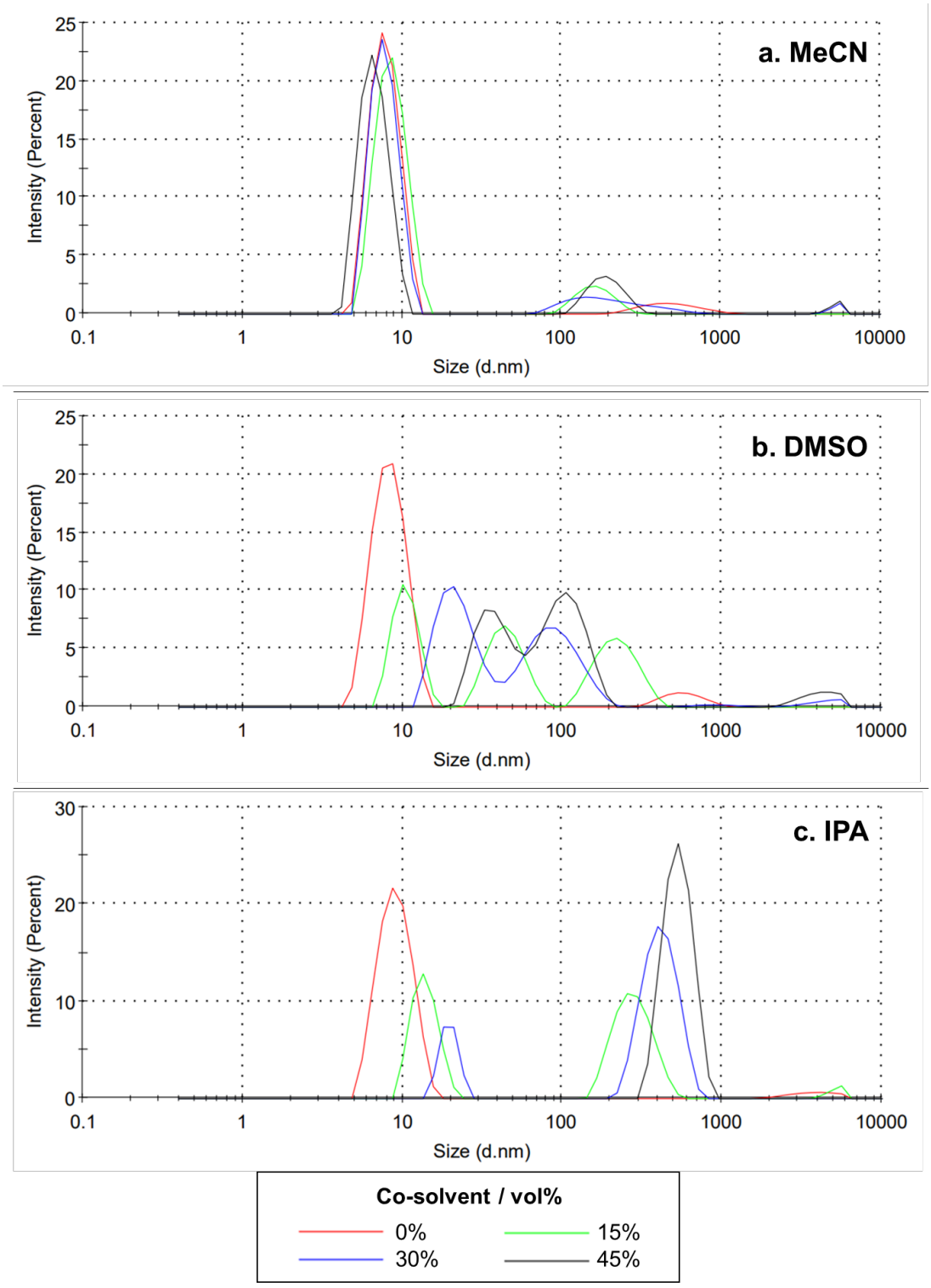


Figure 84 – Particle size distributions by intensity obtained from DLS analysis of 2 wt% TPGS-750-M solutions in water with acetonitrile (a), DMSO (b) or IPA (c).

8 Conclusions and Future Work

Aligning with the 5th of the 12 green chemistry principles, it is vital that future synthetic methods are conscious of the impact that solvent selection has on the sustainability of a route. Micelle solutions have been used in organic synthesis since the 1970's[152] but have gained traction in recent years thanks to pioneering work by Lipshutz and co-workers. These solutions provide a lipophilic area in which reactions may take place whilst using water as the bulk solvent. Further to this, the development of "designer surfactants" that are "benign by design" add to reduction in environmental impact. To this effect, this section of the thesis reported a nickel-catalysed synthesis of isothiouronium salts in micelle solutions (**Figure 85**). Isothiouronium salts are thiophenol surrogates that are non-toxic, crystalline and bench stable. Their synthesis *via* cross-coupling of thiourea and an aryl iodide offers a preferential option to other methods of aryl C–S cross coupling that often employ high temperatures, strong bases or the use of thiols.

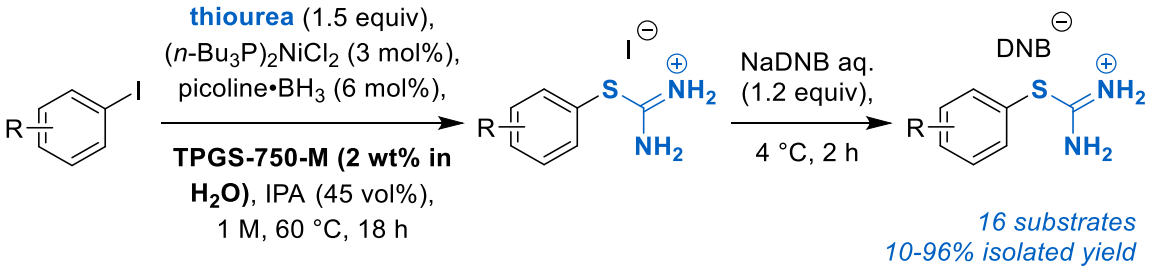


Figure 85 – Ni-catalysed cross-coupling of aryl iodides with thiourea in micelle solutions, thiophenol surrogate isothiouronium salts.

The foundation for this work came from a publication by Magné and Ball, who instead utilised the reprotoxic solvent NMP. In this thesis, TPGS-750-M solutions were used as a greener alternative. After initial experimentation, it was found that co-solvents are necessary to give good yields. This is likely due to a combination of increased reagent solubility and micelle swelling. The choice and volume fraction of co-solvent had a large influence on the outcome of the reaction. DLS data suggested that different solvents

increase the average micelle diameter to different extents. The precise effect that co-solvent has on these TPGS-750-M solutions cannot be deduced, however, without confirmation by cryoTEM imaging.

As can be seen in **Figure 85**, there are many variables involved in this method. The standard one variable at a time method for reaction optimisation would have been very time-consuming and would waste a lot of material. Instead, DoE was used to find the optimal conditions in a fewer number of experiments. Two DoE designs were run, the results of which indicated a strong positive relationship between volume fraction of co-solvent and yield. *N*-substitution at thiourea was also explored and *N*-methylthiourea was highlighted as giving the highest yields of corresponding isothiouronium salt. Despite this, unsubstituted thiourea remained as the preferred sulfur source due to its lower molecular weight, affordability and the low propensity of *N*-methyl salts to precipitate out of solution. The information gathered in these designs gave the conditions stated in **Figure 85** as optimised. Using these conditions, a variety of aryl iodides were screened to explore the scope of this method. The isolated yields varied, and poor yields were due to reagent instability, isolation issues or ortho substitution on the aryl iodide.

As is common for nickel-catalysed cross-couplings, the exact mechanism of this route is unknown. Preliminary mechanistic studies were performed by Magné and Ball which gave insight but did not confirm which species are present in this reaction. In the work reported in this thesis, the change in nickel catalyst resulted in the observation of aryl phosphonium salts. An investigation into the effect that the formation of this salt has on the outcome of the reaction displayed that even in the absence of *n*-Bu_3P ligands, very good conversions can be obtained. This finding adds to the overall picture of what is likely a complex reaction mechanism, but much work is required before a catalytic cycle can be confirmed.

A benefit of using isothiouronium salts is their easy handling compared to their thiophenol counterparts. Additionally, the thiophenol functionality can be exposed on treatment with a weak base. These mild deprotection conditions allow for a wide range of diversification experiments to access other sulfur functionalities, as displayed by Magné and Ball. The range of diversification reactions available, and the reagent separation that micelles may provide, opens avenues to one-pot syntheses of more complex aryl sulfur species.

9 Experimental

General

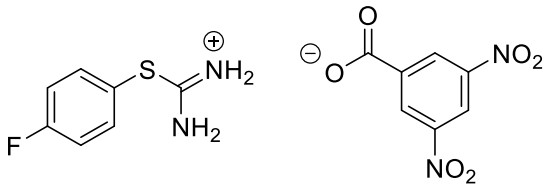
Reagents were purchased from commercial suppliers and used as received. Anhydrous solvents were obtained from in-house solvent purification systems (Inert® Prosolv; dried by passage through activated alumina columns under pressure of Ar). Reactions requiring inert conditions were conducted under an atmosphere of nitrogen using standard Schlenk techniques. All solvents, unless otherwise stated, were degassed prior to addition. For water, this was achieved through a freeze-pump-thaw method.[153] For all other solvents, nitrogen was passed through the solvent for a minimum of 30 minutes. NMR spectra were recorded at 298 K on Bruker Advance-III spectrometers operating at nominal ^{1}H frequencies of 400 MHz. Chemical shifts (δ) are given in ppm and referenced to residual solvent peaks for ^{1}H (DMSO: δ_H = 2.50) and $^{13}C\{^{1}H\}$ (DMSO: δ_C = 39.52). Signals are reported at singlet (s), doublet (d), triplet (t), quartet (q), apparent triplet of doublets (apptd), multiplet (m), broad (br) or combinations of the above. High resolution mass spectroscopy (HRMS was performed using a Bruker MicroTOF spectrometer, with an electrospray ionisation (ESI) ion source. Infrared (IR) spectra were recorded on a Bruker Alpha platinum-ATR with diamond window. Melting points were measured on a Gallenkamp apparatus.

General procedure for the synthesis of isothiouronium salts:

A sealed microwave tube containing solid aryl iodide **18** (0.50 mmol), thiourea **19a** (57 mg, 0.75 mmol), picoline borane complex (3.2 mg, 0.03 mmol) and bis(tributylphosphine)nickel(II) chloride (8.0 mg, 0.015 mmol) was evacuated and backfilled with dinitrogen. If the aryl iodide is liquid, this is added afterwards. Degassed IPA (0.23 mL) then TPGS-750-M in water (2 wt%, 0.28 mL) were added and the resulting

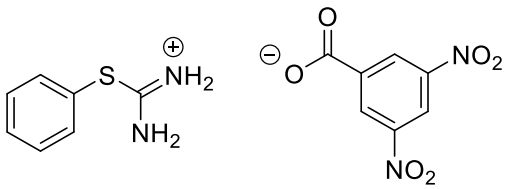
mixture was stirred for 18 h at 60 °C. To this stirred solution, a 0.2 M solution of sodium 3,5-dinitrobenzoate in water (3 mL, 0.6 mmol) was added. The resulting suspension was cooled to 4 °C for 2 hours, then collected by filtration using a Whatman 3-piece filter funnel fitted with glass microfibre filters. The filter cake was then washed with water (4 × 2 mL), ice-cold IPA (2 × 2 mL), then diethyl ether (4 × 2 mL). Drying *in vacuo* afforded the isothiouronium 3,5-dinitrobenzoate salts **27** as powders.

_S_-(4-Fluorophenyl)isothiouronium 3,5-dinitrobenzoate (27a)



Prepared according to the general procedure. Isolated as an off-white powder **27a** (183 mg, 0.48 mmol, 96%). **m.p.** 173-174 °C (lit. 190-192 °C);[57] **^{1}H NMR (400 MHz, DMSO-d_6)** δ = 9.25 (brs, 4H), 8.89 (d, *J* = 2.3 Hz, 2H), 8.83 (t, *J* = 2.3 Hz, 1H), 7.76 (dd, *J* = 8.3, 5.2 Hz, 2H), 7.46-7.39 (m, 2H); **^{13}C{^{1}H} NMR (101 MHz, DMSO-d_6)** δ = 169.8, 165.9, 164.7 (d, *J* = 259.6 Hz), 148.3, 142.8, 139.5 (d, *J* = 9.4 Hz), 128.9, 119.8, 119.6, 118.2 (d, *J* = 22.6 Hz); **^{19}F NMR (376 MHz, DMSO-d_6)** δ = −108.7 (tt, *J* = 8.7, 5.1 Hz); **ν_{max}(neat)/cm^{-1}:** 3457, 3102, 1674, 1615, 1587, 1531, 1490, 1452, 1379, 1346, 1226, 1160, 1014, 842, 720, 522, 49; **HRMS** calcd. for $C_7H_8FN_2S^+$: 171.0387 [M-DNB]$^+$; found (ESI$^+$) 171.0390. Spectroscopic data are in agreement with literature.[57]

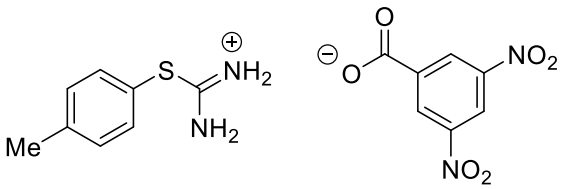
_S_-Phenylisothiouronium 3,5-dinitrobenzoate (27b)



Prepared according to the general procedure. Isolated as an off-white powder **27b** (153 mg, 0.42 mmol, 84%). **m.p.** 189-190 °C (lit. 198-200 °C);[57] **^{1}H NMR (400 MHz, DMSO-d_6)**

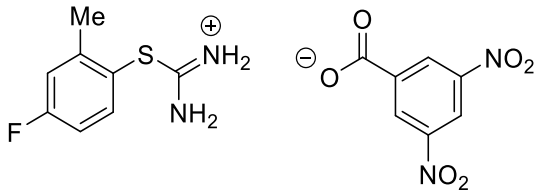
δ = 9.40 (s, 4H), 8.88 (d, *J* = 2.2 Hz, 2H), 8.83 (t, *J* = 2.2 Hz, 1H), 7.71 – 7.54 (m, 5H); **^{13}C{^{1}H} NMR (101 MHz, DMSO-*d*$_6$)** δ = 169.7, 166.5, 148.3, 142.6, 136.4, 132.0, 130.9, 128.9, 124.1, 119.9; **ν_{max}(neat)/cm^{-1}:** 3400, 3098, 2872, 2709, 1739, 1609, 1576, 1534, 1442, 1375, 1217, 1156, 1090, 1073, 920, 873, 758, 727, 653, 557, 524, 489, 443; **HRMS** calcd. for $C_7H_9N_2S^+$: 153.0481 [M-DNB]$^+$; found (ESI$^+$) 153.0487. Spectroscopic data are in agreement with literature.[57]

***S*-(4-Methylphenyl)isothiouronium 3,5-dinitrobenzoate (27c)**



Prepared according to the general procedure. Isolated as an off-white powder **27c** (135 mg, 0.36 mmol, 71%). **m.p.** 186-187 °C (lit. 201-202 °C);[57] **^{1}H NMR (400 MHz, DMSO-*d*$_6$)** δ = 8.95 (brs, 4H), 8.89 (d, *J* = 2.2 Hz, 2H), 8.83-8.80 (m, 1H), 7.58 – 7.53 (m, 2H), 7.39 (d, *J* = 8.0 Hz, 2H), 2.39 (s, 3H); **^{13}C{^{1}H} NMR (101 MHz, DMSO-*d*$_6$)** δ = 170.0, 165.9, 148.3, 143.1, 142.2, 136.5, 131.6, 128.9, 120.3, 119.7, 21.4; **ν_{max}(neat)/cm^{-1}:** 3360, 3258, 3100, 1665, 1609, 1579, 1535, 1447, 1384, 1342, 1187, 1158, 1082, 1071, 922, 856, 817, 792, 730, 709, 520, 488, 455; **HRMS** calcd. for $C_8H_{11}N_2S^+$: 167.0637 [M-DNB]$^+$; found (ESI$^+$) 167.0642. Spectroscopic data are in agreement with literature.[57]

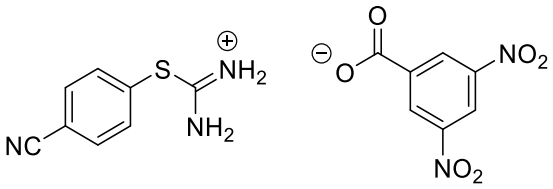
***S*-(4-Fluoro-2-methylphenyl)isothiouronium 3,5-dinitrobenzoate (27d)**



Prepared according to the general procedure. Isolated as an off-white powder **27d** (183 mg, 0.48 mmol, 96%). **m.p.** 185-187 °C (lit. 213-215 °C);[57] **^{1}H NMR (400 MHz, DMSO-*d*$_6$)** δ = 9.81 (brs, 4H), 8.87 (d, *J* = 2.2 Hz, 2H), 8.85 (t, *J* = 2.2 Hz, 1H), 7.73 (dd, *J* = 8.6, 5.9

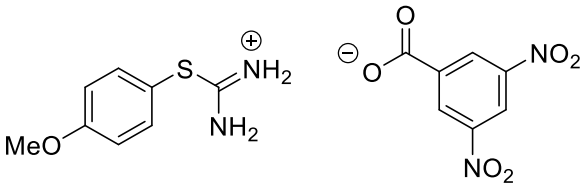
Hz, 1H), 7.41 (dd, *J* = 10.0, 2.9 Hz, 1H), 7.23 (apptd, *J* = 8.6, 2.9 Hz, 1H), 2.43 (s, 3H); **^{13}C{^{1}H} NMR (101 MHz, DMSO-*d*$_6$)** δ = 169.5, 166.7, 164.8 (d, *J* = 249.5 Hz), 148.3, 147.3 (d, *J* = 9.6 Hz), 142.5, 140.5 (d, *J* = 9.6 Hz), 128.9, 119.9, 119.10 (d, *J* = 2.7 Hz), 119.08 (d, *J* = 22.2 Hz), 115.5 (d, *J* = 22.2 Hz), 21.0; **^{19}F NMR (376 MHz, DMSO-*d*$_6$)** δ = −108.15 (ddd, *J* = 9.8, 8.5, 5.7 Hz); **HRMS** calcd. for $C_8H_{10}FN_2S^+$: 185.0543 [M-DNB]$^+$; found (ESI$^+$) 185.0551. Spectroscopic data are in agreement with literature.[57]

S-(4-Cyanophenyl)isothiouronium 3,5-dinitrobenzoate (27e)



Prepared according to the general procedure. Isolated as a pink powder **27e** (162 mg, 0.42 mmol, 83%). **m.p.** 173-174 °C (lit. 195-196 °C);[57] **^{1}H NMR (400 MHz, DMSO-*d*$_6$)** δ = 9.58 (s, 3H), 8.89 (d, *J* = 2.2 Hz, 2H), 8.86 (t, *J* = 2.2 Hz, 1H), 8.02 (d, *J* = 8.4 Hz, 2H), 7.88 (d, *J* = 8.4 Hz, 2H); **^{13}C{^{1}H} NMR (101 MHz, DMSO-*d*$_6$)** δ = 168.7, 166.5, 148.4, 141.0, 136.5, 134.3, 130.9, 129.0, 120.4, 118.6, 114.0; **ν_{max}(neat)/cm^{-1}:** 3444, 3200, 3087, 2234, 1738, 1680, 1620, 1531, 1451, 1379, 1346, 1083, 1018, 922, 840, 791, 723 552, 521, 501, 463, 416; **HRMS** calcd. for $C_8H_8N_3S^+$: 178.0433 [M-DNB]$^+$; found (ESI$^+$) 178.0434. Spectroscopic data are in agreement with literature.[57]

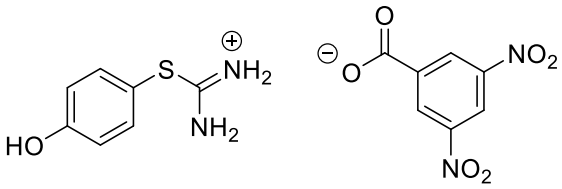
S-(4-Methoxyphenyl)isothiouronium 3,5-dinitrobenzoate (27f)



Prepared according to the general procedure. Isolated as a pale green powder **27f** (166 mg, 0.42 mmol, 84%). **m.p.** 198-200 °C (lit. 214-216 °C);[57] **^{1}H NMR (400 MHz, DMSO-*d*$_6$)** δ = 9.36 (s, 4H), 8.88 (d, *J* = 2.2 Hz, 2H), 8.83 (t, *J* = 2.2 Hz, 1H), 7.64 – 7.58 (m, 2H), 7.15

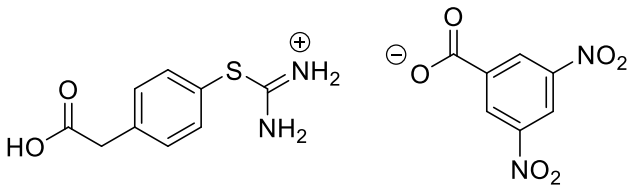
– 7.10 (m, 2H), 3.84 (s, 3H); **^{13}C{^{1}H} NMR (101 MHz, DMSO-d_6)** δ = 170.7, 166.3, 162.4, 148.3, 142.9, 138.6, 128.9, 119.8, 116.6, 113.8, 56.0; **ν_{max}(neat)/cm^{-1}:** 3398, 2970, 2707, 1738, 1666, 1611,1572, 1536, 1495, 1458, 1436, 1378, 1368, 1341, 1296, 1257, 1177, 1086, 1071, 1024, 918, 833, 799, 725, 572, 533, 520, 496, 448; **HRMS** calcd. for $C_8H_{11}N_2OS^+$: 183.0587 [M-DNB]$^+$; found (ESI$^+$) 183.0593. Spectroscopic data are in agreement with literature.[57]

***S*-(4-Hydroxyphenyl)isothiouronium 3,5-dinitrobenzoate (27g)**



Prepared according to the general procedure and on a 5 mmol scale. Isolated as a grey powder **27g** (173 mg, 0.45 mmol, 91%). **m.p.** 199-200 °C (lit. 217-218 °C);[57] **^{1}H NMR (400 MHz, DMSO-d_6)** δ = 9.58 (brs, 4H), 8.89 (d, *J* = 2.2 Hz, 2H), 8.83 (t, *J* = 2.2 Hz, 1H), 7.50 – 7.45 (m, 2H), 6.96 – 6.91 (m, 2H); **^{13}C{^{1}H} NMR (101 MHz, DMSO-d_6)** δ = 171.3, 166.8, 161.4, 148.3, 142.5, 138.7, 128.9, 119.9, 118.1, 111.2; **ν_{max}(neat)/cm^{-1}:** 3607, 3264, 3099, 2970, 2762, 1738, 1673, 1624, 1610, 1580, 1534, 1499, 1452, 1382, 1347, 1276, 1229, 1217, 1177, 1088, 1076, 917, 838, 732, 715, 610, 522, 493, 445; **HRMS** calcd. for $C_7H_9N_2OS^+$: 169.0430 [M-DNB]$^+$; found (ESI$^+$) 169.0434. Spectroscopic data are in agreement with literature.[57]

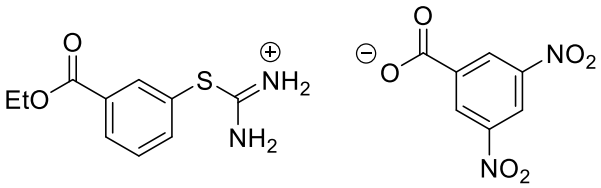
***S*-(4-(Carboxymethyl)phenyl)isothiouronium 3,5-dinitrobenzoate (27h)**



Prepared according to the general procedure. Isolated as a white powder **27h** (148 mg, 0.35 mmol, 70%). **m.p.** 188-190 °C; **^{1}H NMR (400 MHz, DMSO-d_6)** δ = 9.27 (brs, 4H), 8.89

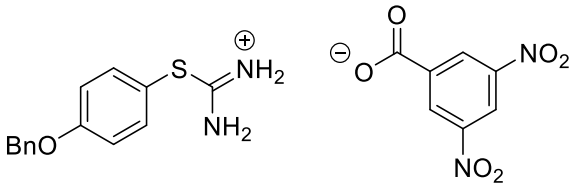
(d, *J* = 2.2 Hz, 2H), 8.86 (t, *J* = 2.2 Hz, 1H), 7.65 – 7.60 (m, 2H), 7.50 – 7.45 (m, 2H), 3.69 (s, 2H); **^{13}C{^{1}H} NMR (101 MHz, DMSO-*d*$_6$)** δ = 169.9, 166.9, 148.3, 142.3, 136.4, 131.9, 130.9, 128.9, 127.6, 124.1, 119.9, 40.1; **ν_{max}(neat)/cm^{-1}:** 3450, 3264, 3101, 2970, 2766, 1737, 1726, 1672, 1608, 1574, 1534, 1461, 1418, 1378, 1344, 1217, 1189, 1163, 1093, 1017, 917, 841, 807, 720, 655, 611, 519, 485, 461, 417; **HRMS** calcd. for $C_9H_{11}N_2O_2S^+$: 211.0536 [M-DNB]$^+$; found (ESI$^+$) 211.0547.

***S*-(3-(Ethoxycarbonyl)phenyl)isothiouronium 3,5-dinitrobenzoate (27i)**



Prepared according to the general procedure. Isolated as a pink powder **27i** (185 mg, 0.42 mmol, 85%). **m.p.** 188-189 °C; **^{1}H NMR (400 MHz, DMSO-*d*$_6$)** δ = 9.53 (brs, 4H), 8.88 (d, *J* = 2.2 Hz, 2H), 8.84 (t, *J* = 2.2 Hz, 1H), 8.18-8.13 (m, 2H), 7.96 (appdt, *J* = 7.8, 1.6 Hz, 1H), 7.72 (appt, *J* = 8.1 Hz, 1H), 4.37 (q, *J* = 7.1 Hz, 2H), 1.35 (t, *J* = 7.1 Hz, 3H); **^{13}C{^{1}H} NMR (101 MHz, DMSO-*d*$_6$)** δ = 169.5, 166.8, 165.2, 148.3, 142.2, 140.9, 136.8, 132.4, 132.3, 131.4, 128.9, 125.1, 120.0, 61.7, 14.6; **ν_{max}(neat)/cm^{-1}:** 3366, 3097, 2970, 2721, 1738, 1708, 1619, 1584, 1534, 1455, 1422, 1512, 1368, 1345, 1289, 1273, 1171, 1133, 1084, 1071, 1011, 919, 794, 756, 722, 682, 581, 492, 444, 419; **HRMS** calcd. for $C_{10}H_{13}N_2O_2S^+$: 225.0692 [M-DNB]$^+$; found (ESI$^+$) 225.0701.

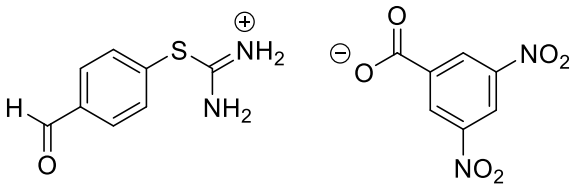
***S*-(4-(Benzyloxy)phenyl)isothiouronium 3,5-dinitrobenzoate (27j)**



Prepared according to the general procedure. Isolated as a grey powder **27j** (31 mg, 0.07 mmol, 13%). **m.p.** 183-188 °C; **^{1}H NMR (400 MHz, DMSO-*d*$_6$)** δ = 9.09 (brs, 4H) 8.89 (d,

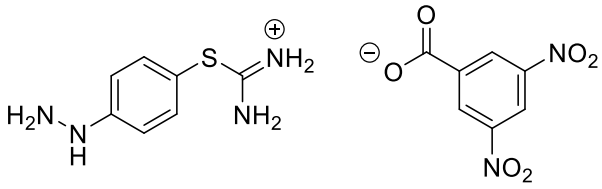
J = 2.3 Hz, 2H), 8.82 (t, *J* = 2.3 Hz, 1H), 7.61 (d, *J* = 8.8 Hz, 2H), 7.50 – 7.34 (m, 5H), 7.20 (d, *J* = 8.8 Hz, 2H), 5.19 (s, 2H); **$^{13}C\{^{1}H\}$ NMR (101 MHz, DMSO-d_6)** δ = 170.8, 166.5, 161.5, 148.3, 142.6, 138.6, 136.9, 129.0, 128.9, 128.5, 128.3, 119.8, 117.3, 114.1, 70.1; **ν_{max}(neat)/cm^{-1}:** 3394, 3102, 1739, 1671, 1609, 1536, 1494, 1452, 1381, 1342, 1255, 1173, 1068, 1018, 912, 883, 831, 796, 747, 722, 698, 583, 533, 497, 443; **HRMS** calcd. for $C_{14}H_{15}N_2OS^+$: 259.0900 [M-DNB]$^+$; found (ESI$^+$) 259.0904.

S-(4-Formylphenyl)isothiouronium 3,5-dinitrobenzoate (27k)



Prepared according to the general procedure. Isolated as a 9:2 mixture of isothiouronium salt and aryl iodide. Obtained as a yellow powder **27k:18k** (9:2, 170 mg, 0.38 mmol, 77%). **m.p.** 149-151 °C; **^{1}H NMR (400 MHz, DMSO-d_6)** δ = 10.12 (s, 1H), 9.80 (brs, 4H), 8.89 (d, *J* = 2.2 Hz, 2H), 8.87 (t, *J* = 2.2 Hz, 1H), 8.07 – 8.03 (m, 2H), 7.93 – 7.89 (m, 2H); **$^{13}C\{^{1}H\}$ NMR (101 MHz, DMSO-d_6)** δ = 193.3, 168.8, 166.4, 148.4, 141.0, 137.9, 136.2, 131.3, 129.0, 121.4, 120.4; **ν_{max}(neat)/cm^{-1}:** 3250, 3100, 2970, 2849, 2743, 1739, 1698, 1675, 1616, 1592, 1532, 1453, 1430, 1377, 1365, 1344, 1229, 1205, 1081, 1013, 915, 889, 824, 791, 731, 720, 610, 521, 483; **HRMS** calcd. for $C_8H_9N_2OS^+$: 181.0430 [M-DNB]$^+$; found (ESI$^+$) 181.0427.

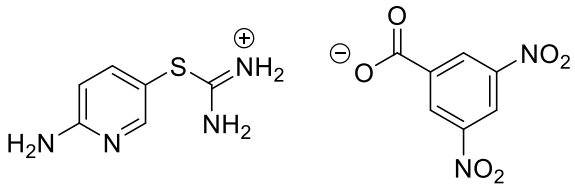
S-(4-Hydrazineylphenyl)isothiouronium 3,5-dinitrobenzoate (27l)



Prepared according to the general procedure. Isolated as a yellow powder **27l** (132 mg, 0.33 mmol, 67%). **m.p.** 133-135 °C; **^{1}H NMR (400 MHz, DMSO-d_6)** δ = 8.98 (t, *J* = 2.1 Hz,

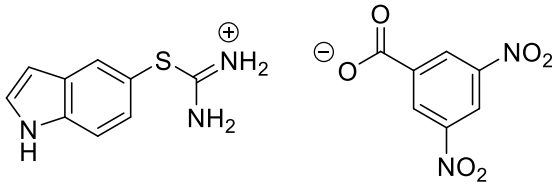
1H), 8.91 (d, *J* = 2.1 Hz, 2H), 7.38 (d, *J* = 8.6 Hz, 2H), 7.08 (s, 4H), 6.63 (d, *J* = 8.6 Hz, 2H); **^{13}C{^{1}H} NMR (101 MHz, DMSO-*d*$_6$)** δ = 172.1, 164.7, 149.1, 148.8, 139.8, 137.5, 129.3, 123.7, 121.6, 115.5; **ν_{max}(neat)/cm^{-1}:** 3252, 3110, 3090, 3015, 2970, 2084, 1739, 1622, 1542, 1530, 1484, 1456, 1377, 1340, 1218, 1164, 1084, 1003, 920, 890, 827, 792, 717, 605, 520, 440; **HRMS** calcd. for $C_7H_{11}N_4S^+$: 183.0699 [M-DNB]$^+$; found (ESI$^+$) 183.0705.

***S*-(6-Aminopyridin-3-yl)isothiouronium 3,5-dinitrobenzoate (27m)**



Prepared according to the general procedure. Isolated as a grey powder **27m** (103 mg, 0.32 mmol, 54%). **m.p.** 170-172 °C (lit. 197-199 °C);[57] **^{1}H NMR (400 MHz, DMSO-*d*$_6$)** δ = 10.28 (s, 4H), 8.89 (d, *J* = 2.2 Hz, 2H), 8.86 (t, *J* = 2.2 Hz, 1H), 8.09 (d, *J* = 2.5 Hz, 1H), 7.54 (dd, *J* = 8.8, 2.5 Hz, 1H), 6.77 (s, 2H), 6.53 (d, *J* = 8.8 Hz, 1H); **^{13}C{^{1}H} NMR (101 MHz, DMSO-*d*$_6$)** δ = 171.6, 166.2, 162.1, 156.4, 148.4, 144.5, 141.5, 129.0, 120.2, 110.0, 104.3; **ν_{max}(neat)/cm^{-1}:** 3468, 3345, 3099, 1671, 1630, 1600, 1531, 1489, 1456, 1382, 1343, 1077, 722, 529, 483, 433; **HRMS** calcd. for $C_6H_9N_4S^+$: 169.0542 [M-DNB]$^+$; found (ESI$^+$) 169.0557. Spectroscopic data are in agreement with literature.[57]

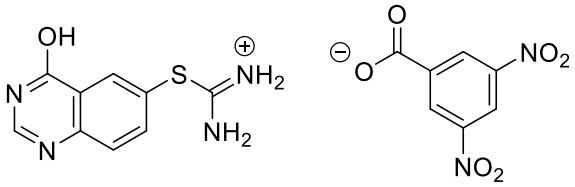
***S*-(1H-Indol-5-yl)isothiouronium 3,5-dinitrobenzoate (27n)**



Prepared according to the general procedure. Isolated as a yellow powder **27n** (147 mg, 0.36 mmol, 73%). **m.p.** 211-213 °C (lit. 229-231 °C);[57] **^{1}H NMR (400 MHz, DMSO-*d*$_6$)** δ = 11.57 (s, 1H), 8.95 (brs, 4H), 8.88 (d, *J* = 2.2 Hz, 2H), 8.80 (t, *J* = 2.2 Hz, 1H), 7.93 (d, *J* =

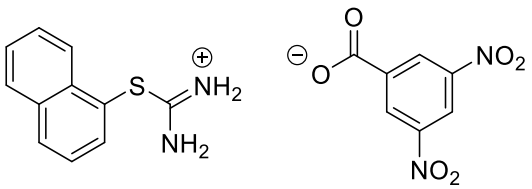
1.8 Hz, 1H), 7.58 (d, *J* = 8.4 Hz, 1H), 7.53 (appt, *J* = 2.7 Hz, 1H), 7.29 (dd, *J* = 8.4, 1.8 Hz, 1H), 6.58 (appt, *J* = 2.7 Hz, 1H); **$^{13}C\{^{1}H\}$ NMR (101 MHz, DMSO-d_6)** δ = 171.7, 166.6, 148.3, 142.7, 137.8, 130.0, 129.5, 128.9, 128.5, 127.9, 119.8, 114.1, 111.6, 102.4; **ν_{max}(neat)/cm^{-1}:** 3400, 3142, 3100, 3028, 2970, 1739, 1639, 1623, 1605, 1565, 1531, 1438, 1379, 1340, 1309, 1229, 1217, 1089, 1070, 925, 891, 795, 771, 722, 703, 643, 556, 526, 480, 418; **HRMS** calcd. for $C_9H_{10}N_3S^+$: 192.0590 [M-DNB]$^+$; found (ESI$^+$) 192.0589. Spectroscopic data are in agreement with literature.[57]

S-(4-Hydroxyquinazolin-6-yl)isothiouronium 3,5-dinitrobenzoate (27o)



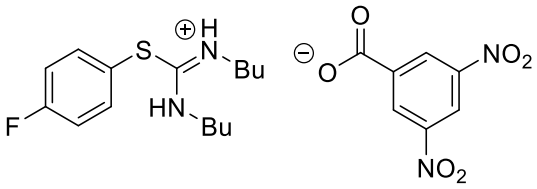
Prepared according to the general procedure. Isolated as a 9:10 mixture of isothiouronium salt and aryl iodide. Obtained as a pink powder **27o:18o** (155 mg, 0.21 mmol, 42%). **m.p.** 170-171 °C (lit. 194-196 °C);[57] **^{1}H NMR (400 MHz, DMSO-d_6)** δ = 9.65 (brs, 4H), 8.89 (d, *J* = 2.3 Hz, 2H), 8.82 (t, *J* = 2.3 Hz, 1H), 8.34 (d, *J* = 2.2 Hz, 1H), 8.25 (s, 1H), 8.01 (dd, *J* = 8.5, 2.2 Hz, 1H), 7.80 (d, *J* = 8.5 Hz, 1H); **$^{13}C\{^{1}H\}$ NMR (101 MHz, DMSO-d_6)** δ = 176.7, 169.6, 165.9, 160.5, 150.9, 148.3, 148.0, 141.9, 135.0, 129.9, 128.9, 122.7, 122.2, 119.8; **ν_{max}(neat)/cm^{-1}:** 3257, 3016, 2970, 2919, 1739, 1670, 1610, 1532, 1457, 1380, 1347, 1281, 1217, 1084, 916, 853, 834, 732, 720, 564, 521, 488, 421; **HRMS** calcd. for $C_9H_9N_4OS^+$: 221.0492 [M-DNB]$^+$; found (ESI$^+$) 221.0489. Spectroscopic data are in agreement with literature.[57]

S-(Naphthalen-1-yl)isothiouronium 3,5-dinitrobenzoate (27p)



Prepared according to the general procedure. Isolated as a grey powder **27p** (103 mg, 0.25 mmol, 50%). **m.p.** 193-194 °C (lit. 207-209 °C);[57] **^{1}H NMR (400 MHz, DMSO-*d*$_6$)** δ = 9.34 (s, 4H), 8.87 (d, *J* = 2.2 Hz, 2H), 8.82 (t, *J* = 2.2 Hz, 1H), 8.26 (d, *J* = 8.4 Hz, 1H), 8.20 (d, *J* = 8.4 Hz, 1H), 8.13 (dd, *J* = 8.1, 1.4 Hz, 1H), 8.05 (dd, *J* = 7.0, 1.2 Hz, 1H), 7.77 (ddd, *J* = 8.4, 7.0, 1.4 Hz, 1H), 7.72 – 7.65 (m, 2H); **^{13}C{^{1}H} NMR (101 MHz, DMSO-*d*$_6$)** δ = 169.6, 166.9, 148.3, 142.3, 138.4, 134.8, 134.3, 133.6, 129.6, 128.9, 128.8, 127.5, 126.9, 124.7, 120.7, 119.9; **ν_{max}(neat)/cm^{-1}:** 3115, 3016, 2970, 1739, 1656, 1627, 1605, 1552, 1526, 1447, 1422, 1379, 1339, 1229, 1217, 1071, 911, 792, 774, 730, 715, 658, 526, 486, 460, 404; **HRMS** calcd. for $C_{11}H_{11}N_2S^+$: 203.0637 [M-DNB]$^+$; found (ESI$^+$) 203.0636. Spectroscopic data are in agreement with literature.[57]

***N, N'*-Dibutyl-*S*-(4-fluorophenyl)isothiouronium 3,5-dinitrobenzoate (31)**



Prepared according to the general procedure. Isolated as a white powder **31** (18.4 mg, 0.07 mmol, 8%). **m.p.** 127-128 °C; **^{1}H NMR (400 MHz, DMSO-*d*$_6$)** δ = 8.90 (d, *J* = 2.2 Hz, 2H), 8.87 (t, *J* = 2.2 Hz, 1H), 7.71 (brs, 2H), 7.66 – 7.60 (m, 2H), 7.40 – 7.33 (m, 2H), 3.32 (br s, 4H), 1.58 – 1.38 (m, 4H), 1.26 (br s, 4H), 0.86 (t, *J* = 7.4 Hz, 6H); **^{13}C{^{1}H} NMR (101 MHz, DMSO-*d*$_6$)** δ = 164.8, 164.4, 163.6 (d, *J* = 248.3 Hz), 148.4, 141.7, 136.8 (d, *J* = 9.7 Hz), 129.0, 123.1, 120.1, 117.8 (d, *J* = 22.5 Hz), 43.8, 32.3, 19.9, 14.1;**^{19}F NMR (376 MHz, DMSO-*d*$_6$)** δ = −108.89 (tt, *J* = 8.5, 4.2 Hz); **ν_{max}(neat)/cm^{-1}:** 3457, 3102, 2959, 2933, 2874, 1638, 1603, 1574, 1538, 1485, 1344, 1223, 1156, 1069, 939, 841, 724, 712, 644, 519; **HRMS** calcd. for $C_{15}H_{24}FN_2S^+$: 283.1639 [M-DNB]$^+$; found (ESI$^+$) 283.1651.

10 References

1 K. A. Scott and J. T. Njardarson, *Top. Curr. Chem.*, 2018, **376**, 5.

2 M. Feng, B. Tang, S. H. Liang and X. Jiang, *Curr. Top. Med. Chem.*, 2016, **16**, 1200–1216.

3 P. Devendar and G.-F. Yang, *Top. Curr. Chem.*, 2017, **375**, 82.

4 E. K. Lee, M. Y. Lee, C. H. Park, H. R. Lee and J. H. Oh, *Adv. Mater.*, 2017, **29**, 1703638.

5 N. Maezaki, A. Sakamoto, N. Nagahashi, M. Soejima, Y.-X. Li, T. Imamura, N. Kojima, H. Ohishi, K. Sakaguchi, C. Iwata and T. Tanaka, *J. Org. Chem.*, 2000, **65**, 3284–3291.

6 J. Sun, C. Zhu, Z. Dai, M. Yang, Y. Pan and H. Hu, *J. Org. Chem.*, 2004, **69**, 8500–8503.

7 V. K. Duong, A. M. Horan and E. M. McGarrigle, *Org. Lett.*, 2020, **22**, 8451–8457.

8 A. Horn and P. H. Dussault, *J. Org. Chem.*, 2019, **84**, 14611–14626.

9 T. Migita, T. Shimizu, Y. Asami, J. Shiobara, Y. Kato and M. Kosugi, *Bull. Chem. Soc. Jpn*, 1980, **53**, 1385–1389.

10 D. Prasad and G. Sekar, *Synthesis*, 2010, **1**, 79–84.

11 O. Campopiano and F. Minassian, in *Encyclopedia of Reagents for Organic Synthesis*, John Wiley & Sons, Ltd, Chichester, UK, 2006.

12 J. A. Rodriguez and J. Hrbek, *Acc. Chem. Res.*, 1999, **32**, 719–728.

13 Y. Liu, S. Liu and Y. Xiao, *Beilstein J. Org. Chem.*, 2017, **13**, 589–611.

14 E. Bellale, M. Chaudhari and K. Akamanchi, *Synthesis*, 2009, **19**, 3211–3213.

15 W. R. Salaneck, N. O. Lipari, A. Paton, R. Zallen and K. S. Liang, *Phys. Rev. B*, 1975, **12**, 1493–1500.

16 Y. Jiang, Y. Qin, S. Xie, X. Zhang, J. Dong and D. Ma, *Org. Lett.*, 2009, **11**, 5250–5253.

17 J. Ham, I. Yang and H. Kang, *J. Org. Chem.*, 2004, **69**, 3236–3239.

18 A. Khazaei, M. Kazem-Rostami, A. Moosavi-Zare, M. Bayat and S. Saednia, *Synlett.*, 2012, **23**, 1893–1896.

19 E. de Souza, T. Chorro and C. Correia, *ChemRxiv*, 2022, 1–10.

20 J. Yi, Y. Fu, B. Xiao, W.-C. Cui and Q.-X. Guo, *Tetrahedron Lett.*, 2011, **52**, 205–208.

21 H. Distler, *Angew. Chem. Int. Ed.*, 1967, **6**, 544–553.

22 J. T. Reeves, K. Camara, Z. S. Han, Y. Xu, H. Lee, C. A. Busacca and C. H. Senanayake, *Org. Lett.*, 2014, **16**, 1196–1199.

23 J. E. Shaw, *J. Org. Chem.*, 1991, **56**, 3728–3729.

24 L. Testaferri, M. Tingoli and M. Tiecco, *Tetrahedron Lett.*, 1980, **21**, 3099–3100.

25 T. Itoh and T. Mase, *Org. Lett.*, 2004, **6**, 4587–4590.

26 G. Schäfer, A. Merot and T. Fleischer, *Org. Process Res. Dev.*, 2022, **26**, 3373–3379.

27 M. Kosugi, T. Shimizu and T. Migita, *Chem. Lett.*, 1978, **7**, 13–14.

28 T. Itoh and T. Mase, *J. Org. Chem.*, 2006, **71**, 2203–2206.

29 T. Gendron, K. Sander, K. Cybulska, L. Benhamou, P. K. B. Sin, A. Khan, M. Wood, M. J. Porter and E. Årstad, *J. Am. Chem. Soc.*, 2018, **140**, 11125–11132.

30 T. Itoh and T. Mase, *Org. Lett.*, 2007, **9**, 3687–3689.

31 M. A. Fernández-Rodríguez, Q. Shen and J. F. Hartwig, *J. Am. Chem. Soc.*, 2006, **128**, 2180–2181.

32 M. Kreis and S. Bräse, *Adv. Synth. Catal.*, 2005, **347**, 313–319.

33 J. C. Arnould, M. Didelot, C. Cadilhac and M. J. Pasquet, *Tetrahedron Lett.*, 1996, **37**, 4523–4524.

34 B. Chekal, D. Damon, D. LaFrance, K. Leeman, C. Mojica, A. Palm, M. St. Pierre, J. Sieser, K. Sutherland, R. Vaidyanathan, J. Van Alsten, B. Vanderplas, C. Wager, G. Weisenburger, G. Withbroe and S. Yu, *Org. Process Res. Dev.*, 2015, **19**, 1944–1953.

35 G. Segalovich-Gerendash, I. Rozenberg, N. Alassad, N. B. Nechmad, I. Goldberg, S. Kozuch and N. G. Lemcoff, *ACS Catal.*, 2020, **10**, 4827–4834.

36 E. de Oliveira Lima Filho and I. Malvestiti, *ACS Omega*, 2020, **5**, 33329–33339.

37 G. Danoun, B. Bayarmagnai, M. F. Gruenberg and L. J. Goossen, *Chem. Sci.*, 2014, **5**, 1312.

38 J. Chen, T. Wang, T. Wang, A. Lin, H. Yao and J. Xu, *Org. Chem. Front.*, 2017, **4**, 130–134.

39 L. Yang, Z.-Y. Tian and C.-P. Zhang, *ChemistrySelect*, 2019, **4**, 311–315.

40 R. Leuckart, *J. Prakt. Chem.*, 1889, **41**, 179–224.

41 L. Wang, W.-Y. Zhou, S.-C. Chen, M.-Y. He and Q. Chen, *Synlett.*, 2011, **2011**, 3041–3045.

42 V. K. Akkilagunta and R. R. Kakulapati, *J. Org. Chem.*, 2011, **76**, 6819–6824.

43 G. Lloyd-Jones, J. Moseley and J. Renny, *Synthesis*, 2008, **5**, 661–689.

44 J. N. Harvey, J. Jover, G. C. Lloyd-Jones, J. D. Moseley, P. Murray and J. S. Renny, *Angew. Chem. Int. Ed.*, 2009, **48**, 7612–7615.

45 A. J. Perkowski, C. L. Cruz and D. A. Nicewicz, *J. Am. Chem. Soc.*, 2015, **137**, 15684–15687.

46 T. Broese, A. F. Roesel, A. Prudlik and R. Francke, *Org. Lett.*, 2018, **20**, 7483–7487.

47 C. Lai and B. J. Backes, *Tetrahedron Lett.*, 2007, **48**, 3033–3037.

48 S. Thea and G. Cevasco, *Tetrahedron Lett.*, 1987, **28**, 5193–5194.

49 S. Thea and G. Cevasco, *Tetrahedron Lett.*, 1988, **29**, 2865–2866.

50 N. Park, K. Park, M. Jang and S. Lee, *J. Org. Chem.*, 2011, **76**, 4371–4378.

51 K. Takagi, *Chem. Lett.*, 1985, **14**, 1307–1308.

52 K. Takagi, *Chem. Lett.*, 1986, **15**, 265–266.

53 K. Takagi, *Chem. Lett.*, 1986, **15**, 1379–1380.

54 C. Tao, A. Lv, N. Zhao, S. Yang, X. Liu, J. Zhou, W. Liu and J. Zhao, *Synlett.*, 2011, **2011**, 134–138.

55 S. Sato, T. Sakamoto, E. Miyazawa and Y. Kikugawa, *Tetrahedron*, 2004, **60**, 7899–7906.

56 A. Pelter, R. M. Rosser and S. Mills, *J. Chem. Soc., Perkin Trans. 1*, 1984, 717–720.

57 V. Magné and L. T. Ball, *Chem. Eur. J.*, 2019, chem.201901874.

58 R. L. Frank and P. V. Smith, *J. Am. Chem. Soc.*, 1946, **68**, 2103–2104.

59 S. Vetter, *Synth. Commun.*, 1998, **28**, 3219–3223.

60 G. I. Matiello, A. Pazini, K. I. M. da Silva, R. G. M. da Costa, G. Ebeling, J. Dupont, J. Limberger and J. D. Scholten, *Tetrahedron Lett.*, 2019, **60**, 780–784.

61 Z. Wu, A. Cao, W. Ding, T. Zhu and P. Shen, *J. Carbohydr. Chem.*, 2016, **35**, 355–366.

62 N. S. Rajapaksa, A. Gobbi, J. Drobnick, S. Do, A. Kolesnikov, J. Liang, Y. Chen, S. Sujatha-Bhaskar, Z. Huang, H. Brightbill, R. Francis, C. Yu, E. F. Choo, K. DeMent, Y. Ran, L. An, C. Emson, J. Maher, J. Wai, B. S. McKenzie, P. J. Lupardus, A. A. Zarrin, J. R. Kiefer and M. C. Bryan, *ACS Med. Chem. Lett.*, 2020, **11**, 327–333.

63 P. W. G. SMITH and A. R. TATCHELL, in *Fundamental Aliphatic Chemistry*, Elsevier, 1965, pp. 267–273.

64 D. Damodara, R. Arundhathi and P. R. Likhar, *Catal. Sci. Technol.*, 2013, **3**, 797–802.

65 H. Firouzabadi, N. Iranpoor and M. Gholinejad, *Adv. Synth. Catal.*, 2010, **352**, 119–124.

66 A. Tait, C. Parenti, M. Di Bella, M. Bondi and G. Quaglio, *Arch. Pharm. (Weinheim)*, 1987, **320**, 203–210.

67 M. A. Düfert, K. L. Billingsley and S. L. Buchwald, *J. Am. Chem. Soc.*, 2013, **135**, 12877–12885.

68 Merck Structure Search. Available at: https://www.sigmaaldrich.com/GB/en/structure-search (Accessed 20 March 2023)

69 B. M. Rosen, K. W. Quasdorf, D. A. Wilson, N. Zhang, A.-M. Resmerita, N. K. Garg and V. Percec, *Chem. Rev.*, 2011, **111**, 1346–1416.

70 A. A. C. Braga, G. Ujaque and F. Maseras, *Organometallics*, 2006, **25**, 3647–3658.

71 G. Wilke, *Angew. Chem. Int. Ed.*, 1988, **27**, 185–206.

72 S. A. Macgregor, G. W. Neave and C. Smith, *Faraday Discuss.*, 2003, **124**, 111–127.

73 V. P. Ananikov, *ACS Catal.*, 2015, **5**, 1964–1971.

74 K. Zhang, M. Conda-Sheridan, S. R. Cooke and J. Louie, *Organometallics*, 2011, **30**, 2546–2552.

75 I. Kalvet, Q. Guo, G. J. Tizzard and F. Schoenebeck, *ACS Catal.*, 2017, **7**, 2126–2132.

76 D. J. Nelson and F. Maseras, *Chem. Commun.*, 2018, **54**, 10646–10649.

77 H. M. Omer and P. Liu, *J. Am. Chem. Soc.*, 2017, **139**, 9909–9920.

78 S. I. Al-Khalil, W. R. Bowman, K. Gaitonde, M. A. Marley (née Nagel) and G. D. Richardson, *J. Chem. Soc., Perkin Trans. 2*, 2001, 1557–1565.

79 J. A. Zoltewicz and T. M. Oestreich, *J. Am. Chem. Soc.*, 1973, **95**, 6863–6864.

80 S. Otsuka, T. Yoshida and Y. Tatsuno, *J. Chem. Soc. D*, 1971, 67-68.

81 W. R. Bowman and P. F. Taylor, *J. Chem. Soc. Perkin 1*, 1990, 919.

82 M. C. R. Symons and W. R. Bowman, *J. Chem. Soc., Perkin Trans. 2*, 1990, 975–979.

83 A. G. Griesbeck and J. Mattay, *Synthetic Organic Photochemistry*, New York, 2004.

84 S. Saito, S. Oh-tani and N. Miyaura, *J. Org. Chem.*, 1997, **62**, 8024–8030.

85 A. C. Albéniz, P. Espinet, R. López-Fernández and A. Sen, *J. Am. Chem. Soc.*, 2002, **124**, 11278–11279.

86 M. E. Greaves, E. L. B. Johnson Humphrey and D. J. Nelson, *Catal. Sci. Technol.*, 2021, **11**, 2980–2996.

87 T. T. Tsou and J. K. Kochi, *J. Am. Chem. Soc.*, 1979, **101**, 6319–6332.

88 R. F. Pratt and T. C. Bruice, *J. Am. Chem. Soc.*, 1972, **94**, 2823–2837.

89 A. Tota, S. St John-Campbell, E. L. Briggs, G. O. Estévez, M. Afonso, L. Degennaro, R. Luisi and J. A. Bull, *Org. Lett.*, 2018, **20**, 2599–2602.

90 C. Swan, L. Maggi, M. Park, S. Taylor, W. Shepherd and L. T. Ball, *Synthesis*, 2022, **54**, 3399–3408.

91 ECHA substance infocard for NMP. Available at: https://echa.europa.eu/substance-information/-/substanceinfo/100.011.662 (Accessed 20 March 2023)

92 M. Cortes-Clerget, J. Yu, J. R. A. Kincaid, P. Walde, F. Gallou and B. H. Lipshutz, *Chem. Sci.*, 2021, **12**, 4237–4266.

93 T. Kitanosono and S. Kobayashi, *Chem. Eur. J.*, 2020, **26**, 9408–9429.

94 T. Kitanosono and S. Kobayashi, *ACS Cent. Sci.*, 2021, **7**, 739–747.

95 M. Parmentier, C. M. Gabriel, P. Guo, N. A. Isley, J. Zhou and F. Gallou, *Curr. Opin. Green Sustain. Chem.*, 2017, **7**, 13–17.

96 P. T. Anastas and J. C. Warner, *Green Chemistry: Theory and Practice*, Oxford University Press, 1998.

97 C. Jiménez-González, A. D. Curzons, D. J. C. Constable and V. L. Cunningham, *Int. J. Life Cycle Assess.*, 2004, **9**, 114–121.

98 D. J. C. Constable, C. Jimenez-Gonzalez and R. K. Henderson, *Org. Process Res. Dev.*, 2007, **11**, 133–137.

99 N. Compagno, R. Profeta and A. Scarso, *Curr. Opin. Green Sustain. Chem.*, 2023, **39**, 100729.

100 D. Prat, O. Pardigon, H.-W. Flemming, S. Letestu, V. Ducandas, P. Isnard, E. Guntrum, T. Senac, S. Ruisseau, P. Cruciani and P. Hosek, *Org. Process Res. Dev.*, 2013, **17**, 1517–1525.

101 R. K. Henderson, C. Jiménez-González, D. J. C. Constable, S. R. Alston, G. G. A. Inglis, G. Fisher, J. Sherwood, S. P. Binks and A. D. Curzons, *Green Chem.*, 2011, **13**, 854.

102 G. La Sorella, G. Strukul and A. Scarso, *Green Chem.*, 2015, **17**, 644–683.

103 M. B. Gawande, V. D. B. Bonifácio, R. Luque, P. S. Branco and R. S. Varma, *Chem. Soc. Rev.*, 2013, **42**, 5522.

104 E. E. Meyer, K. J. Rosenberg and J. Israelachvili, *Proc. Nat. Acad. Sci.*, 2006, **103**, 15739–15746.

105 D. C. Rideout and R. Breslow, *J. Am. Chem. Soc.*, 1980, **102**, 7816–7817.

106 A. Acharjee, A. Rakshit, S. Chowdhury and B. Saha, *J. Mol. Liq.*, 2021, **321**, 114897.

107 B. H. Lipshutz and B. R. Taft, *Org. Lett.*, 2008, **10**, 1329–1332.

108 M. T. De Martino, L. K. E. A. Abdelmohsen, F. P. J. T. Rutjes and J. C. M. van Hest, *Beilstein J. Org. Chem.*, 2018, **14**, 716–733.

109 M. Cortes-Clerget, J. R. A. Kincaid, N. Akporji and B. H. Lipshutz, in *Supramolecular Catalysis*, Wiley, 2022, pp. 467–487.

110 N. Joondan, H. D. Angundhooa, M. G. Bhowon, P. Caumul and S. J. Laulloo, *Tenside Surfactants Deterg.*, 2020, **57**, 361–374.

111 T. Dwars, E. Paetzold and G. Oehme, *Angew. Chem. Int. Ed.*, 2005, **44**, 7174–7199.

112 A. Acharjee, A. Rakshit, S. Chowdhury, S. Malik, M. K. Barman, Md. A. Ali and B. Saha, *J. Mol. Liq.*, 2019, **277**, 360–371.

113 K. Mukherjee, R. Nandi, D. Saha and B. Saha, *Desalination Water Treat.*, 2015, **54**, 525–532.

114 P. Weschayanwiwat, J. F. Scamehorn and P. J. Reilly, *J. Surfactants Deterg.*, 2005, **8**, 65–72.

115 P. S. Hammond, J. S. Forster, C. N. Lieske and H. D. Durst, *J. Am. Chem. Soc.*, 1989, **111**, 7860–7866.

116 H. Borowy-Borowski, M. Sikorska-Walker, P. R. Walker, Water-Soluble Compositions of Bioactive Lipophilic Compounds. U.S. Patent 6,045,826, Apr 4, 2000.

117 H. Borowy-Borowski, M. Sikorska-Walker, P. R. Walker, Water-Soluble Compositions of Bioactive Lipophilic Compounds. U.S. Patent 6,632,443, Oct 14, 2003.

118 B. H. Lipshutz and S. Ghorai, *Aldrichemica Acta*, 2008, **41**, 59-72.

119 T. Lorenzetto, G. Berton, F. Fabris and A. Scarso, *Catal. Sci. Technol.*, 2020, **10**, 4492–4502.

120 B. H. Lipshutz and S. Ghorai, *Aldrichimica Acta*, 2012, **45**, 3–16.

121 B. H. Lipshutz, T. B. Petersen and A. R. Abela, *Org. Lett.*, 2008, **10**, 1333–1336.

122 B. H. Lipshutz, D. W. Chung and B. Rich, *Org. Lett.*, 2008, **10**, 3793–3796.

123 B. H. Lipshutz, G. T. Aguinaldo, S. Ghorai and K. Voigtritter, *Org. Lett.*, 2008, **10**, 1325–1328.

124 B. H. Lipshutz, S. Ghorai and G. T. Aguinaldo, *Adv. Synth. Catal.*, 2008, **350**, 953–956.

125 B. H. Lipshutz, S. Ghorai, A. R. Abela, R. Moser, T. Nishikata, C. Duplais, A. Krasovskiy, R. D. Gaston and R. C. Gadwood, *J. Org. Chem.*, 2011, **76**, 4379–4391.

126 P. T. Anastas and C. A. Farris, *Benign by Design; Alternative Synthetic Design for Pollution Prevention*, American Chemical Society, Washington, DC, 1994, vol. 577.

127 M. P. Andersson, F. Gallou, P. Klumphu, B. S. Takale and B. H. Lipshutz, *Chem. Eur. J.*, 2018, **24**, 6778–6786.

128 B. H. Lipshutz, *Curr. Opin. Green Sustain. Chem.*, 2018, **11**, 1–8.

129 H. Hoffmann and G. Ebert, *Angew. Chem. Int. Ed.*, 1988, **27**, 902–912.

130 C. M. Gabriel, N. R. Lee, F. Bigorne, P. Klumphu, M. Parmentier, F. Gallou and B. H. Lipshutz, *Org. Lett.*, 2017, **19**, 194–197.

131 B. H. Lipshutz, S. Ghorai, W. W. Y. Leong, B. R. Taft and D. V. Krogstad, *J. Org. Chem.*, 2011, **76**, 5061–5073.

132 N. V. Nucci and J. M. Vanderkooi, *J. Mol. Liq.*, 2008, **143**, 160–170.

133 N. Nishikido and R. Matuura, *Bull. Chem. Soc. Jpn*, 1977, **50**, 1690–1694.

134 S. Polarz, M. Kunkel, A. Donner and M. Schlötter, *Chem. Eur. J.*, 2018, **24**, 18842–18856.

135 X. Li, Y. Yang, J. Eastoe and J. Dong, *ChemPhysChem*, 2010, **11**, 3074–3077.

136 J.-K. Kim, E. Lee, Y. Lim and M. Lee, *Angew. Chem. Int. Ed.*, 2008, **47**, 4662–4666.

137 T. Yu, H. Pang, Y. Cao, F. Gallou and B. H. Lipshutz, *Angew. Chem. Int. Ed.*, 2021, **60**, 3708–3713.

138 S. Mattiello, M. Rooney, A. Sanzone, P. Brazzo, M. Sassi and L. Beverina, *Org. Lett.*, 2017, **19**, 654–657.

139 D. J. Lippincott, E. Landstrom, M. Cortes-Clerget, B. H. Lipshutz, K. Buescher, R. Schreiber, C. Durano, M. Parmentier, N. Ye, B. Wu, M. Shi, H. Yang, M. Andersson and F. Gallou, *Org. Process Res. Dev.*, 2020, **24**, 841–849.

140 G. D. Bowden, B. J. Pichler and A. Maurer, *Sci. Rep.*, 2019, **9**, 11370.

141 R. Carlson, *Chemom. Intell. Lab. Syst.*, 2004, **73**, 151–166.

142 S. A. Weissman and N. G. Anderson, *Org. Process Res. Dev.*, 2015, **19**, 1605–1633.

143 I. Bosch, A. González, F. Urpí and J. Vilarrasa, *J. Org. Chem.*, 1996, **61**, 5638–5643.

144 D. W. Allen, I. W. Nowell, L. A. March and B. F. Taylor, *J. Chem. Soc. Perkin 1*, 1984, 2523.

145 D. W. Allen, J. Hawkrigg, H. Adams, B. F. Taylor, D. E. Hibbs and M. B. Hursthouse, *J. Chem. Soc. Perkin 1*, 1998, 335–340.

146 S. Roediger, S. U. Leutenegger and B. Morandi, *Chem. Sci.*, 2022, **13**, 7914–7919.

147 A. Stanger and K. P. C. Vollhardt, *Organometallics*, 1992, **11**, 317–320.

148 A. C. Vetter, K. Nikitin and D. G. Gilheany, *Chem. Commun.*, 2018, **54**, 5843–5846.

149 Ö. Topel, B. A. Çakır, L. Budama and N. Hoda, *J. Mol. Liq.*, 2013, **177**, 40–43.

150 T. Shen, S. Zhou, J. Ruan, X. Chen, X. Liu, X. Ge and C. Qian, *Adv. Colloid Interface Sci.*, 2021, **287**, 102299.

151 A. I. Gómez-Merino, F. J. Rubio-Hernández, J. F. Velázquez-Navarro, J. Aguiar and C. Jiménez-Agredano, *Ceram. Int.*, 2014, **40**, 14045–14050.

152 H. Morawetz, *Catalysis and Inhibition in Solutions of Synthetic Polymers and in Micellar Solutions*, Academic Press 1969, pp. 341–371.

153 A. M. Borys, *Organometallics*, 2023, **42**, 182–196.